



Universidad de Granada – Fundación MEDINA

Doctoral Programme in Pharmacy



Expanding chemical diversity in fungi and evaluation of its application for discovering new antifungal agents

Rachel Serrano Bacallao

PhD Thesis

2024

Thesis Directors

Olga Genilloud Rodríguez

José Rubén Tormo Beltrán



Universidad de Granada – Fundación MEDINA

Programa de Doctorado en Farmacia



Ampliación de la diversidad química en hongos y evaluación de su aplicación para el descubrimiento de nuevos agentes antifúngicos

Rachel Serrano Bacallao

Tesis Doctoral

2024

Directores de Tesis

Olga Genilloud Rodríguez

José Rubén Tormo Beltrán

Editor: Universidad de Granada. Tesis Doctorales
Autor: Rachel Serrano Bacallao
ISBN: 978-84-1195-787-8
URI: <https://hdl.handle.net/10481/103737>

La presente Tesis Doctoral se ha llevado a cabo en los Departamentos de Microbiología, Química y Screening de Fundación MEDINA bajo la supervisión de los doctores Olga Genilloud Rodríguez y José Rubén Tormo Beltrán, en la línea de Investigación de Nuevas Dianas Terapéuticas del Programa de Doctorado en Farmacia (B15.56.1) de la Escuela de Doctorado de Ciencias de la Salud de la Universidad de Granada. Este trabajo ha sido financiado íntegramente por Fundación MEDINA.

Para la obtención de la Mención Internacional se realizó una estancia durante cuatro meses, del 1 de mayo de 2017 al 1 de septiembre de 2017, en National and Kapodistrian University of Athens, Atenas, Grecia, bajo la supervisión de Dr. Nikolas Fokialakis, donde se llevó a cabo la evaluación biológica inicial de extractos de origen microbiano frente a hongos fitopatógenos de interés agrícola como *Rhizoctonia* sp. y *Botrytis* sp., así como su caracterización química para la identificación de nuevos metabolitos secundarios.

Los resultados de esta Tesis Doctoral han sido publicados o están en vías de publicación en las siguientes revistas científicas:

- **Serrano, R., González-Menéndez, V., Rodríguez, L., Martín, J., Tormo, J.R. and Genilloud, O.** (2017). Co-culturing of fungal strains against *Botrytis cinerea* as a model for the induction of chemical diversity and therapeutic agents. *Frontiers in Microbiology*, 8: 649. doi: 10.3389/fmicb.2017.00649. JCR 4.019, Q2, total journal citations 25,111.
- **Serrano, R., González-Menéndez, V., Martínez, G., Toro, C., Martín, J., Genilloud, O. and Tormo, J.R.** (2021). Metabolomic analysis of the chemical diversity of South Africa leaf litter fungal species using an epigenetic culture-based approach. *Molecules*, 26: 4262. <https://doi.org/10.3390/molecules26144262>. JCR 4.927, Q2, total journal citations 128,386.
- **Serrano, R., González-Menéndez, V., Tormo, J.R. and Genilloud, O.** (2023). Development and validation of a HTS Platform for the discovery of new antifungal agents against four relevant fungal phytopathogens. *Journal of Fungi*, 9: 883. <https://doi.org/10.3390/jof9090883>. JCR 4.2, Q2, total journal citations 15,491.
- **Serrano, R., González-Menéndez, V., Pérez-Victoria, I., Sánchez, I., Toro, C., Mackenzie, T.A., Martín, J., Tormo, J.R. and Genilloud, O.** (submitted) Leaf-litter-associated fungi from South Africa to control fungal plant pathogens. *Scientific Reports*. JCR 3.8, Q1, total journal citations 734,947.

Además, parte de los resultados derivados de esta Tesis Doctoral han sido presentados en los siguientes congresos:

- **Rachel Serrano**, Víctor González-Menéndez, Clara Toro, Isabel Sánchez, Jesús Martín, José R. Tormo, Olga Genilloud. Leaf-litter-associated fungi for the Discovery of new antifungal agents against fungal phytopathogens. **POSTER**. 12th International Mycological Congress. Agosto 2024. Maastricht, Netherlands.

- **Rachel Serrano**, Víctor González-Menéndez, José R. Tormo, Olga Genilloud. PHYTOPATHOGENS HTS-PLATFORM: Development and validation of a HTS platform for the discovery of new antifungal agents against fungal plant pathogens. **POSTER**. SLAS2024 International Conference and Exhibition. February 2024. Boston, USA.
- **Rachel Serrano**, Víctor González-Menéndez, Clara Toro, Jesús Martín, José R. Tormo, Olga Genilloud. Un nuevo linaje de hongos de la hojarasca de Sudáfrica, fuente de metabolitos bioactivos frente hongos fitopatógenos. **POSTER**. Sociedad Española de Microbiología SEM2023. Junio 2023. Burgos, España.
- **Rachel Serrano**, Víctor González-Menéndez, Germán Martínez, Clara Toro, Jesús Martín, Olga Genilloud y José R. Tormo. Epigenética de hongos de la hojarasca de Sudáfrica como fuente de metabolitos bioactivos frente hongos fitopatógenos. **POSTER**. XV Congreso Nacional de Micología. Septiembre 2022. Valencia, España.
- **Rachel Serrano**, Víctor González-Menéndez, José R. Tormo y Olga Genilloud. Puesta a punto y validación de ensayos de inhibición del crecimiento de hongos fitopatógenos. **POSTER**. XV Congreso Nacional de Micología. Septiembre 2022. Valencia, España.
- **Rachel Serrano**, Víctor González-Menéndez, Ignacio González, José R. Tormo and Olga Genilloud. Development and validation of four fungal phytopathogen HTS assays for Natural Product biocontrol discovery. **POSTER**. International Symposium miCROPe, Julio 2022. Viena, Austria.
- **Rachel Serrano**, Víctor González-Menéndez, Germán Martínez, Clara Toro, Jesús Martín, Olga Genilloud, José R. Tormo. Epigenética de hongos de la hojarasca de Sudáfrica como fuente de metabolitos bioactivos frente hongos fitopatógenos. **POSTER**. II Congreso Investigación PTS. Febrero 2022. Granada, España.
- **Rachel Serrano**, Víctor González-Menéndez, Germán Martínez, Clara Toro, Jesús Martín, Olga Genilloud, José R. Tormo. Metabolomic analyses of the chemical diversity of leaf-litter fungal species using an epigenetic culture-based approach. **POSTER**. World Microbe Forum. Junio 2021, online.
- **Rachel Serrano**, Víctor González-Menéndez, José R. Tormo, Olga Genilloud. Puesta a punto y validación de ensayos de inhibición del crecimiento de hongos fitopatógenos. **POSTER**. XXVII Congreso Nacional de Microbiología SEM. Julio 2019, Málaga, Spain.
- **Rachel Serrano**, Víctor González-Menéndez, Clara Toro, Jesús Martín, José R. Tormo, Olga Genilloud. Fungal grass endophytes as biocontrol agents against fungal phytopathogens. **ORAL**. XIV Congreso Nacional de Micología. Septiembre 2018, Tarragona, España.
- **Rachel Serrano**, Víctor González-Menéndez, Lorena Rodríguez, Jesús Martín, José R. Tormo, Olga Genilloud. Co-culturing of fungal strains with the phytopathogen *Botrytis cinerea* induces the production of chemical diversity, with application as agrochemical and therapeutic agents. **POSTER**. Congreso Nacional de Biotecnología BIOTEC, Junio 2017, Murcia, España. 7th Congress of European Microbiologists FEMS, Julio 2017, Valencia, España. MICROPE: Microbe-assisted Crop production opportunities, challenges & needs, Diciembre 2017, Viena, Austria.

RESUMEN

Los hongos fitopatógenos son la principal causa de pérdidas en el sector agrícola, responsables de graves daños ecológicos y económicos. A pesar de que el uso de agroquímicos es el método preferido para el control de estos patógenos de plantas, presentan desafíos medioambientales. Por ello, se necesitan nuevas alternativas para controlar su infección en plantas con bajo riesgo para el medio ambiente y la salud humana. Hoy en día, el uso de cepas microbianas y su actividad antagonica presentan ventajas para el biocontrol de fitopatógenos. Los hongos se consideran una de las fuentes más prolíficas de Productos Naturales, con una amplia diversidad estructural y biológica. Sin embargo, la mayor parte de su potencial biosintético permanece inactivo en condiciones estándares de laboratorio, lo que requiere aplicar aproximaciones basadas en técnicas de cultivo efectivas para explorar su diversidad química única. Este estudio evaluó diferentes métodos innovadores para inducir la producción de metabolitos secundarios bioactivos en una amplia diversidad de hongos, y la evaluación de su potencial como fungicidas frente a cuatro hongos fitopatógenos relevantes.

Las interacciones microbianas juegan un papel crucial en su entorno natural a través de la producción de metabolitos/señales. Estas interacciones naturales pueden ser imitadas artificialmente mediante técnicas de co-cultivo. Inicialmente, se co-cultivaron 762 cepas aisladas de numerosos orígenes geográficos frente al hongo fitopatógeno *Botrytis cinerea*, resultando en 93 antagonismos positivos (12% de tasa de éxito). Las zonas de inhibición y micelio inhibido del fitopatógeno fueron extraídas para identificar los metabolitos responsables de los antagonismos. Los análisis de espectrometría de masas revelaron una clara comunicación bidireccional entre ambas cepas co-cultivadas, y más interesante aún, las interacciones fúngicas con *B. cinerea* indujeron la activación de rutas silenciosas para la biosíntesis de nuevos metabolitos.

Se exploró una segunda metodología para maximizar la producción de nuevos compuestos bioactivos, involucrando condiciones nutricionales específicas combinado con el modificador epigenético SAHA, en una nueva selección de cepas fúngicas aisladas de muestras de hojarasca recolectadas en Sudáfrica. Estudios de metabolómica no dirigida mostraron que las variaciones en la composición del medio indujeron importantes cambios en los perfiles metabolómicos, siendo determinante para la producción de metabolitos únicos, donde la fermentación en estado sólido en el medio BRFT fue la condición más productiva. Además, la adición de SAHA aumentó significativamente la diversidad y la cantidad de metabolitos en todos los medios de fermentación.

Métodos avanzados de cribado de alto rendimiento (HTS) permitieron desarrollar una plataforma efectiva y robusta para identificar nuevos agentes antifúngicos frente a *Botrytis cinerea*, *Colletotrichum acutatum*, *Fusarium proliferatum* y *Magnaporthe grisea*. Esta plataforma HTS fue validada para una amplia variedad de muestras, desde compuestos sintéticos hasta mezclas naturales complejas. El método HTS por microdilución mostró mayor eficiencia para evaluar el potencial antifúngico, el cual fue aplicado para caracterizar la diversidad química inducida en hongos asociados a hojarasca. El cribado primario reveló un alto número de extractos activos (n=340, 14% tasa de éxito), explicado por una amplia variedad de compuestos bioactivos conocidos. Además, el SAHA mejoró la diversidad química general y, en consecuencia, las tasas de acierto de actividad antifúngica, permitiendo identificar metabolitos poco expresados como la nueva molécula *libertamide*, producida por la cepa *Libertasomyces aloeticus* CF-168990, que

resultó ser un posible nuevo biofungicida para la mancha foliar de septoria causada por *Zymoseptoria tritici*.

En resumen, este estudio ha integrado diferentes enfoques basados en el cultivo de una amplia diversidad de cepas fúngicas, con el objetivo de explorar su potencial biosintético silente para producir metabolitos bioactivos. Además, la implementación de métodos analíticos avanzados, tanto en la caracterización química como en la actividad biológica, facilitó el descubrimiento de posibles nuevos fungicidas para el biocontrol de hongos fitopatógenos relevantes.

ABSTRACT

Fungal phytopathogens are the major cause of agricultural losses, responsible for severe ecological and economic damage. Despite agrochemical agents are the preferred method to control these plant pathogens, they present environmental challenges. Therefore, new alternatives are needed to control plant diseases with low risk to the environment and human health. Nowadays, the use of microbial strains and their antagonistic activities present advantages for the biocontrol of phytopathogens. Fungi are considered one of the most prolific sources of Natural Products with a broad structural and biological diversity. However, most of their biosynthetic potential remain inactive under standard laboratory conditions, which requires effective cultured-based approaches to explore their unique chemical diversity. This study assessed different innovative methods to induce the production of bioactive secondary metabolites in a broad diversity of fungal strains, as well as the evaluation of their potential as fungicides against four relevant phytopathogens.

Microbial interactions play a crucial role within their natural environment through the production of metabolites/signals. These natural interactions can be artificially mimicked by co-culturing techniques. Initially, 762 strains isolated from numerous geographical origins were co-cultured with the fungal phytopathogen *Botrytis cinerea*, resulting in 93 positive antagonisms (12% hit-rate). The inhibition zones and inhibited mycelia of the phytopathogen were extracted to identify the metabolites responsible for the antagonisms. Mass spectrometry analyses revealed a clear bidirectional communication between both co-cultured strains, and more interestingly, fungal interactions with *B. cinerea* induced the activation of silent pathways for the biosynthesis of new metabolites.

A second methodology was explored to maximize the production of novel bioactive compounds, involving specific nutritional arrays combined with the epigenetic elicitor SAHA, on a new selection of fungal strains isolated from leaf-litter collected in South Africa. Untargeted metabolomics showed that variations in the medium composition induced important changes in the metabolomic profiles, determining the production of unique metabolites, being the solid-state fermentation in the medium BRFT the most productive condition. Moreover, the addition of SAHA significantly increased the diversity and amounts of metabolites in all fermentation media.

Advanced high-throughput screening (HTS) methods allowed to develop an effective and robust platform to identify new antifungal agents against *Botrytis cinerea*, *Colletotrichum acutatum*, *Fusarium proliferatum* and *Magnaporthe grisea*. The HTS Platform has been validated for a wide range of samples from synthetic compounds to complex natural mixtures. This HTS microdilution method showed greater efficiency to assess the antifungal potential, that was applied to characterize the chemical diversity induced in leaf-litter-associated fungi. The primary screening revealed a high number of active extracts (n=340, 14% hit-rate), what was explained by a broad variety of known bioactive compounds. Moreover, SAHA enhanced the general chemical diversity, and consequently the antifungal activity hit-rates, allowing the identification of poorly expressed metabolites such as the novel molecule *libertamide*, produced by the strain *Libertasomyces aloeticus* CF-168990, a potential new bio-fungicide for septoria leave blotch caused by *Zymoseptoria tritici*.

In summary, this study has integrated different culture-based approaches on a wide diversity of fungal strains to successfully explore their cryptic biosynthetic potential to produce bioactive metabolites. Furthermore, the implementation of advanced analytical methods, both in chemical and biological activity characterization, has facilitated the discovery of possible new fungicides for the biocontrol of relevant phytopathogens.

Index

I. INTRODUCTION	
1. Natural Products from fungi	2
2. Leaf-litter-associated fungi	6
3. Culture-based approaches for new chemical production	8
3.1. Nutritional arrays and fermentation formats	
3.2. Epigenetic modulation by chemical elicitors	
3.3. Microbial interaction for metabolite induction	
4. Metabolomic tools for chemical analyses	15
5. High-Throughput Screening Platforms for bioactivity evaluation	17
6. Fungal plant pathogens	18
7. Current status of Natural Product-based fungicides	23
II. OBJECTIVES	25
III. RESULTS	27
Chapter 1. Co-culturing of fungal strains against <i>Botrytis cinerea</i> as a model for the induction of chemical diversity and therapeutic agents	30
Introduction	
Materials and Methods	
Results	
Discussion	
Conclusions	
References	
Chapter 2. Metabolomic analysis of the chemical diversity of South Africa leaf litter fungal species using an epigenetic culture-based approach	56
Introduction	
Results and Discussion	
Materials and Methods	
Conclusions	
References	
Chapter 3. Development and validation of a HTS Platform for the discovery of new antifungal agents against four relevant fungal phytopathogens	81
Introduction	
Materials and Methods	
Results and Discussion	
Conclusions	
References	

	Chapter 4. Leaf-litter-associated fungi from South Africa to control fungal plant pathogens	108
	Introduction	
	Results	
	Discussion	
	Materials and Methods	
	Conclusions	
	References	
IV.	GENERAL DISCUSSION	136
V.	CONCLUSIONS	150
VI.	REFERENCES	152
VII.	ANNEXES	166

LIST OF ABBREVIATIONS

28S	28S ribosomal RNA
Ac-CoA	Acetyl Coenzyme A
BCA	Biocontrol Agent
BGC	Biosynthetic Genes Cluster
DAD	Diode Array Detector
DNA	Deoxyribonucleic Acid
DNMT	DNA Methyltransferase
DNP	Chapman & Hall Dictionary of Natural Products
DMSO	Dimethyl Sulfoxide
DRC	Dose Response Curve
ED₅₀	Effective Dose for 50% of the Population
EPA	USA Environmental Protection Agency
ESI	Electrospray Ionization
FADH	Flavin Adenine Dinucleotide reduced
FAO	Food and Agriculture Organization of the United Nations
GCF	Gene Cluster Family
HATs	Histone Acetyl Transferases
HDAC	Histone Deacetylase
HepG2	Human hepatocellular carcinoma cell line
HPLC	High Performance Liquid Chromatography
HTS	High-Throughput Screening
IC₅₀	Inhibitory Concentration for 50% of Inhibition
ITS	Internal Transcribed Spacer
LC-MS	Liquid Chromatography Mass Spectrometry
LC-LRMS	Liquid Chromatography Low Resolution Mass Spectrometry
LC-HRMS	Liquid Chromatography High Resolution Mass Spectrometry
NMR	Nuclear Magnetic Resonance
NP	Natural Product
m/z	Mass to Charge Ratio
MIC	Minimal Inhibitory Concentration
MS	Mass Spectrometry
MTT	3-(4,5-dimethylthiazol-2-yl)-2,5,-diphenyltetrazolium bromide
MTS	3-(4,5-dimethylthiazol-2-yl)-5-(3-carboxymethoxyphenyl)-2-(4-sulphophenyl)-2H-tetrazolium
NADPH	Nicotinamide Adenine Dinucleotide Phosphate reduced
NADH	Nicotinamide Adenine Dinucleotide reduced

OSMAC	One Strain Many Compounds
PAINS	Pan-Assay Interference Compounds
PRC2	Polycomb Repressive Complex 2
rDNA	Ribosomal Deoxyribonucleic Acid
RNA Pol II	RNA Polymerase II
ROS	Reactive Oxygen Species
RT	Retention Time
SAM	S-adenosylmethionine
SAHA	Suberoylanilide Hydroxamic Acid
SBHA	Suberohydroxamic Acid
SM	Secondary Metabolite
SmF	Submerged Liquid Fermentation
SSF	Solid-State Fermentation
UPGMA	Unweighted Pair Group Method using Arithmetic Averages
UV	Ultraviolet
VA	Veratryl Alcohol
XTT	2,3-Bis(2-methoxy-4-nitro-5-sulfophenyl)-2H-tetrazolium-5-carboxanilide
ZOI	Zone of Inhibition

I. Introduction

1. NATURAL PRODUCTS FROM FUNGI

Natural Products (NPs) are molecules produced through diverse biosynthetic processes by living organisms such as animals, plants, and microorganisms (Bills & Gloer, 2016; Katz & Baltz, 2016). For several decades, NPs have been identified as unlimited sources of bioactive compounds, with several chemical structures with relevant stereochemical complexity and a broad spectrum of biological activities. NPs have been ‘optimized’ by evolution to perform specific biological functions, including the interaction among different organisms, which explained the interest of pharmaceutical industry on them for the discovery of novel drugs (Atanasov et al., 2021). Furthermore, many NPs show limited field persistence, short shelf life, and present no residual threats, which has attracted other sectors such as the agriculture industry for the development of agrochemicals (Xu et al., 2021).

Specifically, microbial NPs are considered one of the most important sources for the discovery of novel bioactive compounds. Among microorganisms, fungi are one of the most prolific producers and present a unique biosynthetic potential (Keller et al., 2005; Niego et al., 2023). So far, more than 45% of known bioactive NPs have been described to be produced by the secondary metabolism of fungi, with a broad structural and biological diversity (Bérđy, 2012; Riedling et al., 2024). Fungal Secondary Metabolites (SMs) are defined as non-essential compounds for the growth or survival of their producers, but are crucial for their ecological success. These metabolites provide strong selective advantages to nutrient acquisition, virulence, communication, defense, stress protection, reproduction, and pigmentation (Bills & Gloer, 2016; Rodrigo et al., 2021). These variety of functions have led to the discovery of fungal NPs with applications within the pharmaceutical, agrochemical and cosmetic industries. Examples of valuable biological activities have been described for several fungal SMs such as **antibacterial agents** against Gram-positive and negative bacteria (e.g. *penicillins*, *cephalosporin C*, *pleuromutilin* and *fusidic acid*), **antifungals** for human infections (e. g. *griseofulvin*, *echinocandins* and *enfumafungin*), **immunosuppressants** (e. g. *cyclosporin A*, *mycophenolic acid* and *mizoribine*), **hypercholesterolemia agents** (e. g. *lovastatin* and *compactin*), **antioxidants** (*kojic acid*), **anthelmintic agents** (*PF1022A*), **fungicides against phytopathogens** (*strobilurins A-D*), **plant growth promoters** (*gibberellic acid*), **insecticides** (*fumagillin*), among other important applications (Table 1).

Fungal SMs can be classified within a wide range of chemical classes (Figure 1) such as **alkaloids** (e.g. *cytochalasins*, *indoles*, *diketopiperazines*), **terpenoids** (*monoterpenoids*, *sesquiterpenes*, *cyclohexanoids*), **polyketides** (e.g. *isocoumarin*, *quinones*, *macrolides*, *benzopyrones*), **non-ribosomal peptides** (e.g. *echinocandins*, *cyclosporins* and *emerincins*), for which specialized biosynthetic programs are broadly distributed (Bills & Gloer, 2016; Gouda et al., 2016; Rodrigo et al., 2021; Xu et al., 2021). This complex and rich secondary metabolism is highly developed in the filamentous fungi belonging to *Ascomycota* and *Basidiomycota* classes, while it is underdeveloped in their unicellular forms and in *Zygomycota*, *Blastocladiomycota*, and *Chytridiomycota* classes (Bills & Gloer, 2016). The synthesis of SMs is controlled by the expression of biosynthetic gene clusters (BGCs). Generally, BGCs contain multiple genes encoding for enzymes involved in the synthesis of the core metabolite and the control of its transport, transcription and self-resistance, which are co-regulated and often co-localized along the fungal chromosome (Rokas et al., 2021; Zhang et al., 2024). Recent genome mining studies of 1,037 fungal genomes have identified 36,399 BGCs organized into a network of 12,067 gene cluster families (GCFs), suggesting an extensive and

Introduction

unexplored reservoir of potentially novel Natural Products, besides those that are commonly identified in culture-based studies (Robey et al., 2021; Zhang et al., 2024).

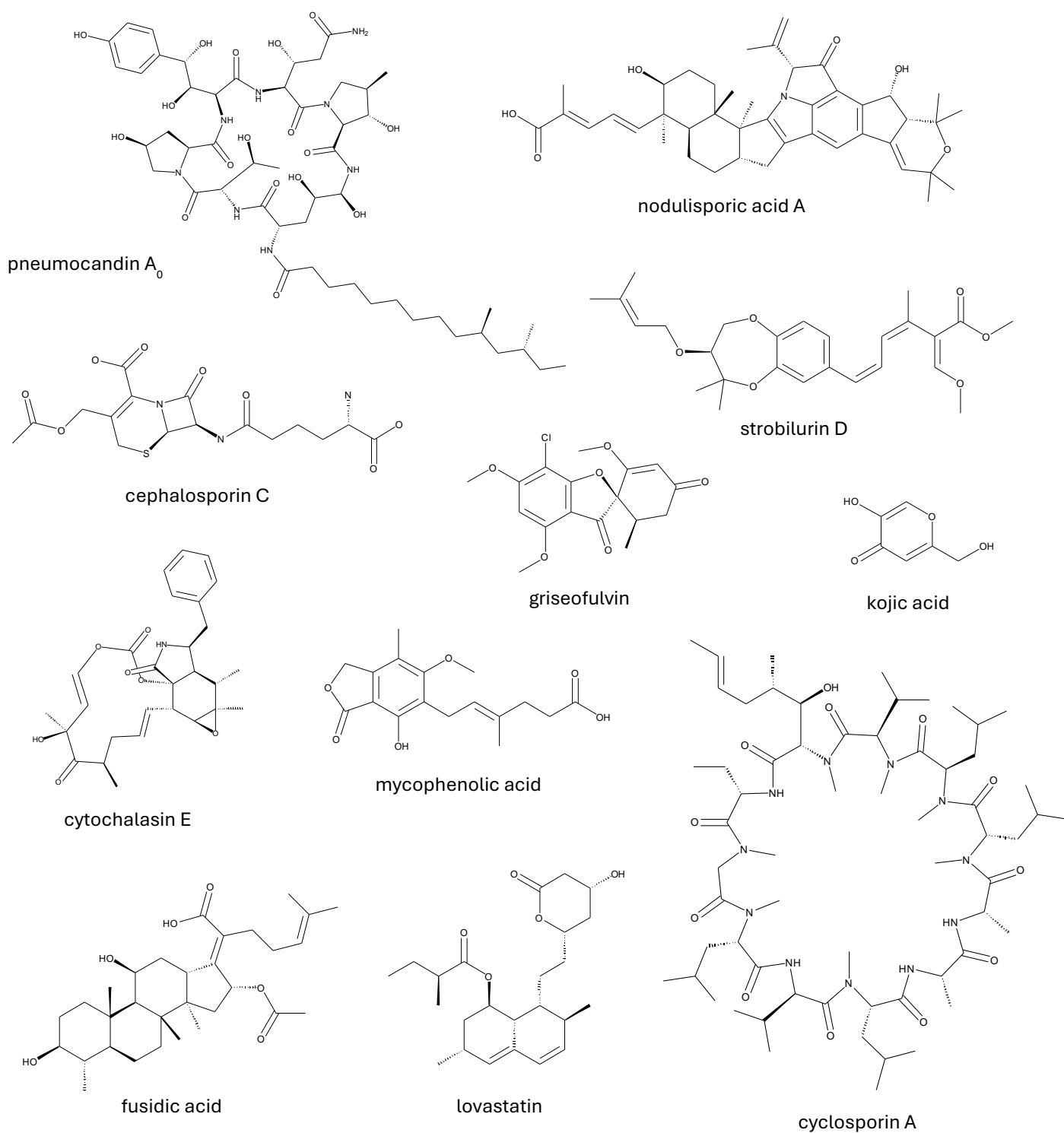


Figure 1. Chemical structure of bioactive fungal metabolites with relevant biological activities.

Table 1. Examples of fungal metabolites developed in pharmaceutical, agrochemical and cosmetic industrial sectors. Based on Bills & Gloer, 2016.

Metabolite	Source species	Structural classification	Commercial products	Mode of action and target	Activity
Human Health					
penicillins G & V	<i>Penicillium rubens</i> , <i>P. chrysogenum</i>	Nonribosomal peptide	Benzylpenicillin, phenoxymethylpenicillin, 6-aminopenicillanic acid	Biosynthesis of cell wall peptidoglycans	Antibiotic: Gram-positive and -negative bacteria
cephalosporin C	<i>Acremonium chrysogenum</i>	Nonribosomal peptide	7-amino cephalosporanic acid derivatives	Biosynthesis of cell wall peptidoglycans	Antibiotic: Gram-positive and -negative bacteria
pleuromutilin	<i>Clitopilus passeckerianus</i> , <i>Clitopilus</i> spp.	Diterpene	Retapamulin, tiamulin, valnemulin	Targets peptidyl transferase	Antibiotic: Gram-positive bacteria
fusidic acid	<i>Acremonium fusidioides</i>	Triterpene	Usidin, Fucidin, Fucicort, Fucibet, Taksta	Translocation of the elongation factor G	Antibiotic: Gram-positive bacteria, MRSA
griseofulvin	<i>Penicillium griseofulvum</i> , <i>P. aethiopicum</i> , <i>P. coprophilum</i>	Halogenated polyketide	Fulcin, Fulsovin, Grisovin	Bind tubulin preventing polymerization	Antifungal
echinocandins	<i>Aspergillus pachycristatus</i> , <i>Glarea lozoyensis</i> , <i>Coleophoma empetri</i>	Nonribosomal peptide acylated to fatty acid	Anidulifungin (Eraxis), Caspofungin (Cancidas), Micafungin (Mycamine)	β -1,3 glucan synthase & cell wall biosynthesis inhibitor	Antifungal
enfumafungin	<i>Hormonema carpetanum</i>	Triterpene glycoside	Scy-078, Ibrexafungerp	β -1,3 glucan synthase and cell wall biosynthesis	Antifungal
cyclosporin A	<i>Tolypocladium inflatum</i>	Nonribosomal peptide	Cyclosporine A (Sandimmune, Neoral, Restasis, Gengraf)	Bind cyclophilin A, calcineurin inhibition	Immunosuppressant
mycophenolic acid	<i>Penicillium brevicompactum</i> , <i>Penicillium</i> spp.	Meroterpenoid	Mycophenolate mofetil (Cellcept), mycophenolate sodium (Myfortic)	Inosine monophosphate dehydrogenase (IMPDH) inhibitor	Immunosuppressant
mizoribine	<i>Penicillium brefeldianum</i>	Imidazole nucleoside	Bredinin	Competitive inhibitor of IMPDH	Immunosuppressant
myriocin	<i>Isaria sinclairii</i>	Amino acid lipid	Fingolimod (Gilenya)	Bind extracellular G protein-coupled receptors	Immunosuppressant
ergotamine	<i>Claviceps purpurea</i> , <i>C. fusiformis</i> , <i>C. paspali</i>	Prenylated nonribosomal peptide	Ergotamine tartrate (Ergomar, Migril), dihydroergotamine mesylate (Migranal)	Agonist of 5-OH tryptamine (5-HT ₂) receptor 1B	Vasoconstrictor
ergometrine	<i>C. purpurea</i> , <i>C. fusiformis</i> , <i>C. paspali</i>	Prenylated nonribosomal peptide	Ergometrine maleate (Ergotrate, Ergovin)	Serotonin antagonist, activate /block 5-HT ₂ receptors	Vasoconstrictor

Introduction

Table 1 (continued).

Metabolite	Source species	Structural classification	Commercial products	Mode of action and target	Activity
Human Health					
lovastatin	<i>Aspergillus terreus</i> , <i>Monascus purpureus</i> , <i>Pleurotus ostreatus</i>	Polyketide	Mevacor, Simvastatin (Zocor, Simvacor, Simvastin)	3-hydroxy-3-methylglutaryl-coA reductase inhibitor	Hypercholesterolemia
mevastatin	<i>Penicillium citrinum</i> , <i>P. solitum</i> , <i>Penicillium</i> spp.	Polyketide	Pravachol, Selektine, Lipostat	3-hydroxy-3-methylglutaryl-coA reductase inhibitor	Hypercholesterolemia
Animal Health					
PF1022A	<i>Rosellinia</i> sp.	Nonribosomal peptide	Emodepside	nematode neuromuscular function	Anthelmintic
Cosmetic sector					
kojic acid	<i>Aspergillus oryzae</i> , <i>A. tamarii</i> , <i>A. flavus</i>	Pyrone derived from glucose	Kojic dipalmitate	Inhibits tyrosinase & suppresses melanogenesis	Antioxidant in cosmetic products
Agricultural sector					
strobilurins A-D	<i>Strobilurus tenacellus</i>	Polyketide with benzoyl CoA starting unit	azoxystrobin, fenamidone, fluoxastrobin, kresoxim methyl, trifloxystrobin	mitochondrial cytochrome b, respiratory electron transport	Fungicide broad spectrum against phytopathogens
fumagillin	<i>Aspergillus fumigatus</i>	Meroterpenoid	Bicyclohexyl ammonium fumagillin	Inhibits methionine aminopeptidase2 (MetAP2)	Fungicide for <i>Nosema apis</i> in honeybees
nodulisporic acid	<i>Nodulisporium</i> sp.	Diterpene	Nodulisporic acid A	glutamate-gated chloride channels	Insecticide
gibberellic acid	<i>Fusarium fujikuroi</i>	Diterpene	Fermentation of <i>F. fujikuroi</i>	Promotes plant growth	Plant growth hormone

2. LEAF-LITTER-ASSOCIATED FUNGI

Fungi are ubiquitous microorganisms that can colonize numerous ecosystems with large variations of pH and temperature, due to their capacity to adopt various forms and produce a high diversity of enzymes and metabolites. Fungal populations have key roles in multiple environmental processes such as nitrogen fixation, hormone production, biological control of pathogens, and organic material decomposition, which provides the essential nutrients for maintaining fertility of soils in forest ecosystems (Frąc et al., 2018). In terrestrial habitats fungi are crucial in carbon and nutrient cycling through the decomposition of organic material. The process of **leaf-litter decomposition** presents a high complexity where fungi are an essential element given their ability to degrade recalcitrant components such as cellulose, lignin and suberin (Foster et al., 2022; Grossman et al., 2020; Voříšková & Baldrian, 2013). Consequently, fungal communities associated with leaf-litter have been extensively studied, and a considerable number of rare and unique species are presented in this ecological habitat, being **one of the most diverse mycological assemblages** (Bills & Polishook, 1994; Collado et al., 2007; Crous et al., 2006; Foster et al., 2022; Voříšková & Baldrian, 2013).



Figure 2. Example of fungal fruiting bodies developed on leaf-litter material.

Despite the high biodiversity in leaf-litter communities, fungal strains are continually changing due to variations in the chemical and physical conditions of leaf-litter mixtures (Gao et al., 2015). Furthermore, the fungal community associated with leaf-litter is dominated by the phylum *Ascomycota*, followed by *Basidiomycota*, especially by saprotrophic cord-forming fungi, both considered to possess the richest secondary metabolomic potential (Bills & Gloer, 2016). Several reports have assessed the taxonomic diversity of leaf-litter-associated fungi from different geographical areas and their decomposer ability, but poor studies have exploited the biosynthetic potential of this large biodiversity of strains. However, some interesting fungal strains have been described as producers of important bioactive molecules (Table 2).

Introduction

Among leaf-litter studies, multiple works have been focused on describing fungal populations associated with leaf-litter in South Africa, mainly from litter material of endemic plants such as *Proteaceae* (proteas) and *Restionaceae* (restios). **South Africa** is considered one of the **worldwide biodiversity “hotspots”**, including areas such as the Cape Floral Kingdom which is the smallest and most biodiverse biome dominated by numerous endemic plants (Crous et al., 2006; Mamathaba et al., 2022; Goldblatt & Manning, 2000). Several novel fungal genera and species have been described in this geographical area, including *Bactrodesmium* sp., *Brachydesmiella* sp., *Circinotrichum* sp., *Coniosporium* sp., *Periconiella* sp., *Sporidesmium* sp., *Parasarcopodium ceratocaryi* and *Rhexodenticula elegiae* (Crous et al., 2006; Lee et al., 2004; Mel’nik et al., 2004; Taylor et al., 2001).

In this context, South Africa offers unique and valuable conditions for the development of a highly diverse leaf-litter material, with promising opportunities to discover new fungal strains with undescribed biosynthetic potential to produce novel bioactive metabolites.

Table 2. Examples of fungal strains described as producers of bioactive molecules, that were isolated from leaf-litter samples collected in different geographical areas.

Producer Strains	Origin	Bioactive molecule	Reference
<i>Plenodomus enteroleucus</i> CF-146176	Leaf-litter of <i>Fraxinus angustifolia</i> , Spain	campafungin : antifungal against <i>Candida albicans</i> & <i>Cryptococcus neoformans</i>	Perlatti et al., 2020
<i>Hormonema carpetanum</i> F-154715 & F-154786	Leaf-litter of <i>Cistus albidus</i> and <i>Juniperus sabina</i> , Spain	enfumafungin : antifungal against <i>Candida</i> sp. & <i>Aspergillus fumigatus</i>	Bills et al., 2004
<i>Arthrinium phaeospermum</i> F-044878	Leaf-litter, Congo	arundifungin : antifungal against <i>Candida</i> & <i>Aspergillus</i> strains	Cabello et al., 2001
<i>Fusarium larvarum</i> var. <i>rubrum</i> CF-253264	Mixed leaf-litter of <i>Pinus nigra</i> , Georgia	parnafungin : antifungal against <i>C. albicans</i>	Bills et al., 2017
<i>Lachnum</i> sp. F-266039	Leaf-litter, USA	virgineone : antimicrobial against <i>Staphylococcus aureus</i> , <i>Candida</i> sp. & <i>Aspergillus fumigatus</i>	Ondeyka et al., 2009
<i>Emericella variegata</i> F-202719	Leaf-litter of <i>Quercus Iberica</i> , Georgia	desferritriacetylusigen : antibacterial against <i>Staphylococcus aureus</i> MB5393	De la Cruz et al., 2012
<i>Lasionectria</i> sp. CF-176994	Forest leaf-litter, Equatorial Guinea	lasionectrin : antimalarial	Poral et al., 2015
<i>Hypoxylon pulicicidum</i> MK6321	Forest leaf-litter, Mauritius island & Peru	nodulisporic acid : anti-parasitic agent	Platas et al., 2009, Bills et al., 2012

3. CULTURE-BASED-APPROACHES FOR NEW CHEMICAL PRODUCTION

As indicated above, microbial NPs are untapped sources of bioactive molecules, that have been used for decades in a variety of screening programs with numerous biotechnological applications (Wilson et al., 2020). Despite their described ability to produce a broad diversity of compounds, most taxonomic orders are still poorly explored, besides the 80% of the fungal secondary metabolome remains unknown, what means a high number of potential new molecules waiting to be discovered (Hautbergue et al., 2018; Robey et al., 2021). However, the activation of these cryptic BGCs proposes severe challenges under laboratory culture conditions (Figure 3), where **genetic engineering approaches** have only been efficiently applied for improving the yields of a few specific metabolites, after manipulation of the expression and regulation of certain BGCs (Scherlach & Hertweck, 2009a; Selegato & Castro-Gamboa, 2023).

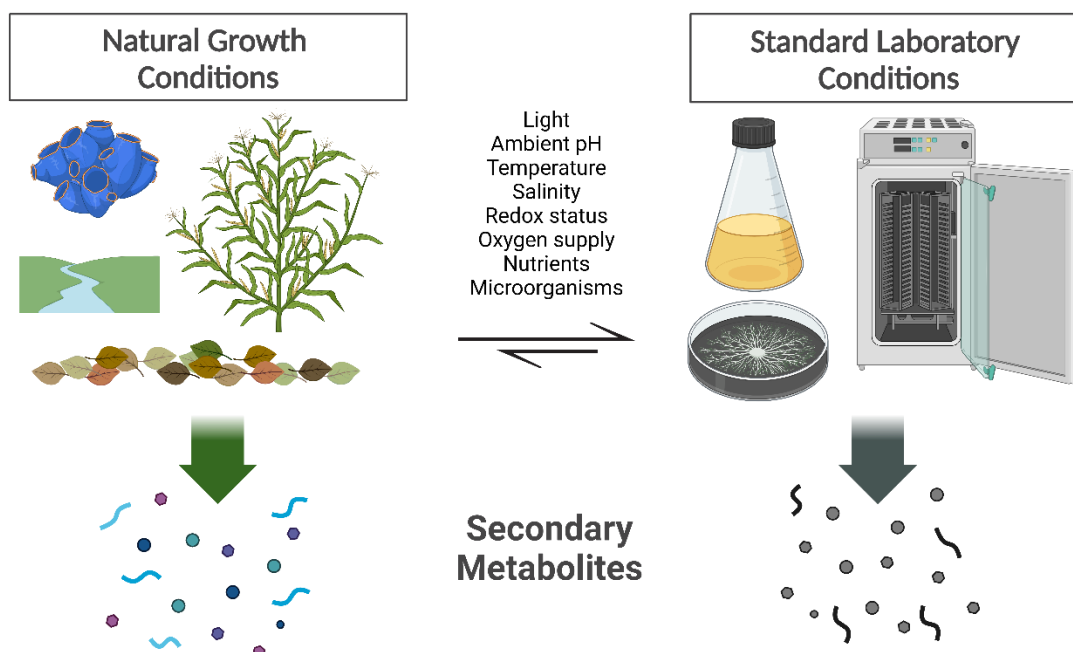


Figure 3. Differences between natural growth and standard laboratory conditions for fungi in terms of physical, chemical and interspecies cross-talk parameters involved in the production of fungal secondary metabolites. Figure adapted from Hautbergue et al., 2018.

Culture-based approaches can expand the chemical diversity without a direct manipulation of the genome. Many culture-based approaches have been proposed in recent years to unlock this cryptic biosynthetic potential encoded in fungal genomes, involving variations in **culture medium** compositions, **co-cultivation** with different microorganisms or **epigenetic** metabolism elicitation. In addition, the application of these approaches in combination with an increase in the **diversity** of species from the most diverse ecological and geographical areas, could also contribute to expand the chemical diversity obtained from fungal sources (Reyes et al., 2022).

3.1 Nutritional arrays and fermentation formats

The cultivation environment is one of the main factors that controls metabolite production. Fungi modulate the synthesis of SMs depending on their mechanisms of defense and/or environment colonization (Hautbergue et al., 2018). The term “**OSMAC**” (**One Strain-Many Compounds**) refers to how changes in growth conditions can significantly modulate metabolite production profiles in fungi. Variations in the culture parameters such as carbon and nitrogen sources, temperature, pH, salinity, light, aeration, or even the culture format set-up (static, shaken, liquid or solid) have proven to be successful strategies for the induction of new bioactive metabolites (Abdelwahab et al., 2018; Gakuubi et al., 2022; Scherlach & Hertweck, 2009; Wei et al., 2021). Even the quality of water used in the culture medium can alter the metabolite production in fungal strains (Paranagama et al., 2007).

Furthermore, numerous reports have demonstrated the importance of **nutrient sources** to induce the production of fungal SMs. The nutritional requirements of fungi to produce certain SMs are complex, diverse and specific for each strain. For example, Wiemann et al., 2009 demonstrated that nitrogen availability affected considerably the expression of 35 of the 40 gene clusters of *Fusarium fujikuroi*. Similarly, Scherlach & Hertweck in 2006 identified genes in the *Aspergillus nidulans* genome encoding for the synthesis of alkaloid precursors, which were not produced when the strain was cultured in a standard laboratory medium. However, fungal cultivation on rice medium led to the discovery of *aspoquinolones A-D*. Another example was reported by Hemphill et al., 2017, revealing the influence of fruit and vegetable juices as supplement of solid rice media to improve the production of bioactive metabolites by *Fusarium tricinctum*.

Besides the nutrient composition of media, **solid supports** are also commonly used to induce changes in chemical profiles. Previous studies have reported considerable metabolomic differences when microorganisms were grown in liquid vs. solid (Bader et al., 2021; Bigelis et al., 2006; Bills et al., 2012; Webb & Manan, 2017). Bigelis et al., in 2006 revealed that solid-state fermentations (SSF) of fungi clearly influenced growth, morphology and production of bioactive SMs of *Cylindrocarpon* sp. LL-Cyan426 and *Acremonium* sp., in comparison to their conventional liquid submerged fermentations (SmF). The use of SSF with fungi could bring them closer to their natural conditions, offering potential benefits for the metabolite production.

3.2 Epigenetic modulation by chemical elicitors

The activation of cryptic biosynthetic pathways is often controlled by epigenetic modifications of the chromatin structure that do not involve alterations in the DNA sequence (Toghueo et al., 2020; Xue et al., 2023). Several small molecule elicitors have been described with the ability to generate histone modifications that consequently have effects on the chromatin structure and modulate the expression of specific BGCs. Their mechanisms of action involve epigenetic regulation of chromatin by processes of acetylation, methylation, ubiquitination, phosphorylation, sumoylation, glycosylation, or neddylation (Hautbergue et al., 2018; Toghueo et al., 2020). Specifically, fungal BGCs are frequently located in distal regions of chromosomes in heterochromatin state, where gene transcription is regulated by reversible epigenetic modifications such as **histone acetylation** and **DNA methylation** (Toghueo et al., 2020) (Figure 4). Numerous inhibitors of histone

deacetylase (HDAC) and DNA methyltransferase (DNMT) have proven to be efficient tools to induce the production of fungal metabolites through the activation of silent or under-expressed BGCs involved in the biosynthesis of specific metabolites (Table 3).

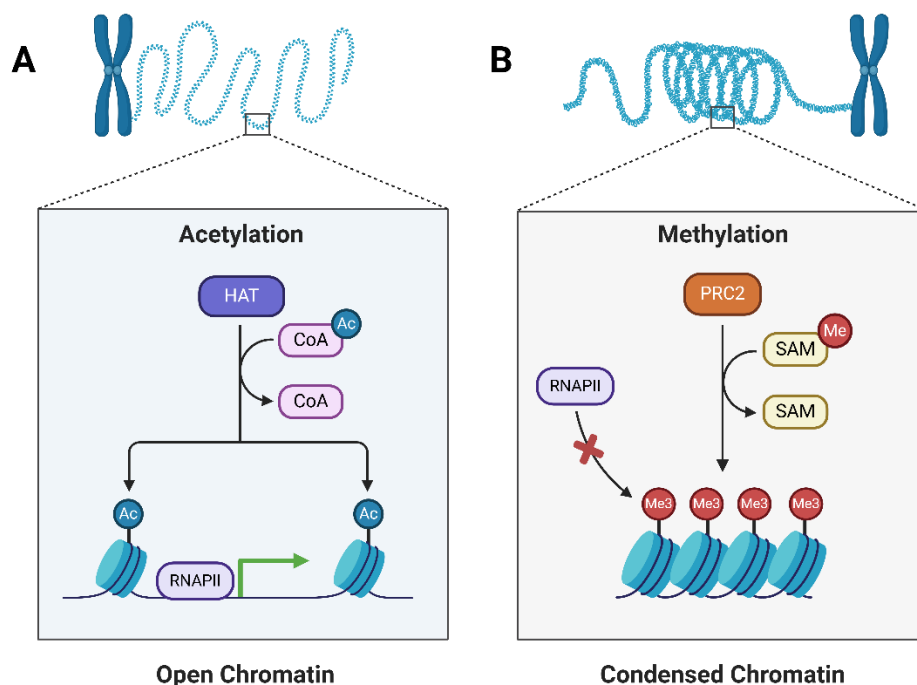


Figure 4. A) Histone acetylation is performed by Histone Acetyl Transferases (HATs) by using Ac-CoA as donor, opening the chromatin that allows the binding of RNA Pol II to a promoter to induce target gene expression. **B)** DNA methylation is performed by Polycomb Repressive Complex 2 (PRC2) by transferring a methyl group from S-adenosylmethionine (SAM) to cytosine, condensing the chromatin that inhibits the transcription by preventing RNA Pol II binding. Figure adapted from Scrivano, 2020 Biorender.

Furthermore, the use of epigenetic elicitors has also resulted in a significant enhancement of the production of some of the existing metabolites, that were poorly detected under normal growth conditions. Chen et al., in 2016 identified a significant increase in the production of *diethylene glycol phthalate ester monomers* and *oligomers* when the marine-derived *Cochliobolus lunatus* TA26-46 was grown with the DNMT inhibitor 5-azacytidine. (Siless et al., 2018) reported the use of SAHA and other HDAC inhibitors in a culture of *Drechslera* sp. to improve the production of *benzophenone*. In addition, the treatment of *Alternaria alternata* and *Penicillium expansum* with the HDAC inhibitor trichostatin A generated a considerable increase in numerous unidentified metabolites for both species (Shwab et al., 2007).

Among the wide variety of epigenetic elicitors, **Suberoylanilide Hydroxamic Acid (SAHA)** is one of the most frequently used inhibitors for inducing new bioactive metabolites in numerous epigenetic studies. The following metabolites were only produced when fungal strains were cultured with SAHA: *nygerone A* by *Aspergillus niger* (Henrikson et al., 2009); induction of several mycotoxins in

Introduction

Alternaria alternata (Sun et al., 2012); the anti-infective *cytosporones* by the marine fungus *Leucostoma persoonia* (Beau et al., 2012); (10'S)-*verruculide B*, *vermistatin* and *dihydrovermistatin* by *Phoma* sp. LG0217 (Gubiani et al., 2017); various bioactive *dihydroisocoumarins*, including five unknown brominated and two chlorinated compounds produced by *Lachnum palmae* (Zhao et al., 2018); production of *versiperol A*, *2,4-dimethoxyphenol* and *diorcinol* by *Aspergillus versicolor* (Zhu et al., 2019); and the two new natural *sclerotioramine* derivatives, *isochromophilone* XIV and XV, and two known compounds *sclerotioramine* and (+)-*sclerotiorin* induced in the insect-associated fungi *Penicillium mallochii* CCH01, being this last compound a potent inhibitor of phytopathogenic strains (Zhang et al., 2019).

Table 3. Examples of small molecule epigenetic elicitors that induced the production of diverse secondary metabolites in fungi.

Epigenetic elicitor	Mechanism of action	Fungal species	Induced compounds	References
5-azacytidine	Inhibition of DNMT	<i>Diatrype</i> sp.	lunalides A and B	Williams et al., 2008
		<i>Pestalotiopsis crassiuscula</i>	4,6-dihydroxy- 7-hydroxymethyl-3-methoxymethylcoumarin	Yang et al., 2014
suberoylanilide hydroxamic acid (SAHA)	Inhibition of HDAC	<i>Phoma</i> sp. LG0217	(10'S)-verruculide B, vermistatin, dihydrovermistatin	Gubiani et al., 2017
		<i>Microascus</i> sp.	EGM-556	Vervoort et al., 2011
suberohydroxamic acid (SBHA)	Inhibition of HDAC	<i>Fusarium oxysporum</i> f. sp. <i>conglutinans</i>	5-butyl-6-oxo-1,6-dihydropyridine-2-carboxylic acid, 5-(but-9-enyl)-6-oxo-1,6-dihydropyridine-2-carboxylic acid	Chen et al., 2013
SBHA + 5-azacytidine	Inhibition of HDAC & DNMT	<i>Pestalotiopsis acaciae</i>	prenyldepsides and methylcoumarins	Yang et al., 2013
nicotinamide	Inhibition of HDAC	<i>Chaetomium cancroideum</i>	chaetophenol G, cancrolides A and B	Asai et al., 2015
		<i>Penicillium brevicompactum</i>	<i>p</i> -anisic acid, <i>p</i> -anisic acid methyl ester, benzyl anisate, syringic acid, acetosyringone, sinapic acid, gentisaldehyde and <i>p</i> -hydroxy benzaldehyde	El-Hawary et al., 2018
sodium butyrate	Inhibition of HDAC	<i>Penicillium brevicompactum</i>	anthranilic acid, ergosterol peroxide	El-Hawary et al., 2018
valproic acid	Inhibition of HDAC	<i>Diaporthe</i> sp.	xylarolide A and B, diaportharine A	Sharma et al., 2018

Despite epigenetic elicitors clearly influence the fungal metabolite profiles, these treatments also have shown effect on the morphological characteristics of the fungal cultures. For example, when the strain *Hypoxylon* sp. CI-4A was exposed to SAHA and 5-azacytidine it showed variations in pigmentation and growth rates, in addition to significant differences in the bioactivities of the produced volatile organic compounds (Ul-Hassan et al., 2012).

Therefore, the use of these chemical elicitors is a simple, cost-effective and easily implementable approach that is emerging as a valuable tool in fungal biotechnology. Moreover, these processes could be combined with optimized culture conditions to improve the production of novel bioactive compounds.

3.3 Microbial interactions for metabolite induction

In natural environments, microorganisms are commonly living in microbial consortia, involving complex interactions between different organisms (Guo et al., 2024). Microbial interactions play a crucial role in communication or competition within the **microbial community**, that clearly influences their growth, morphology and development (Bertrand et al., 2014; Knowles et al., 2022). These interactions can be mediated by the production of metabolites/signals, through mechanisms of mutualism, commensalism, neutralism, competition, amensalism, parasitism and predation (Moody, 2014). Furthermore, biosynthesis of microbial SMs is tightly regulated by complex signaling cascades, where metabolic pathways are regulated by genes that can be influenced by external factors. For example, in competitive environments, microorganisms constantly interact with neighbors, competitors, and hosts, resulting in phenotypic and genotypic effects that ensure the survival of the microbial community (Moody, 2014; Selegato & Castro-Gamboa, 2023). Specific BGCs for certain metabolites that are silent in monocultures could be activated by interspecies communications which trigger the production of undiscovered molecules. Therefore, mining these microbial interactions could be a promising strategy to explore their untapped biosynthetic potential for producing novel bioactive compounds, as well as for identifying antagonistic strains.

Co-culturing techniques pursue to mimic *in vitro* the interaction conditions of natural habitats, where two or more microorganisms co-inhabit in a single confined environment and compete for resources (Abdelwahab et al., 2018; Nonaka et al., 2011; Wang et al., 2013). Microorganisms could sense the presence of other microorganisms, triggering an antagonist response that can involve morphological changes in confronted strains and stimulate the production of unique SMs (Hautbergue et al., 2018; Knowles et al., 2022). The co-culture approach has been described between bacteria-bacteria, fungus-fungus, bacteria-fungus, and even with microalgae (Alanzi et al., 2023; Leng et al., 2021). Microbial co-culturing has been broadly applied to improve biochemical processes in industrial sectors, such as the fermentation processes to enhance flavour profiles and production of biofuels, biomaterials, and other products (Bader et al., 2010; Guo et al., 2024). More interestingly, several works have reported the discovery of new bioactive microbial NPs by co-culture approaches that have been used in the treatment of different diseases. For example, Oh et al. in 2007 showed that the co-culture of the marine-derived fungus *Emericella* sp. and actinomycete *Salinispora arenicola* induced the production of *emicellamides A* and *B*, which present moderate antibiotic activity against methicillin-resistant *Staphylococcus aureus*. The common strategy to identify the induced compounds involves a comparison of the chemical profiles of mono- and co-culture extracts (Hautbergue et al., 2018). Thus, signals present in the co-culture, but absent in their mono-cultures, indicate the induction SMs specifically synthesized in response to the interaction between the two microorganisms (Figure 5).

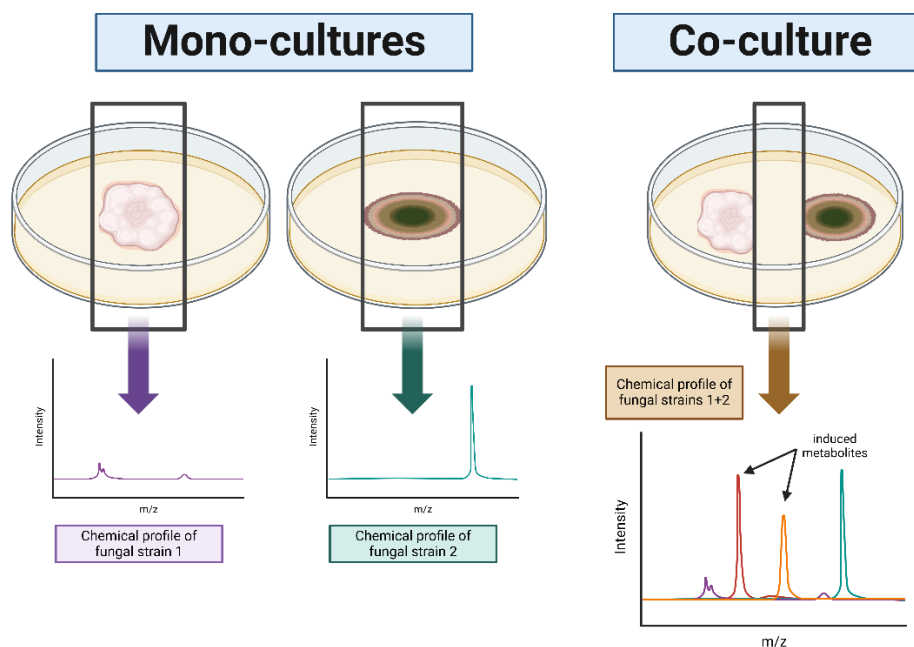


Figure 5. Co-culturing of two different fungal strains to promote the production of secondary metabolites. Chemical profiles from the mono- and co-cultures are analyzed to identify metabolomic changes.

The best known example of co-culturing was the discovery of *penicillin* by Alexander Fleming in 1929, as a result of the microbial interactions between *Penicillium notatum* and *Staphylococcus* sp., one of the most important scientific research in medicine. Another example of the effects of microbial interactions during co-culturing was the production of *bacillomycin D* and *fengycin*, when *Bacillus velezensis* was confronted with the fungus *Trichoderma* spp. The use of this microbial consortium has become a successful tool for the biological control of the *Fusarium* wilt (Izquierdo-García et al., 2020). Similarly, the co-culture of the endophyte *Paraconiothyrium* sp. with the bark fungus *Alternaria* sp. enhanced the *paclitaxel* production. More interestingly, the addition of another community member to the co-culture (*Phomopsis* sp.) led to an eight-fold increase in the production of *paclitaxel* (Soliman & Raizada, 2013). Table 4 summarizes additional studies which have also described the improvement of metabolite production and/or the induction of new SMs by microbial interactions during co-culturing.

Therefore, the implementation of this technic has proven to be a promising tool to stimulate the fungal biosynthetic potential, triggering the expression of cryptic BGCs that are silent when individual fungi are cultured alone, as well as to identify antagonistic strains against a target pathogen.

Table 4. Examples of compounds identified from microbial interactions during microbial co-culturing.

Compound	Co-cultured microorganisms	Reference
acremostatins A-C	<i>Acremonium</i> sp. & <i>Mycogone rosea</i>	Degenkolb et al., 2002
aspergicin	<i>Aspergillus</i> sp. & <i>Aspergillus</i> sp.	Zhu et al., 2011
austin	<i>Talaromyces purpurogenus</i> & <i>Phanerochaete</i> sp.	Do Nascimento et al., 2020
cyclo-(L-leucyl-trans-4-hydroxy-L-prolyl-D-leucyl-trans-4-hydroxy-L-proline)	<i>Phomopsis</i> sp. & <i>Alternaria</i> sp.	Li et al., 2014
5-epi-pestafolide A	<i>Trichocladium</i> sp. & <i>Bacillus subtilis</i>	Tran-Cong et al., 2019
fumicycline A	<i>Aspergillus nidulans</i> & <i>Streptomyces rapamycinicus</i>	König et al., 2013
2-heptyl-4-hydroxyquinolone, henazine-1-carboxylic acid, Phenazine-1-carboxamide	<i>Pseudomonas aeruginosa</i> & <i>Fusarium tricinctum</i>	Moussa et al., 2020
hydroxylated O-methylmelleins	<i>Eutypa lata</i> & <i>Botryosphaeria obtusa</i>	Glauser et al., 2009
4-hydroxysulfoxy-2-dimethyltelavin P	<i>Trichophyton rubrum</i> & <i>Bionectria ochroleuca</i>	Bertrand et al., 2013
ibomycin	Actinomycete WAC2288 & <i>Cryptococcus neoformans</i>	Robbins et al., 2016
macrocarpon C, 2-(carboxymethylamino) benzoic acid, (-)-citreoisocoumarinol	<i>Fusarium tricinctum</i> & <i>Bacillus subtilis</i>	Ola et al., 2013
nigrolactone, multiplolide B, 15α-diol	<i>Nigrospora</i> sp. & <i>Stagonosporopsis</i> sp.	Chen et al., 2022
11-O-methylpseurotin A₂	<i>Aspergillus fumigatus</i> & <i>Streptomyces bullii</i>	Rateb et al., 2013
oosponol, oospoglycol, melledonal A & C	<i>Gloeophyllum abietinum</i> & <i>Heterobasidion annosum</i>	Sonnenbichler et al., 1994
orsellinic acid	<i>Aspergillus nidulans</i> & <i>Streptomyces rapamycinicus</i>	Nützmann et al., 2011
soudanone A & E, (3R)-soudanone D, isochromanones	<i>Cosmospora</i> sp. & <i>Magnaporthe oryzae</i>	Oppong-Danquah et al., 2022
stemphyperyleneol, alterperyleneol	<i>Alternaria tenuissima</i> & <i>Nigrospora sphaerica</i>	Chagas et al., 2013

4. METABOLOMIC TOOLS FOR CHEMICAL ANALYSES

The discovery of new bioactive compounds from microbial sources requires valuable metabolomic technologies to allow us to study the chemical composition of these complex biological systems. Metabolomics studies are divided into targeted and untargeted approaches. **Targeted metabolomics** require prior knowledge of the molecule of interest, in order to design tailored analytical methods to evaluate the presence and content of this molecule in a complex sample. Dereplication analysis is a critical step in NP discovery to avoid the rediscovery of known compounds and guide the analysis of undescribed molecules. In general, MEDINA dereplication processes start with Liquid Chromatography Low Resolution Mass Spectrometry (LC-LRMS) analyses, that allow to compare retention time, ultraviolet signal, positive and negative mass data of every component present in the sample with the MEDINA's internal database of known NPs (Pérez-Victoria et al., 2016). Then, Liquid Chromatography High Resolution Mass Spectrometry (LC-HRMS) provides an accurate mass and predicted molecular formulae, that can be combined with the taxonomic information of the producer to facilitate the identification of compounds in commercial and public databases such as Chapman & Hall Dictionary of Natural Products (DNP) and the Natural Products Atlas (Pérez-Victoria, 2024). In addition, the characterization of new molecules requires valuable efforts regarding scale-up fermentations, whole broth extractions, solvent partition, low and high-pressure chromatographic purifications, and finally, structural elucidation by Nuclear Magnetic Resonance (NMR) combined with additional Mass Spectrometry (MS) with molecule fragmentation. Bio-guided purifications are commonly implemented in the identification of microbial metabolites. This method involves recurrent fractionations steps to isolate the active molecule. Nevertheless, this approach requires the integration of an activity evaluation platform for a rapid identification of bioactive fractions with a targeted biological effect.

However, **untargeted metabolomics** employ early data-mining strategies aimed at detecting as many metabolites as possible in a sample, in order to determine trends and prioritize conditions (Figure 6) (Alarcon-Barrera et al., 2022; Martínez et al., 2017). Liquid Chromatography Mass Spectrometry (LC-MS) is the technique of choice in metabolomic studies because it provides complex information, with a fast and robust sensitivity to detect a wide range of metabolites. This method allows a comprehensive evaluation of several hundreds of molecular species within a single analysis, making it an excellent technology for improving early dereplication steps in NP research (Alarcon-Barrera et al., 2022; Hautbergue et al., 2018).

Technological advances in LC-MS and big data analyses have significantly increased the number of untargeted metabolomics studies and different applications in NP research. Kang et al., in 2011 analyzed the SMs of seven species of *Trichoderma* using the genomic and metabolomic data to develop a chemotaxonomic identification of fungal strains. They found that the chemical taxonomy based on SMs was more accurate than its genome sequence and identified a previously unknown group of *Trichoderma*. Moreover, metabolomics can explain how fungi respond to stress through chemical evaluation of their changes in endogenous metabolite production. For example, Miura et al., in 2004 studied the white rot basidiomycete *Phanerochaete chrysosporium* under air ambient and 100% oxygen, resulting in the identification of three metabolites associated with the oxygen stress response: *veratryl alcohol* (VA), *threonate*, and *erythronate*. Elevated levels of reactive oxygen species (ROS) could directly activate the VA synthesis, which increased directly the intracellular oxygen concentration, while the resistance of *threonate* and *erythronate* to hyperoxia involved a

progressive accumulation process. Moreover, untargeted metabolomic analyses are optimal methods for screening hundreds of NPs simultaneously for dereplication studies, identification of bioactive compounds, discovery and relative quantification of unknown metabolites (Li et al., 2022).

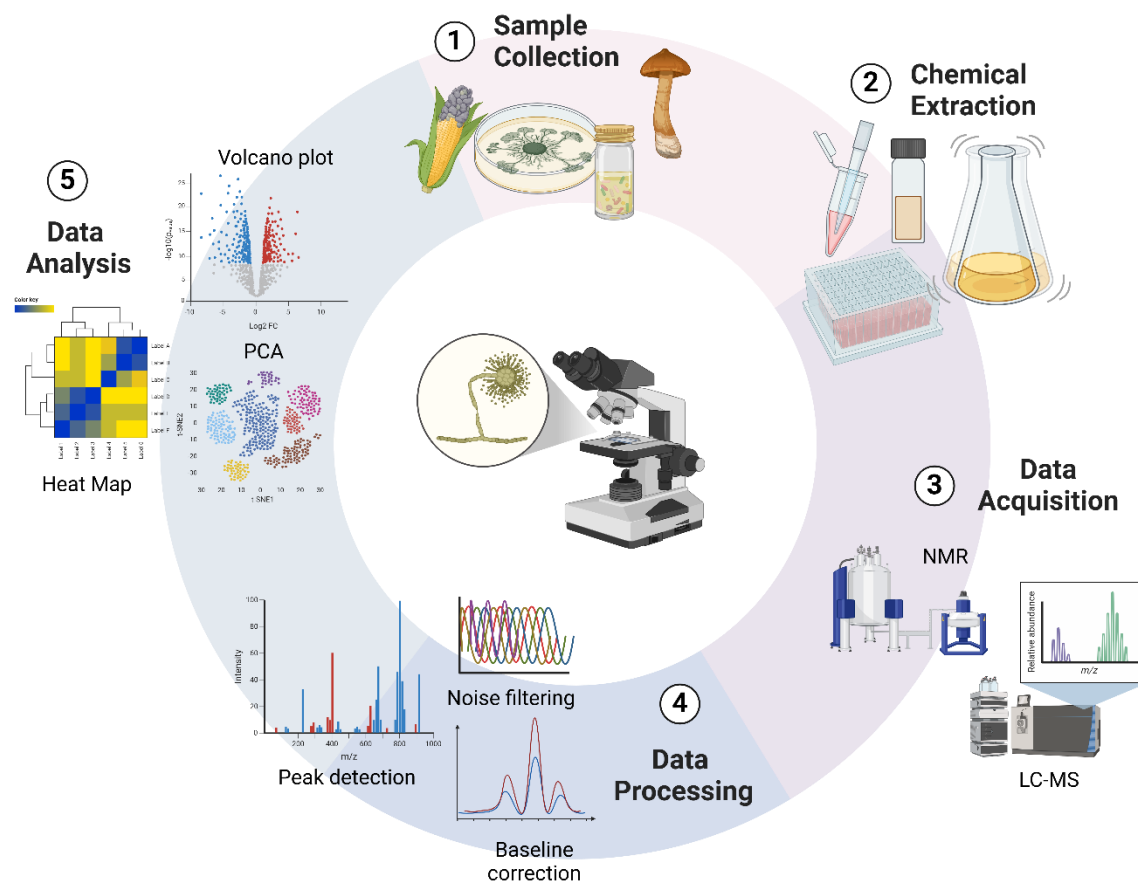


Figure 6. General workflow of analytical methods implemented in untargeted metabolomics applied to fungal metabolite studies.

Untargeted metabolomics can generate large datasets with hundreds of MS spectra per experiment, leading to the development of computational tools that help in data mining (Hautbergue et al., 2018; Li et al., 2022). Specifically, **MASS Studio** is a software developed at MEDINA that allows a metabolomic evaluation of the chemical diversity of samples in the context of NP research (Martínez et al., 2017). This software simplifies the complexity of LC-MS data when comparing thousands of samples by collapsing the time dimension and keeping the mass signal information. The resulting metabolomics data matrixes can be analyzed with any multivariate statistical analysis software such as BioNumerics® to identify significant trends. MASS Studio offers various applications in metabolomics, such as the evaluation of chemical diversity of microbial NP Libraries and relative quantification of metabolites, which allows the prioritization of strains, fermentation conditions or metabolites of interest.

5. HIGH-THROUGHPUT-SCREENING PLATFORMS FOR BIOACTIVITY EVALUATION

Historically, microbial NPs have been the most relevant source for bioactive compounds, especially for antimicrobial compounds. The complexity of NP extracts and fractions have led to the development of a variety of compatible screening approaches to test their antimicrobial potential, from the phenotypic whole-cell growth inhibition tests with wild type strains grown on agar plates to cell-free biochemical assays looking for a specific mechanism of action (Miethke et al., 2021; Singh et al., 2011). Whole-cell growth inhibition assays are major approaches for the identification of antifungal agents against phytopathogens, being agar dilution and disc diffusion assays on Petri dishes the most common methodologies (Huang et al., 2018; Jiménez et al., 2011; Yang et al., 2012). These traditional methods are laborious, time-consuming, have limited reproducibility, and require large quantities of test material, making unsuitable their automation for large High-Throughput Screenings (HTS) (Rampersad, 2011).

The pharmaceutical industry introduced **HTS agar-based assays** for antifungal drug discovery, that fixed some of the issues associated with traditional and manual agar tests (Bills et al., 2008; De La Cruz et al., 2012). A HTS methodology based on agar assays in microplates and an automated imaging system was developed to identify antifungal agents against target fungal pathogens such as *Candida albicans*. This agar method recorded and measured automatically the zones of inhibition (ZOIs) generated by active samples using an image analysis, which significantly reduced the time required to obtain results, opposed to traditional agar tests that required manual measurements. However, this type of HTS still exhibits drawbacks such as the fusion of closely located ZOIs that hinders the hit selection, and the limitations in accurate identification of intermediate sensitivity to specific samples (density of ZOIs) (Bills et al., 2008; Rampersad, 2011).

Alternatively, the **microdilution method** has been extensively applied in fungal inhibition studies. This methodology provides several advantages related to simplicity, reliability, time and cost-effectiveness, and could be scalable for large number of samples, which makes it ideal for screening campaigns. Numerous reports have described the development of microdilution assays based on methodologies using colorimetric dyes such as resazurin or the tetrazolium salts MTT, XTT and MTS. **Resazurin** is the preferred redox dye to measure cell proliferation, viability, and cytotoxicity of various cell types in medical research (Chadha & Kale, 2015; Monteiro et al., 2012; Rampersad, 2011). This dye shows a non-fluorescent blue color that turns fluorescent pink when is reduced to resorufin by mitochondrial enzymes, by accepting the electrons from cytochromes, NADH, FADH, NADPH. This change in color can be easily visualized and precisely measured in a spectrophotometer, reducing time costs (Figure 7).

Therefore, these colorimetric assays are useful tools for the development of HTS antifungal platforms. A clear example is the HTS developed for antifungal drug discovery against the human pathogen *Aspergillus fumigatus* (Monteiro et al., 2012). In addition, few reports have described HTS methods based on colorimetric microdilution assays to be applied in new fungicide discovery against different plant pathogens: *Botrytis cinerea* (Pelloux-Prayer et al., 1998), *Verticillium dahliae* (Rampersad, 2011), *Alternaria alternata* (Vega et al., 2012) and *Magnaporthe oryzae* (Chadha & Kale, 2015). However, fluorescence of resazurin can be easily affected by colored or fluorescent molecules present in NP extracts, challenging the identification of hits from microbial samples which contain complex mixtures of compounds (Wilson et al., 2020). Therefore, appropriate

screening methods to study the antifungal activity of microbial resources are required for the discovery of the next-generation of fungicides.

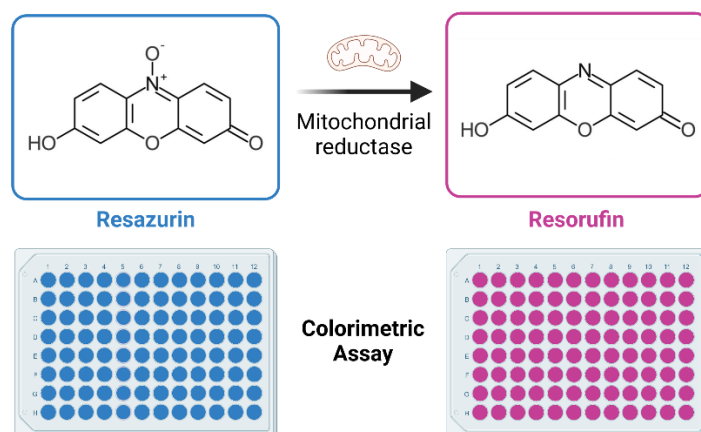


Figure 7. Scheme of the colorimetric reaction of resazurin (blue color) into resorufin (fluorescent pink color) mediated by mitochondrial reductase enzymes, as indicative of metabolic activity and cell viability.

6. FUNGAL PLANT PATHOGENS

Plant pathogens are a broad and phylogenetically diverse group of microorganisms responsible for a variety of serious plant diseases (Jayawardena et al., 2021; Pandit et al., 2022; Sharma, 2021). The Food and Agriculture Organization of the United Nations (FAO) estimates that plant diseases cost around US\$220 billion per year, corresponding to 20-40% of losses in global crop production (“Pathogens, Precipitation and Produce Prices”, 2021; Savary et al., 2019). Fungal phytopathogens are widely distributed and can infect numerous cereal crops, vegetables and fruits through various mechanisms of pathogenesis, generating the most important damage in worldwide agriculture. Phytopathogenic fungi have developed specialized and highly regulated infection strategies, ranging from the generation of structures such as appressoria and haustoria for penetrating plant tissues, to the production of enzymes, toxins and growth regulators to modulate the plant metabolism (Leiva-Mora et al., 2024; Sharma, 2021). Traditionally, fungal plant pathogens are divided into two main groups: **necrotrophs** such as *Botrytis cinerea*, that can induce the death of plant tissues and subsequently feed on the necrotic material by secreting toxins; and **biotrophs** such as *Puccinia graminis* f. sp. *tritici*, that can colonize living tissues by producing effector molecules to suppress cell death and manipulate the plant response. Both types of pathogens produce enzymes that degrade the carbohydrate polymers in plant cell walls which weaken the primary defenses of plants (Fillinger & Elad, 2016). Furthermore, there is another group of **hemibiotrophic** pathogens, such as *Colletotrichum* spp., which start the colonization as biotrophs and then switch to become necrotrophs.

Most fungal phytopathogens belong to the *Ascomycota* and the *Basidiomycota* classes. Based on their scientific and economic importance, the top ten phytopathogenic fungi have been listed in the following order by (Dean et al., in 2012): (i) *Magnaporthe oryzae*, (ii) *Botrytis cinerea*, (iii) *Puccinia* spp., (iv) *Fusarium graminearum*, (v) *Fusarium oxysporum*, (vi) *Blumeria graminis*, (vii) *Zymoseptoria tritici*, (viii) *Colletotrichum* spp., (ix) *Ustilago maydis* and (x) *Melampsora lini*. The first position of the ranking corresponds to (i) ***Magnaporthe oryzae*** due to the economic impact of its damage on rice crops, one of the major global basic foods. Additionally, *M. oryzae* and *M. grisea* are the main causal agents of rice blast disease, considered the most destructive infection that generates losses up to 100% of production (Dean et al., 2012; Kohli et al., 2011). Secondly, (ii) ***Botrytis cinerea*** is responsible for the grey mold in numerous plants by using a broad range of pathogenic factors: lytic enzymes, activated oxygen forms, toxins and plant hormones (Fillinger & Elad, 2016; Couderchet, 2003). *B. cinerea* is considered the most important post-harvest decay pathogen of fresh fruits and vegetables. The costs of damage caused by this phytopathogen are incalculable worldwide, specifically for the wine sector in the use of botryticides in vineyards. The genus (iii) ***Puccinia*** is responsible for causing three types of rust diseases in *Triticum aestivum*, primarily carried out by three species *P. graminis*, *P. striiformis*, and *P. triticina*, which poses severe impact to the wheat productions (Dean et al., 2012). In the fourth and fifth positions of the ranking are species of the genus ***Fusarium***. *Fusarium* sp. belongs to a ubiquitous group of fungi that has been extensively studied not only for causing the two major diseases of wheat (*Fusarium* head blight and *Fusarium* crown rot), but also for producing numerous mycotoxins that contaminate the grain harvested and cause potential risk to human and animal health. (iv) *Fusarium graminearum*, (v) *Fusarium oxysporum*, and *Fusarium proliferatum* can infect a broad range of crops such as maize, wheat, rice, soybean, barley, fruit, and even ornamental plants, where the most significant damage is root rot (Arias et al., 2013). (vi) ***Blumeria graminis*** is the causal agent of powdery mildew in barley and wheat crops and is considered a high-risk pathogen because of its ability to change its virulence (Lalošević et al., 2021). Following, (vii) ***Zymoseptoria tritici*** is responsible for one of the most important wheat diseases (septoria leaf blotch), with a high percentage of infection that generates significant damage (Ababa, 2023). In the eighth position is the genus (viii) ***Colletotrichum*** sp., one of the most common and important genera of phytopathogenic fungi, which promotes the anthracnose disease in more than 3,000 plants, leading considerable losses of fruits and vegetables (da Silva et al., 2020). In Spain, the species *C. acutatum* and *C. gloeosporioides* represent a severe problem for the olive oil sector, responsible for soapy olive effects (Oliveira et al., 2005; Rouhma et al., 2010). Otherwise, (ix) ***Ustilago maydis*** is a homobasidiomycete that normally infects maize through a complex pathogenic process, including morphogenetic transitions until complete its sexual cycle, placed on the ninth position (Méndez-Morán et al., 2005). Finally, (x) ***Melampsora lini*** is responsible for the rust disease on *Linum usitatissimum*, which causes severe losses in seed yields, as well as fiber quality reduction in flax plants (Lawrence et al., 2007).

Most fungal diseases of plants are efficiently managed through the application of a great variety of synthetic agrochemicals (Table 5). However, the indiscriminate use of these synthetic fungicides during the last decades has promoted undesirable consequences, which have generated important hazards to the health of humans, animals, and the environment (Zaker, 2016). Frequent use of pesticides and fertilizers can lead to the pollution of soil and water, ecological imbalances, and potential toxicity to humans and other organisms. Moreover, the use of fungicides has led to the emergence of pathogens with multiple fungicide resistances, which further complicated the

management of the diseases (Xu et al., 2021). Today, there are strict regulations on chemical pesticide use and there is a political pressure to remove the most hazardous agrochemicals from the market. Therefore, the challenge nowadays is to develop new and eco-friendly alternatives for the safe control of these pathogens, which pose low risk to human health and the environment.

Table 5. Examples of synthetic agrochemicals used for the control of fungal plant diseases (Fillinger & Elad, 2016).

Mode of action	Common name	Selected trade names
Multisite	folpet	Folpan
	thiram	Pomarsol, Thiram
	chlorothalonil	Fongistop
Respiration	azoxystrobin	Amistar, Heritage
	pyraclostrobin	Pristine
	boscalid	Endura, Cantus, Pristine
	fluopyram	Luna privilege
Cystoskeleton	carbendazim	Bavistin, Derosal
	diethofencarb	Sumico, Jonk
Osmoregulation	iprodione	Kidan, Rovral
	fludioxonil	Geoxe, Switch
Cid synthesis	cyprodinil	Switch
	pyrimethanil	Scala
Sterol synthesis	prochloraz	Octave, Sportak
	tebuconazole	Horizon
	fenhexamid	Teldor, Lazulie
	fenpyrazamine	Prolectus

Biological control of plant diseases has been considered a viable alternative method to manage phytopathogen infections. Biological control is defined as the inhibition of growth, infection or reproduction of one organism by its natural enemies. This term includes the use of microbial antagonists or products extracted or fermented from various natural sources, to suppress the disease. Furthermore, these NPs should have minimum adverse effects on the physiological processes of plants, they are easily convertible into common eco-friendly organic materials and are generally assumed to be more tolerant and less hazardous for the ecosystems (Chuang et al., 2007; Gnanamanickam, 2002).

The most common Biocontrol Agents (BCAs) are usually fungi or bacteria isolated from the phyllosphere, endosphere or rhizosphere, which can exhibit direct or indirect mechanisms of action to control the pathogen. These mechanisms include (i) **antibiosis** where an inhibitory metabolite is produced by the antagonist; (ii) **mycoparasitism** where the antagonist derives nutrients from the fungal host, (iii) **induced resistance** where microorganisms induce plant defense responses against phytopathogens, and (iv) **growth enhancement** where BCAs promote plant growth through

the production of microbial hormones such as indoleacetic acid and gibberellic acid (Fillinger & Elad, 2016; Rodrigo et al., 2021; Zabalgoitia, 2008). Secretion of extracellular hydrolytic enzymes, competition for space and nutrients between organisms and detoxification of virulence factors are among the actions involved in biological disease control (Heydari and Pessarakli, 2010; Chandrashekhara et al., 2012; Singh, 2014; Zhang et al., 2014; Deketelaere et al., 2017).

The term **biopesticide** refers to preparations that are based on living microorganisms and substances of natural origin, including plant and microbial extracts, minerals, and organic compounds (Fillinger & Elad, 2016). The strategy consists of applying NPs to control plant diseases without affecting the ecological environment. There are currently 390 biochemical and microbial active ingredients registered as biopesticides by USA Environmental Protection Agency (EPA) (Koul, 2023). Moreover, the global market is expected to grow significantly in the coming years in demand for sustainable agricultural practices. Specifically, biopesticides derived from microorganisms are gaining the attention of many researchers due to their lower toxicity and costs. Major commercial biopesticides in the current market correspond to microbial strains (Table 6). However, in some cases it is not necessary that microorganisms are alive in the product due to the presence of secondary metabolites, which generate the inhibition of the pathogens (Serenade® Max containing *agrastatins* and Companion® containing *iturins*).

Furthermore, the use of BCAs for controlling plant diseases also presents some limitations such as their variability of effects, regulatory constraints, and they are usually difficult to import into new regions due to concerns around exotic organism introductions (T. R. Glare et al., 2016). Therefore, the use of their **active metabolites** might be a promising strategy for the development of new bio-fungicides. Moreover, microbial SMs produced by fermentation processes can be optimized and scale-up to reduce costs. In general, regulations of the use of microbial SMs are similar to their synthetic equivalence, making them easier to incorporate in current pest management program regulations (T. R. Glare et al., 2016).

Several studies have focused on the chemical composition of bioactive microorganisms to biocontrol phytopathogens, in contrast to the use of the whole organism. For example, *griseofulvin* and *dechlorogriseofulvin* isolated from various species of fungi, including endophytic strains of *Penicillium canescens* and *Xylaria* sp., demonstrated direct inhibitory effects against diverse phytopathogens: *Botrytis cinerea*, *Blumeria graminis*, *Colletotrichum orbiculare*, *Corticium sasakii*, *Didymella bryoniae*, *Magnaporthe grisea*, *Sclerotinia sclerotiorum* (Park et al., 2005; Wang et al., 2010). Similarly, compounds such as *sterols*, have shown antifungal activity against *Bipolaris sorokiniana*, a common root rot pathogen of wheat and barley crops (Lu et al., 2000). In addition, *epoxycytochalsin H* and *cytochalsins N* and *H* were obtained from the endophyte *Phomopsis* sp., and exhibited potent inhibition of *Bipolaris sorokiniana*, *B. maydi*, *Botrytis cinerea*, *Rhizoctonia cerealis*, *Sclerotinia sclerotiorum* and *Fusarium oxysporum* (Jing et al., 2011). Finally, the family of bioactive compounds *strobilurins*, first identified from the culture of the basidiomycete *Strobilurus tenacellus*, have played a key role in the development of the β -methoxyacrylate class of relevant agricultural fungicides (Niego et al., 2023).

Most of those natural compounds act as specific inhibitors of fungal cellular or metabolic processes to inhibit the growth of the pathogen. Therefore, the development of new microbial NPs fungicides represents a promising tool to manage and control agricultural destructive fungal diseases.

Table 6. Commercial biopesticides based on microorganisms for the management of plant diseases. Based on (Fillinger & Elad, 2016).

Active Ingredient	Product	Mode of Action	Company
<i>Melaleuca alternifolia</i>	Timorex Gold ®	Antifungal	STK Stockton Group
<i>Reynoutria sachalinensis</i>	Regalia ®	ISR	Marrone Bio Innovations
<i>Ampelomyces quisqualis</i>	AQ10 ®	Fungicide	Ecogen Inc
<i>Psuedozyma flocculosa</i>	Sporodex L	Competition	Plant Products Co.
<i>Aureobasidium pullulans</i> strains 14940/14941	Botector ®	Competitive exclusion	Bio-ferm
<i>Bacillus amyloliquefaciens</i>	Double Nickel 55WDG/LC™	Antimicrobial	Certis USA
<i>B. subtilis</i> QST 713	Serenade ® Max	Antimicrobial (agrastatins), induction of plant defences	Bayer Crop Science
<i>B. subtilis</i> GB03	Companion ®	Antibiosis (iturins), ISR	Growth Products
<i>B. megaterium</i>	Bio Arc	Enzymatic action	Sphere Bio-Arc PVT Ltd
<i>Candida oleophila</i>	Aspire	Competition	Ecogen Inc
<i>Chlonostachys rosea</i>	Endofine ®	Competition	Adjuvants Plus
<i>Fusarium oxysporum</i> (non-pathogenic)	Fusaclean & Biofox C	Competition	SIAPA & Natural Plant Protection
<i>Gliocladium catenulatum</i> J1446	Prestop ®	Competition, hyperparasitism	Verdera Oy
<i>Paraphaeosphaeria minitans</i>	Contans WG; KONI	Competition	Prophyta Biologischer Pflanzenschutz GmbH
<i>Phebiopsis gigantea</i>	Rotstops ®	Antifungal (phlebiopsins)	Kemira Agro Oy
<i>Pseudomonas syringae</i> ESC-10	Bio-save ®	Competition	Jet Harvest Solutions
<i>Streptomyces griseoviridis</i> K61	Mycostop ®	Competition	Verdera Oy
<i>S. lydicus</i> WYCD108	Actinovate ®	Competition, antibiosis	Novozymes
<i>Trichoderma atroviride</i> LC52	Sentinel ®	Competitive exclusion	Agrimm Technologies Ltd
<i>T. harzianum</i> + <i>T. polysporum</i>	Binab TF	Antibiosis, SAR	BINAB Bio-Innovation AB
<i>T. harzianum</i>	RootShield ® & Trichodex ®	Competition	Bioworks Inc & Makhteshim Agan Industries
<i>T. virens</i>	Soilgard ®	Competition	Certis
<i>T. viride</i>	<i>Trichoderma Viridae</i> Trieco	Competition	Ecosense
<i>Ulocladium oudemansii</i>	Botryzen ®	Competitive exclusion	Botryzen NZ Ltd
Mineral oils	Neem oil Trilogy ®	Fungicidal	Certis USA
Paraffinic oil	JMS Stylet Oil ® & Suffoil-X ®	Fungistatic	JMS Flower Farms Inc & Bioworks
Thyme oil	Promax™	Fungicidal	Bio Huma Netics Inc

^aISR Induced systemic resistance, SAR Systemically acquired resistance

7. CURRENT STATUS OF NATURAL PRODUCT-BASED FUNGICIDES

Synthetic fungicides are the preferred strategy for managing plant diseases, but their continuous use generates severe damage to environmental and human health. Therefore, there is an urgent need to develop safe and efficient next-generation of fungicides based on natural resources (Späth & Loiseleur, 2024). To date, the use of living microorganisms is considered the strategy of choice to control fungal infections because of their numerous advantages. Several commercial products are in the market as biopesticides. However, biocontrol through microbial agents also presents impediments, mainly related to loss of efficiency. Therefore, numerous studies are focused on the chemical components of the bioactive extracts obtained from the biocontrol microorganism, instead of on the use of the whole organism.

Microbial NPs are valuable sources of novel chemical structures with diverse biological activities, which has generated an interest in the discovery of crop protection products. Xu et al., in 2021 summarized a total of 132 metabolites isolated from fungal endophytes in the past two decades, with moderate and potent antifungal activities against fungal phytopathogens, that could be considered candidates for the development of natural agrochemicals. Furthermore, the discovery of novel NPs also can inspire innovative solutions to transform them into optimized products for agriculture (Späth & Loiseleur, 2024). For example, the *strobilurins* were inspired by the natural fungicide derivatives of β -methoxyacrylic acid, and are one of the most important classes of agricultural fungicides (Bartlett et al., 2002; Niego et al., 2023). Therefore, chemical exploration of NPs Libraries might lead the efforts to develop new strategies for crop protection.

The discovery of novel NP fungicides requires a multidisciplinary approach, starting with the isolation and characterization of microbial strains with the potential to produce bioactive SMs, followed by innovative analytical techniques for metabolomics and HTS methods for an accurate evaluation of bioactivity. Fungi could be an important source of new fungicide agents because of their great biosynthetic potential encoded in their genomes (Zhang et al., 2024). Despite this biosynthetic richness, 80% of the fungal secondary metabolome remains unknown, but numerous culture-based approaches such as variations in culture media, the use of epigenetic elicitors, and the co-cultivation with different microorganisms have proven to be efficient strategies to expand fungal chemical diversity (Hautbergue et al., 2018). Furthermore, advances in untargeted metabolomics facilitate studying fungal metabolome and the selection of strains, culture conditions or compounds of interest. The development of new methodologies to evaluate the inhibition effects of fungal metabolites in an efficient and robust manner, as well as the correct selection, are crucial to identify potential candidates for further characterization as novel next-generation fungicides.

II. Objectives

Fungi represent one of the most prolific sources of novel secondary metabolites (SMs) with a great variety of biological activities, and one of the major potential reservoirs of novel Natural Products (NPs). However, the challenge remains to activate the large biosynthetic potential encoded in their genomes, which could lead to the discovery of novel compounds with relevant biological and industrial importance.

Therefore, the general objective of this work was to study the **activation of silent biosynthetic pathways by different culture-based approaches across a wide biodiversity of fungal strains, and their chemical and bioactivity evaluation**, with the aim of **expanding the fungal metabolite diversity and discovering novel fungicide molecules against relevant fungal phytopathogens**. Accordingly, the following specific objectives were established:

1. Study of fungal **co-cultivation on agar plates** using the fungal phytopathogen *Botrytis cinerea* CBS 102414 as a model system against a wide ecological and taxonomical set of fungi to identify **antagonistic strains**, evaluating the potential of **fungal interactions** to determine metabolomic changes in the **production of bioactive SMs**.
2. Design specific **nutritional arrays in liquid and solid conditions** to exploit the metabolomic potential of fungal strains isolated from leaf-litter samples collected in South Africa.
3. **Untargeted metabolomics** to assess the effects generated by the presence of **suberoylanilide hydroxamic acid (SAHA) on nutritional arrays** to induce the production of novel fungal SMs.
4. Implement of a **High-Throughput Screening (HTS) Platform** of assays against four relevant **fungal phytopathogens** based on agar-based and liquid microdilution methods, to improve the activity evaluation of fungicides.
5. Application of the HTS Platform to assess the **antifungal potential** of the generated fungal extract library against a panel of four **fungal phytopathogens**.
6. Build a proof of concept pipeline for the identification of **novel fungal bioactive molecules** as potential new fungicide agents to control plant diseases, among the hits detected in the HTS campaigns.

III. Results

This research work describes the implementation of different strategies that were developed to enhance the expression of the large biosynthetic potential encoded in the genomes of a wide biodiversity of fungi, and the development of new methods to evaluate their potential applications in the discovery of novel bioactive molecules. The results of this Thesis correspond to four scientific publications that compile the work developed, with the aim of expanding the access to fungal chemical potential and to identify new fungicide agents against relevant phytopathogens.

Chapter 1 focused on the work described in manuscript **“Co-culturing of fungal strains against *Botrytis cinerea* as a model for the induction of chemical diversity and therapeutic agents”**. In this study I co-cultivated on agar plates a selection of 762 fungal strains with a broad ecological and taxonomical diversity, to study fungal interactions and to identify potential inhibitors of the phytopathogen *Botrytis cinerea* CBS 102414. Furthermore, interaction zones from the positive antagonisms revealed a clear communication between co-cultured strains, that generated important alterations in their metabolomic expression. Results confirmed the effectiveness of the co-culturing method on agar plates in activating the expression of fungal biosynthetic gene clusters (BGCs) encoding bioactive metabolites, which remain silent in axenic cultures.

However, the agar-based co-culturing technique on agar presented significant limitations for large scale production of induced novel bioactive molecules (*Phoma* sp. CF-090072 and *Skeletocutis amorphia* CF-190679). Therefore, subsequent efforts for the discovery of new bioactive fungicides were focused on a second strategy aimed to optimize culture-based approaches.

Given that the leaf-litter associated fungi were the most active group in the co-cultivation approach, I decided to further explore this group of fungi, focusing on their metabolomic potential to produce Secondary Metabolites (SMs). Chapter 2, entitled **“Metabolomic analysis of the chemical diversity of South Africa leaf litter fungal species using an epigenetic culture-based approach”**, describes the effects of a specifically designed OSMAC (One Strain Many Compounds) approach on a new selection of fungal strains isolated from leaf-litter collected in South Africa, one of the worldwide biodiversity “hotspots”. A total of 232 fungal strains were cultured in four liquid fermentation media (SmF) and one solid-state fermentation (SSF), in presence and absence of the epigenetic elicitor suberoylanilide hydroxamic acid (SAHA), to maximize the chances for inducing the production of new SMs. Here, I discuss the application of metabolomics algorithms highlighting the SSF as the most productive cultivation format. Furthermore, the incorporation of the epigenetic elicitor SAHA into the OSMAC approach additionally improved the chemical diversity identified in the nutritional array for the entire fungal population.

The great chemical diversity induced by the OSMAC approach was further studied for the discovery of new potential fungicide agents. For this purpose, a more rapid and effective approach than the agar-based methodology was optimized for the screening of Natural Product (NP) samples, as detailed in the Chapter 3 **“Development and validation of a HTS Platform for the discovery of new antifungal agents against four relevant fungal phytopathogens”**. The High-Throughput Screening (HTS) platform allowed to efficiently profile a wide variety of synthetic and natural compounds and mixtures using both agar-based and liquid microdilution assays. The resulting platform was validated as an efficient tool to facilitate the discovery of next-generation fungicides for the biocontrol of the plant pathogens *Botrytis cinerea*, *Colletotrichum acutatum*, *Fusarium proliferatum* and *Magnaporthe grisea*.

Results

Subsequently, this HTS microdilution methodology for the discovery of phytopathogen inhibitors, was used for the evaluation of the antifungal activity of the enhanced library of extracts from leaf-litter-associated fungi. The results of this screening campaign are described in Chapter 4 “**Leaf-litter-associated fungi from South Africa to control fungal plant pathogens**”, where primary screenings against *B. cinerea*, *C. acutatum*, *F. proliferatum* and *M. grisea* provided a high number of hits with promising inhibitory effects that were further characterized. Dereplication analyses revealed a high chemical richness that was improved by the SAHA addition to fungal fermentations. Finally, as a proof of concept, this study described the identification of the novel antifungal molecule *libertamide* ($C_{16}H_{27}NO_2$) produced by the strain *Libertasomyces aloeticus* CF-168990, a potential biocontrol agent of the septoria leaf blotch caused by *Zymoseptoria tritici*.

In summary, the implementation of different culture-based methods such as co-cultivations of different fungal strains, modifications in culture media and the addition of SAHA, combined with the identification of new taxonomic species, have led to an efficient induction of several fungal metabolites bioactive against fungal phytopathogens, which were silent or poorly expressed under standard laboratory conditions.

Chapter 1

Co-culturing of fungal strains against *Botrytis cinerea* as a model for the induction of chemical diversity and therapeutic agents

Rachel Serrano, Víctor González-Menéndez, Lorena Rodríguez, Jesús Martín, José R.
Tormo, Olga Genilloud

Frontiers in Microbiology, 2017

Sec. Antimicrobials, Resistance and Chemotherapy

Volume 8, 649, <https://doi.org/10.3389/fmicb.2017.00649>

JCR 4.019, Q2, total journal citations 25111

ABSTRACT

New fungal SMs have been successfully described to be produced by means of in vitro-simulated microbial community interactions. Co-culturing of fungi has proved to be an efficient way to induce cell–cell interactions that can promote the activation of cryptic pathways, frequently silent when the strains are grown in laboratory conditions. Filamentous fungi represent one of the most diverse microbial groups known to produce bioactive Natural Products. Triggering the production of novel antifungal compounds in fungi could respond to the current needs to fight health compromising pathogens and provide new therapeutic solutions. In this study, we have selected the fungus *Botrytis cinerea* as a model to establish microbial interactions with a large set of fungal strains related to ecosystems where they can coexist with this phytopathogen, and to generate a collection of extracts, obtained from their antagonistic microbial interactions and potentially containing new bioactive compounds. The antifungal specificity of the extracts containing compounds induced after *B. cinerea* interaction was determined against two human fungal pathogens (*Candida albicans* and *Aspergillus fumigatus*) and three phytopathogens (*Colletotrichum acutatum*, *Fusarium proliferatum*, and *Magnaporthe grisea*). In addition, their cytotoxicity was also evaluated against the human hepatocellular carcinoma cell line (HepG2). We have identified by LC-MS the production of a wide variety of known compounds induced from these fungal interactions, as well as novel molecules that support the potential of this approach to generate new chemical diversity and possible new therapeutic agents.

Keywords: co-culturing, fungal interactions, phytopathogens, antifungal agents

INTRODUCTION

The continued emergence of new resistances to the existing drugs, even for the most common organisms, is challenging the future use of the limited current therapies. Invasive fungal infections are an important cause of morbidity and mortality, especially in immunocompromised patients, and the limited therapeutic options require new approaches to replenish the drug discovery pipeline with novel potential drug candidates that might respond to these unmet clinical needs (Roemer and Krysan, 2014). Microbial Natural Products represent one of the most important resources for the discovery of novel drugs (Koehn and Carter, 2005). So far more than 42% of known bioactive compounds have been described as produced by filamentous fungi and many of these molecules with pharmacological applications were developed to the clinic and have been broadly used as antibiotics and antifungals among other applications (Demain, 2014; Schueffler and Anke, 2014). Despite the capacity to produce a broad diversity of compounds, most orders of filamentous fungi still remain poorly explored and are potential sources of novel molecules with applications not only in human health, but as well in agriculture and other industrial sectors (Bacon and White, 2000; Strobel and Daisy, 2003; Kusari et al., 2012). Furthermore, mining of fungal genomes has revealed the high number of gene clusters involved in the biosynthesis of fungal SMs (SMs) that are not detected in strains cultivated in laboratory conditions and many approaches have been proposed in the recent years to (Brakhage et al., 2008; Rank et al., 2010).

SMs have been proposed to be produced as defense mechanisms in the microbial environment (Davies, 1990), but recent hypothesis suggest their role as chemical signals in microbial cell communication between organisms of the same and distinct species as well as with host cells (Partida-Martinez and Hertweck, 2005). Bacteria and fungi are in constant interaction in their natural environment, living in close contact and competing for resources. Microbial interactions with different combinations of microorganisms have been extensively reported and have shown how they can modulate fungal metabolism and to induce the production of new bioactive molecules (Brizuela et al., 1998; Brakhage et al., 2008; Combès et al., 2012). These interactions can lead to the activation of complex regulatory mechanisms, and finally unlock the biosynthesis of a broad diversity of Natural Products (Bertrand et al., 2014).

Co-cultures have proved to be an effective tool to simulate the physiological conditions that occur during the interactions of fungi in their natural environment and may have an enormous potential for the discovery of new molecules with industrial applications (Bader et al., 2010; Brakhage, 2013; Netzker et al., 2015). Whereas traditional screening processes involve culturing a single microbial strain to discover new bioactive compounds, the use of co-cultures present new opportunities for the activation of cryptic biosynthetic pathways. Microorganisms can sense the presence of other microorganisms, triggering a general response derived from this antagonistic reaction that promotes changes in the morphology of both microorganisms in the interaction zone and the induction of SMs, enzymes, and other compounds in the area of communication (Hynes et al., 2007).

Such culturing conditions have facilitated the detection of compounds which are not produced when individual fungi are cultured alone (Hynes et al., 2007). Analytical methods have permitted to detect changes in the metabolite profiles that vary depending on the interacting fungi (Peiris et al., 2008; Rodriguez-Estrada et al., 2011). Different co-culturing techniques have been developed for this purpose including liquid and solid media, but all approaches consist on culturing two or more microorganisms in a single confined environment to facilitate interactions and induce further chemical diversity (Bertrand et al., 2013). Some examples of compounds derived from these interactions include long-distance growth inhibitors reported between *Trichophyton rubrum* and *Bionectria ochroleuca* (Bertrand et al., 2013), the production of acremostatins A–C, by *Acremonium* sp. when cultivated in mixed culture with *Mycogone rosea* (Degenkolb et al., 2002), the production of aspergicin, by a co-culture of two *Aspergillus* species (Zhu et al., 2011) or the production of cyclo-(l-leucyl-trans-4-hydroxy-l-prolyl-d-leucyl-trans-4-hydroxy-l-proline), when the two mangrove strains of *Phomopsis* sp. and *Alternaria* sp. are co-cultured in liquid media (Li et al., 2014). Additional studies have also reported the increase of metabolite production and the induction of new SMs during microbial interactions such as the variation of the metabolite expression detected by LC-MS in the interaction between the phytopathogen *Fusarium verticillioides* and the endophyte *Ustilago maydis* (Rodriguez-Estrada et al., 2011), or the induction of 12 metabolites by *Paraconiothyrium variable* when co-cultured with *F. oxysporum* (Combès et al., 2012).

Phytopathogen fungi are a wide and phylogenetically diverse group of microorganisms infecting plants or even causing serious plant diseases (Heydari and Pessarakli, 2010). *Botrytis cinerea* is one of the most important phytopathogen fungi according to the economic impact of the damages produced by its high infection rates (Dean et al., 2012). *B. cinerea* is the causing agent of the gray mold in a wide number of plants during all production cycle, including their storage and transport (Couderechet, 2003; Soylu et al., 2010; Dean et al., 2012; Wang et al., 2012). Furthermore, *B. cinerea*

is an excellent model for the study of fungal infection processes given its polyphagic and necrotrophic characteristics. This fungus promotes a rapid destruction of the tissues of the host plant by using a broad range of pathogenic factors (lytic enzymes, activated oxygen forms, toxins or plant hormones). Access to its genome and transcriptomic analyses have identified many genes and functions involved in the infectious process (Fillinger and Elad, 2016). As a phytopathogenic fungus, *B. cinerea* is a natural competitor for many fungal strains isolated from plants. Therefore, we propose in this study the use of fungal co-cultures with *B. cinerea* to challenge and activate cryptic pathways in fungal strains isolated from diverse plant environments and to identify potential producers of new antifungals. Chemical dereplication of known antifungals and an initial characterization of induced activities against a panel of human and plant fungal pathogens was also carried out to perform an extensive evaluation of this model interaction in the discovery of new antifungal agents.

MATERIALS AND METHODS

Fungal Strains

Fungal strains used in this work were obtained from Fundación MEDINA Culture Collection. The 762 wild-type strains were grown on Petri dishes of 55 mm of diameter with 10 mL of YM medium (yeast extract Difco™ 1 g, malt extract Difco™ 10 g, agar 20 g, and 1000 mL deionized H₂O), and incubated in darkness for 10–14 days at 22°C and 70% relative humidity (RH). Strains were selected from different environments, to ensure a broad and representative fungal community from soils, leaf litters, plant endophytes and epiphytes, and rhizosphere isolates from different geographical origins and environments.

Four phytopathogenic fungi were also used: *B. cinerea* CBS 102414, *Colletotrichum acutatum* CF-137177, *F. proliferatum* CBS 115.97 and *Magnaporthe grisea* CF-105765. Human pathogens used in the agar based assays include *Aspergillus fumigatus* ATCC 46645 and *Candida albicans* MY 1055.

MEDINA fungal Collection strains were identified according to their morphological characters, the ITS1-5.8S-ITS2 region and the first 600 nt of the 28S gene of each strain were sequenced and compared with GenBank® or the NITE Biological Resource Center¹ databases by using the BLAST® application.

B. cinerea Co-culturing Induction on Agar

Fungal strains were confronted against *B. cinerea* using coculturing methods on agar. *B. cinerea* strain that was grown in 250 mL Erlenmeyer flasks containing 50 mL of SMYA medium (neopeptone Difco™ 10 g, maltose Fisher™ 40 g, yeast extract Difco™ 10 g, agar 4 g, and 1000 mL deionized H₂O), and incubated at 220 rpm, 22°C and 70% RH for 3 days. Co-culture Petri dishes of 55 mm with 10 mL of 2% malt agar (malt extract Difco™ 20 g, agar 20 g, and 1000 mL deionized H₂O), were inoculated with 0.2 mL of *B. cinerea* liquid culture on one side of the plate, and an agar plug of the test strain to be induced was placed on the opposite site of the plate. All Petri dishes were incubated

at 22°C and 70% RH in darkness for 10 days. In parallel, axenic strains were inoculated using the same methodology.

Generation of Extracts from Agar Zones of Positive Interactions

Extracts were prepared from two areas of the inhibition zones formed in the co-culturing plates: (a) the growth inhibition area established between the growth of both fungal strains, and (b) the edge of *B. cinerea* inhibited mycelium. Similar agar areas were extracted from the axenic controls. Agar blocks were cut using a sterilized scalpel, and extracted with acetone (3 mL) in two Falcon tubes. Falcon tubes were centrifuged at 5000 rpm for 5 min and supernatants were collected. The extraction process was repeated twice for ensuring an efficient extraction and supernatants were combined. The extracts were concentrated to dryness under heated nitrogen stream. Hundred microliters of DMSO and 400 mL of H₂O were added sequentially to reconstitute the samples, that were transferred to HTS 96-well AB-gene® plates with an automatic liquid handler Multiprobe IIR robot. Extracts were filtered in 96 format with 0.22 mm MultiScreen® filter plates by 2000 rpm centrifugation for 5 min. Finally, the plates were heat-sealed and stored at 4°C until tested.

In Vitro Antimicrobial Assays Against Fungal Pathogens

Agar-Based Assay for Antifungal Evaluation

Media used for agar-based antifungal assays were SDA (sabouraud dextrose agar Difco™ 65 g and 1000 mL H₂O), Malt (malt extract Difco™ 20 g, agar 20 g, and 1000 mL deionized H₂O), YM (malt extract Difco™ 10 g, yeast extract Difco™ 2 g, agar 20 g, 1000 mL deionized H₂O). Depending on the phytopathogen fungus used, conidia concentration was also adjusted in a range from 1×10^4 to 5×10^7 conidia/mL (Moreira et al., 2014; Li et al., 2015; Ong and Ali, 2015) and plates were prepared in a temperature range between 30 and 45°C of the media for microbial damage. Twenty-five microliter of agar media containing conidia or spores were dispensed in OmniTray® of 86 mm×128 mm assay plates. Once solidified, samples were dispensed on top of the plates (10 mL) using an automated liquid handler (BiomekFX™, Beckman Coulter®). Five antifungal agents were evaluated as positive controls, in order to determine the optimal concentrations for a standard curve for each phytopathogenic strain from 5 mg/mL to 0.005 mg/mL: amphotericin B, cycloheximide, fluconazole, itraconazole, and voriconazole. Results (not shown) indicated amphotericin B as the best standard for reference.

The assay plates were incubated in dark at 25°C and 70% RH during 24 h. The diameter and turbidity of the inhibition halos were measured to assess the antimicrobial activity using a proprietary Image Analyzer® software and a stereoscope microscope (Leica™ MZ16). In the first column, each assay plate contained alternated, four positive control points corresponding to amphotericin B 1 mg/mL, and four DMSO 20% negative controls. The last column contained a specific standard curve of amphotericin B, different for each pathogen. Extracts were evaluated per duplicate for each pathogen.

***Aspergillus fumigatus* Agar-based Assay**

The *A. fumigatus* ATCC 46645 stock conidial suspension was prepared in Petri dishes of PDA and incubated at 37°C during 48 h. The plate surface was scraped with Tween 80 solution 0.1% (v/v) and a sterile loop to obtain a conidia suspension that was filtered with a sterile gauze. The conidia

suspension was inoculated at a final concentration of 1×10^5 spores/mL in yeast nitrogen base-dextrose agar medium, in OmniTray® assay plates of 86 mm×128 mm. Amphotericin B 1 mg/mL and DMSO 20% were used as positive and negative controls, respectively. Concentrations for the standard curve of amphotericin B were: 0.06 mg/mL–0.04 mg/mL–0.02 mg/mL–0.01 mg/mL.

***Candida albicans* Agar-based Assay**

Frozen stocks of *C. albicans* MY1055 were used to inoculate Sabouraud Dextrose Agar (SDA) plates and were incubated for 24 h, at 37°C. Grown colonies were suspended in Sabouraud Dextrose Broth (SDB) and incubated at 37°C and 250 rpm during 18–20 h. The OD660 was adjusted to 0.4 using SDB as diluent and blank. It was used 30 mL of this overnight inoculum to inoculate 1 L of yeast nitrogen base-dextrose agar medium (YNB 67 g/L, Dextrose 10 g/L, Agar 15 g/L), dispensing in assay plates OmniTray® of 86 mm×128 mm (de la Cruz et al., 2012). Amphotericin B 1 mg/mL and DMSO 20% were used as positive and negative controls, respectively. Concentrations for standard curve finally was determined by four points of amphotericin B: 0.06 mg/mL–0.04 mg/mL–0.02 mg/mL–0.01 mg/mL.

Generation of Conidia and Spores for Agar-based Assays

The evaluation against the three phytopathogens *Colletotrichum acutatum*, *Fusarium proliferatum*, and *Magnaporthe grisea*, required an optimization of the assay and in each case to define the optimum method for obtaining conidia to be used in the assay. For the sporulation of the phytopathogen fungi six different solid media were tested: CMD (cornmeal agar Microkit™ 17 g, glucose Sigma–Aldrich™ 1 g, agar 4 g, and 1000 mL deionized water), MALT 2% (malt extract Difco™ 20 g, agar 20 g, and 1000 mL deionized water), OAT-MEAL (oatmeal 60 g, agar 20 g, and 1000 mL deionized water), PDA (potato dextrose agar Difco™ 20 g and 1000 mL deionized water), SNA (KH₂PO₄ Merck™ 1 g, KNO₃ Merck™ 1 g, MgSO₄·7H₂O Merck™ 0.5 g, KCl Merck™ 0.5 g, glucose Sigma–Aldrich™ 0.2 g, sucrose Fisher™ 0.2 g, agar 20 g, and 1000 mL deionized water), V8-AGAR (V8 juice 200 mL, agar 20 g, and CaCO₃ Panreac™ 3 g and 1000 mL deionized water) and YM. *C. acutatum*, *F. proliferatum*, and *M. grisea* strains were cultured in these media by putting three mycelial agar plugs on Petri dishes of 90 mm, and were incubated at 22°C and 70% RH for 21–28 days depending on the strain. After this incubation, all plates were evaluated under the stereoscope (Leica™ MZ16), to identify the presence of conidia or spores. The best medium to induce their sporulation was selected in each case and the culturing was repeated until obtaining enough conidia to be used in the inhibition assays.

Two methods were evaluated for obtaining the highest quantity of conidia or spores: cultivating the fungal strain in submerged culture conditions during 24 h (overnight), or directly scraping the produced conidia or spores from the solid medium. In the first case, 50 mL of liquid medium were inoculated in 250 mL Erlenmeyer flasks with 12 agar plugs of mycelia grown in Petri dishes containing conidia and spores. Two different liquid media: SDB (sabouraud dextrose broth Difco™ 30 g and 1000 mL deionized water) and SMY (neopeptone Difco™ 20 g, maltose Fisher™ 40 g, yeast extract Difco™ 10 g and 1000 mL deionized water) were tested. Flasks were incubated at 220 rpm, 22°C and 70% RH during 24 h. In the second case, the surface of the sporulated fungus growing on solid media was scraped using a Tween 80 solution 0.1% (v/v) and a sterile loop to detach conidia or spores. Conidia were washed sequentially with sterile water to remove any remaining Tween 80. Finally, the resulting liquid culture was filtered with sterile gauzes to obtain a homogeneous solution

of conidia and spores. The resulting solution of conidia and spores was counted in a Neubauer chamber 0.0025 mm² and was adjusted the solution to the optimum concentration of conidia per milliliter.

***Colletotrichum acutatum* Agar-based Assay**

The optimum method for obtaining conidia was to directly scrap a sporulated culture in medium YM after 21 days of incubation. Conidia were tested at several concentrations (conidia/mL): 1×10^5 , 5×10^5 , 1×10^6 , 5×10^6 , 1×10^7 , and 5×10^7 and 1×10^7 conidia/mL was selected as the optimum concentration for *C. acutatum*, permitting the best definition of inhibition halos. The amphotericin B standard curve included four points: 0.06 mg/mL–0.04 mg/mL–0.02 mg/mL–0.01 mg/mL.

***Fusarium proliferatum* Agar-based Assay**

For this phytopathogen the method used to obtain a conidial suspension was to incubate the fungus overnight in liquid in SMY media, where the fungus was able to produce a large quantity of conidia and few hyphae. The different concentrations of conidia/mL were evaluated, and 1×10^6 conidia/mL resulted the optimum concentration to ensure clear inhibition halos. Four concentrations of amphotericin B were used in the standard curve (0.50 mg/mL–0.10 mg/mL–0.05 mg/mL–0.01 mg/mL).

***Magnaporthe grisea* Agar-based Assay**

To obtain a solution enriched in conidia of *M. grisea*, the fungus was grown in CMD medium to achieve sporulation and spores were directly scraped from the plate surface and the best inoculum concentration in the assay was established in 1×10^6 conidia/mL. The amphotericin B standard curve contained four concentrations: 0.50 mg/mL–0.10 mg/mL–0.05 mg/mL–0.01 mg/mL.

Evaluation of Cytotoxicity on HepG2 Cell Line

MTT (3-(4,5-dimethylthiazol-2-yl)-2,5-diphenyltetrazolium bromide) reduction rate is an indicator of the functional integrity of the mitochondria and used to evaluate cellular viability (Corine et al., 1998; Liu and Nair, 2010). In order to evaluate the cytotoxicity of extracts obtained from positive co-cultures and the corresponding axenic strains, the extracts were tested using the MTT assay against the HepG2 cell line (hepatocellular carcinoma, ATCC HB 8065) (de Pedro et al., 2013) after 24 h of incubation. Extracts were evaluated per duplicate.

Chemical Characterization of Positive Microbial Interactions

In order to identify known antifungals and induced Natural Products, the active extracts identified from the co-culture of *B. cinerea* with the tested fungi were analyzed by LC-MS and their chemical profiles were compared to internal proprietary databases of more than 900 known active molecules. LC-MS and database matching of known SMs were based on the LC-MS analyses in the low (LR) or high resolution (HR) mode and were performed as previously described (Martín et al., 2014; Pérez-Victoria et al., 2016). Database searching was performed against the MEDINA proprietary database of microbial metabolites or the Chapman & Hall Dictionary of Natural Products (v25.1).

RESULTS

Fungal Strains Confronted to *B. cinerea*

The study has evaluated the induction of new SMs from a wide population of 762 fungal strains of high taxonomic and geographic diversity when co-cultured with *B. cinerea*. The fungal strains were selected according to ecological characteristics of the environment where they were isolated, in the aim of prioritizing ecosystems where possible interactions with *B. cinerea* could be present. The strains were isolated from environmental samples collected in four climatic regions including: (a) a temperate group of 125 strains ranging from Argentina to Japan, New Zealand, the Republic of Georgia and western Europe, (b) an arid climate group of 102 strains from arid areas in Australia, Chile, Arizona (USA) and Almeria (Spain), (c) a tropical group of 282 strains selected from different tropical forests in Africa, Central and South America and Indic Ocean countries, and (d) a Mediterranean group with 253 strains from Southern Europe and South Africa.

The fungal strain population was selected from a wide diversity of habitats, identifying among them fruiting bodies (77), herbivore dung (27), leaf litter (187), lichens (18), plant rhizospheres (20), soils (148), and other plant materials (285). The largest group of strains was represented by strains isolated from leaf litter (187) and soils (148) associated to agricultural crops. Leaf litter is a unique source of saprophytic fungi decomposers of plant organic matter (Bills and Polishook, 1994; Lunghini et al., 2013) and soil fungi have an important function in the recycling of habitats of high fungal diversity (Sayer, 2006; Nihorimbere et al., 2011; Chandrashekar et al., 2014). Strains isolated from different plant rhizospheres are of special interest given their ability to generate interactions with plant roots to ensure absorption of nutrients and protection against other microbial pathogens. Finally, endophytes and epiphytes isolated from plants are natural competitors with plant phytopathogenic fungus, what can facilitate finding strains antagonistic to *B. cinerea*.

Eliciting Positive Microbial Interactions on Agar Plates

Fungal co-culturing techniques have been used previously to mimic in vitro microbial interactions occurring in their natural environment and to identify new antifungal compounds (Liu et al., 2001; Kim et al., 2015; Lopes et al., 2015; Ting and Jioe, 2016). We selected *B. cinerea* as a model to be used in fungal co-cultures and to induce the production of new SMs derived from fungal interactions. *B. cinerea* is a worldwide spread fungus that can be found in most of the environments where strains were isolated. In addition, it is an invasive fungus with fast growth, which facilitates the identification of antagonisms presented by other fungi.

Fungal co-cultures on solid media were incubated for 10 days, the time required by *B. cinerea* to grow and invade the whole Petri dish. From the 762 strains studied, 93 presented a positive antagonism (12% hit rate) observing a clear inhibition of the growth of *B. cinerea*. These 93 strains were evenly distributed among the different groups of strains of the tested population, both according to climatic and ecological aspects (Results not shown), indicating that the antagonism against *B. cinerea* was uniformly distributed within our group of strains.

In addition, to the growth inhibition, we observed differences in the growth morphology and colony-front pattern of *B. cinerea* including: (i) a clear front formed from a homogeneous mycelium (**Figures**

1a,d,e,i); (ii) a diffused front with overgrown aerial mycelium (**Figures 1b,h**); (iii) a diffused front with an homogenous pigmented mycelium (**Figures 1c,g**), and (iv) a clear front with accumulation of pigments at the front of the inhibited mycelium (**Figure 1f**). Typically, it is possible to identify SMs that diffused in the inhibition zone from the induced strains and that are diffusing as a gradient across the agar. These molecules can include both signalling and reacting compounds induced as result of the interaction as well as other SMs produced constitutively by each of the strains (Schulz et al., 2015).

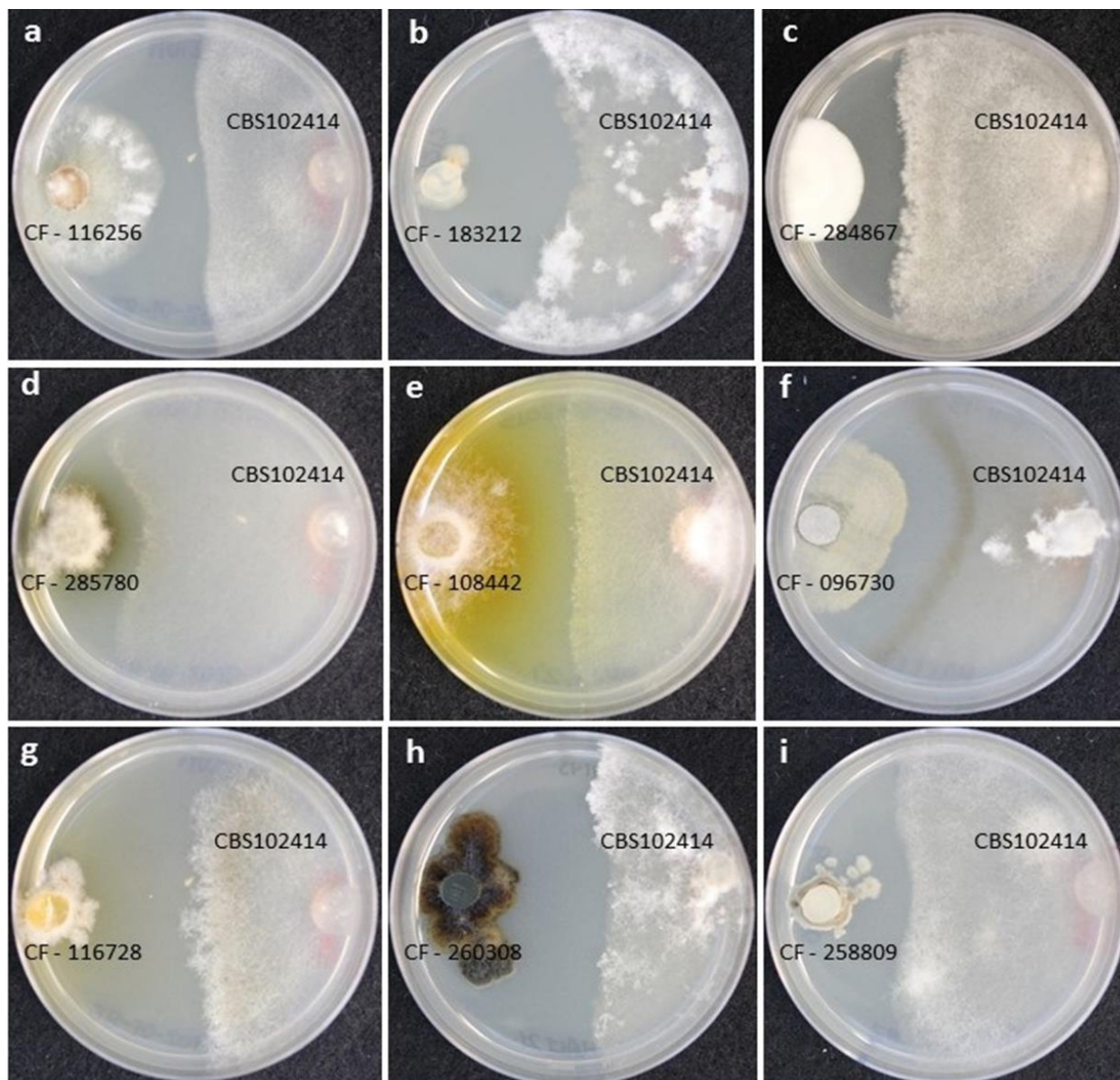


Figure 1. (a–i) Different growth morphologies and colony-front patterns in *Botrytis cinerea* CBS102414 as a response to the microbial interaction with wild-type fungal strains.

Each area of inhibition resulting from a positive interaction on the agar plate and the diffusion of chemical signals was extracted, as well as the front-colony area of the *B. cinerea* mycelium where the fungus may be responding to the challenge (**Figure 2**). This differentiation of two zones has permitted to evaluate the relative amounts of any compound contained in the extract and to indicate according to its diffusion gradient the source of the compound. With the aim of better understanding and evaluating the nature of the active molecules induced from the fungal interactions with *B. cinerea*, we screened the extracts against a panel of fungal pathogens to evaluate their antifungal specificity and performed a LC-MS chemical profiling as a first attempt to characterize the chemical composition in the extracts (**Figure 2**).

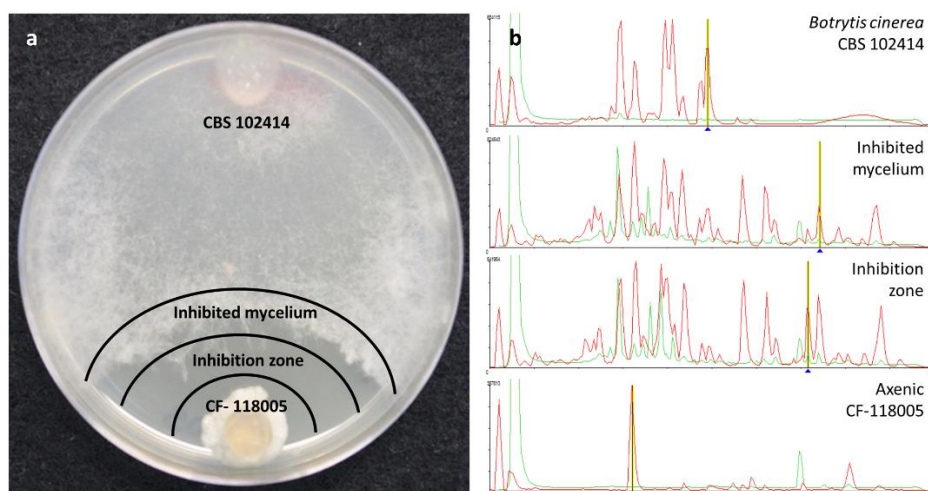


Figure 2. (a) Zones of microbial interaction evaluated for antifungal activities and (b) LC-MS chemical profiling.

Antifungal Activities against the Plant Pathogens

We selected three different phytopathogen to test the antifungal activities contained in the zone of inhibition extracts, evaluate their antifungal spectrum and characterize their specificity. The genus *Colletotrichum* is one of the most common and important genera among the phytopathogenic fungi, due to the capability to induce the anthracnosis in fruits and vegetables (Cacciola et al., 2012; Dean et al., 2012; Gang et al., 2015). Species as *C. acutatum* and *C. gloeosporioides* are serious threats for olive crops (*Olea europea*) an important cause of large losses in this agricultural sector (Oliveira et al., 2005; Rouhma et al., 2010). *Fusarium* spp. involve a lot of plant pathogenic species, and affect a large variety of crops, ranging from corn to wheat and other cereals, as well as the majority of fruits and even ornamental plants (Díaz et al., 2013). The third phytopathogen is *M. oryzae*, one of the most important phytopathogen given damages impact on rice (*Oryza sativa*). In addition, *M. oryzae* is the type of organism used in the research on the interactions between this pathogen and its hosts plant (Dean et al., 2012). Two species of the genus *Magnaporthe* (*M. grisea* and *M. oryzae*) are the main causative agent of rice blast disease, that is considered the most destructive infection that can promote losses up to 100% of ground production (Viaud et al., 2002; Kohli et al., 2011; Koeck et

al., 2012). In general, all three phytopathogenic species are very studied due to the wide range of plants they can infect, above and especially cereal crops (Kohli et al., 2011).

Most of the co-culture extracts presented a broad antifungal spectrum against the plant pathogens. As many as 51 extracts from the 93 strains that had a positive interaction with *B. cinerea*, presented activity against *C. acutatum*. From these 29 antifungal activities (57%) were not produced by the corresponding axenic controls, and had been subsequently induced with the co-culture. Similarly, 57 extracts were active against *F. proliferatum*, from which 31 (55%) were not present in the corresponding axenic controls. Finally, as many as 82 extracts were also active against *M. grisea* with 51 of the activities only observed in co-cultures (62%). There are also cases of strain extracts that presented antifungal activity against the phytopathogens *C. acutatum* (10 extracts), and *F. proliferatum* (5 extracts) when cultured axenically, but lost the activity when co-cultured with *B. cinerea*, were 10 for *C. acutatum*, 5 for *F. proliferatum* and none for *M. grisea* (**Figure 3**).

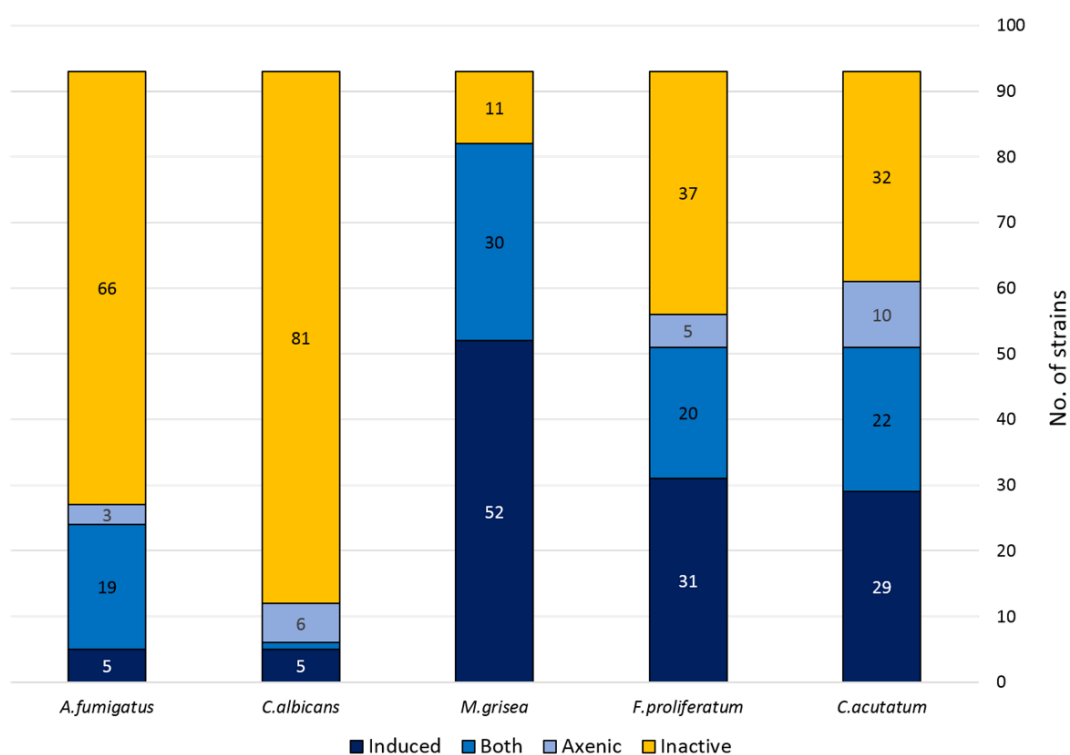


Figure 3. Antifungal activity distribution of the co-culture extracts.

Antifungal Activity Against Human Pathogens

The active extracts were also screened against the human pathogens *Candida albicans* and *A. fumigatus*. In this case the active extracts were detected to a lesser extent than those previously observed against the phytopathogen panel. Only 6 from the 93 co-culture extracts were active against *Candida albicans*. From these, 5 of these activities (83%) were only observed in the co-culture and were not observed in the extracts prepared from their axenic controls. An opposite

situation was found with another group of six strains that only produced antifungal activities against *C. albicans* when grown axenically, and that were not detected in co-culture. In the case of *A. fumigatus*, 24 extracts showed some activity against this pathogen, but only 5 of them (21%) were induced by the interaction, and only 3 were active when obtained from strains cultured axenically (Figure 3).

Chemical Dereplication and Characterization of Induced Antifungals

The active extracts were dereplicated by LC-MS against our databases of known compounds (Pérez-Victoria et al., 2016), and the following antifungal molecules were identified by fingerprint matching of HPLC retention time, UV and LC-LRMS spectra data: cercosporamide, 7-chloro-6-methoxymellein, cyclosporin A, equisetin, gliotoxin, globosuxanthone, griseofulvin, mycophenolic acid, mycorrhizin, palmarumycin C₁₅, preussomerin, thricothecin, virescenoside C, violaceol I/II.

Among them preussomerins were the family of molecules most frequently detected in the active extracts, especially the preussomerin analogs F and B, and followed in frequency by preussomerin A. These antifungal metabolites have been described in *Sporormiaceae*, the genus *Preussia* sp. and one species of *Dothidiales* (*Hormonema dematioides*) (Quesada et al., 2004). Palmarumycin C₁₅, closely related structurally to preussomerins and produced by species of *Pleosporales*, was the second most abundant molecule dereplicated. Other known antifungals such as equisetin (produced by several species of *Fusarium* sp.), globosuxanthone A (produced by species of *Hypocreales* and *Pleosporales*), griseofulvin (produced by several species of *Penicillium* sp.) and virescenoside C (produced by species of *Hypocreales*) (Cagnoli-Bellavita et al., 1970; Burke et al., 2005; Chooi et al., 2010; Yamazaki et al., 2012) were detected only in one or two strains.

Most of the de-replicated known antifungals were detected both in the inhibition zones and the *B. cinerea* mycelium front, being the differences in their LC-LRMS areas indicating their diffusion gradients and in consequence the producer organism. This allowed to identify if they active compounds were produced by the strain confronted to *B. cinerea* or by *B. cinerea* itself as a mechanism of defense.

Despite the presence of some known compounds the initial dereplication did not find any known antifungals in as many as 70% of the co-culture extracts. To evaluate the efficiency of the co-culturing approach with *B. cinerea* to induce chemical diversity we compared the metabolite profiles of the extracts independently of their biological activities. For this purpose, we analyzed by LC-HRMS the extracts and predicted tentative molecular formulas of their major components in order to identify the new induced compounds, disregarding constitutive metabolites (Pérez-Victoria et al., 2016).

Cytotoxicity of Active Extracts

The extracts were tested against the human HepG2 cell line to evaluate the production of cytotoxic compounds. Regarding specificity against the plant pathogens and their cytotoxicity against the human HepG2 cell line, 4 extracts (14%) that presented activity against *C. acutatum*, and one

against *F. proliferatum* (3%) were all of them as well cytotoxic; finally, from the 23 extracts with activity with *M. grisea* (45%), 7 of them were cytotoxic.

Among the compounds dereplicated in the extracts by LC-LRMS, most of them were identified as known cytotoxic agents or antibiotics. This identification was also dependent on the amounts of the cytotoxic compound in the extracts above the detection limits. For amounts of active compounds under the level of detection of LC-LRMS, we analyzed in detail the LC-HRMS profiles to check if any of those components was present in traces. A general evaluation of the number of induced SMs detected by LC-LRMS indicated that, as average the number of components produced in high titers in the extracts from positive interactions were 21.2 ± 4.8 and they were equivalent to doubling the number of metabolites observed in the extracts from the axenic control (12.2 ± 3.1). When these components were analyzed in detail by LC-HRMS and their molecular formula predicted by HRMS isotope patterns, we could identify as average 9.3 ± 2.3 metabolites produced by *B. cinerea* and present in the interactions. Clearly, the difference observed in the number of metabolites detected in the microbial interactions was due to the addition of the compounds resulting from the interaction between the confronted strains.

LC-HRMS Profiling of Active Extracts

The chemical dereplication of the 93 positive antagonisms indicated that 70% of the co-cultured pairs presented antifungal activities that were not identified as already known Natural Products when compared by LCMS to our database with more than 900 standards of families of known compounds. To look for the presence of other known compounds not contained in our databases, we analyzed the LC-HRMS profiles of every extract obtained for each strain in an interaction. In general, whereas the total number of SMs was similar to the addition of those observed in the axenic cultures, in many cases the molecules were different, confirming that the microbial interactions had induced changes the secondary metabolite profiles on the confronted strains. A tailor-made analysis of each pair was clearly necessary to understand each interaction and to explain the different responses that their extracts presented when characterized for antifungal activities.

We could identify tentatively the SMs induced in *B. cinerea* as a reaction to the microbial interaction, according to the molecular formula prediction and unique matching with metabolites described from *B. cinerea* in the Chapman & Hall Dictionary of Natural Products: 11-hydroxy-dehydro-botrydienol ($C_{15}H_{22}O_3$), botrytisic acid A ($C_{15}H_{20}O_3$), botrytisic acid B ($C_{15}H_{18}O_4$), dehydro-botrydienol ($C_{15}H_{22}O_2$), 3-hydroxy-4-oxocyclofarnesa-2,5,7,9-tetraen-11,8-olide ($C_{15}H_{16}O_4$), norbotrydialone acetate ($C_{16}H_{22}O_4$), botrydial phytotoxin ($C_{15}H_{20}O_2$), 10-oxo-dehydro-dihydro-bodtrydial ($C_{15}H_{18}O_2$), hydratedbotryenalol ($C_{17}H_{26}O_4 \cdot H_2O$), and dehydro-botrydienal ($C_{15}H_{18}O_2$) (**Figure 4**).

The active compounds identified by LC-HRMS dereplication in as many as 25 strains corresponded to molecules contained both in the axenic and co-culture extracts. The molecules 2-(-hydroxy-5-methoxyphenoxy)acrylic acid, integrastin B and palmarumycin C_{15} were dereplicated among other unknown Natural Products produced in the axenic controls in the strains CF-185391, CF-177133, CF-192842, CF-111323, CF-200182, and CF-210766. Similarly, the strains CF-116869, CF-096730, CF-195204, produced australifungin, botrydial phytotoxin, and tentatively a molecule identified as cissetin. Other molecules such as 3-O-acetyl-botcineric acid, equisetin, enniantin I and G,

11,12-hydroxy-eudesm-4-en-3-one, cordyol C, illudin C₃, illudinic acid, integrastin B, 7-chloro-6-methoxymellein, cis-4-hydroxy-6-deoxy-scytalone or xylarine, and tentatively, citreoviridin licicolinic acid A, 4-hydroxy-5-methylmellein, were also dereplicated by LCMS within this group of strains.

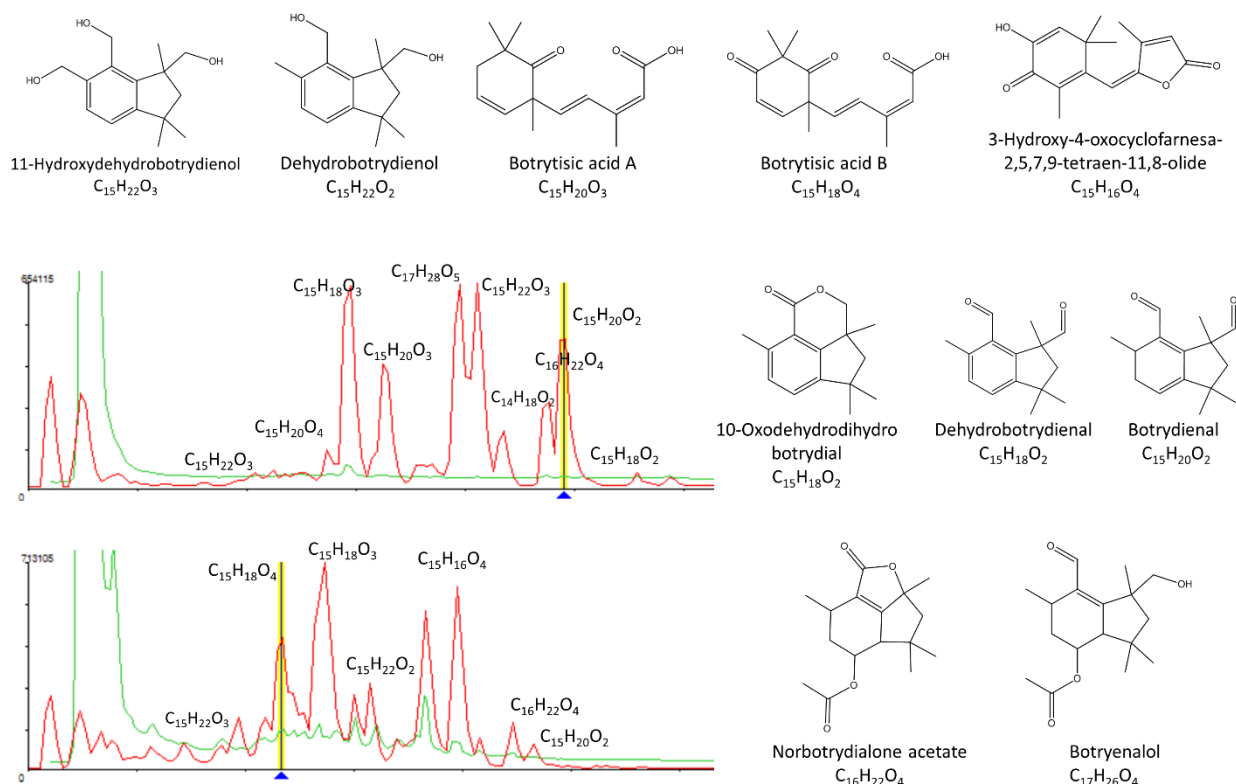


Figure 4. Tentative identification of secondary metabolites induced in *B. cinerea* as a response to the microbial interactions.

Once identified most of the known metabolites produced by *B. cinerea*, and those produced by the other fungal strains independently of the interaction, we studied the molecules only present in the co-culturing extracts that could correspond to induced compounds produced by each of the other fungi in the microbial interaction. These compounds were more abundant in the inhibition area and in less amount or not present both in the axenic strain or in the *B. cinerea* inhibited mycelium. Upon LC-HRMS analysis and molecular formula prediction of the three extracts for each co-cultured pair of strains, we could identify some molecules that were only present in the co-culturing inhibition extract for each pair.

One of these examples is chaetoxanthone C that was only detected in the extract from the inhibition zone of the co-culture of CF-108442 *Verticillium* sp. (**Figure 5**).

Chapter 1

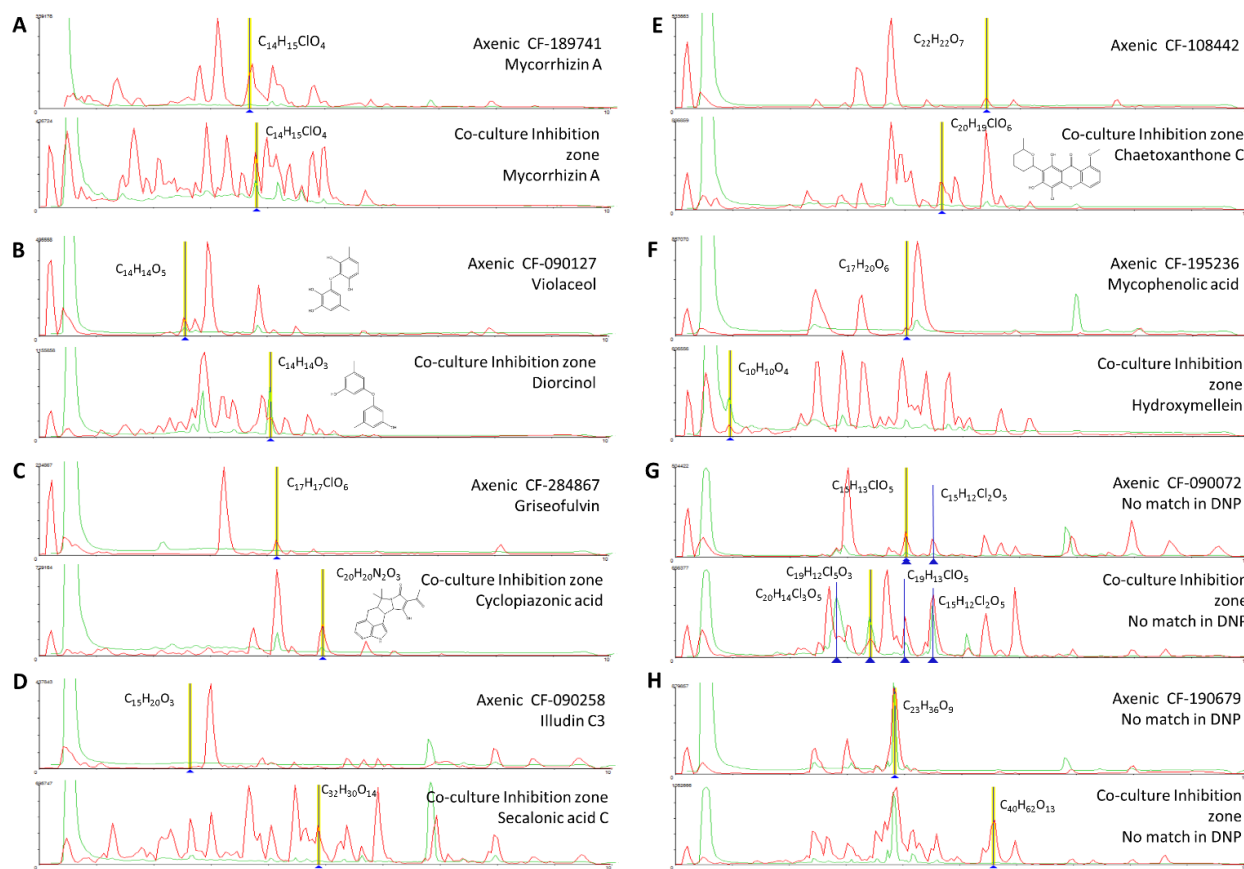


Figure 5. (a-h) Comparison of the secondary metabolite profiles produced by each axenic wild type fungal strains and its co-culturing with *B. cinerea*. Tentative LCMS identification of the main induced secondary metabolites is highlighted in each case.

Among the strains that produced induced antifungal activities against human fungal pathogens we can highlight the extract from the co-culture with the strain CF-118005 was found to contain as many as 21 induced metabolites without considering the known compounds produced by *B. cinerea*. One of them could be tentatively identified as SNF 4794-7 against our database of known compounds. Similarly, in the strain CF-183212 we identified induced components with m/z 312.1930 (CHO). Cordyol C was induced in the strain CF-187233, along with $C_{15}H_{16}O_4$, a component possibly related to the original $C_{15}H_{16}O_5$ detected in its axenic culture. In the case of CF-189741, 17 components were induced in this strain including a family of 210 nm UV absorbing metabolites, including mycorrhizin A and a chlorinated $C_{14}H_{15}ClO_4$ among them. The strain CF-246868 also produced 19 induced SMs that included palmarumycins C_7 and C_{15} and other preussomerin UV-like spectrum components. A similar situation could be observed for CF-090071 with a family of induced UV absorbance components. Finally, CF-268787 produced penicillic acid when confronted to *B. cinerea* among other 11 induced components.

In the group of five strains that produced induced antifungal extracts with a broad spectrum against the three plant pathogens we identified very few UV absorbing components in CF-116728, chaetoxanthone C, and one chlorated compound ($C_{20}H_{19}ClO_6$) among other 7 components in CF-

108442, palmarumycin C₁₃ as well as other 6 components in CF-176883, and 8 and 12 induced metabolites in CF-185636 and CF-262323 respectively. In addition, two strains CF-288225 and CF-185653 presented 13 and 9 clearly induced SMs.

The strain CF-190679 with specific activity against *Fusarium*, presented multiple components (12), many of them with molecular formulas not described for any known Natural Products and without match in the Chapman & Hall Dictionary of Natural Products (DNPv25.1). The co-culture extracts of CF-090258 and CF-153629, with specific activity against *C. acutatum*, contained, respectively, the secalononic acid C along other 14 SMs, and several induced metabolites, some of them with molecular formulas (i.e., C₁₁H₁₅ClO₅) not described previously for known fungal Natural Products.

Among the nine strains with induced activities specific to *M. grisea* (CF-090072, CF-090127, CF-110925, CF-118101, CF-195236, CF-209253, CF-213368, CF-284867, and CF-285353) we identified the production of diorcinol, destruxin A₁/A₄, antibiotic FR-49175, bis-dethio-bis-methyl-thiogliotoxin, 3-hydroxymellein, 3,4-dihydro-3,8-dihydroxy-3-methyl-1H-2-benzopyran-1-one, pleuromutilin, cyclopiazonic acid, and a range of 7 to 19 additional SMs not present in the DNP.

DISCUSSION

Distribution of the Positive Interactions Among the Population of Confronted Fungi

The distribution of the strains that presented positive antagonism against *B. cinerea* presented similar distribution the initial population of strains confronted, both in climate and ecological isolation origins, confirming that all climates and ecological source niches included in the study presented strains equally susceptible of respond to interactions with *B. cinerea*. Among them only 34% of the strains produced broad-spectrum antifungal compounds in the interaction zone showing activity against all three plant pathogens.

Identification of Metabolites Produced in the Axenic Cultures

Two groups of toxins have been described in literature to be produced by *B. cinerea*: the sesquiterpene botryanes and the polyketides botcinins. Both may facilitate its plant infection process (Reino et al., 2004; Tani et al., 2006; Collado et al., 2007). As response to the attack of the co-culturing strain, we confirmed that *B. cinerea* produced some of these Natural Products that were included among the group of molecules that were detected in the LC-HRMS chemical profiles of the active extracts. These molecules were present in higher amounts in the extracts obtained at the front of the colony of the *B. cinerea* inhibited mycelium than in the inhibition area between confronted strains (as indicated by area comparison of their LC-HRMS peaks between both extracts per each co-culture analyzed).

For the remaining strains, the LC-HRMS characterization and dereplication of compounds from axenic versus co-cultures against databases of know compounds indicated that, for 25 strains, their positive antagonistic interaction with *B. cinerea* could be explained by the presence of constitutive

molecules also present in the corresponding axenic culture and were not induced as a reaction to the attack of the confronted strain. None of them presented inhibition of human pathogenic fungi, but they could be classified in two groups formed by nine strains with extracts with broad spectrum against the plant pathogens and 16 strains with active extracts specific to *M. grisea*. In the first group are included the strains CF-185391, CF-177133, CF-192842, CF-111323, CF-200182, and CF-210766, that produce 2-(-hydroxy-5-methoxyphenoxy) acrylic acid, integrastin B and palmarumycin C₁₅ dereplicated among other unknown Natural Products in the axenic controls. Among the group of extracts with broad spectrum antifungal plant pathogens and with activity only when obtained from the *B. cinerea* inhibited mycelium, the strains CF-116869, CF-096730, CF-195204 presented australifungin, botryendial phytotoxin, and tentatively cisetin.

Strains that produced compounds with specific activity to *M. grisea*, but that did not show induced SMs when co-cultured with *B. cinerea*, constituted the largest group of the positive microbial interactions. Extracts from these 25 confronted strains (data not shown) presented, when dereplicated by LCMS 3-O-acetyl-botcineric acid, botryendial phytotoxin, equisetin, enniantin I and G, 11,12-hydroxyeudesm-4-en-3-one, cordyol C, illudin C3, illudinic acid, integrastin B, 7-chloro-6-methoxy-mellein, cis-4-hydroxy-6-deoxy-scytalone or xylarine, and tentatively, botrystic acid B, botrydial, citreoviridin licicolinic acid A, 4-hydroxy-5-methylmellein.

Metabolites Induced When Co-culturing with *B. cinerea*

The most significant group of results are represented by seven strains in which the co-culture induced the production of antifungal activities against human and plant fungal pathogens and an important number of new SMs were only detected in the extracts from the co-cultures. The most clearly effect was observed in strain CF-118005 producing a broad spectrum antifungal activity in co-culture against *Aspergillus fumigatus* and the three plant pathogens. The LC/MRMS profiles show the production of as many as 21 induced metabolites, including a molecule tentatively identified as SNF 4794-7. Similar observations were obtained for other strains such as in the strain CF-183212 with broad spectrum antifungal activity against *Candida albicans* and the three plant pathogens, presented induced metabolites in co-culture; cordyol C and a component with formula C₁₅H₁₆O₄ related to the component C₁₅H₁₆O₅ found in axenic cultures was induced in the strain CF-187233. Other broad spectrum activity extracts against both *C. albicans* and *A. fumigatus* and the three human pathogens were obtained from the strain CF-189741 where we identified mycorrhizin A and a chlorinated C₁₄H₁₅ClO₄ metabolite among 17 different induced components. Similarly, in the strains CF-246868, CF-090071, and CF-268787 multiple secondary metabolites were induced including some known compounds such as palmarumycins C₇ and C₁₅ and other preussomerin UV-like spectrum components, or penicillic acid. Further follow-up will be required to purify the individual components in these extracts and evaluate the antifungal spectrum of activity of these metabolites.

The analysis of the antifungal extracts that presented antifungal activity against all or individual plant pathogens has also shown the high number of new induced metabolites that be detected as result of the interaction. This study permitted to identify the production of known molecules such as chaetoxanthone C (CF-108442), palmarumycin C₁₃ (CF-176883), secalonic acid C (CF-090258), components with no match in the Chapman & Hall Dictionary of Natural Products (DNPv25.1) such

as the chlorated metabolite $C_{20}H_{19}ClO_6$ (CF-108442) or $C_{11}H_{15}ClO_5$ (CF-153629) not described previously for known fungal Natural Products, and of a large number of components ranging from 8 to 14 induced metabolites (CF-185636, CF-262323, CF-190679, CF-153629) that will require further characterization. The large number of specific activities specific to *M. grisea* (CF-090072, CF-090127, CF-110925, CF-118101, CF-195236, CF-209253, CF-213368, CF-284867, and CF-285353) and their lack of cytotoxicity that contrasts with the few specific activities obtained against *C. acutatum* or *F. proliferatum* suggests a higher sensitivity of the *M. grisea* assay to the presence of antifungals.

Given the high number of induced metabolites observed in the co-culturing study we focused the analysis on the most significant metabolite inductions. These are represented by 8 examples in which the induction of different SMs in extracts with antifungal against human and plant pathogens were detected in the inhibition zone (**Figure 4**).

In the case of the fungus *Lachnum* sp. CF-189741, the co-culture extract that presented a broad spectrum of activity against both *C. albicans* and *A. fumigatus* and the three plant pathogens showed among other 19 induced components a chlorinated metabolite ($C_{14}H_{15}ClO_4$) and a significant increase in the production of the mycotoxin mycorrhizin A, when compared to the axenic culture. Mycorrhizin A was previously described from the ectendomycorrhizal fungus *Monotropia hypopitys* (Trofast and Wickberg, 1977) and later reported as the responsible for the antimicrobial activity of extracts from various fungal endophytes (Pimentel et al., 2010; Hussain et al., 2014) (**Figure 5A**).

Axenic cultures of the strain *A. nidulans* CF-090127 (**Figure 5B**) produced violaceol, whereas in co-culturing we observed the induction of diorcinol. Both SMs were previously isolated from a marine-derived isolate of *A. versicolor* and were shown to have antibiotic activities (Fremlin et al., 2009). Recent genome analysis of the *A. nidulans* has evidenced that the polyketide synthase *orsA*, a member of the F9775 secondary metabolite gene cluster, is required for the biosynthesis of F9775, orsellinic acid and violaceol (Nielsen et al., 2011), and deletions of other putative orsellinic acid/F9775 cluster resulted in accumulation of the bioactive compounds gerfelin and diorcinol (Sanchez et al., 2010). Our data suggest that in this case the putative expression of this pathway may be repressed in the co-culturing, resulting in the formation of diorcinol and suppression of violaceol.

The strain *Penicillium* sp. CF-284867 was shown to produce griseofulvin and dechlorogriseofulvin when growth axenically, though in co-culturing the production of these two molecules was significantly increased, together with the induction of the mycotoxin cyclopiazonic acid (CPA) (**Figure 5C**). CPA has been described as the main toxic principle of a strain of *Penicillium cyclopium* (Holzapfel, 1968) but is also known to be produced by several species of *Aspergillus* and *Penicillium* (Frisvad et al., 2006). Griseofulvin was first isolated from *Penicillium griseofulvum* (Oxford et al., 1939) and later from other species of *Penicillium*, and is known to inhibit the mycelial growth of fungi but has no effect on yeasts. This fungistatic drug is used in animals and humans, in treatment of fungal infections of the skin and nail (Borgers, 1980). The co-culture induced Natural Product CPA is a known iron chelator and has been shown to be a specific inhibitor of Ca²⁺ ATPase of the sarcoplasmic reticulum (Seidler et al., 1989). The benefit of CPA to the producing fungi is not clear and there is no literature supporting specific antimicrobial activity.

In co-culture the endophyte *Stagonospora* sp. CF-090258 induced the production of secalonic acid C that showed activity against *C. acutatum* (**Figure 5D**). Secalonic acids are members of the ergochrome group of SMs, and can be isolated from the plant pathogenic fungus *Claviceps purpurea* as well as from other fungi, including *Aspergillus* spp. and *Penicillium* spp.

Among the molecules that were only produced in the zone of inhibition of the co-culture, we identified chaetoxanthone C as produced by the strain of *Verticillium* sp. CF-108442. This compound was only detected in the extract from the inhibition zone of the co-culture and the extract produced growth inhibition in all three plant pathogens. Xanthenes are well known for their pharmacological activities (Hostettmann and Hostettmann, 1989) such as antibacterials and antifungals (Braz-Filho, 1999; Beerhues et al., 2000). Chaetoxanthone C has been previously described from the marine-derived fungus *Chaetomium* sp., with specific antimalarial activity and low cytotoxicity (Pontius et al., 2008), but this study is the first report of the production of this compound by a *Verticillium* sp. From a terrestrial origin (**Figure 5E**). Furthermore, our results are in line with a similar study of a co-culture broth of two marine fungi, and the induction of a new xanthone with antifungal activity (Li et al., 2011). Xanthenes are known to be elicited in plants, where they play a dual function during biotic stress: as antioxidants to protect the cells from oxidative damage and as phytoalexins to impair the pathogen growth (Franklin et al., 2009). A similar role could be proposed for these compounds in fungal interactions.

The co-culture of the unidentified endophyte CF-195236 that showed a specific activity against *M. grisea* induced the production hydroxymellein, a metabolite not detected when the strain was grown axenically (**Figure 5F**). Hydroxymellein is a mellein derivative reported recently in antimicrobial extracts from fungal endophytes (Oliveira et al., 2009; Santiago et al., 2014) and our results suggest that the production of this compound can be the result of a crosstalk resulting from the induction of potentially silent biosynthetic gene clusters.

Another strain producing a specific activity against *M. grisea* is the *Phoma* sp. CF-090072. The strain is a prolific producer of new multi-chlorinated Natural Products (chemical formula with no match in DNP), most unusual in fungi. In axenic cultures, we only detected a low yield of the compounds $C_{15}H_{13}ClO_5$ and $C_{15}H_{12}Cl_2O$, while in co-cultures with *B. cinerea* the production titer for these compounds was significantly increased, and we could detect the induction of two additional multi-chlorinated compounds ($C_{20}H_{14}Cl_3O_5$ and $C_{19}H_{12}Cl_5O_3$) (**Figure 5G**). A search in DNP for fungal-derived polychlorinated Natural Products shows that only 64 were found to have three or more chlorides, and only 11 possess five or more chlorides. This is another example of unusual secondary metabolites that can be elicited by co-culturing, and efforts to scale up and isolate these chlorinated compounds are under way.

The extract of the co-culture of strain *Skeletocutis amorphia* CF-190679 that showed activity against *F. proliferatum* presented multiple components (12), many with molecular formulas not described for known Natural Products with no match in the Chapman & Hall Dictionary of Natural Products (DNPv25.1). The strain produced among others a possible new compound $C_{23}H_{36}O_9$ when grown axenically and in co-culture, as well as a potential new compound $C_{40}H_{62}O_{13}$ only induced in co-culture (**Figure 5H**). *Skeletocutis* is a genus of more than 60 species belonging to the *Polyporales* (Kirk et al., 2008) and key players in the carbon cycle, and the white-rot members of the order are among the most efficient lignin decayers in the biosphere (Floudas et al., 2012; Riley et al., 2014).

To date Natural Product derived from fungal species have been reported so far and efforts to scale up and isolate such novel compounds without no match in DNP, are under way.

In most of the extracts the LC-MS analysis did not detect any known molecules that could explain the inhibitory activity, especially in the case of the extracts with specific activity against one of three phytopathogens. Even in the case of the production of preussomerin B and F, equisetin and griseofulvin, all well known as broad spectrum antifungal agents, we did not observe any inhibition of the growth of *C. acutatum* and *F. proliferatum*, an observation that can be related to the low concentration of these molecules below the minimal inhibitory concentration (MIC) for these phytopathogens.

In summary, follow-up analysis including co-cultivation scaleup, chemical fractionation and purification of several compounds from the positive microbial interactions are currently being performed for the identification of SMs responsible for their biological activities. This will permit to characterize the novelty of the compounds and the activity profile against these pathogens.

CONCLUSIONS

Co-culturing with *B. cinerea* has proven to be a successful way of inducing antifungals with activity against both human and plant pathogens. The strain interaction determines dramatic changes in the number and levels of SMs detected with significative changes in the metabolite profiles.

Although *B. cinerea* is a good candidate in co-culturing experiments to induce new activities in the population of confronted strains, the highest number of positive antagonism compounds were obtained against plant pathogens, and only in a reduced number of cases we could confirm the production of antifungal activities against human pathogens. These results suggest that the selection of human pathogens such as *A. fumigatus* or *C. albicans* could be a more suitable co-culture inducer to trigger the production of new antifungals against human pathogens.

Further follow-up studies that are in progress in our laboratory to characterize the most interesting activities and potentially novel compound will permit to confirm the antifungal spectrum of these components and identify the diversity of novel components that have been elicited upon microbial interaction.

REFERENCES

- Bacon, C. W., and White, J. F. (2000). *Microbial Endophytes*. New York, NY: CRC Press.
- Bader, J., Mast-Gerlach, E., Popović, M. K., Bajpai, R., and Stahl, U. (2010). Relevance of microbial coculture fermentations in biotechnology. *J. Appl. Microbiol.* 109, 371–387. doi: 10.1111/j.1365-2672.2009.04659.x
- Beerhues, L., Barillas, W., Peters, S., and Schmidt, W. (2000). “Biosynthesis of plant xanthenes,” in *Bioorganic Chemistry*, eds U. Diederichsen, T. K. Lindhorst, B. Westermann, and L. A. Wessjohann (Weinheim:Wiley-VCH), 322–328.
- Bertrand, S., Bohni, N., Schnee, S., Schumpp, O., Gindro, K., and Wolfender, J.-L. (2014). Metabolite induction via microorganism co-culture: a potential way to enhance chemical diversity for drug discovery. *Biotechnol. Adv.* 32, 1180–1204. doi: 10.1016/j.biotechadv.2014.03.001
- Bertrand, S., Schumpp, O., Bohni, N., Monod, M., Gindro, K., and Wolfender, J.-L. (2013). Denovo production of metabolites by fungal co-culture of *Trichophyton rubrum* and *Bionectria ochroleuca*. *J. Nat. Prod.* 76, 1157–1165. doi: 10.1021/np400258f
- Bills, G. F., and Polishook, J. D. (1994). Abundance and diversity of microfungi in leaf litter of a lowland rain forest in Costa Rica. *Mycology* 2, 187–198. doi: 10.2307/3760635
- Borgers, M. (1980). Mechanism of action of antifungal drugs, with special reference to the imidazole derivatives. *Rev. Infect. Dis.* 2, 520–534. doi: 10.1093/clinids/2.4.520
- Brakhage, A. A. (2013). Regulation of fungal secondary metabolism. *Nat. Rev. Microbiol.* 11, 21–32. doi: 10.1038/nrmicro2916
- Brakhage, A. A., Schuemann, J., Bergmann, S., Scherlach, K., Schroeckh, V., and Hertweck, C. (2008). “Activation of fungal silent gene clusters: a new avenue to drug discovery,” in *Natural Compounds as Drugs*, eds F. Petersen and R. Amstutz (Basel: Birkhäuser), 1–12.
- Braz-Filho, R. (1999). Brazilian phytochemical diversity: bioorganic compounds produced by secondary metabolism as a source of new scientific development, varied industrial applications and to enhance human health and the quality of life. *Pure Appl. Chem.* 71, 1663–1672. doi: 10.1351/pac199971091663
- Brizuela, M. A., García, L., Pérez, L., and Mansur, M. (1998). Basidiomicetos: nueva fuente de metabolitos secundarios. *Rev. Iberoam. Micol.* 15, 69–74.
- Burke, L. T., Dixon, D. J., Ley, S. V., and Rodríguez, F. (2005). Total synthesis of the *Fusarium* toxin equisetin. *Org. Biomol. Chem.* 3, 274–280. doi: 10.1039/B411350K
- Cacciola, S. O., Faedda, R., Sinatra, F., Agosteo, G. E., Schena, L., Frisullo, S., et al. (2012). Olive anthracnose. *J. Plant Pathol.* 94, 29–44.
- Cagnoli-Bellavita, N., Ceccherelli, P., Mariani, R., Polonsky, J., and Baskevitch, Z. (1970). Structure du virescenoside C, nouveau métabolite de *Oospora virescens*. *FEBS J.* 15, 356–359. doi: 10.1111/j.1432-1033.1970.tb01015.x
- Chandrashekar, M. A., Pai, K. S., and Raju, N. S. (2014). Fungal diversity of rhizosphere soils in different agricultural fields of Nanjangud Taluk of Mysore District, Karnataka, India. *Int. J. Curr. Microbiol. Appl. Sci.* 5, 559–566.

- Chooi, Y. H., Cacho, R., and Tang, Y. (2010). Identification of the viridicatumtoxin and griseofulvin gene clusters from *Penicillium aethiopicum*. *Chem. Biol.* 17, 483–494. doi: 10.1016/j.chembiol.2010.03.015
- Collado, I. G., Sánchez, A. J., and Hanson, J. R. (2007). Fungal terpene metabolites: biosynthetic relationships and the control of the phytopathogenic fungus *Botrytis cinerea*. *Nat. Prod. Rep.* 24, 674–686. doi: 10.1039/b603085h
- Combès, A., Ndoye, I., Bance, C., Bruzaud, J., Djediat, C., Dupont, J., et al. (2012). Chemical communication between the endophytic fungus *Paraconiothyrium variabile* and the phytopathogen *Fusarium oxysporum*. *PLoS ONE* 7:e47313. doi: 10.1371/journal.pone.0047313
- Corine, V., Coiffard, C., Coiffard, L. J. M., Rivalland, P., and de Roeck-Holtzhauer, Y. (1998). In vitro correlation between two colorimetric assays and the pyruvic acid consumption by fibroblasts cultured to determine the sodium laurylsulfate cytotoxicity. *J. Pharmacol. Toxicol.* 39, 143–146. doi: 10.1016/S1056-8719(98)00016-1
- Couderchet, M. (2003). Benefits and problems of fungicide control of *Botrytis cinerea* in vineyards of Champagne. *Vitis* 42, 165–171.
- Davies, J. (1990). What are antibiotics? Archaic functions for modern activities. *Mol. Microbiol.* 4, 1227–1232. doi: 10.1111/j.1365-2958.1990.tb00701.x
- de la Cruz, M., Martín, J., González-Menéndez, V., Pérez-Victoria, I., Moreno, C., Tormo, J. R., et al. (2012). Chemical and physical modulation of antibiotic activity in *emericella* species. *Chem. Biodiv.* 9, 1095–1113. doi: 10.1002/cbdv.201100362
- de Pedro, N., Cautain, B., Melguizo, A., Cortes, D., Vicente, F., Genilloud, O., et al. (2013). Analysis of cytotoxic activity at short incubation times reveals profound differences among *Annonaceus* acetogenins, inhibitors of mitochondrial Complex I. *J. Bioenerg. Biomembr.* 45, 145–152. doi: 10.1007/s10863-012-9490-8
- Dean, R., Van Kan, J. A. L., Pretorius, Z. A., Hammond-Kosack, K. E., Di Pietro, A., Spanu, P. D., et al. (2012). The top 10 fungal pathogens in molecular plant pathology. *Mol. Plant Path.* 13, 414–430. doi: 10.1111/j.1364-3703.2011.00783.x
- Degenkolb, T., Heinze, S., Schlegel, B., Strobel, G., and Gräfe, U. (2002). Formation of new lipoaminopeptides, acremostatins A, B, and C, by co-cultivation of *Acremonium* sp. Tbp-5 and *Mycogonerosea* DSM12973. *Biosci. Biotechnol. Biochem.* 66, 883–886. doi: 10.1271/bbb.66.883
- Demain, L. A. (2014). Importance of microbial Natural Products and the need to revitalize their discovery. *J. Ind. Microbiol. Biot.* 41, 185–201. doi: 10.1007/s10295-013-1325-z
- Díaz, M. M., Leandro, L. F., and Munkvold, G. P. (2013). Aggressiveness of *Fusarium* species and impact of root infection on growth and yield of soybeans. *Phytopathology* 103, 822–832. doi: 10.1094/PHYTO-08-12-0207-R
- Fillinger, S., and Elad, Y. (2016). *Botrytis* - the Fungus, the Pathogen and its Management in Agricultural Systems. Berlin: Springer. doi: 10.1007/978-3-319-23371-0
- Floudas, D., Binder, M., Riley, R., Barry, K., Blanchette, R. A., Henrissat, B., et al. (2012). The Paleozoic origin of enzymatic lignin decomposition reconstructed from 31 fungal genomes. *Science* 336, 1715–1719. doi: 10.1126/science.1221748

- Franklin, G., Conceição, L. F., Kombrink, E., and Dias, A. C. (2009). Xanthone biosynthesis in *Hypericum perforatum* cells provides antioxidant and antimicrobial protection upon biotic stress. *Phytochemistry* 70, 60–68. doi: 10.1016/j.phytochem.2008.10.016
- Fremlin, L. J., Piggott, A. M., Lacey, E., and Capon, R. J. (2009). Cottoquinazoline A and cotteslosins A and B, metabolites from an australian marine-derived strain of *Aspergillus versicolor*. *J. Nat. Prod.* 72, 666–670. doi: 10.1021/np800777f
- Frisvad, J. C., Larsen, T. O., Dalsgaard, P. W., Seifert, K. A., Louis-Seize, G., Lyhne, E. K., et al. (2006). Four psychrotolerant species with high chemical diversity consistently producing cycloaspeptide A, *Penicillium jamesonlandense* sp. nov., *Penicillium ribium* sp. nov., *Penicillium soppii* and *Penicillium lanosum*. *Int. J. Syst. Evol. Microbiol.* 56, 1427–1437. doi: 10.1099/ijs.0.64160-0
- Gang, G. H., Cho, H. J., Kim, H. S., Kwack, Y. B., and Kwak, Y. S. (2015). Analysis of fungicide sensitivity and genetic diversity among *Colletotrichum* species in sweet persimmon. *Plant Path.* 31, 115–122. doi: 10.5423/PPJ.OA.03.2015.0033
- Heydari, A., and Pessarakli, M. (2010). A review on biological control of fungal plant pathogens using microbial antagonists. *J. Biol. Sci.* 10, 273–290. doi: 10.3923/jbs.2010.273.290
- Holzappel, C. W. (1968). The isolation and structure of cyclopiazonic acid, a toxic metabolite of *Penicillium cyclopium* westling. *Tetrahedron* 24, 2101–2119. doi: 10.1016/0040-4020(68)88113-X
- Hostettmann, K., and Hostettmann, M. (1989). “Xanthones,” in *Methods in Plant Biochemistry: Plant Phenolics*, Vol. 1, eds P. M. Dey and J. B. Harborne (New York, NY: Academic Press), 493–508.
- Hussain, H., Kliche-Spory, C., Al-Harrasi, A., Al-Rawahi, A., Abbas, G., Green, I. R., et al. (2014). Antimicrobial constituents from three endophytic fungi. *Asian Pac. J. Trop. Med.* 7S1, S224–S227. doi: 10.1016/S1995-7645(14)60236-4
- Hynes, J., Müller, C. T., Jones, T. H., and Boddy, L. (2007). Changes in volatile production during the course of fungal mycelial interactions between *Hypholoma fasciculare* and *Resinicium bicolor*. *J. Chem. Ecol.* 33, 43–57. doi: 10.1007/s10886-006-9209-6
- Kim, H. M., Lee, K. J., and Chae, J. C. (2015). Postharvest biological control of *Colletotrichum acutatum* on apple by *Bacillus subtilis* HM1 and the structural identification of antagonists. *J. Microbiol. Biotechnol.* 11, 1954–1959. doi: 10.4014/jmb.1507.07100
- Kirk, P. M., Cannon, P. F., Minter, D. W., and Stalpers, J. A. (2008). *Dictionary of the Fungi*, 10th Edn. Wallingford: CAB International, 771.
- Koeck, M., Hardham, A. R., and Dodds, P. N. (2012). The role of effectors of biotrophic and hemibiotrophic fungi in infection. *Cell Microbiol.* 12, 1849–1857. doi: 10.1111/j.1462-5822.2011.01665.x
- Koehn, F. E., and Carter, G. T. (2005). The evolving role of natural products in drug discovery. *Nat. Rev. Drug Discov.* 4, 206–220. doi: 10.1038/nrd1657
- Kohli, M. M., Mehta, Y. R., Guzman, E., de Viedma, L., and Cubilla, L. E. (2011). *Pyricularia* blast – a threat to wheat cultivation. *Czech J. Genet. Plant Breed.* 47, S130–S134. doi: 10.3767/003158516X692149
- Kusari, S., Hertweck, C., and Spiteller, M. (2012). Chemical ecology of endophytic fungi: origins of SMs. *Chem. Biol.* 19, 792–798. doi: 10.1016/j.chembiol.2012.06.004

- Li, C., Wang, J., Luo, C., Ding, W., and Cox, D. G. (2014). A new cyclopeptide with antifungal activity from the co-culture broth of two marine mangrove fungi. *Nat. Prod. Res.* 28, 616–621. doi: 10.1080/14786419.2014.887074
- Li, R. Y., Wu, X. M., Yin, X. H., Long, Y. H., and Li, M. (2015). Naturally produced citral can significantly inhibit normal physiology and induce cytotoxicity on *Magnaporthe grisea*. *Pestici. Biochem. Phys.* 118, 19–25. doi: 10.1016/j.pestbp.2014.10.015
- Li, Z. L., Liu, D., Li, D. Y., and Hua, H. M. (2011). A novel prenylated xanthone from the stems and leaves of *Calophyllum inophyllum*. *Nat. Prod. Res.* 25, 905–908. doi: 10.1080/14786419.2010.513977
- Liu, C. H., Zou, W. X., Lu, H., and Tan, R. X. (2001). Antifungal activity of *Artemisia annua* endophyte cultures against phytopathogenic fungi. *J. Biotechnol.* 88, 277–282. doi: 10.1016/S0168-1656(01)00285-1
- Liu, Y., and Nair, M. G. (2010). An efficient and economical MTT assay for determining the antioxidant activity of plant natural product extracts and pure compounds. *J. Nat. Prod.* 73, 1193–1195. doi: 10.1021/np1000945
- Lopes, M. R., Klein, M. N., Ferraz, L., da Silva, A. C., and Kupper, K. C. (2015). *Saccharomyces cerevisiae*: a novel and efficient biological control agent for *Colletotrichum acutatum* during pre-harvest. *Microbiol. Res.* 175, 93–99. doi: 10.1016/j.micres.2015.04.003
- Lunghini, D., Granito, V. M., di Leonardo, D. P., Maggi, O., and Persiani, A. M. (2013). Fungal diversity of saprotrophic litter fungi in a Mediterranean maquis environment. *Mycologia* 105, 1499–1515. doi: 10.3852/13-103
- Martín, J., Crespo, G., González-Menéndez, V., Pérez-Moreno, G., Sánchez-Carrasco, P., and Pérez-Victoria, I. (2014). MDN-0104, an antiplasmodial betaine lipid from *Heterospora chenopodii*. *J. Nat. Prod.* 77, 2118–2123. doi: 10.1021/np500577v
- Moreira, R. R., Nesi, C. N., and de Mio, L. L. M. (2014). *Bacillus* spp. And *Pseudomonas putida* as inhibitors of the *Colletotrichum acutatum* group and potential to control *Glomerella* leaf spot. *Biol. Control* 72, 30–37. doi: 10.1016/j.biocontrol.2014.02.001
- Netzker, T., Fischer, J., Weber, J., Mattern, D. J., König, C. C., Valiante, V., et al. (2015). Microbial communication leading to the activation of silent fungal secondary metabolite gene clusters. *Front. Microbiol.* 6:299. doi: 10.3389/fmicb.2015.00299
- Nielsen, M. L., Nielsen, J. B., Rank, C., Klejnstrup, M. L., Holm, D. K., Brogaard, K. H., et al. (2011). A genome-wide polyketide synthase deletion library uncovers novel genetic links to polyketides and meroterpenoids in *Aspergillus nidulans*. *FEMS Microbiol. Lett.* 321, 157–166. doi: 10.1111/j.1574-6968.2011.02327.x
- Nihorimbere, V., Ongena, M., Smargiassi, M., and Thonart, P. (2011). Beneficial effect of the rhizosphere microbial community for plant growth and health. *Biotechnol. Agron. Soc.* 15, 327–337. doi: 10.1038/srep35825
- Oliveira, R., Bouhmidi, K., Trapero, A., and del Moral, J. (2005). Caracterización morfológica y cultural de aislados de *Colletotrichum* spp. Causantes de la Antracnosis del olivo. *Bol. San. Veg. Plagas* 31, 531–548.
- Oliveira, C. M., Silva, G. H., Regasini, L. O., Zanardi, L. M., Evangelista, A. H., Young, M. C., et al. (2009). Bioactive metabolites produced by *Penicillium* sp. 1 and sp. 2, two endophytes associated with *Alibertia macrophylla* (Rubiaceae). *Z. Naturforsch. C.* 64, 824–830. doi: 10.1515/znc-2009-11-1212

- Ong, M. K., and Ali, A. (2015). Antifungal action of ozone against *Colletotrichum gloeosporioides* and control of papaya anthracnose. *Postharvest Biol. Technol.* 100, 113–119. doi: 10.1016/j.postharvbio.2014.09.023
- Oxford, A. E., Raistrick, H., and Simonart, P. (1939). Studies in the biochemistry of micro-organisms: griseofulvin, C(17)H(17)O(6)Cl, a metabolic product of *Penicillium griseo-fulvum* Dierckx. *Biochem. J.* 33, 240–248. doi: 10.1042/bj0330240
- Partida-Martinez, L. P., and Hertweck, C. (2005). Pathogenic fungus harbours endosymbiotic bacteria for toxin production. *Nature* 437, 884–888. doi: 10.1038/nature03997
- Peiris, D., Dunn, W. B., Brown, M., Kell, D. B., Roy, I., and Hedger, J. N. (2008). Metabolite profiles of interacting mycelial fronts differ for pairings of the wood decay basidiomycete fungus, *Stereum hirsutum* with its competitors *Coprinus micaceus* and *Coprinus disseminates*. *Metabolomics* 4, 52–62. doi: 10.1007/s11306-007-0100-4
- Pérez-Victoria, I., Martín, J., and Reyes, F. (2016). Combined LC/UV/MS and NMR strategies for the dereplication of marine natural products. *Planta Med.* 82, 857–871. doi: 10.1055/s-0042-101763
- Pimentel, M. R., Molina, G., Dionísio, A. P., Junior, M. R. M., and Pastore, G. M. (2010). The use of endophytes to obtain bioactive compounds and their application in biotransformation process. *Biotechnol. Res. Int.* 2011:576286. doi: 10.4061/2011/576286
- Pontius, A., Krick, A., Kehraus, S., Brun, R., and König, G. M. (2008). Antiprotozoal activities of heterocyclic-substituted xanthenes from the marine-derived fungus *Chaetomium* sp. *J. Nat. Prod.* 71, 1579–1584. doi: 10.1021/np800294q
- Quesada, E., Stockley, M., and Taylor, R. J. K. (2004). The first total syntheses of (–)-Preussomerins K and L using 2-arylacetal anion technology. *Tetrahedron Lett.* 45, 4877–4881. doi: 10.1016/j.tetlet.2004.04.143
- Rank, C., Larsen, T., and Frisvad, J. (2010). “Functional systems biology of *Aspergillus*,” in *Aspergillus: Molecular Biology and Genomics*, eds M. Machida and K. Gomi (Wymondham: Caister Academic Press), 173–198.
- Reino, J. L., Hernandez-Galan, R., Duran-Patron, R., and Collado, I. G. (2004). Virulence-toxin production relationship in isolates of the plant pathogenic fungus *Botrytis cinerea*. *J. Phytopathol.* 152, 563–566. doi: 10.1111/j.1439-0434.2004.00896.x
- Riley, R., Salamov, A. A., Brown, D. W., Nagy, L. G., Floudas, D., Held, B. W., et al. (2014). Extensive sampling of basidiomycete genomes demonstrates inadequacy of the white-rot/brown-rot paradigm for wood decay fungi. *Proc. Natl. Acad. Sci. U.S.A.* 111, 9923–9928. doi: 10.1073/pnas.1400592111
- Rodriguez-Estrada, A. E., Hegeman, A., Kistler, H. C., and May, G. (2011). In vitro interactions between *Fusarium verticillioides* and *Ustilago maydis* through real-time PCR and metabolic profiling. *Fungal Genet. Biol.* 48, 874–885. doi: 10.1016/j.fgb.2011.06.006
- Roemer, T., and Krysan, D. J. (2014). Antifungal drug development: challenges, unmet clinical needs, and new approaches. *Cold Spring Harb. Perspect. Med.* 4:a019703. doi: 10.1101/cshperspect.a019703
- Rouhma, A., Triki, M. A., and Msallem, M. (2010). First report of olive anthracnose caused by *Colletotrichum gloeosporioides* in Tunisia. *Phytopathol. Mediterr.* 49, 95–98.

- Sanchez, J. F., Chiang, Y. M., Szewczyk, E., Davidson, A. D., Ahuja, M., Oakley, C. E., et al. (2010). Molecular genetic analysis of the orsellinic acid/F9775 gene cluster of *Aspergillus nidulans*. *Mol. Biosyst.* 6, 587–593. doi: 10.1039/b904541d
- Santiago, C., Sun, L., Munro, M. H., and Santhanam, J. (2014). Polyketide and benzopyran compounds of an endophytic fungus isolated from *Cinnamomum mollissimum*: biological activity and structure. *Asian Pac. J. Trop. Biomed.* 4, 627–632. doi: 10.12980/APJTB.4.2014APJTB-2014-0030
- Sayer, E. J. (2006). Using experimental manipulation to assess the roles of leaf litter in the functioning of forest ecosystems. *Biol. Rev.* 81, 1–31. doi: 10.1017/S1464793105006846
- Schueffler, A., and Anke, T. (2014). Fungal natural products in research and development. *Nat. Prod. Rep.* 31, 1425–1448. doi: 10.1039/c4np00060a
- Schulz, B., Haas, S., Junker, C., Andrée, N., and Schobert, M. (2015). Fungal endophytes are involved in multiple balanced antagonisms. *Curr. Sci.* 109, 39–45.
- Seidler, N. W., Jona, I., Vegh, M., and Martonosi, A. (1989). Cyclopiazonic acid is a specific inhibitor of the Ca²⁺-ATPase of sarcoplasmic reticulum. *J. Biol. Chem.* 264, 17816–17823.
- Soylu, E. M., Kurt, S., and Soyulu, S. (2010). In vitro and in vivo antifungal activities of the essential oils of various plants against tomato grey mould disease agent *Botrytis cinerea*. *Int. J. Food Microbiol.* 143, 183–189. doi: 10.1016/j.ijfoodmicro.2010.08.015
- Strobel, G., and Daisy, B. (2003). Bioprospecting for microbial endophytes and their natural products. *Microbiol. Mol. Biol. Rev.* 67, 491–502. doi: 10.1128/MMBR.67.4.491-502.2003
- Tani, H., Koshino, H., Sakuno, E., Cutler, H. G., and Nakajima, H. (2006). Botcinins E and F and botcinolide from *Botrytis cinerea* and structural revision of botcinolides. *J. Nat. Prod.* 69, 722–725. doi: 10.1021/np060071x
- Ting, A. S. Y., and Jioe, E. (2016). In vitro assessment of antifungal activities of antagonistic fungi towards pathogenic *Ganoderma boninense* under metal stress. *Biol. Control* 96, 57–63. doi: 10.1016/j.biocontrol.2016.02.002
- Trofast, J., and Wickberg, B. (1977). Mycorrhizin A and chloromycorrhizin A, two antibiotics from a mycorrhizal fungus of *Monotropa hypopitys* L. *Tetrahedron Lett.* 33, 875–879. doi: 10.1016/0040-4020(77)80038-0
- Viaud, M. C., Balhadere, V., and Talbot, N. J. (2002). A *Magnaporthe grisea* cyclophilin acts as a virulence determinant during plant infection. *Plant Cell* 14, 917–930. doi: 10.1105/tpc.010389
- Wang, Q., Tao, S., Dub'e, C., Tury, E., Hao, Y. J., Zhang, S., et al. (2012). Postharvest changes in the total phenolic content, antioxidant capacity and L-phenylalanine ammonia-lyase activity of strawberries inoculated with *Botrytis cinerea*. *J. Plant Stud.* 2, 11–18. doi: 10.5539/jps.v1n2p11
- Yamazaki, H., Rotinsulu, H., Kaneko, T., Murakami, K., Fujiwara, H., Ukai, K., et al. (2012). A new dibenz[b,e]oxepine derivative, 1-hydroxy-10-methoxy-dibenz[b,e]oxepin-6,11-dione, from a marine-derived fungus, *Beauveria bassiana* TPU942. *Mar. Drugs* 10, 2691–2697. doi: 10.3390/md10122691
- Zhu, F., Chen, G., Chen, X., Huang, M., and Wan, X. (2011). Aspergicin, a new antibacterial alkaloid produced by mixed fermentation of two marine-derived mangrove epiphytic fungi. *Chem. Nat. Comp.* 47, 767–769. doi: 10.1007/s10600-011-0053-8

Chapter 2

Metabolomic analysis of the chemical diversity of South Africa leaf litter fungal species using an epigenetic culture-based approach

Rachel Serrano, Víctor González-Menéndez, Germán Martínez, Clara Toro, Jesús Martín,
Olga Genilloud, José R. Tormo

Molecules, 2021

Special Issue Analytical Microbiology

Volume 26 (14), 4262, <https://doi.org/10.3390/molecules26144262>

JCR 4.927, Q2, total journal citations 128386

Abstract

Microbial Natural Products are an invaluable resource for the biotechnological industry. Genome mining studies have highlighted the huge biosynthetic potential of fungi, which is underexploited by standard fermentation conditions. Epigenetic effectors and/or cultivation-based approaches have successfully been applied to activate cryptic biosynthetic pathways in order to produce the chemical diversity suggested in available fungal genomes. The addition of Suberoylanilide Hydroxamic Acid to fermentation processes was evaluated to assess its effect on the metabolomic diversity of a taxonomically diverse fungal population. Here, metabolomic methodologies were implemented to identify changes in secondary metabolite profiles to determine the best fermentation conditions. The results confirmed previously described effects of the epigenetic modifier on the metabolism of a population of 232 wide diverse South Africa fungal strains cultured in different fermentation media where the induction of differential metabolites was observed. Furthermore, one solid-state fermentation (BRFT medium), two classic successful liquid fermentation media (LSFM and YES) and two new liquid media formulations (MCKX and SMK-II) were compared to identify the most productive conditions for the different populations of taxonomic subgroups.

Keywords: fungal fermentations; epigenetic modifier; metabolomic; chemical diversity

1. Introduction

Microorganisms are known to be a rich source of new bioactive molecules with a wide range of biotechnological applications in the pharmaceutical, agrochemical and cosmetic industries. The rediscovery of already known structures, the usual low production yields and the difficulty in activating cryptic biosynthetic gene clusters (BGCs) under laboratory conditions are some of the limitations to exploit their huge chemical production capability [1,2,3]. Recent advances in laboratory automation and detection technologies, such as chromatography coupled to mass spectrometry, have contributed to the rapid and efficient generation of large Libraries of Natural Products [2,3,4]. Moreover, different approaches through the variations in nutritional and culturing factors have been extensively applied in order to exploit the biosynthetic potential revealed from genome-based studies [5,6,7].

Fungi stand out for their ability to produce a high diversity of metabolites with biological activities as antibacterial, antifungal or cytotoxic agents [8,9,10,11,12]. Orders *Chaetothyriales*, *Dothideales*, *Eurotiales*, *Helotiales*, *Hypocreales* and *Pleosporales* are well known to produce a broad range of high chemically diverse active molecules [12]. In addition, fungi play an important role in organic matter decomposition and especially in leaf litter with complex processes of nutrient recycling [13,14]. Leaf litter is a well-studied environment, and many reports have revealed its great fungal diversity, dominated by Ascomycota species. The leaf litter fungal community also harbors a high proportion of rare species associated with the decomposition of wide diverse plants, invertebrates and animal excrements [14,15,16,17,18]. Among leaf litter studies, South Africa is a high biodiversity hotspot with multiple works focused on describing its fungal populations associated

with leaf litter with many unique genera and species described: *Bactrodesmium* sp., *Brachydesmiella* sp., *Circinotrichum* sp., *Coniosporium* sp., *Periconiella* sp., *Sporidesmium* sp., *Parasarcopodium ceratocaryi* and *Rhexodenticula elegiae* [15,16,17,18].

Historically, variations in cultivation conditions have successfully been applied for exploiting the chemical diversity of fungal metabolism and increasing the chances of finding new bioactive molecules during fermentation processes [1,7,9,12]. The term “OSMAC” (One Strain Many Compounds), referred to modifications of media composition, aeration, culture format and temperature, is often applied on microbial fermentations to induce the production of additional compounds in response to these variables [1,9,12]. Besides the nutrient composition of fermentation media, the use of solid supports to promote cell differentiation and the addition of metabolic inductors are some approaches commonly used to enhance the probability for inducing changes in chemical profiles [4,8].

Transcription of BGCs is often controlled by epigenetic regulation such as histone deacetylation and DNA methylation. Small molecule epigenetic modifiers can modulate the microbial metabolism through the activation of cryptic biosynthetic pathways. Several reports have revealed the ability of epigenetic modifiers to alter the expression of silent or under-expressed BGCs, resulting in the modulation of the metabolomic profile and enhancement of the production of metabolites that were not synthesized under normal growth conditions [1,5,6,7,11,12,19,20,21,22,23,24,25,26,27]: Treatment of *Alternaria alternata* and *Penicillium expansum* with the histone deacetylase inhibitor trichostatin A resulted in a statistically significant increase in numerous unidentified metabolites for both species [21]. The addition of 5-azacytidine to cultures of *Cladosporium cladosporioides* stimulated the production of several oxylipins, and, when the culture was supplemented with suberoylanilide hydroxamic acid, it led to the isolation of two new perylenequinones (cladochromes F and G), four known cladochromes A, B, D, E and calphostin B [5]. Treatment of *Penicillium brevicompactum* with nicotinamide in static liquid fermentation induced the production of nine new compounds p-anisic acid, p-anisic acid methyl ester, benzyl anisate, syringic acid, sinapic acid, acetosyringone, phenyl acetic acid, gentisaldehyde and phydroxy benzaldehyde [23].

Suberoylanilide Hydroxamic Acid (SAHA) is one of the most frequently used inhibitors for inducing new bioactive metabolites in numerous epigenetic studies. The following metabolites were only produced when the strains were cultured with SAHA: Nygerone A produced by *Aspergillus niger* in semi-solid culture with vermiculite [24]; the anti-infective cytosporones by the marine fungus *Leucostoma persoonia* [25]; (10'S)-verruculide B, vermistatin and dihydrovermistatin induced in the endophytic fungus *Phoma* sp. nov. LG0217 [26]; two new natural sclerotioramine derivatives, isochromophilone XIV and XV, and two known compounds, sclerotioramine and (+)-sclerotiorin induced in the insect-associated fungi *Penicillium mallochii* CCH01 [27].

On another note, advances in Liquid Chromatography Mass Spectrometry (LC-MS) technologies have exponentially increased metabolomic studies. LC-MS detection provides complex information in a fast and robust way, with a high sensitivity to detect a wide range of microbial metabolites, establishing it as a very useful technology for improving early dereplication in drug discovery processes [2,4,28,29]. MASS Studio 2.3 is a software tool created by our group that allows the evaluation of the chemical diversity of microbial Natural Product Libraries using large LC-MS datasets. This methodology simplifies the complexity of LC-MS data when comparing hundreds of

samples by collapsing the time dimension and keeping the mass signal information [28,29]. MASS Studio allows multiple applications on metabolomics including, among others, the categorization of different fermentation conditions, the quantification of differentially induced metabolites, or the use of chemical metabolite information for the identification of species-specific chemotypes, a very useful tool for the prioritization of strains or metabolites for further studies [28,29].

The main goal of this study was to evaluate the effects of the addition of SAHA during the inoculum and fermentation stages, on a broad range of taxonomically diverse fungal strains isolated from leaf litter material collected in South Africa, where the influence of different fermentation conditions on the fungal metabolite production was characterized by the implementation of metabolomic analyses.

2. Results and Discussion

2.1 Fungal Fermentations

A taxonomically diverse group of fungal strains isolated from leaf litter samples of 17 local plants collected in South Africa was selected from the Fundación MEDINA Fungal Collection. A total of 232 fungal strains were identified and classified based on their morphology and ribosomal DNA sequences. As a result, more than 11 different fungal classes were identified, with *Agaricomycetes*, *Dothideomycetes*, *Eurotiomycetes*, *Leotiomycetes* and *Sordariomycetes* being the most representative. As many as 33 taxonomic orders, 77 families and more than 145 genera were identified, highlighting the large taxonomic diversity represented by fungi associated to leaf litter [14,15,16,17,18] (Table S1). The class *Dothideomycetes* grouped the highest number of fungal strains (n=119), with members of the order *Pleosporales* (n=94) as the most represented and diverse group of strains. When analyzed at the family level, this order included more than 20 families where *Didymellaceae* (n=19), *Phaeosphaeriaceae* (n=16), *Cucurbitariaceae* (n=7) and *Didymosphaeriaceae* (n=7) were the most predominant. The class *Sordariomycetes* (n=34) was the second more representative class of the fungal population, with *Hypocreales* (n=12) and *Xylariales* (n=8) being the major orders. The classes *Leotiomycetes* (n=28) and *Eurotiomycetes* (n=15) were mainly represented by the orders *Helotiales* (n=19) and *Chaetothyriales* (n=7), respectively. All of basidiomycete strains belonged to the class *Agaricomycetes* (n=11) including five different orders but with a low number of fungal strains. Other minor classes could be identified with a smaller number of strains that did not allow statistical determination of metabolomic trends: *Pezizomycetes* (n=3), *Cystobasidiomycetes* (n=1), *Microbotryosmycetes* (n=1), *Orbiliomycetes* (n=1), *Umbelopsidomycetes* (n=1) and *Wallemiomycetes* (n=1). Finally, due to their uniqueness, 17 fungal strains could not be assigned to any class and were classified as *Incertae sedis*.

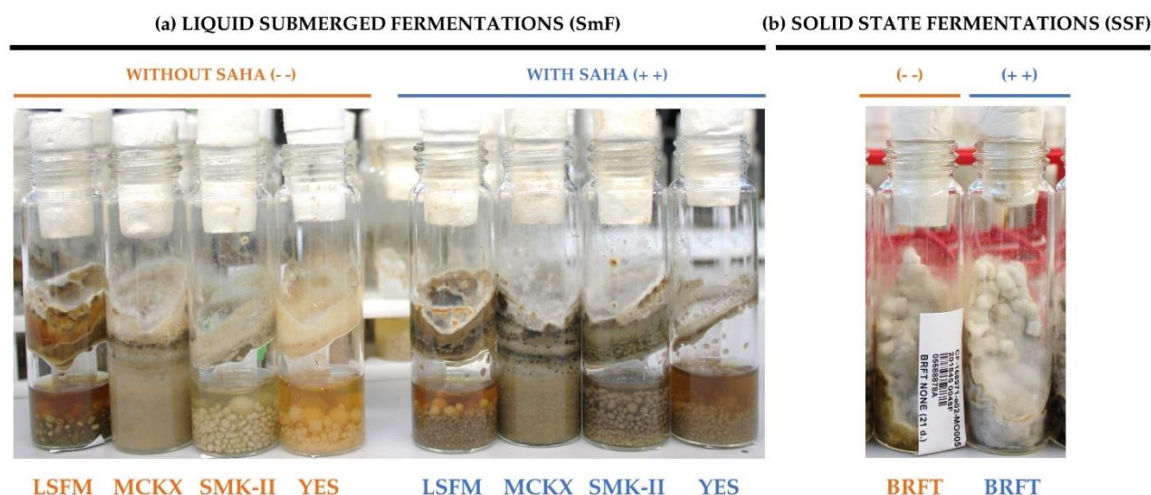


Figure 1. Example of *Parastagonospora* sp. CF-168971 showing different morphologies when grown in 10 fermentation conditions. **(a)** Fungal strain grown in liquid submerged fermentations (SmF) in four media LSFM, MCKX, SMK-II and YES without SAHA (-) (four EPA vials on the left) and supplemented with SAHA (++) (four EPA vials on the right) after 14 days of incubation. **(b)** Fungal strain grown on solid-state fermentation (SSF) in BRFT medium without SAHA (-) (EPA vial on the left) and with SAHA (++) (EPA vial on the right) after 21 days of incubation.

Each fungal strain was cultured in four different liquid fermentation media and one solid-state fermentation condition (SSF) to maximize the chances for inducing the production of secondary metabolites. The SSF BRFT medium was selected to include a rice-based medium, with brown rice as carbon source and yeast extract as a nitrogen source, with excellent reports on induction on chemical diversity. Regarding the liquid submerged fermentations (SmF), we selected two of the media due to their reported ability to enhance bioactive metabolite production (LSFM and YES) [9,10,11,12] and designed two new formulations for this work (MCKX and SMK-II). All of these fermentation conditions were evaluated with and without the epigenetic modifier SAHA (added during both the inoculum and fermentation stages) to evaluate the effects on the metabolite production. All of the studied fungal strains were well grown and many showed clear changes in color, texture and morphologies between the tested fermentation conditions, which could be indicative of changes in their secondary metabolite production (Figure 1a,b). After chemical extraction, a library of 2,362 fungal extracts and blanks was obtained and compiled in 96-well plates, which were analyzed by LC-MS. The raw data files resulting from the different batches of analytical runs were processed with the MASS Studio tool, which generated a matrix of more than twenty-seven thousand different [rt-m/z] chemical components.

2.2 Influence of Media Composition on Fungal Fermentations

Secondary Metabolite (SM) profiles of the selected 232 fungal strains, grown in five fermentation media with and without SAHA, were compared in detail to identify differences between the growth conditions after subtraction of media components. Initially, no statistical differences in the average of the number of [rt-m/z] components detected per strain were observed for each of the five

fermentation media (Figure 2a). All fermentation conditions seem to be contributing with a large number of metabolites ranging as average from 230 to 253 molecular components per strain. However, when the number of accumulated m/z produced by all fungal strains was compared, a slight increase was observed in BRFT fermentations. The SSF in BRFT medium showed higher total number of $[rt-m/z]$ components for both SAHA (9253) and without SAHA (8022) conditions, always higher than the corresponding liquid conditions (Figure 2b). The number of exclusive different components produced with and without SAHA was also averaged per strain and medium (Figure 2c). Although fungal fermentations in BRFT resulted the best conditions, we could not statistically determine significant differences, probably due to the wide diversity of the selected fungal population. More interestingly, the accumulated number of exclusive components clearly highlighted BRFT medium as the most productive condition for the studied strains (Figure 2d). Specifically, fungal fermentations in BRFT with SAHA provided the highest number of $[rt-m/z]$ components (1842), which were not detected in any of the other fermentation conditions. Previous studies have reported that SSF generally exhibits more complex metabolite profiles than the same strains when grown in liquid submerged conditions [4,8,30,31,32]. The use of SSF with fungi brings them closer to the conditions of their natural habitats, offering potential benefits for the microbial cultivation and metabolite production [30,31,32]. However, regarding whether the BRFT medium was a successful medium because of being a solid-state fermentation or because of its nutrient composition, and/or a synergy in both factors, it cannot be assured, since the different media were used in different culture systems. What can be confirmed is that BRFT with SAHA was the best medium for generating metabolomic changes on the wide taxonomically diverse fungal strains studied.

Regarding the four liquid fermentation media, two new designed media, MCKX and SMK-II, were prepared with specific media components in order to activate the huge metabolic capacity of the studied fungal population. On the one hand, MCKX medium has a rich base formulation which includes mannitol and yeast extract as carbon and nitrogen sources, ingredients used in other previously described production media MMK2 [10,11,12], but xylose was also added to present the same carbon source found in leaf litter environments, as it is the most abundant sugar in plant cell walls [33]. On the other hand, different carbon and nitrogen sources were selected for the fermentation medium SMK-II, including soluble starch, maltose and soybean flour, also reported to be components of successful formulations for bioactive metabolite production [10,11,12]. This fermentation medium was supplemented with L-proline, an amino acid that has been reported to be crucial in the production of antifungal compounds such as pneumocandin by *Glarea lozoyensis* [34]. Furthermore, Murashige and Skoog, a widely used plant growth medium that has been a common ingredient in some formulations for fungal growth [10,11,12,35], was added to both new production media MCKX and SMK-II to stimulate the growth and development of fungal strains able to metabolize leaf litter components. Classic LSFM and YES media, previously reported to be successful formulations to promote chemical changes during fungal fermentations and to enhance the production of fungal SMs [9,10,11,12], resulted to be the most productive conditions, followed by the new MCKX and SMK-II (Figure 2d). Despite fungal fermentations in both new media providing a lower number of exclusive and total $[rt-m/z]$ components, no significative differences were observed when compared to the other classic liquid formulations. Therefore, both new formulations resulted effective to induce the production of a considerable range of unique metabolites.

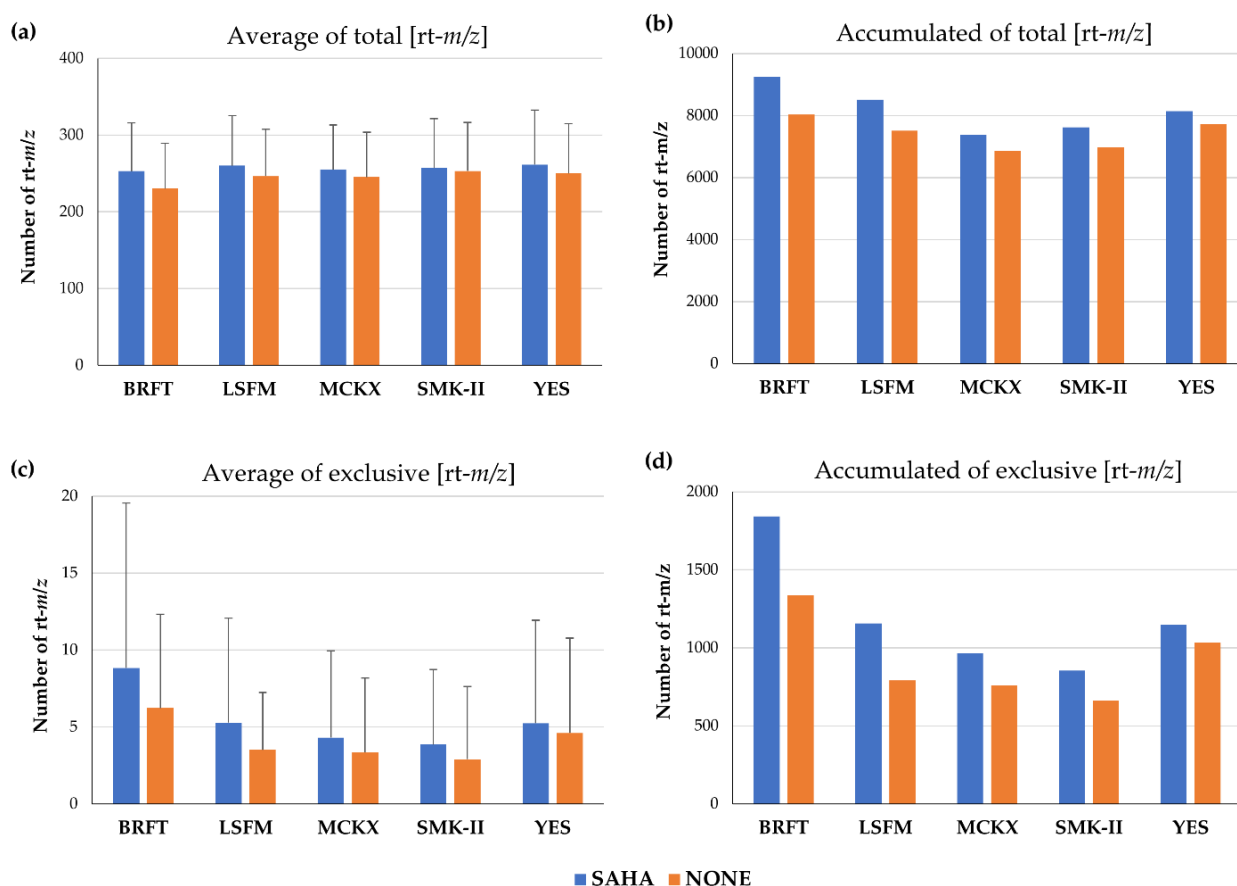


Figure 2. (a) Average of all [rt-m/z] components produced per strain in the five fermentation media with and without SAHA addition. (b) Accumulated differential components detected per fermentation medium. (c) Average of exclusive components produced per strain in the five fermentation media with and without SAHA addition. (d) Accumulated exclusive components detected per fermentation media. All values were calculated after subtraction of blank media components.

2.3 Chemical Evaluation of SAHA Addition during Fungal Fermentations

Several studies have reported the use of epigenetic modifiers for inducing metabolomic changes during fungal fermentations through the activation of biosynthetic pathways that are silent under standard culture conditions [1,5,6,7,11,12,19,20,21,22,23,24,25,26,27]. Specifically, SAHA is the most used histone deacetylase inhibitor due to its capacity to modulate the fungal SM profiles and to induce the production of new metabolites in specific fungal strains [24,25,26,27]. However, the ability of SAHA to enhance the chemical diversity on a wide diverse fungal population set has never been analytically supported. In this work, the metabolomic effects of the SAHA addition during every fermentation stage (inoculum and production) for five different media were evaluated. In general, the addition of SAHA to the fermentation processes of the studied fungal population always improved the number of [rt-m/z] chemical components in every medium tested. Moreover, an increase in the exclusive components was also detected when SAHA was present during all

fermentation processes (7132 [rt-m/z] components) in comparison to the same conditions without the addition of the epigenetic modifier (5267 [rt-m/z] components) (Figure 3).

Furthermore, the distribution of the exclusive [rt-m/z] components detected across the whole 232 fungal strains cultured with and without SAHA was compared after removing the common [rt-m/z] ones. In positive ionization mode of Mass Spectroscopy (MS), 4758 unique [rt-m/z] components were detected in fermentations with SAHA, whereas 3194 [rt-m/z] components were found in the same conditions without the epigenetic modifier. The total number of exclusive [rt-m/z] components detected in negative ionization mode, generally lower than positive, resulted to be 2374 with SAHA and 2073 without SAHA. The statistical mode of m/z values were similar in presence of SAHA for both detection modes (Table 1). However, the statistical mode was notably higher for positive ionization in conditions without SAHA. Regarding the retention times (rt), histograms show a bimodal distribution of data, where statistical mode intervals were similar between the conditions. Despite the discrepancies between positive and negative MS detection modes, generally related to the typical variances in the ionization of SMs [4], the addition of SAHA clearly improved the total number of exclusive [rt-m/z] components.

Dereplication analyses by LC-MS and HR-MS were applied against MEDINA's internal databases of known Natural Products and commercial database Dictionary of Natural Products (DNP), in order to evaluate further the effects of SAHA on the fungal fermentations [11,12,36]. As a result, 132 known metabolites (from 118 strains) were dereplicated in fungal fermentations with SAHA, without SAHA and common to both conditions (Figure 4, Table S1). Altenusin, Aposphaerin C, Citreoviridin, Melinacidin II, Mycophenolic acid, O-7-Methylfulvin acid, Photinide A as well as Ustilaginoidin A and J were only produced in fermentation conditions without SAHA. This is while 22 known metabolites with a high chemical diversity were only induced by the addition of SAHA to fungal fermentations: 9-O-Methylalternariol, Altenuic acid I, Anhydrosepedonin, Cytochalasin F or B, Dihydroaltenuene A, Leucinostatin A and B, Lucilactaene, MDN 0104, Naematolin, Palmarumycin C₁₁ and C₁₂, 6-Methoxyvestitol, Pandangolide 2, PF 1140, Phomalairdenone, Pycnidione, Quinolactacin A₂, Deoxyradicinin, Violaceol, Terricolin and 5,6-Dehydrozearalenone (Figure 5). The remaining dereplicated molecules were produced constitutively by specific fungal strains cultured in conditions with and without SAHA.

Table 1. Statistical mode value intervals calculated for each histogram of positive and negative ionization detection modes in Mass Spectroscopy (MS), based on the population of m/z and retention time (rt) values.

	SAHA	NONE
Exclusive m/z (MS positive mode)	[350, 400]	[400, 450]
Exclusive m/z (MS negative mode)	[-350, -400]	[-350, -400]
Exclusive rt (MS positive mode)	[0.5, 1.0], [2.5, 3.0]	[0.5, 1.0], [3.5, 4.0]
Exclusive rt (MS negative mode)	[-0.5, -1.0], [-3.5, -4.0]	[-0.5, -1.0], [-3.5, -4.0]

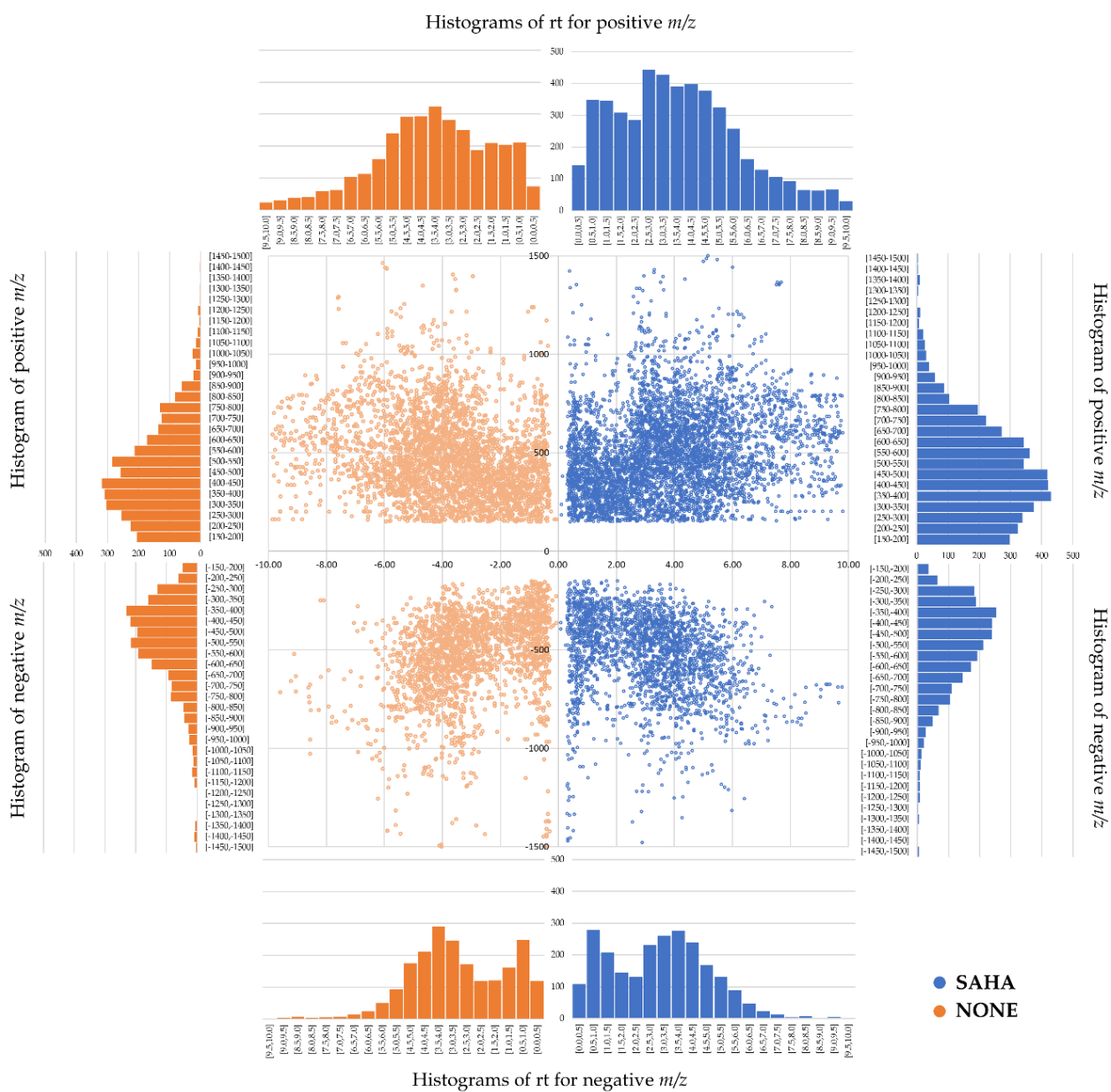


Figure 3. Distribution of all exclusive $[rt-m/z]$ components for positive (top) and negative (bottom) ionization mode, detected in leaf litter fungal population fermented in the presence of SAHA (blue) and the absence of SAHA (orange).

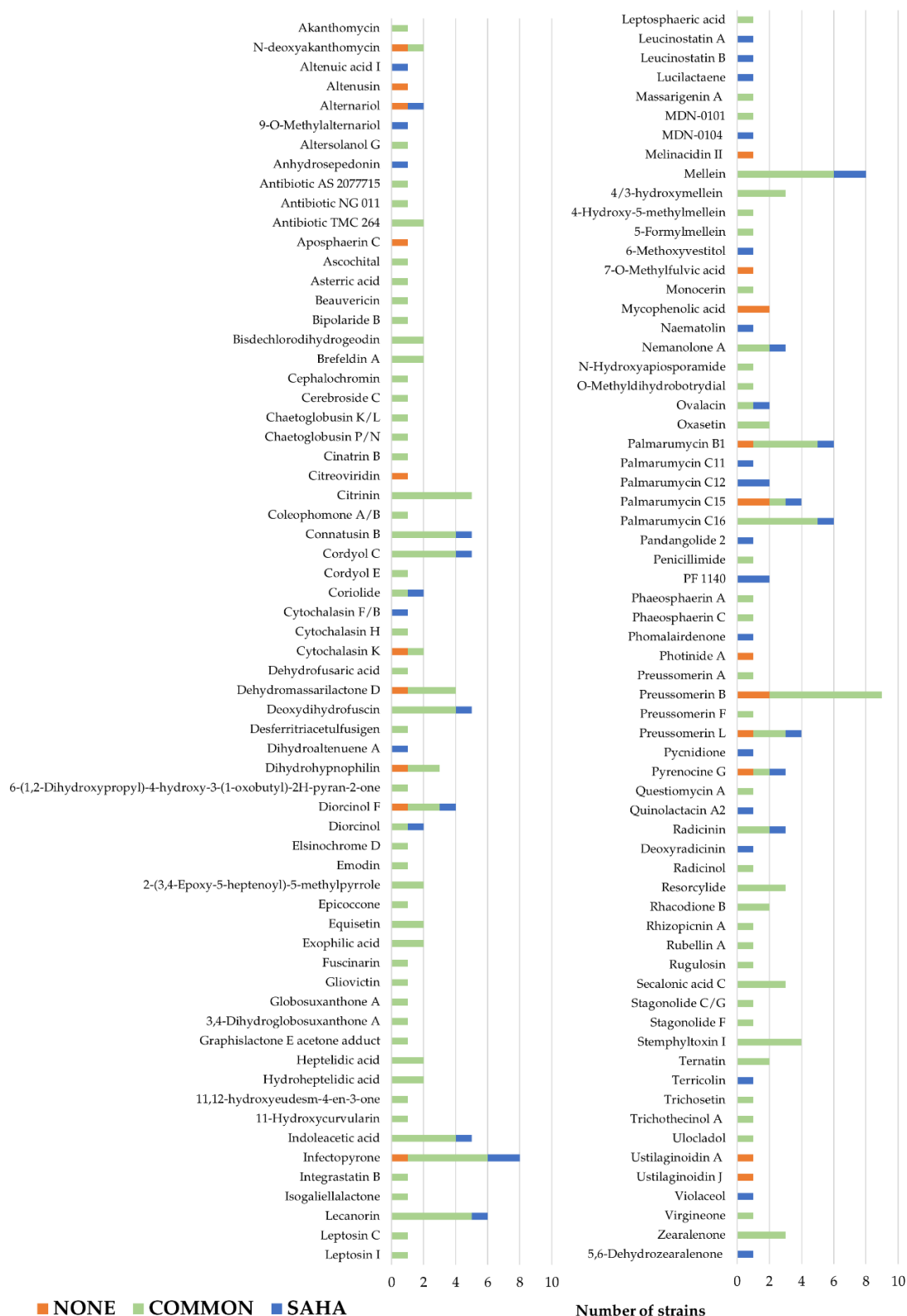


Figure 4. Distribution of known metabolites dereplicated for the leaf litter fungal population, only produced in fermentations supplemented with SAHA (blue), without SAHA (orange) and common to both conditions (green).

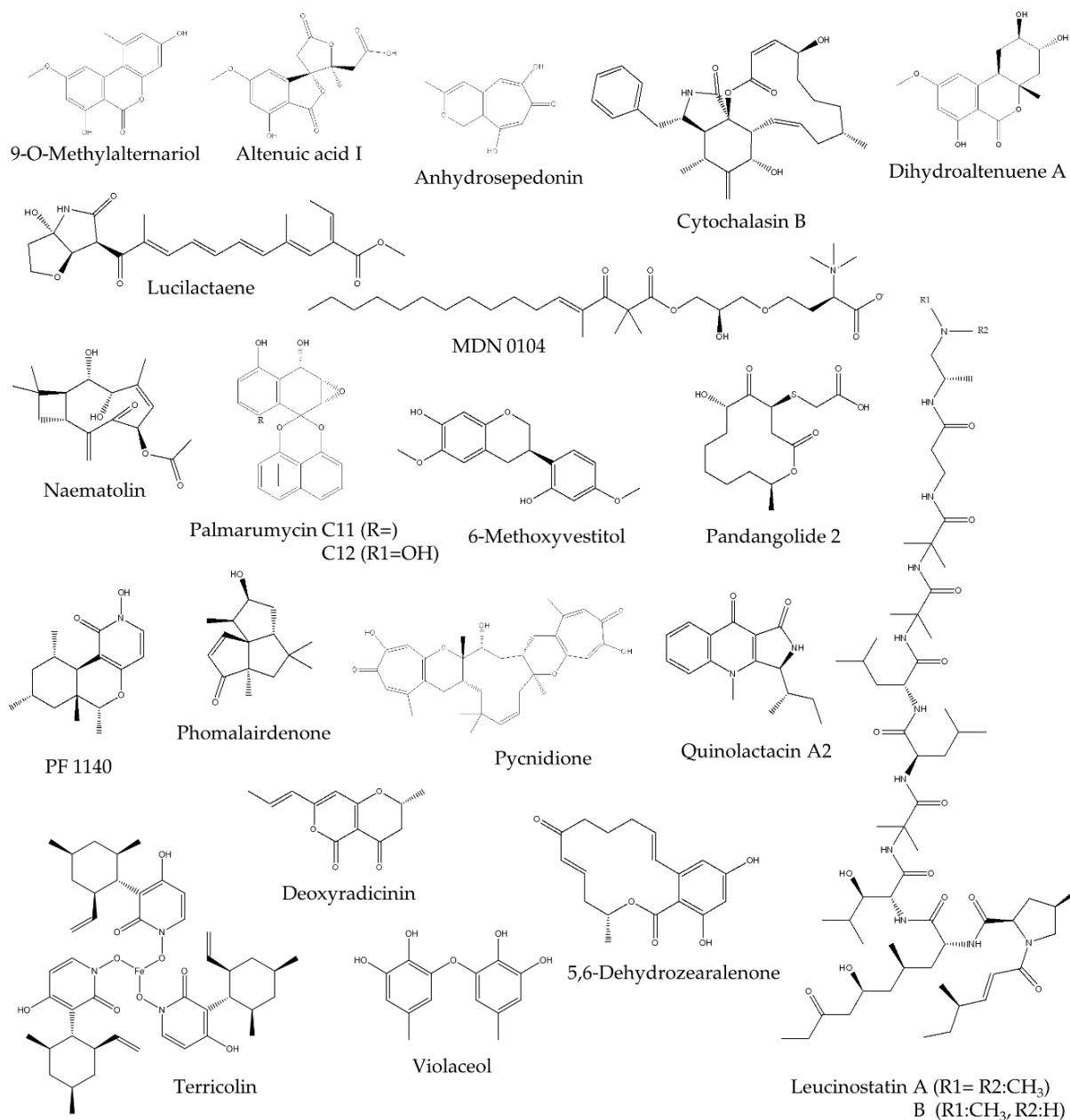


Figure 5. Chemical structures of dereplicated known metabolites induced by the addition of SAHA to fermentations of leaf litter fungal strain population.

In addition, MASS Studio 2.3 was implemented to characterize the chemical diversity and the amounts of metabolites produced by the addition of SAHA across all fungal fermentations. The software ranked and prioritized the different fermentation conditions from the best to the worst in inducing metabolomic changes [37,38,39]. The ranking processes consist of selecting the condition that generated the highest number of [rt-m/z] components as indicative of the chemical diversity achieved (Figure 6a), or the largest corresponding accumulated areas as indicative of the amount of produced SM (Figure 6b). Subsequently, the determination of the remaining condition that

generates the highest number of components not previously contemplated or their accumulated areas are performed until all fermentation conditions have been ranked from highest to lowest diversity/quantity productions [9,10,37,38,39]. According to this methodology, divergence from the 1:1 diagonal lineal correlation indicates its difference from the average. Following this criterion, the fermentation conditions were ranked based on the generation of chemical diversity in BRFT+SAHA > BRFT > LSFM+SAHA > YES+SAHA > SMK-II+SAHA > MCKX+SAHA > YES > LSFM > SMK-II > MCKX (see from top left to bottom right following the diagonal arrow, Figure 6a). Regarding the accumulated area (production quantity), the liquid submerged fermentations are grouped close to the diagonal (Figure 6b); this indicates that the SmF conditions provided lower diversity and quantity of metabolites compared with the SSF for equivalent extracted biomasses. Both graphics show the BRFT solid medium in the upper part of the diagonal line, highlighting it as the most productive condition among the set. Furthermore, the addition of SAHA clearly influenced the ranking positions, so every fermentation medium with SAHA was selected in the ranking prior to its corresponding medium without the epigenetic modifier. These results, with such a large fungal population, have confirmed that the addition of SAHA during fermentation processes can activate the metabolomic capacity of a wide taxonomically diverse fungal population, in line with the reported effects of SAHA for individual fungal species [1,5,6,7,11,12,19,20,21,22,23,24,25,26,27]. Remarkably, none of the tested fermentation conditions was discarded by the software, confirming that all of them were effective for inducing changes in the metabolomic profiles of leaf litter fungal strains.

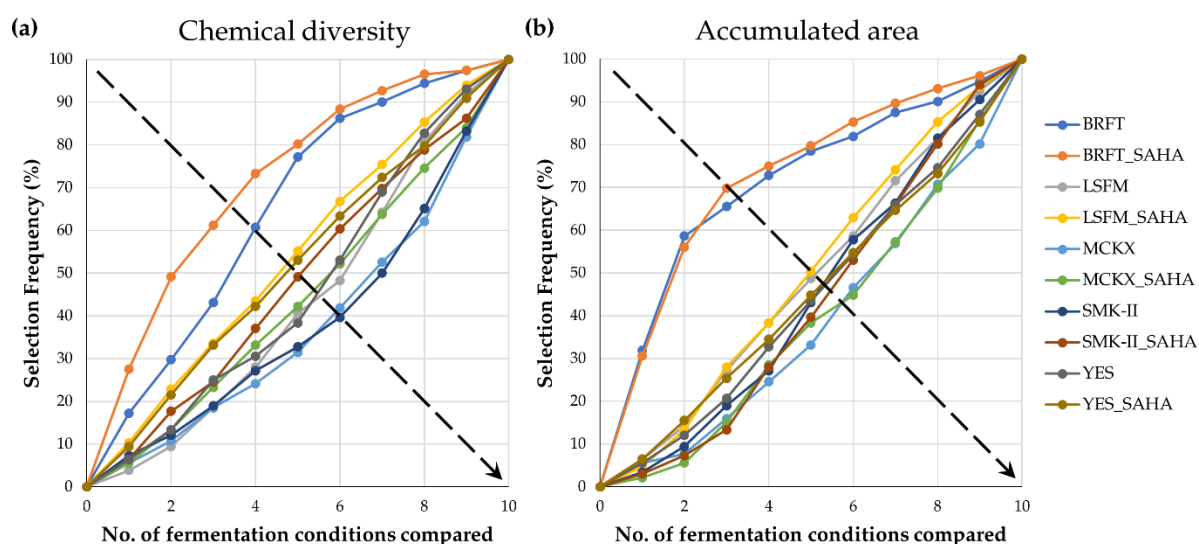


Figure 6. Ranking of all fermentation conditions studied in the total fungal population (n=232); **(a)** based on the exclusive chemical diversity generated (presence or absence of [rt-m/z] components); **(b)** based on the amount of metabolites (as accumulated area of [rt-m/z] components).

2.4 Effect of SAHA Addition to Different Taxonomic Orders

Due to the high taxonomic diversity of the studied fungal strains, we also focused on a detailed analysis of the potentially different effects of SAHA on taxonomic subgroups. For this purpose, we selected the most representative taxonomic orders within the major classes. In general, the solid-state fermentations in BRFT medium (with and/or without SAHA) were also able to provide the highest chemical diversity, being the first choice for the orders *Pleosporales*, *Capnodiales*, *Xylariales*, *Helotiales* and *Chaetothyriales* (Figure 7). In agreement with the general population, the ranking for each taxonomic group again showed that fungal fermentations with SAHA were ranked higher on presenting chemical diversity, compared with their corresponding conditions without the epigenetic modifier; however, some specific taxonomic groups showed some interesting differences.

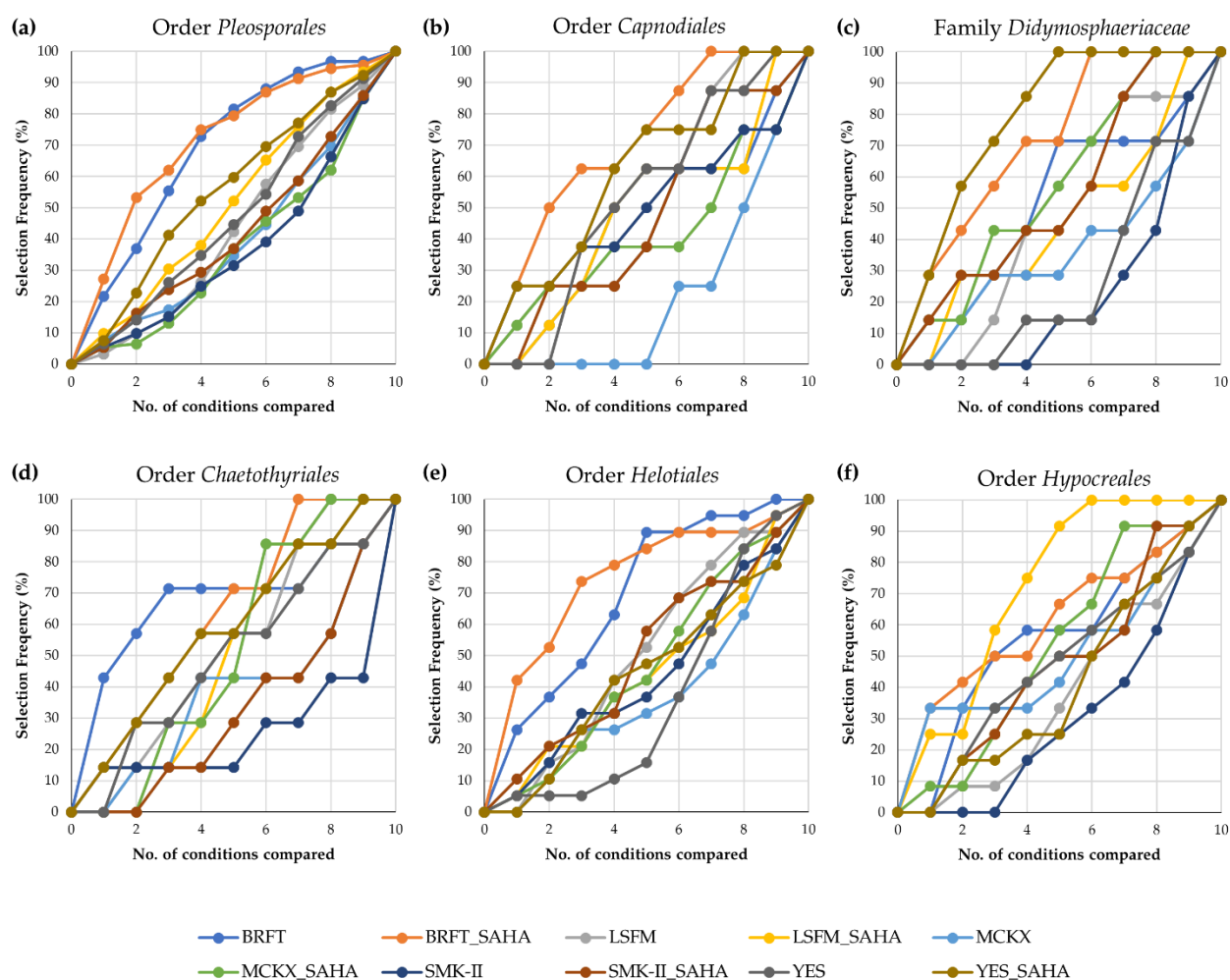


Figure 7. Rankings of the fermentation conditions based on the exclusive chemical diversity generated in different taxonomic groups: (a) order *Pleosporales* (n=94), (b) order *Capnodiales* (n=8), (c) family *Didymosphaeriaceae* (n=7), (d) order *Chaetothyriales* (n=7), (e) order *Helotiales* (n=19) and (f) order *Hypocreales* (n=12).

Within the class *Dothideomycetes*, fermentations of the orders *Pleosporales* and *Capnodiales* in YES with SAHA stand out as the most productive SmF condition (Figure 7a,b), in line with the reported ability of this medium to produce a wide range of fungal metabolites [9,10]. Given that the order *Pleosporales* showed similar behavior to the general population (Figure 6a and Figure 7a) and was the most abundant of the studied fungal group (94/232), we decided to study in more detail the four major families within this order. Among them, the liquid medium YES supplemented with SAHA was determined to be a better condition than BRFT, only for the family *Didymosphaeriaceae*, followed by this SSF condition (Figure 7c).

In the case of the order *Chaetothyriales* (class *Eurotiomycetes*), fermentations in YES with SAHA were able to produce a high SM diversity similar to the one obtained by the SSF in BRFT with SAHA (Figure 7d), confirming the previously described condition for this medium. Only the order *Helotiales* (class *Leotiomycetes*) produced a high number of chemical components in the new formulation SMK-II supplemented with SAHA (Figure 7e). This behavior of *Helotiales* strains could be related to the reported ability of this fungal group to grow on maltose, one of the carbon sources used in the formulation of this medium [40].

By contrast, rankings of the class *Sordariomycetes* showed LSFM medium with SAHA as the best SmF condition for inducing chemical diversity in the two studied orders (*Xylariales* and *Hypocreales*), contrary to its corresponding medium without SAHA, which occupied the last positions. Interestingly, fermentations of *Hypocreales* strains in LSFM with SAHA were highlighted as the first selected condition for producing more chemical components than the SSF (Figure 7f). This is the unique taxonomic order in this study where an SmF supplemented with SAHA produced higher chemical diversity than the SSF, followed closely by the BRFT conditions (with and without SAHA).

On another note, the class *Agaricomycetes* is one of the most important groups of leaf litter decomposers and includes quite different fungal strains with high metabolic potential [13]. Here, we studied a group of 11 basidiomycetes where the addition of SAHA to the fermentation media ensured a high improvement on the chemical diversity in BRFT, LSFM and MCKX media. Although the best fermentation condition was again BRFT with SAHA, the same medium without SAHA was unusually in the fourth place of the ranking (Figure 8). Moreover, fermentations of *Agaricomycetes* strains in MCKX with the epigenetic modifier significantly increased the chemical diversity, in contrast to the same medium without SAHA. The capacity of most of the basidiomycetes to degrade complex litter material could explain their ability to metabolize the xylose present in the formulation of the newly designed MCKX medium, producing a wide variety of metabolites [13].

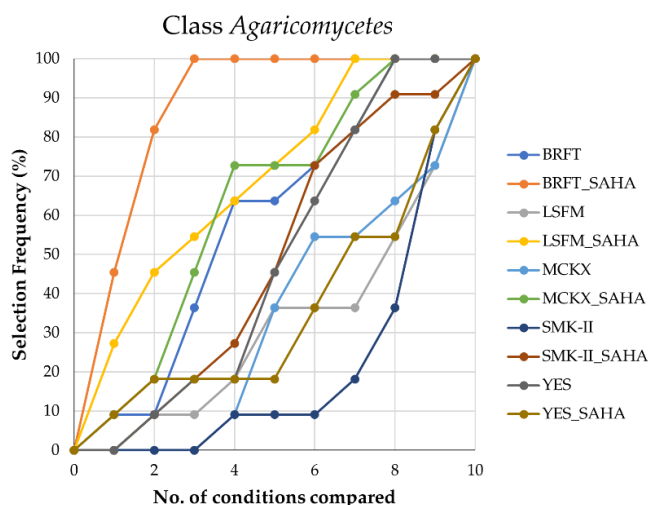


Figure 8. Ranking of the different conditions based on the exclusive chemical diversity generated from fermentations of the class *Agaricomycetes* (n=11).

2.5 Chemometrical Analysis of Chemical Profiles

Cluster analysis using Dice similarity coefficient (presence or absence), with simple matching by UPGMA, was performed in order to represent the general similarity and relationships between SM profiles for the different fermentation conditions after removing media components. According to this statistical analysis, the dendrogram grouped the metabolomic profiles of the different fermentation media in pairs: with and without SAHA (Figure 9). In general, chemical profiles from the same fermentation medium with and without SAHA showed higher similarity percentages. Fungal fermentations in BRFT medium were highlighted again as the ones with the most different metabolomic profiles, compared with the remaining liquid conditions LSFM, MCKX, SMK-II and YES. The same statistical relationship was observed when the Pearson correlation coefficient, based on the area of [rt-m/z], was applied to the population (data not shown).

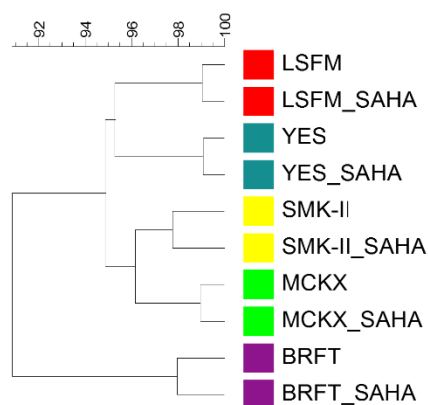


Figure 9. Dice-UPGMA dendrogram of similarity relationship between the metabolomic profiles of the fungal population (n=232) cultured in five fermentation media with and without SAHA.

After the initial untargeted metabolomic studies by low resolution mass spectrometry data, subsequent detailed characterization of specific ions of interest (targeted metabolomics) by high resolution mass spectroscopy (HR-MS) was performed. HR-MS analyses allowed us to compare the chemical profiles generated from the addition of SAHA during fungal fermentations and to identify some of the enhancement effects in the metabolite production for specific strains in certain conditions. HR-MS provided more complex information and allowed to identify effects that included: (i) conditions where the addition of SAHA did not affect the metabolomic profile; (ii) conditions with clear improvement in the production titer of given compounds in the presence of SAHA; and/or (iii) compounds that only were produced in presence of SAHA.

An example of metabolomic changes by the addition of SAHA is the strain *Corticium* sp. CF-166036, which showed some differences in the LC-MS profiles of the fermentation conditions when they were compared using the Dice similarity coefficient. Fermentations of this strain in BRFT and SMK-II media presented clear similarity between both conditions with and without SAHA. However, LSFM, MCKX and YES media showed metabolomic variations between conditions with and without SAHA, grouping them in different clusters of the dendrogram (Figure 10a). Moreover, interesting chemical changes were found after HR-MS profiles' comparison (Figure 11). In general, fermentations of the strain *Corticium* sp. CF-166036 in the BRFT medium provided more complex HR-MS profiles in comparison to the other SmF conditions, but no significant differences were found between conditions with and without SAHA. Nevertheless, fermentations in the four liquid conditions LSFM, MCKX, SMK-II and YES with SAHA induced important changes in metabolite production. Several known metabolites that were induced by the addition of SAHA could be identified by comparing results with our internal database and the commercial Dictionary of Natural Products (DNP) [11,12,36]. This strain produced, in the presence of SAHA, Terricolin (m/z 842.367; $C_{45}H_{60}FeN_3O_9$) in LSFM, Leucinostatin B (m/z 1203.8174; $C_{61}H_{109}N_{11}O_{13}$) in MCKX and Leucinostatin A (m/z 1,217.8363; $C_{62}H_{111}N_{11}O_{13}$) in MCKX and YES media. In addition, three differential m/z detected could not be identified: m/z 264.1474 ($C_{14}H_{20}N_2O_3$) induced in MCKX with SAHA, as well as m/z 581.3664 ($C_{30}H_{51}N_3O_8$) and m/z 362.2119 ($C_{18}H_{34}N_3O_5S$), both induced in YES with SAHA.

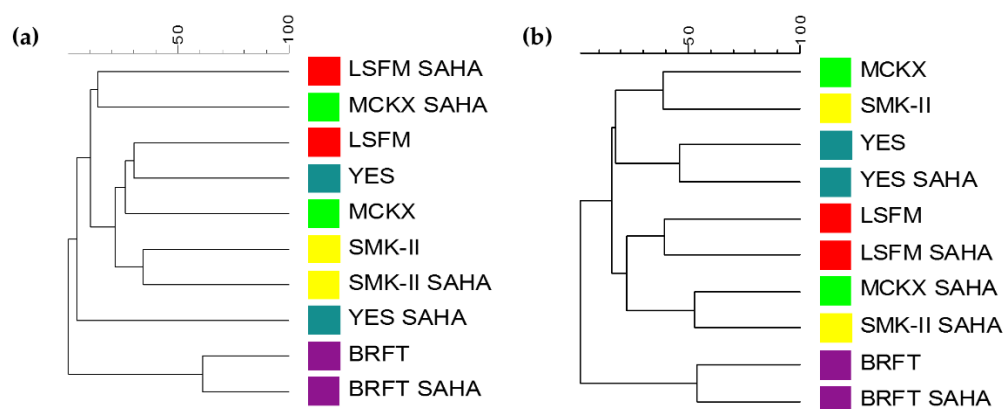


Figure 10. Dice-UPGMA dendrograms of metabolite profiles detected for the fungal strains; **(a)** *Corticium* sp. CF-166036 and **(b)** *Microxyphium* sp. CF-164412 grown in five fermentation media with and without SAHA.

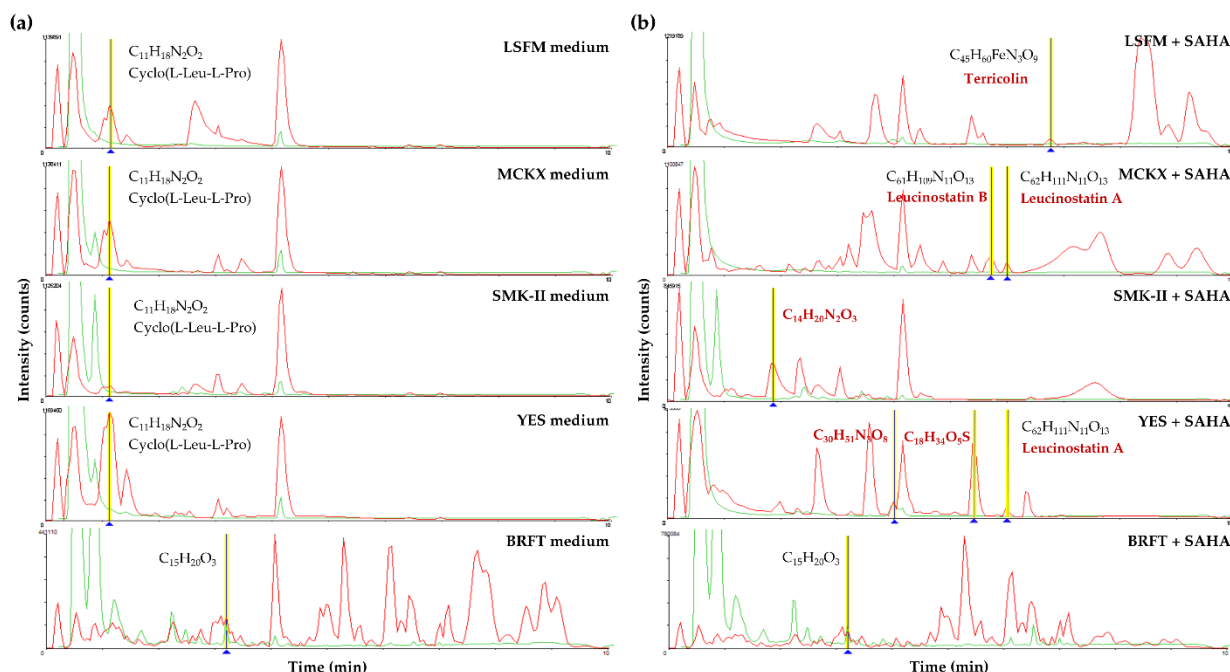


Figure 11. Comparative analysis of HR-MS profiles produced by fermentation of the strain *Corticium* sp. CF-166036 in five different media **(a)** without SAHA addition and **(b)** supplemented with SAHA. HPLC/UV at 210 nm profiles in green and HPLC/HR-MS profiles in red.

Another interesting example of metabolite induction during fermentation in the presence of SAHA is the strain *Microxyphium* sp. CF-164412. LC-MS profiles generated from fermentations in YES, LSFM and BRFT media showed similarities between their conditions with and without SAHA, grouping them in the same clusters (Figure 10b). By contrast, fermentations of this strain in the two new formulations supplemented with SAHA (MCKX and SMK-II media) induced important changes in their chemical profiles, placing both in different clusters distant from their corresponding conditions without SAHA. After comparing HR-MS profiles of this strain, several known and new metabolites were identified in the different fermentation conditions (Figure 12). The described Quinolactacin A₂ (m/z 270.1362; C₁₆H₁₈N₂O₂) was detected only in MCKX and SMK-II media supplemented with SAHA. Moreover, two new metabolites without matches in our internal database or the DNP were identified; m/z 510.2801 (C₂₈H₃₈N₄O₅) was induced by the addition of SAHA to MCKX and SMK-II media and m/z 362.1076 (C₁₇H₁₈N₂O₇) was produced in YES medium with and without the addition of SAHA. Furthermore, a clear improvement in the amounts of Radicinin (m/z 236.0702; C₁₂H₁₂O₅) was observed when this strain was grown in LSFM and YES media in the presence of SAHA.

Both examples demonstrated that the addition of SAHA during fermentations can enhance the production of specific metabolites in individual fungal strains, as well as improving the general diversity and the quantity of metabolites of a wide range of fungal strains.

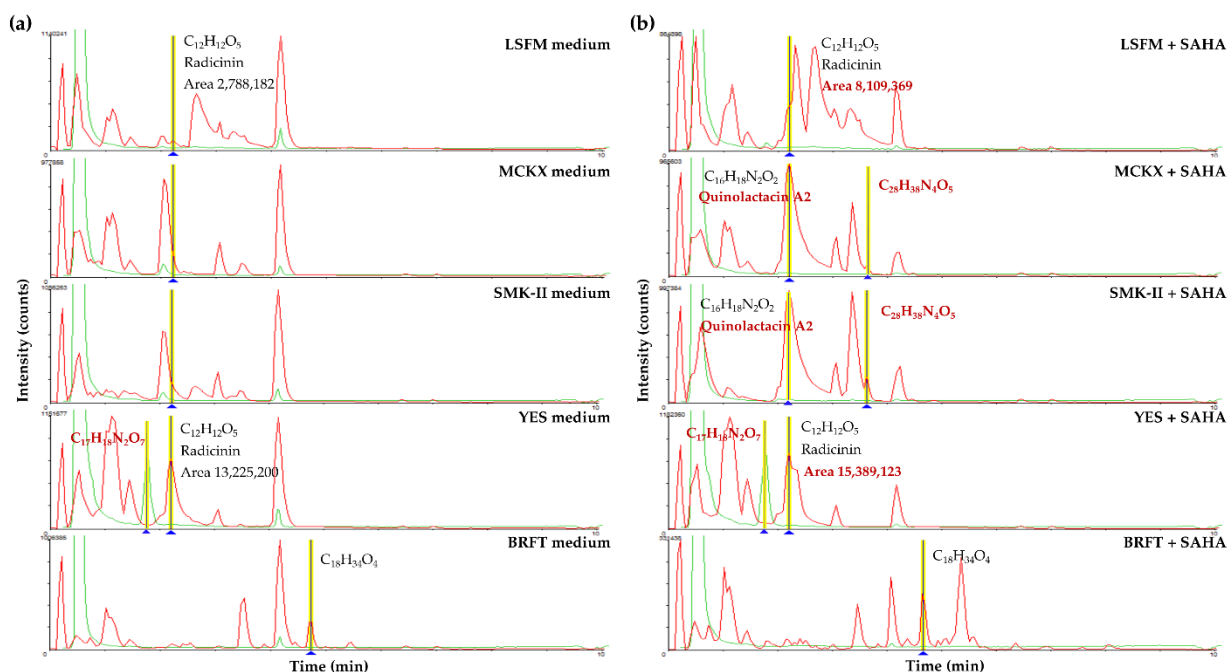


Figure 12. Comparative analysis of HR-MS profiles produced by fermentation of the strain *Microxyphium* sp. CF-164412 in five different media **(a)** without SAHA addition and **(b)** supplemented with SAHA. HPLC/UV at 210 nm profiles in green and HPLC/HR-MS profiles in red.

3. Materials and Methods

3.1. Fungal Strains

A taxonomically diverse subset of 232 fungal strains isolated from leaf litter collected in South Africa was selected for this study. Fungal strains were deposited in the Fundación MEDINA Culture Collection, one of the world's most diverse and productive collections of filamentous fungi. Frozen cryotubes containing fungal inoculum or mycelia discs were cultured in Petri dishes containing YM agar as previously described [10,11,12]. After 7–14 days of incubation, five mycelial discs were transferred and crushed in the bottom of tubes containing 12 mL of SMYA medium in order to obtain a homogeneous mycelia inoculum of each strain. Inoculum tubes were supplemented by the epigenetic modifier Suberoylanilide Hydroxamic Acid (SAHA, TCI H1388), a histone deacetylases inhibitor. SAHA was dissolved in DMSO and adjusted at the final concentration of 100 μ M in inoculum tubes and was incubated on an orbital shaker during 7 days at 22 $^{\circ}$ C and 70% RH [11].

3.2. Fermentation Conditions

Fungal cultures were inoculated by the addition of 0.3 mL of inoculum into EPA vials containing the five production media with the different carbon and nitrogen sources and fermentation states (SmF and SSF). Three of the selected culture media had been commonly used in fungal fermentation: BRFT medium (SSF) [41], LSFM medium and YES medium (SmF) [10,11,12]. Two new formulations

have been developed in this work: MCKX medium (mannitol VWR 25311.297 40 g/L, corn meal yellow SIGMA C6304 10 g/L, yeast extract DIFCO 212750 5 g/L, Murashige and Skoog salts SIGMA M5524 4.3 g/L, xylose SIGMA X1500 10 g/L and deionized water to 1 L) and SMK-II medium (soluble starch from potato PANREAC 121096 40 g/L, maltose FISHER BP 684-500 40 g/L, soybean flour SIGMA S9633 1 g/L, L-proline MERCK 1.07434.0500 3 g/L, Murashige and Skoog salts SIGMA M-5524 4.3 g/L and deionized water to 1 L). SAHA dissolved in DMSO was added to each EPA vial at the final concentration of 100 μ M [11]. Fermentations were incubated at 22 °C and 70% RH for 14 days with the SmF (LSFM, MCKX, SMK-II and YES) media and for 21 days with the BRFT SSF medium.

3.3. Chemical Extraction

After incubation time, fermentation broths from the liquid media were extracted by adding equal volume of acetone [10,11,12] or equivalent volume of methyl-ethyl-ketone (MEK) for solid fermentation, as previously described [30,41], using a Multiprobe II robotic liquid handler (PerkinElmer, Waltham, MA, USA) and shaking at 220 rpm for 1 h. Acetone, miscible with water, has been described as the solvent of choice for whole broth extractions of liquid submerged fermentations [10,11,12], whereas MEK, immiscible with water, extracts just the region of medium to low polarity compounds, but has been reported to be more successful on ensuring maximum extraction of SM for solid state fermentations [9]. The samples were centrifuged, and 12 mL of supernatant from each vial was transferred to glass tubes containing 0.6 mL of DMSO and mixed. The amount of 5 mL of water was added to the solid fermentation extracts and organic solvents, and parts of water were evaporated under a heated nitrogen stream to a final volume of 3 mL (80/20 water/DMSO solution), along with a final concentration of 2 \times WBE [10]. Each fermentation batch included extracts from control media to discriminate their components.

3.4. LC-MS Profile Analysis and Database Matching of Known Metabolites

Fermentations extracts (4 μ L) were analyzed by Liquid Chromatography Mass Spectrometry (LC-MS), with a 10 min gradient using a Zorbax SB-C8 column (3.5 μ m; 2.1 \times 30 mm), on an Agilent 1100 single Quadrupole MSD Low Resolution Mass Spectrometer (Santa Clara, CA, USA). Solvent A consisted of 10% acetonitrile and 90% water with 0.01% trifluoroacetic acid and of 1.3 mM ammonium formate, while solvent B was 90% acetonitrile and 10% water with 0.01% trifluoroacetic acid and 1.3 mM ammonium formate [10,11,12]. The gradient started at 10% of solvent B and went to 100% in 6 min, kept at 100% of solvent B for 2 min and returned to 10% for 2 min to initialize the system, maintained at 40 °C and with a flow rate of 300 μ L/min [10,11,12]. Full diode array UV scans from 100 to 900 nm were collected in 4 nm steps at 0.25 sec/scan. Ionization of eluting solvent was obtained using the standard Agilent 1100 ESI source adjusted to a drying gas flow of 11 L/min at 325 °C and a nebulizer pressure of 40 psig. The capillary voltage was set to 3500 V. Mass spectra were collected as full scans from 150 to 1500 m/z, with one scan every 0.77 s, in both positive and negative modes. Methanol blanks were injected every 80 samples for monitoring each analytical batch.

The obtained chemical raw data consisted in two sets of [rt-m/z] data for each extract in negative and positive ionization modes [28,29]. The sample information regarding each fungal strain, the fermentation medium, additives, extraction procedures and the plate map position in the storage plates were recorded in an Oracle system database (Nautilus LIMS by Thermo) [10,28,29,37,38,39].

Database matching was performed using an in-house developed application where the DAD, retention time, positive and negative mass spectra of the samples were compared to the UV-LC-MS data of known metabolites, stored in a proprietary database where metabolite standard data were obtained using the exact same LC-MS conditions as the samples under analysis [36].

3.5. MASS Studio 2.3 Processing

The LC-MS raw data files were managed in the MASS Studio 2.3 software. This tool allowed the comparison of the [rt-m/z] components detected in all injected samples and to correlate to their corresponding control media [28,29]. Characterization of the generated library of extracts allowed the ranking of the different tested fermentation conditions as previously described [37,38,39]. The prioritization process consisted in the sequential selection of the medium which generated the highest number of [rt-m/z] components or accumulated area of [rt-m/z], indicating the highest chemical diversity achieved and the amount of detectable material [10,37,38,39]. The metabolomic data matrixes were statistically analyzed with the commercial BioNumerics® 6.6 software (Applied Maths™) to generate similarity matrixes according to Dice (presence/absence) and Pearson (area/intensity) coefficients and simple matching UPGMA.

3.6. HR-MS Profile Analysis and Database Matching of Known Metabolites

Selected extracts (2 μ L) were analyzed by HPLC/HR-MS on an Agilent (Santa Clara, CA, USA) 1200, using a Zorbax SB-C8 column (2.1 \times 3.0 mm), maintained at 40 °C with a flow rate of 300 μ L/min. Solvent A consisted of 10% acetonitrile and 90% water with 0.01% trifluoroacetic acid and 1.3 mM ammonium formate, while solvent B was 90% acetonitrile and 10% water with 0.01% trifluoroacetic acid and 1.3 mM ammonium formate. The gradient started at 10% of solvent B and went to 100% in 6 min, kept at 100% of B for 2 min and returned to 10% B for 2 min to initialize the system. Full diode array UV scans from 100 to 900 nm were collected in 4 nm steps at 0.25 sec/scan.

Mass spectrometry acquisition was performed on a Bruker maXis HR-QTOF mass spectrometer (Bruker Daltonics GmbH, Bremen, Germany) coupled to the previously described LC system. Ionization of the eluting solvent was obtained using the standard maxis ESI source adjusted to a drying gas flow of 11 L/min at 200 °C and a nebulizer pressure of 40 psig. The capillary voltage was set to 4000 V. Mass spectra were collected from 50 to 2000 m/z in positive mode.

Chemical profiles were compared to MEDINA's internal database of known Natural Products by fingerprint matching of their retention time, ultraviolet signal and mass spectrometry data [11,12,36]. Compounds that were not identified were further analyzed by HR-MS for tentative identification by matching their predicted molecular formulae with the commercial Chapman & Hall Dictionary of Natural Products (DNP).

4. Conclusions

In summary, this study is the first systematic metabolomic analysis of the effects of SAHA on nutritional arrays of a large number of taxonomically diverse fungal strains cultured in solid and liquid state conditions. The results confirmed that changes in the medium composition influenced largely in their metabolomic profiles. Fermentation conditions were ranked in order to determine the best conditions to improve SM diversity production for each taxonomic group. This was the first chemometric confirmation that supports the solid-state fermentation BRFT as the most productive formulation that generated greater metabolomic changes, which is in line with the described benefits of its culturing for a significant enhancement of SM production. The results also supported the hypothesis that the addition of SAHA during fungal fermentations can determine substantial metabolomic changes of the chemical profiles for entire fungal populations as well as for different taxonomic classes, orders or families. Furthermore, studies on the evaluation of the potential activity of the generated library of extracts are currently in progress, besides the isolation and characterization of the most interesting and unknown metabolites induced by the addition of SAHA to specific fungal fermentations.

References

1. Li, C.Y.; Chung, Y.M.; Wu, Y.C.; Hunyadi, A.; Wang, C.C.; Chang, F.R. Natural products development under epigenetic modulation in fungi. *Phytochem. Rev.* 2020, 19, 1323–1340. [Google Scholar] [CrossRef]
2. Brice, A.P.; Wilson, B.A.; Thornburg, C.C.; Henrich, C.J.; Grkovic, T.; O’Keefe, B.R. Creating and screening natural product libraries. *Nat. Prod. Rep.* 2020, 37, 893–918. [Google Scholar]
3. Hernandez, A.; Nguyen, L.T.; Dhakal, R.; Murphy, B.T. The need to innovate sample collection and library generation in microbial drug discovery: A focus on academia. *Nat. Prod. Rep.* 2021, 38, 292–300. [Google Scholar] [CrossRef]
4. Bader, C.D.; Haack, P.A.; Panter, F.; Krug, D.; Müller, R. Expanding the scope of detectable microbial natural products by complementary analytical methods and cultivation systems. *J. Nat. Prod.* 2021, 84, 268–277. [Google Scholar] [CrossRef] [PubMed]
5. Williams, R.B.; Henrikson, J.C.; Hoover, A.R.; Lee, A.E.; Cichewicz, R.H. Epigenetic remodeling of the fungal secondary metabolome. *Org. Biomol. Chem.* 2008, 6, 1895–1897. [Google Scholar] [CrossRef]
6. Scherlach, K.; Hertweck, C. Triggering cryptic natural product biosynthesis in microorganisms. *Org. Biomol. Chem.* 2009, 7, 1753–1760. [Google Scholar] [CrossRef] [PubMed]
7. Pettit, R.K. Small-molecule elicitation of microbial secondary metabolites. *Microb. Biotechnol.* 2011, 4, 471–478. [Google Scholar] [CrossRef] [PubMed] [Green Version]
8. Bigelis, R.; He, H.; Yang, H.Y.; Chan, L.; Greenstein, M. Production of fungal antibiotics using polymeric solid supports in solid-state and liquid fermentation. *J. Ind. Microbiol. Biotechnol.* 2006, 33, 815–826. [Google Scholar] [CrossRef]
9. Bills, G.F.; Platas, G.; Fillola, A.; Jiménez, M.R.; Collado, J.; Vicente, F.; Martín, J.; González, A.; Bur-Zimmermann, J.; Tormo, J.R.; et al. Enhancement of antibiotic and secondary metabolite detection from filamentous fungi by growth on nutritional arrays. *J. Appl. Microbiol.* 2008, 104, 1644–1658. [Google Scholar] [CrossRef]
10. González-Menéndez, V.; Asensio, F.; Moreno, C.; de Pedro, N.; Monteiro, M.C.; de la Cruz, M.; Vicente, F.; Bills, G.F.; Reyes, F.; Genilloud, O.; et al. Assessing the effects of adsorptive polymeric resin additions on fungal secondary metabolite chemical diversity. *Mycology* 2014, 5, 179–191. [Google Scholar] [CrossRef]
11. González-Menéndez, V.; Pérez-Bonilla, M.; Pérez-Victoria, I.; Martín, J.; Muñoz, F.; Reyes, F.; Tormo, J.R.; Genilloud, O. Multicomponent analysis of the differential induction of secondary metabolite profiles in fungal endophytes. *Molecules* 2016, 21, 234. [Google Scholar] [CrossRef] [Green Version]
12. González-Menéndez, V. Enhancement of chemical diversity in fungal endophytes from arid plants of Andalusia. Ph.D. Thesis, University of Granada, Granada, Spain, 2018. [Google Scholar]
13. Schneider, T.; Keiblinger, K.M.; Schmid, E.; Sterflinger-Gleixner, K.; Ellersdorfer, G.; Roschitzki, B.; Richter, A.; Eberl, L.; Zechmeister-Boltenstern, S.; Riedel, K. Who is who in litter decomposition? Metaproteomics reveals major microbial players and their biogeochemical functions. *ISME J.* 2012, 6, 1749–1762. [Google Scholar] [CrossRef] [Green Version]
14. Bills, G.F.; Polishook, J.D. Abundance and diversity of microfungi in leaf litter of a lowland rain forest in Costa Rica. *Mycologia* 1994, 86, 187–198. [Google Scholar] [CrossRef]

15. Joanne, E.; Taylor, J.E.; Lee, S.; Crous, P.W. Biodiversity in the Cape Floral Kingdom: Fungi occurring on Proteaceae. *Mycol. Res.* 2001, 105, 1480–1484. [Google Scholar]
16. Crous, P.W.; Rong, I.H.; Wood, A.; Lee, S.; Glen, H.; Botha, W.; Slippers, B.; de Beer, W.Z.; Wingfield, M.J.; Hawksworth, D.L. How many species of fungi are there at the tip of Africa? *Stud. Mycol.* 2006, 55, 13–33. [Google Scholar] [CrossRef] [Green Version]
17. Lee, S.; Mel Nik, V.; Taylor, J.E.; Crous, P.W. Diversity of saprobic hyphomycetes on Proteaceae and Restionaceae from South Africa. *Fungal Diversity* 2004, 17, 91–114. [Google Scholar]
18. Mel Nik, V.; Lee, S.; Groenewal, J.Z.; Crous, P.W. New hyphomycetes from Restionaceae in fynbos: *Parasarcopodium ceratocaryi* gen. et sp. nov., and *Rhexodenticula elegiae* sp. nov. *Mycol. Progress* 2004, 3, 19–28. [Google Scholar]
19. Magotra, A.; Kumar, M.; Kushwaha, M.; Awasthi, P.; Raina, C.; Gupta, A.P.; Shah, B.A.; Gandhi, S.G.; Chaubey, A. Epigenetic modifier induced enhancement of fumiquinazoline C production in *Aspergillus fumigatus* (GA-L7): An endophytic fungus from *Grewia asiatica* L. *AMB Expr.* 2017, 7, 43. [Google Scholar] [CrossRef]
20. Zhu, J.X.; Ding, L.; He, S. Discovery of a new biphenyl derivative by epigenetic manipulation of marine-derived fungus *Aspergillus versicolor*. *Nat. Prod. Res.* 2019, 33, 1191–1195. [Google Scholar] [CrossRef]
21. Kouipou, R.; Sahal, D.; Boyom, F. Recent advances in inducing endophytic fungal specialized metabolites using small molecule elicitors including epigenetic modifiers. *Phytochemistry* 2020, 174, 112338. [Google Scholar]
22. Shwab, E.K.; Bok, J.W.; Tribus, M.; Galehr, J.; Graessle, S.; Keller, N.P. Histone deacetylase activity regulates chemical diversity in *Aspergillus*. *Eukaryot. Cell* 2007, 6, 1656–1664. [Google Scholar] [CrossRef] [PubMed] [Green Version]
23. El-Hawary, S.S.; Sayed, A.M.; Mohammed, R.; Hassan, H.M.; Zaki, M.A.; Mostafa, E.; Rateb, M.E.; Mohammed, T.A.; Amin, E.; Abdelmohsen, U.R. Epigenetic modifiers induce bioactive phenolic metabolites in the marine-derived fungus *Penicillium brevicompactum*. *Mar. Drugs* 2018, 16, 253. [Google Scholar] [CrossRef] [PubMed] [Green Version]
24. Henrikson, J.C.; Hoover, A.R.; Joyner, P.M.; Cichewicz, R.H. A chemical epigenetics approach for engineering the in situ biosynthesis of a cryptic natural product from *Aspergillus niger*. *Org. Biomol. Chem.* 2009, 7, 435–438. [Google Scholar] [CrossRef] [PubMed]
25. Beau, J.; Mahid, N.; Burda, W.N.; Harrington, L.; Shaw, L.N.; Mutka, T.; Kyle, D.E.; Barisic, B.; Van Olphen, A.; Baker, B.J. Epigenetic tailoring for the production of anti-infective cytosporones from the marine fungus *Leucostoma persoonia*. *Mar. Drugs* 2012, 10, 762–774. [Google Scholar] [CrossRef] [PubMed]
26. Gubiani, J.R.; Kithsiri, E.M.; Shi, T.; Araujob, A.R.; Arnold, E.; Chapman, E.; Gunatilaka, A.A. An epigenetic modifier induces production of (10'S)-verruculide B, an inhibitor of protein tyrosine phosphatases by *Phoma* sp. nov. LG0217, a fungal endophyte of *Parkinsonia microphylla*. *Bioorg. Med. Chem.* 2017, 25, 1860–1866. [Google Scholar] [CrossRef] [PubMed] [Green Version]
27. Zhang, S.; Fang, H.; Yin, C.; Wei, C.; Hu, J.; Zhang, Y. Antimicrobial metabolites produced by *Penicillium mallochii* CCH01 isolated from the gut of *Ectropis oblique*, cultivated in the presence of a histone deacetylase inhibitor. *Front. Microbiol.* 2019, 10, 2186. [Google Scholar] [CrossRef] [PubMed]

28. Martínez, G.; González-Menéndez, V.; Martín, J.; Reyes, F.; Genilloud, O.; Tormo, J.R. MASS Studio: A novel software utility to simplify LC-MS analyses of large sets of samples for metabolomics. In *Proceedings of the Bioinformatics and Biomedical Engineering: 5th International Work-Conference, IWBBIO, Granada, Spain, 26–28 April 2017*; Ignacio Rojas, Francisco Ortuño; *Lecture Notes in Computer Science*, volume 10208; Springer: Cham, Switzerland, 2017. [Google Scholar]
29. González-Menéndez, V.; Martínez, G.; Serrano, R.; Muñoz, F.; Martín, J.; Genilloud, O.; Tormo, J.R. Ultraviolet (IUV) and mass spectrometry (IMS) imaging for the deconvolution of microbial interactions. *BMC Syst. Biol.* 2018, 12, 99. [Google Scholar] [CrossRef] [Green Version]
30. Bills, G.F.; Dombrowski, A.W.; Goetz, M.A. The “FERMEX” Method for Metabolite-Enriched Fungal Extracts. In *Fungal Secondary Metabolism: Methods and Protocols, Methods in Molecular Biology*; Keller, N.P., Turner, G., Eds.; Springer Science+Business Media: Totowa, NJ, USA, 2012; Volume 944, pp. 79–96. [Google Scholar]
31. Barrios-González, J.; Mejía, A. Production of secondary metabolites by solid-state fermentation. *Biotechnol. Annu. Rev.* 1996, 2, 85–121. [Google Scholar]
32. Manan, M.A.; Webb, C. Design aspects of solid state fermentation as applied to microbial bioprocessing. *J. Appl. Biotechnol. Bioeng.* 2017, 4, 511–532. [Google Scholar]
33. Yao, F.; Liu, S.C.; Wang, D.N.; Liu, Z.J.; Hua, Q.; Wei, L.J. Engineering oleaginous yeast *Yarrowia lipolytica* for enhanced limonene production from xylose and lignocellulosic hydrolysate. *FEMS Yeast Res.* 2020, 20, 6. [Google Scholar] [CrossRef]
34. Petersen, L.A.; Hughes, D.L.; Hughes, R.; Di Michele, L.; Salmon, P.; Connors, N. Effects of amino acid and trace element supplementation on pneumocandin production by *Glarea lozoyensis*: Impact on titer, analogue levels, and the identification of the new analogues of pneumocandin B0. *J. Ind. Microbiol. Biotechnol.* 2001, 26, 216–221. [Google Scholar] [CrossRef]
35. Fernández-Miranda, E.; Casares, A. Influence of the culture media and the organic matter in the growth of *paxillus ammoniavirescens* (Contu & Dessi). *Mycobiology* 2017, 45, 172–177. [Google Scholar]
36. Pérez-Victoria, I.; Martín, J.; Reyes, F. Combined LC/UV/MS and NMR strategies for the dereplication of marine natural products. *Planta. Med.* 2016, 82, 857–871. [Google Scholar] [CrossRef] [PubMed] [Green Version]
37. García, J.B.; Tormo, J.R. HPLC-studio: A novel software utility to perform HPLC chromatogram comparison for screening purposes. *J. Biomol. Screen* 2003, 8, 305–315. [Google Scholar] [CrossRef] [PubMed] [Green Version]
38. Tormo, J.R.; García, J.B.; De Antonio, M.; Feliz, J.; Mira, A.; Díez, M.T.; Hernández, P.; Peláez, F. A method for the selection of production media for actinomycete strains based on their metabolite HPLC profiles. *J. Ind. Microbiol. Biotechnol.* 2003, 30, 582–588. [Google Scholar] [CrossRef] [PubMed]
39. Tormo, J.R.; Garcia, J.B. Automated Analyses of HPLC Profiles of Microbial Extracts: A new tool for drug discovery screening. In *Natural Products: Drug Discovery and Therapeutic Medicine*; Zhang, L., Demain, A.L., Eds.; Humana Press: Totowa, NJ, USA, 2005; Volume 3, pp. 57–75. [Google Scholar]
40. Knapp, D.G.; Kovács, G.M. Interspecific metabolic diversity of root-colonizing endophytic fungi revealed by enzyme activity tests. *FEMS Microbiol. Ecol.* 2016, 92, 1–10. [Google Scholar] [CrossRef] [PubMed] [Green Version]

Chapter 2

41. Peláez, F.; Cabello, A.; Platas, G.; Díez, M.T.; González, A.; Basilio, A.; Martán, I.; Vicente, F.; Bills, G.F.; Giacobbe, R.A.; et al. The discovery of enfumafungin, a novel antifungal compound produced by endophytic *Hormonema* species, biological activity, and taxonomy of the producing organisms. *Syst. Appl. Microbiol.* 2000, 23, 333–343. [Google Scholar] [CrossRef]

Chapter 3

Development and validation of a HTS Platform for the
discovery of new antifungal agents against four
relevant fungal phytopathogens

Rachel Serrano, Víctor González-Menéndez, José R. Tormo, Olga Genilloud

Journal of Fungi, 2023

Special Issue Plant Protection: New Green Antifungal Agents

9 (9), 883; <https://doi.org/10.3390/jof9090883>

JCR 4.2, Q2, total journal citations 15491

Abstract

Fungal phytopathogens are the major agents responsible for causing severe damage to and losses in agricultural crops worldwide. *Botrytis cinerea*, *Colletotrichum acutatum*, *Fusarium proliferatum*, and *Magnaporthe grisea* are included in the top ten fungal phytopathogens that impose important plant diseases on a broad range of crops. Microbial Natural Products can be an attractive alternative for the biological control of phytopathogens. The objective of this work was to develop and validate a High-throughput Screening (HTS) Platform to evaluate the antifungal potential of chemicals and Natural Products against these four important plant pathogens. Several experiments were performed to establish the optimal assay conditions that provide the best reproducibility and robustness. For this purpose, we have evaluated two media formulations (SDB and RPMI-1640), several inoculum concentrations (1×10^6 , 5×10^5 and 5×10^6 conidia/mL), the germination curves for each strain, each strain's tolerance to dimethyl sulfoxide (DMSO), and the Dose Response Curves (DRC) of the antifungal control (Amphotericin B). The assays were performed in 96-well plate format, where absorbance at 620 nm was measured before and after incubation to evaluate growth inhibition, and fluorescence intensity at 570 nm excitation and 615 nm emission was monitored after resazurin addition for cell viability evaluation. Quality control parameters (RZ' Factors and Signal to Background (S/B) ratios) were determined for each assay batch. The assay conditions were finally validated by titrating 40 known relevant antifungal agents and testing 2400 microbial Natural Product extracts from the MEDINA Library through both HTS agar-based and HTS microdilution-based set-ups on the four phytopathogens.

Keywords: phytopathogenic fungi; fungicides; high-throughput screening; biocontrol agents

1. Introduction

Plant pathogens are one of the major problems affecting agriculture worldwide. They are responsible for the loss of one third of the crops produced annually [1,2]. Fungal phytopathogens are widely distributed and can impose plant diseases on a large variety of plants, including cereals, vegetables, and fruit. They can infect plants through various mechanisms of pathogenesis, often accompanied by the biosynthesis of mycotoxins, which generates important yield losses that have a considerable economic impact on the agricultural sector [3].

Based on their scientific/economic importance, the top ten fungal phytopathogens have been identified [4] in rank order as (i) *Magnaporthe oryzae*, a phytopathogen model for plant host studies that, together with *M. grisea*, is one of the main causal agents of blast rice, the most destructive plant disease [5,6,7]; (ii) *Botrytis cinerea*, responsible for gray mold, which generates severe damages and losses in fruit, vegetables, and ornamental plants during both pre- and post-harvesting steps [4,8,9,10]; (iii) *Puccinia* spp., the cause of three types of royal diseases in *Triticum aestivum* which seriously impact wheat production, mainly via the infection of *P. graminis*, *P. striiformis*, and *P. tritricina* [4]; the genus *Fusarium*, which includes a high number of pathogenic species, can produce numerous mycotoxins and colonize plants in a wide range of climatic areas; (iv) *Fusarium graminearum*, (v) *Fusarium oxysporum*, and *Fusarium proliferatum*, which can infect a broad range of crops such as maize, wheat, rice, soybean, barley, fruit, and even ornamental plants, where one of the most significant damages is root rot [11]; (vi) *Blumeria graminis*, which is

the causal agent of powdery mildew in barley and wheat crops and is considered a high-risk pathogen because of its potential to change its virulence [12]; (vii) *Zymoseptoria tritici*, which is responsible for the most important wheat disease, the Septoria leaf blotch, with a high percentage of infection, inducing significant damages; (viii) *Colletotrichum* spp., which are the genera that promote the anthracnose disease in more than 3000 plant species and can alternate between different infection stages (hemibiotrophic, necrotrophic, and biotrophic), making it very efficient in propagation and leading to considerable worldwide economic losses in fruit and vegetable crops [4,13,14,15,16]; (ix) *Ustilago maydis*, a homobasidiomycete that normally infects maize (*Zea mays*) through a complex pathogenic process, including morphogenetic transitions until its sexual cycle is completed [17]; and finally, (x) *Melampsora lini*, responsible for the rust disease on *Linum usitatissimum*, which causes severe losses in seed yields as well as a fiber quality reduction in flax plants [18].

Nowadays, the preferred strategy for managing plant diseases and crop protection is the use of a broad range of chemical agents such as fungicides combined with herbicides and insecticides. The use of synthetic fungicides has enabled the efficient control of fungal infections and improved the production yields and quality of crops [19,20,21]. However, the continuous and extended use of these agrochemicals has shown a severe negative impact on both environmental and human health [19,22]. Chemical fungicides accumulated in soils, plants, and water may seriously affect humans through the food chain [22], and their application has become strictly regulated to reduce their toxicity in agricultural fields and guarantee food safety. Given these current limitations, there is an urgent need to develop safe, efficient, and environmentally friendly next-generation fungicides.

The most common methods to identify antifungal agents against filamentous fungi include agar dilution and disc diffusion assays on Petri dishes [23,24]. These manual methods are time-consuming, expensive, and require large quantities of material to be tested [23]. The introduction of a miniaturized High-throughput Screening (HTS) Platform for agar-based assays by our group fixed some of these problems [25]. However, to date, few methods for the determination of the susceptibility of phytopathogens to fungicides in in vitro set-ups using liquid conditions have been reported. Specifically, the microdilution methodology provides the advantages of simplicity, reliability, and time- and cost-effectiveness and could be scalable for a large number of samples, which makes it ideal for wide screening campaigns looking for new fungicide agents [23,24].

Microbial Natural Products are an untapped source of new bioactive molecules with broad applications. The use of natural agents for the biocontrol of phytopathogens offers an attractive alternative to enable economical and environmentally sustainable agriculture in the forthcoming decades [26,27,28]. HTS approaches with Natural Products allow for both the evaluation of pure compounds and the extraction of mixtures for the rapid identification of new potential antifungal agents with a simple and accurate detection technique in a miniaturized assay with reduced costs.

Therefore, in this study, we have developed two miniaturized HTS methodologies based on agar and liquid assays to identify and characterize the antifungal properties of a wide variety of samples (pure compounds and Natural Product mixtures) against four relevant fungal phytopathogens: *Botrytis cinerea*, *Colletotrichum acutatum*, *Fusarium proliferatum*, and *Magnaporthe oryzae*. In this sense, the final objective of this study was to provide a validated HTS platform to enable the efficient discovery of next-generation fungicides for the biocontrol of these four important phytopathogens.

2. Materials and Methods

2.1. Fungal Strains and Conidia Production

Four fungal strains were obtained from CBS-KNAW Fungal Biodiversity Centre, CECT Spanish Type Culture Collection and MEDINA Fungal Collection. *Botrytis cinerea* B05.10 (CECT 20754) was isolated from *Vitis vinifera* in Italy, *Colletotrichum acutatum* CF-137177 was isolated from a dead leaf collected in Mexico, *Fusarium proliferatum* CBS 115.97 was isolated from *Dianthus caryophyllus* in Italy, and *Magnaporthe grisea* CF-105765 was isolated from the ear blast on *Eleusine indica* collected in Argentina.

Each phytopathogen was cultured in five solid media and five liquid media to optimize their sporulation process. The solid media evaluated were 2% malt agar (MEA), corn meal agar (CMA), oatmeal agar (OAT), potato dextrose agar (PDA), and yeast-malt agar (YM) [25]. The submerged culture conditions assessed were also achieved by using three traditional media following a previously described protocol (SDB, PDB, and SMY) [25,29,30] and two new formulations: GMS medium (glycerol 5 g/L, Bacto malt extract 10 g/L, Difco soy peptone 10 g/L, Difco dextrose 4 g/L, ammonium sulfate 2 g/L, KH_2PO_4 1 g/L, $\text{MgSO}_4 \cdot 7\text{H}_2\text{O}$ 0.5 g/L, $\text{FeSO}_4 \cdot 7\text{H}_2\text{O}$ 0.005g/L, pH adjusted at 7) and VME medium (vegetable peptone Biochemika 10 g/L, Bacto malt extract 40 g/L, Difco yeast extract 0.4 g/L, $(\text{NH}_4)_2\text{SO}_4$ 2.4 g/L, pH adjusted at 6.6).

Conidia solutions were obtained following different protocols depending on the sporulation condition (solid or liquid). After 14–28 days of incubation (specific timing for each strain, the surfaces of the sporulated agar plates ($n=5$) were scraped with a sterile loop and a Tween 80 solution 0.1% (v/v), and the resulting suspension was filtered through sterile cotton gauzes. In the case of cultures in liquid conditions, each inoculum tube containing 16 mL of media was directly filtered and washed to remove medium remains and therefore obtain a final homogeneous solution. The resulting conidia stocks were adjusted to a final volume of 10 mL, and the concentration of conidia per milliliter was determined by counting in a Neubauer chamber 0.0025 mm^2 . All experiments were performed on three different days/batches to compare the robustness of production and select the optimal condition and method for each fungal strain.

2.2. Agar-Based Assays against Fungal Phytopathogens

Agar-based assays against *C. acutatum*, *F. proliferatum*, and *M. grisea* have been already described by our group [25], where the optimal conditions were successfully determined to allow for the evaluation of the antifungal activity of microbial extracts. However, the agar-based assay of *B. cinerea* required new adjustments to be made to the different parameters. Following the steps described for the other three phytopathogens [25], *B. cinerea* conidia were inoculated in Sabouraud Dextrose Agar medium (SDA) adjusted in a range from 1×10^4 to 5×10^7 conidia/mL. Once solidified, the samples were dispensed on the top of the agar containing the inoculum. Five antifungal compounds were evaluated as positive controls to determine the optimal concentrations for a reference Dose Response Curve (DRC): amphotericin B (AmB), azoxystrobin, cycloheximide, cyproconazole, and econazole. The plates were incubated at 25 °C and 70% relative humidity (RH) at different times, with 48 h proving to be the optimum time. The diameter and turbidity of the

inhibition halos were calculated using proprietary Image Analyzer® software (version 1.0.3393.20294) and a stereoscope (Leica™ MZ16).

2.3. Liquid-Based Assays against Fungal Phytopathogens

The methodology developed in this work was adapted from the previously described HTS protocol for the human fungal pathogen *Aspergillus fumigatus* [31]. Two media formulations were compared to select the assay medium: Sabouraud Dextrose Broth (SDB) was the reference medium for the agar-based assay and is commonly used in mycology laboratories [25,32,33], and RPMI-1640 was already used for the *A. fumigatus* antifungal assays and is also recommended by the CLSI (Clinical & Laboratory Standards Institute) and the EUCAST (European Committee on Antimicrobial Susceptibility Testing) [31]. Several experiments were performed to establish the optimal inoculum concentration which provided the highest reproducibility and robustness for each phytopathogen: 1×10^6 conidia/mL (same used in the agar-based assay), 5×10^5 , and 5×10^6 conidia/mL. Plates were incubated at 25 °C and 70% RH from 8 to 168 h to define the growth curve for each phytopathogen and determine the optimal incubation times. Absorbance at 620 nm was measured in a spectrofluorometer ENVISION™ Multilabel Reader (PerkinElmer, Waltham, MA, USA) before and after incubation. Finally, for the cell viability evaluation, 10 µL of resazurin at 0.02% (w/v) was added, and fluorescence intensity at 570 nm excitation and 615 nm emission was monitored from 5 min to 4 h of incubation at 37 °C for dye reduction evaluation [23,31,32].

2.4. Validation of Assay Conditions

Once the optimal assay conditions were established for each plant pathogen, primary screening with 40 known antifungal standards was performed to validate the assay parameters. The samples were tested in triplicate, and active compounds were evaluated in DRC. Finally, the assays were also validated with a subset of 2400 microbial extracts (Natural Products mixtures). For this purpose, extracts were selected from the MEDINA microbial extract Library, obtained from microbial fermentations of both actinomycetes and fungi.

The assays were performed in Corning® Costar™ 96-well plates containing a set of control wells in the first and last columns according to the following layout: the four top wells of the first column (1A–1D wells) with the positive control (inoculum + AmB in DMSO), the four bottom wells (1E–1H) with the negative control (inoculum + 2% DMSO), and the last column (A12–H12) containing a reference DRC of AmB in 2% DMSO. The samples were first dispensed (2–10 µL) in columns 2–11 with an automated liquid handler Biomek i7, Beckman Coulter® (Life Sciences Division Headquarters, Indianapolis, IN, USA), then the inoculum was added to a final volume of 100 µL using a Thermo Scientific Multidrop Combi (MTX Lab System, Vienna, VA, USA).

2.5. Data Analysis

Absorbance and fluorescence raw data were used to calculate antifungal activity via the Genedata Screener® software (Genedata AG, Basel, Switzerland). Absorbance values for each well were obtained from the difference between the absorbance measured before and after incubation time. The percentage of inhibition (% INH) was determined for each sample by the following equations integrated in the software. For the absorbance-based assay, $\% \text{ INH} = (\text{Abs}_{\text{test}} - \text{Abs}_{\text{pos}}) / (\text{Abs}_{\text{neg}} - \text{Abs}_{\text{pos}})$, where Abs_{test} was the absorbance of the evaluated sample, and Abs_{pos} and Abs_{neg} were the absorbances for the positive and negative controls. For the fluorescence-based assay, $\% \text{ INH} = 100 - \% \text{ Reduction}$ and $\% \text{ Reduction} = 100 \times (\text{Fl}_{\text{test}} - \text{Fl}_{\text{pos}}) / (\text{Fl}_{\text{neg}} - \text{Fl}_{\text{pos}})$, where Fl_{test} , Fl_{pos} , and Fl_{neg} corresponded to the fluorescence intensity of a given evaluated sample and positive and negative controls, respectively.

DRCs of the studied standards were calculated following a sigmoidal shape and adjusted to a classical hill equation integrated in the software: $E/E_{\text{max}} = A^n / (IC_{50}^n + A^n)$, where E corresponded with the response, A was the compound concentration, IC_{50} was the compound concentration that produced 50% of the maximal response, and n was the Hill coefficient, which was calculated using the following formula: $n = \log(81) / \log(EC_{90}/EC_{10})$, with EC_{90} and EC_{10} being the concentrations that produced 90% and 10% of the maximal response, respectively. The quality control (QC) parameters—Robust Z Factor (RZ' Factor), Signal/Background ratio (S/B), and the IC_{50} ($\mu\text{g/mL}$) of the positive control AmbB—were determined for each batch of assay plates.

Additional statistical analysis using JMP® software was applied to distribute and categorize the activity population obtained from the piloting HTS approach).

3. Results and Discussion

3.1. Induction of the Sporulation of Fungal Phytopathogens

The first step of the HTS assay development involved the definition of a standardized method for conidia production. The optimal condition to induce the sporulation was specific for each of the four phytopathogens tested (Table 1). *B. cinerea* only produced a sufficient concentration of conidia for the assay on solid media, specifically when it was cultured on OAT medium for 21 days at 25 °C (where the concentration obtained was $3.7 \times 10^7 \pm 1.9$ conidia/mL). The other three strains produced conidia in both solid and liquid culture conditions (Table 1). In the case of *C. acutatum*, no significant differences were observed in the concentration of conidia: $8.8 \times 10^7 \pm 1.7$ conidia/mL from solid culture on YM medium after 21 days, and $7.8 \times 10^7 \pm 1.9$ conidia/mL from submerged culture in SMY liquid medium (220 rpm) for 3 days. For *F. proliferatum*, the best sporulation was obtained from the overnight inoculum in SMY medium ($2.5 \times 10^8 \pm 0.4$ conidia/mL), in agreement with previous published data [25]. Finally, *M. grisea* produced the highest concentration of conidia on CMA agar plates ($2.7 \times 10^8 \pm 1.0$ conidia/mL), although no significant differences were observed in liquid conditions when cultured for 2 days in the new medium formulation VME ($2.3 \times 10^8 \pm 0.9$ conidia/mL).

Table 1. Conidia concentrations obtained from the cultivation of the four phytopathogens in the 10 studied culture conditions. The most productive conditions for each fungal strain are highlighted in bold. Average and standard deviations were calculated with triplicate data from different batches.

Culture Media	Concentration (conidia/mL)			
	<i>B. cinerea</i>	<i>C. acutatum</i>	<i>F. proliferatum</i>	<i>M. grisea</i>
Solid Culture Media				
CMA	-	-	$2.4 \times 10^7 \pm 1.3$	$2.7 \times 10^8 \pm 1.0$
MEA	$5.9 \times 10^5 \pm 1.9$	$1.3 \times 10^6 \pm 0.9$	$1.2 \times 10^8 \pm 1.0$	$9.3 \times 10^7 \pm 1.2$
OAT	$3.7 \times 10^7 \pm 1.5$	$4.6 \times 10^7 \pm 3.4$	$1.9 \times 10^7 \pm 0.6$	-
PDA	$6.7 \times 10^5 \pm 2.9$	$3.3 \times 10^7 \pm 1.7$	$1.3 \times 10^8 \pm 0.5$	$1.3 \times 10^8 \pm 0.8$
YM	$8.3 \times 10^5 \pm 2.9$	$8.8 \times 10^7 \pm 1.7$	$1.4 \times 10^8 \pm 0.8$	$1.9 \times 10^8 \pm 0.9$
Liquid Culture Media				
SDB	-	$5.3 \times 10^6 \pm 3.3$	$9.0 \times 10^7 \pm 1.4$	$9.3 \times 10^7 \pm 2.3$
SMY	-	$7.8 \times 10^7 \pm 1.9$	$2.5 \times 10^8 \pm 0.4$	$1.9 \times 10^8 \pm 1.1$
PDB	-	$2.0 \times 10^6 \pm 0.4$	$8.7 \times 10^7 \pm 1.0$	$9.7 \times 10^7 \pm 2.4$
GMS	-	$8.7 \times 10^6 \pm 2.1$	$8.7 \times 10^7 \pm 1.3$	$1.5 \times 10^8 \pm 0.6$
VME	-	$2.9 \times 10^7 \pm 1.3$	$1.4 \times 10^8 \pm 0.5$	$2.3 \times 10^8 \pm 0.9$

(-) No conidia obtained after filtration, only mycelium development observed.

In general, the best conditions for the sporulation of *B. cinerea* and *F. proliferatum* were cultivation in OAT agar plates and in the SMY submerged tube, respectively. However, for *C. acutatum* and *M. grisea*, both solid and liquid cultures provided similar conidia production rates. Significant advantages in time and cost requirements were clearly observed for liquid cultivation when compared to solid conditions (Table 2), and therefore, the liquid culture in SMY was selected for the sporulation of *C. acutatum*, and VME was selected for *M. grisea*.

Table 2. Comparison of requirements to obtain a stock solution of fungal conidia from solid and liquid culture conditions.

Parameters	Solid medium	Liquid medium
Time of incubation	10 - 21 days	24 - 72 hours
Volume of inoculum	200 mL (5 Petri plates)	16 mL (1 Test tube)
Time to obtain conidia solution	1h (Scraping + Filtration)	30 min (Filtration)

3.2. *Botrytis cinerea* Agar-Based Assay

Four final concentrations of *B. cinerea* conidia in SDA medium were compared: 1×10^5 , 5×10^5 , 1×10^6 , and 5×10^6 conidia/mL (Figure 1) [25,34]. Concentrations of 1×10^5 and 5×10^5 conidia/mL generated a very sparse and translucent layer of mycelium growth that required long incubation times to show good defined inhibition halos (Figure 1a,b). On the contrary, 5×10^6 conidia/mL generated a very dense mycelium growth more resistant to AmB (Figure 1d). The concentration of 1×10^6 conidia/mL showed the best definition of the inhibition zones for the AmB curve, providing a good assay window between positive and negative controls (Figure 1c). Therefore, the optimal concentration for the *B. cinerea* agar-based assay was considered to be 1×10^6 conidia/mL. AmB at 100 $\mu\text{g/mL}$, and 20% DMSO were used as positive and negative controls, respectively. The AmB reference curve included 1:2 serial dilution concentrations from 50 $\mu\text{g/mL}$ to 6.25 $\mu\text{g/mL}$. The plates were incubated for 48 h at 25 °C and 70% RH to ensure clear zones of inhibition.

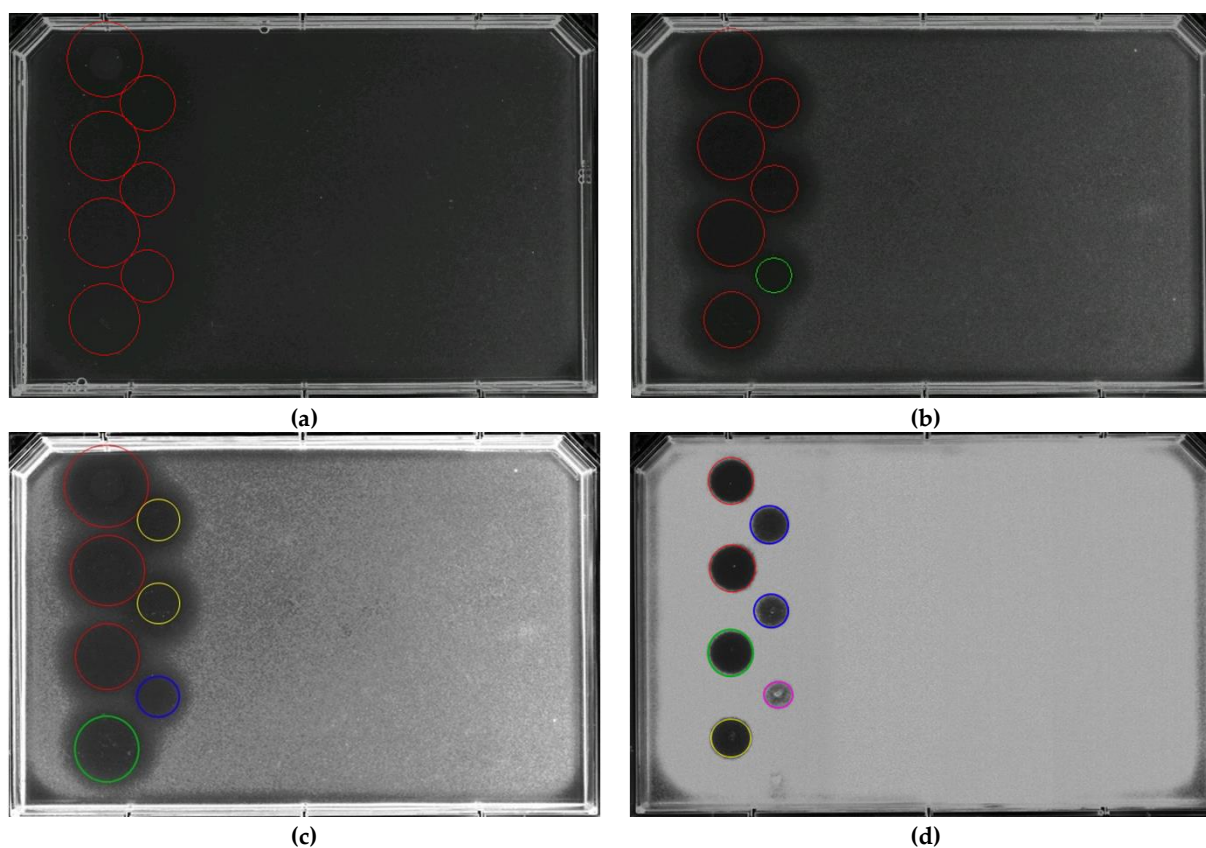


Figure 1. Agar-based assay using four different concentrations of *Botrytis cinerea* conidia: **(a)** 1×10^5 conidia/mL, **(b)** 5×10^5 conidia/mL, **(c)** 1×10^6 conidia/mL, and **(d)** 5×10^6 conidia/mL. Inhibition zones corresponded to the AmB curve starting at 200 $\mu\text{g/mL}$ with eight-point 1:2 serial dilutions to 1.56 $\mu\text{g/mL}$. Inhibition halos were highlighted based on diameter (cm) and turbidity (circle color) to assess the antifungal activity of the compounds. The halos were sorted into five categories depending on the conidia germination rates: halo A (red) corresponds to the highest activity where germination was not observed, halo B (green) where 25% of conidia started to germinate, halo C (yellow) for 50% of germination, halo D (blue) for 75% of germination, and halo E (pink) for 100% germination with high turbidity, indicating the lowest activity.

3.3. *Botrytis cinerea* Microdilution Assay

The first step to develop the antifungal assay with *Botrytis cinerea* using the microdilution method was to determine the best liquid medium that allowed for optimal signal detection from the two different media under comparison: SDB and RPMI-1640 [25,31,32,33]. *B. cinerea* developed good growth in both media, with all conidia germinating and developing mycelium. The absorbance raw data was similar in both media, but the fluorescence readouts showed some differences that could be observed visually and when fluorescence intensity was measured. Positive control wells remained blue (indicating absence of metabolic activity and no germination), whereas negative control wells turned into a fluorescent pink color (indicating metabolic activity and conidia germination) [31]. When *B. cinerea* was grown in the RPMI medium, we observed that the described blue color in the inhibited wells (Figure 2aP) corresponded to a fluorescence intensity of 605 ± 10 RFU, and a fluorescent pink color in the negative control wells (Figure 2aN) corresponded to a higher fluorescence intensity of $13,450 \pm 292$ RFU. However, the viability assay in SDB medium showed a purple color in negative controls (Figure 2bN), with lower fluorescence values of 8063 ± 420 RFU. In addition, the two specific fungi media SMF1 [35] and PDB [30] were evaluated, showing similar results for the fluorescence readouts than those obtained for the SDB medium [30,35]. After statistical analysis, the S/B and RZ' factors were determined (120 wells of negative controls and 120 wells of positive controls) and were significantly better in the RPMI medium, highlighting it as the optimal medium for signal detection.

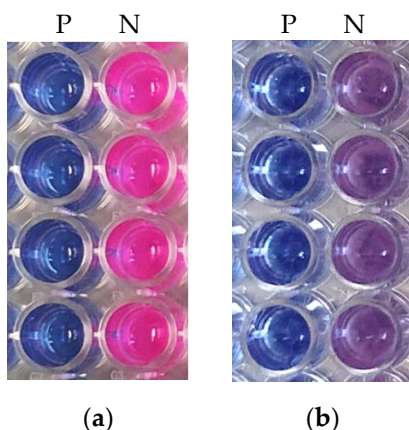


Figure 2. Resazurin reaction in the control wells in (a) RPMI-1640 medium and (b) SDB medium. **P** indicates the positive control wells (growth inhibition), whereas **N** indicates the negative control wells (normal growth).

The best three inoculum concentrations obtained from the *B. cinerea* agar-based assay were evaluated for the microdilution assay: 5×10^5 , 1×10^6 and 5×10^6 conidia/mL. The growth inhibition assay showed that 5×10^6 conidia/mL generated very dispersed absorbance data with considerably low QC parameters (Table 3 and Figure 3). This could be due to the saturated background generated by the addition of a high concentration of *B. cinerea* conidia. Lower concentrations of 5×10^5 and 1×10^6 conidia/mL presented more homogeneous and robust absorbance data without significant differences between RZ' factors (0.77 and 0.79, respectively) (Table 3). However, the viability assay clearly supported 1×10^6 conidia/mL as the optimal concentration, with the highest RZ' (0.89) and

S/B (23.19), in agreement with Pelloux-Prayer et al. 1998, who reported this conidia concentration as the best one for a fluorescence test using Alamar blue [36]. Therefore, 1×10^6 conidia/mL was selected as the optimal concentration that provided robust data with a broad assay window for absorbance and fluorescence readouts for the *B. cinerea* assay.

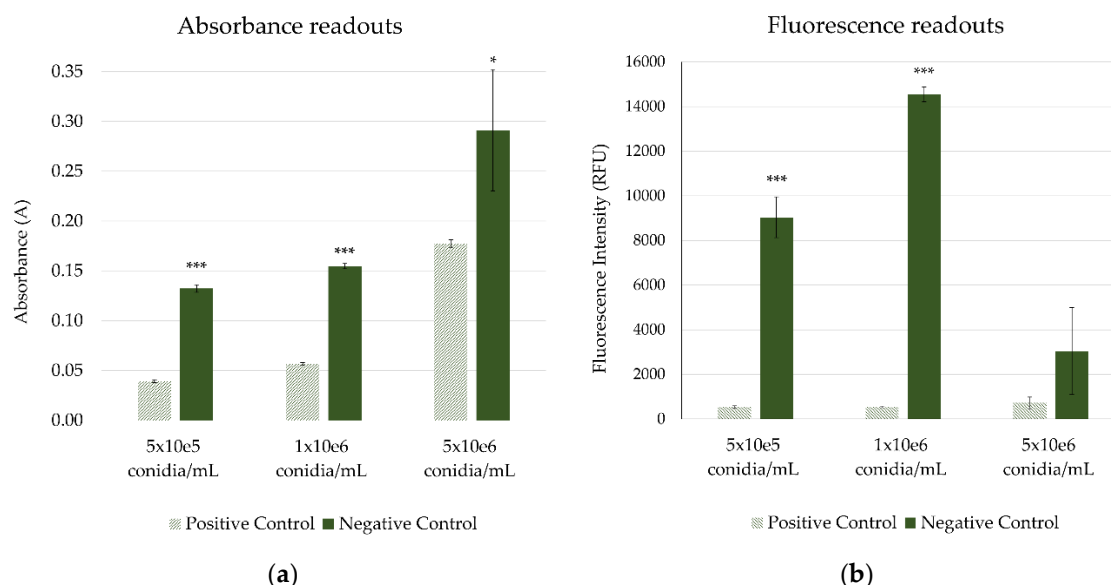


Figure 3. Influence of three concentrations of *Botrytis cinerea* conidia on **(a)** absorbance and **(b)** fluorescence readouts in RPMI-1640 medium. Positive control corresponds to AmB at 100 μ g/mL in 2% DMSO, and negative control corresponds to 2% DMSO (final concentrations). * $p < 0.05$, *** $p < 0.001$.

Table 3. Quality control parameters obtained for three different *B. cinerea* conidia concentrations for absorbance and fluorescence readouts. The condition that provided the most robust data is highlighted in bold.

Concentration of inoculum	Absorbance		Fluorescence	
	S/B	RZ'	S/B	RZ'
5×10^5 conidia/mL	15.31	0.76	11.74	0.76
1×10^6 conidia/mL	37.40	0.77	23.19	0.90
5×10^6 conidia/mL	2.33	< 0	7.65	0.55

The growth curve of *Botrytis cinerea* in the presence of positive and negative controls was analyzed to determine the optimal time for assay incubation. The absorbance values of the negative controls increased with time, while the positive controls remained constant (Figure 4, both green lines). Consequently, the S/B ratio also increased at longer incubation times after 48 h. The RZ' factors showed robustness until 120 h of incubation ($RZ' > 0.7$); hence, the optimal time for the absorbance readout was determined to be in the range of 48 to 120 h. On the other hand, the fluorescence readouts presented the highest assay window when resazurin was added after 24 h of incubation

but decreased with longer incubation times as the fluorescence of negative controls could not reach the maximum fluorescence intensity. This effect could be related to the presence of a high metabolic activity due to the high amount of germinated conidia, which could rapidly reduce the resazurin to hydroresorufin (non-fluorescent) and generate a false signal of viability. The RZ' factor also decreased with longer times, being acceptable until 72 h of incubation ($RZ' > 0.7$). Then, the best readout time for the viability assay of *B. cinerea* (fluorescence) was defined to be in the range of 24 to 72 h, with incubation for 72 h allowing for the evaluation of both the growth inhibition and cell viability of *B. cinerea* conidia within the same plate set-up.

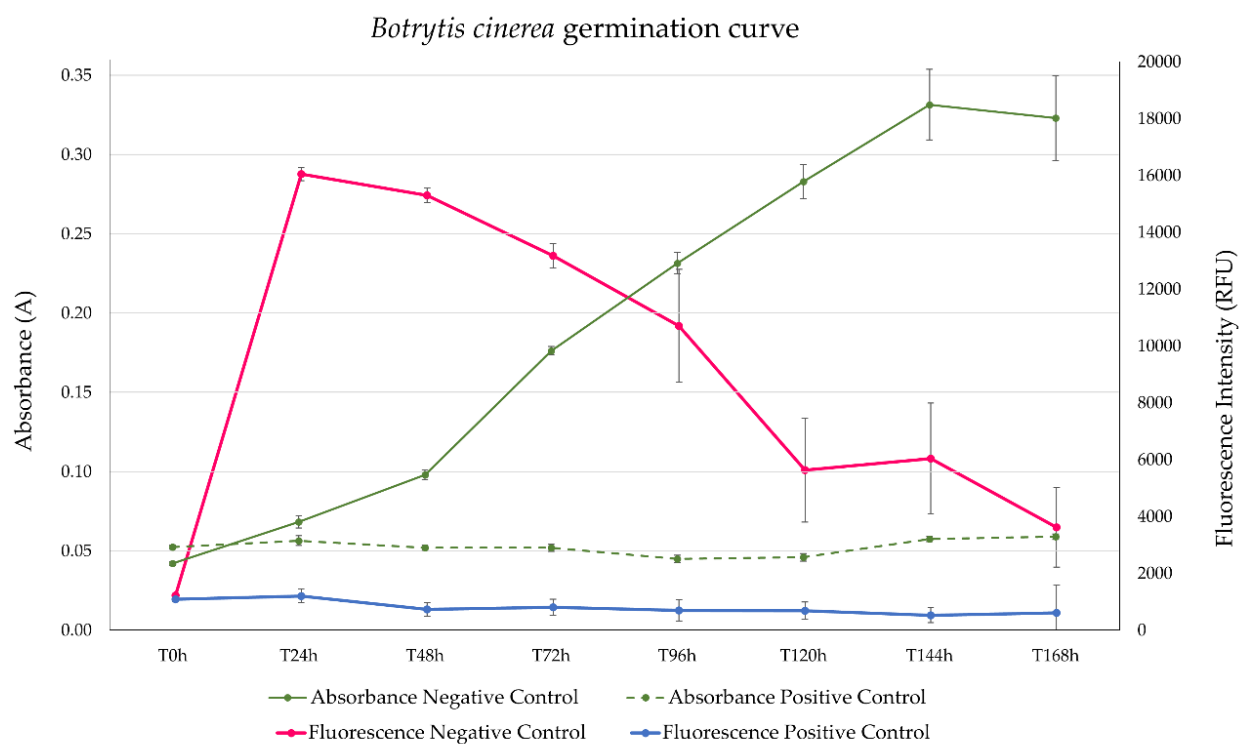


Figure 4. Germination curves of *Botrytis cinerea* conidia based on absorbance at 612 nm (green lines) and fluorescence at 570 nm excitation and 615 nm emission (pink and blue lines). The left axis quantifies the absorbance values of negative controls (green continued line) and positive controls (green discontinued line). The right axis measures the fluorescence intensities of negative controls (pink line) and positive controls (blue line). Each data point represents an average of 40 wells with their corresponding standard deviation.

In order to evaluate the reproducibility of the method based on the QC parameters, the antifungal assay was performed on three different days using three independent batches of sporulated plates and fresh reagents. The growth inhibition assay showed absorbance values for *B. cinerea* similar for each replicate (0.23 ± 0.01 A), RZ' factors higher than 0.70 (0.80 ± 0.05), and good S/B ratios (48.95 ± 10.10). Regarding the viability assay, it showed greater homogeneity with the fluorescence data of the negative controls ($13,173 \pm 427$ RFU), with RZ' factors close to 1.00 (0.94 ± 0.03) and S/B ratios (24.98 ± 5.00) slightly lower than absorbance readouts but with less variability. In general, these

parameters indicated that the established assay conditions provided data that were robust enough to evaluate the antifungal activity of large sets of samples against *Botrytis cinerea* in HTS format.

The tolerance of *B. cinerea* to dimethyl sulfoxide (DMSO), the most common solvent used in compound libraries, was determined to evaluate its possible effect on conidia germination. Figure 5 shows the germination inhibition in a 1:2 serial dilution concentration-dependent curve starting at 8% DMSO. A final concentration of 4% DMSO still induced significant effects on fungal growth (Figure 5a) and on the viability of *B. cinerea* conidia (Figure 5b), where the IC_{50} was determined to be between 3.43 (absorbance) and 4.01% (fluorescence). *B. cinerea* germination exhibited a clear decrease when conidia were exposed to concentrations higher than 2%. These results showed that Natural Product extracts and compound libraries prepared in DMSO can be tested using this methodology if the final assay concentration of this solvent remains below 2%.

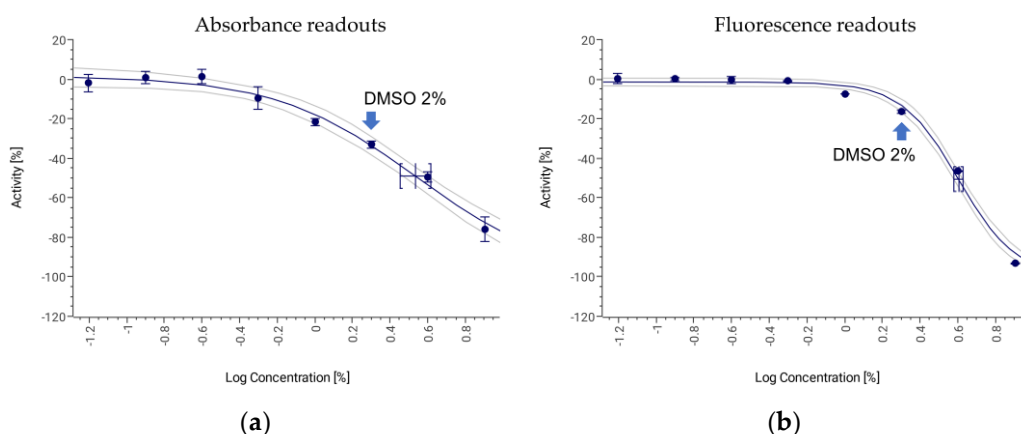


Figure 5. Tolerance of *Botrytis cinerea* conidia to different DMSO concentrations **(a)** based on absorbance readouts ($R^2 = 0.97$) and **(b)** fluorescence readouts ($R^2 = 0.99$).

The broad spectrum antifungal agent Amphotericin B (AmB) was tested as the positive control. This natural polyene inhibits human and plant pathogens by binding with ergosterol [37,38,39,40,41]. Different stock concentrations of AmB dissolved in 100% DMSO were tested in a DRC to determine the IC_{50} ($\mu\text{g/mL}$) and the sensitivity of the assay. The AmB DRC started at a final concentration of 200 $\mu\text{g/mL}$ with eight-point 1:5 serial dilutions to 2.56 ng/mL . The IC_{50} of AmB for *B. cinerea* for absorbance readouts was 0.45 $\mu\text{g/mL}$ (0.33–0.60 $\mu\text{g/mL}$), and for the fluorescence intensity, the IC_{50} was 0.27 $\mu\text{g/mL}$ (0.25–0.30 $\mu\text{g/mL}$) (Figure 6a,b).

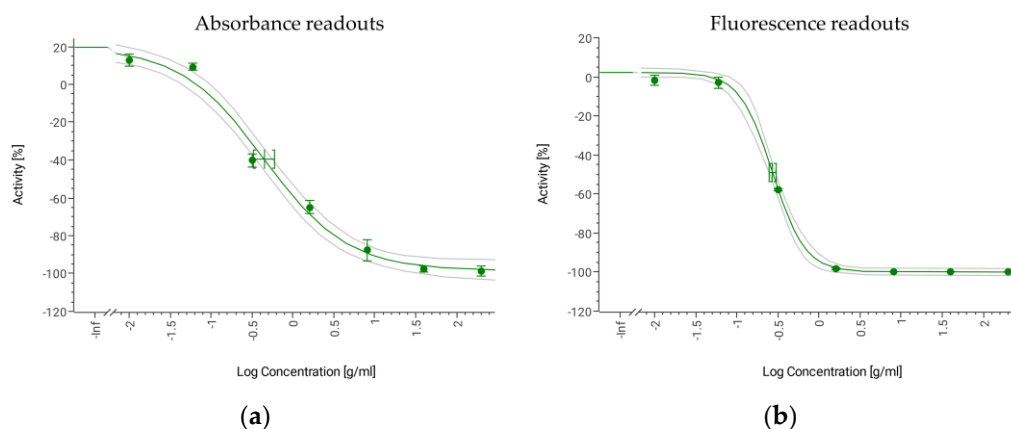


Figure 6. AmB DRC against *Botrytis cinerea* based on **(a)** absorbance readout $IC_{50} = 0.45 \mu\text{g/mL}$ ($0.33\text{--}0.60 \mu\text{g/mL}$) ($R^2 = 0.98$) and **(b)** fluorescence readout $IC_{50} = 0.27 \mu\text{g/mL}$ ($0.25\text{--}0.30 \mu\text{g/mL}$) ($R^2 = 0.99$).

3.4. *Colletotrichum acutatum* Microdilution Assay

The same steps and QC parameters were evaluated for the development of the *C. acutatum* antifungal assay. Two concentrations of conidia (5×10^5 and 1×10^6 conidia/mL) were evaluated to select the optimal inoculum concentration based on the results obtained for *B. cinerea*. Although no significant differences were observed between the assay window at both concentrations (S/B was 47.18 and 55.12 for absorbance and 15.68 and 18.76 for fluorescence, respectively), the RZ' factors were slightly higher with 1×10^6 conidia/mL ($RZ' = 0.76$), and this concentration was selected for the *C. acutatum* assay. The germination of *C. acutatum* in RPMI medium was monitored at 8 h intervals given the rapid germination and growth of this pathogen. After 24 h of incubation, the RZ' factors started to increase (>0.5), but the S/B was still low (11.70). The optimal incubation time for the *C. acutatum* assay plates was 40 h with the following RZ' and S/B values: absorbance readouts $RZ' = 0.75 \pm 0.01$ and $S/B = 53.05 \pm 5.50$ and fluorescence readouts $RZ' = 0.91 \pm 0.01$ and $S/B = 17.01 \pm 1.35$. The DMSO-tolerance evaluation revealed that this strain remained unaffected up to 2% DMSO and exhibited a significant decrease in growth when it was exposed to concentrations higher than 4%. The AmB DRC with eight-point 1:2 serial dilutions for *C. acutatum* starting at $10 \mu\text{g/mL}$ final concentration enabled the determination of an IC_{50} of $1.25 \mu\text{g/mL}$ ($1.12\text{--}1.33 \mu\text{g/mL}$) for the absorbance readouts and $1.21 \mu\text{g/mL}$ ($1.19\text{--}1.23 \mu\text{g/mL}$) for the fluorescence readouts (Table 4).

Table 4. Optimized conditions for the microdilution assays against the four phytopathogens.

Parameters	<i>B. cinerea</i> B05.10	<i>C. acutatum</i> CF-137177	<i>F. proliferatum</i> CBS 115.97	<i>M. grisea</i> CF-105765
Sporulation condition	OAT plates	SMY tube	SMY tube	VME tube
Time for sporulation	14 - 28 days	3 days	2 days	3 days
Assay medium	RPMI-1640	RPMI-1640	RPMI-1640	RPMI-1640
Concentration of conidia	1×10 ⁶ conidia/mL	1×10 ⁶ conidia/mL	1×10 ⁶ conidia/mL	1×10 ⁶ conidia/mL
Tolerance to DMSO	2 %	2 %	4 %	2 %
Growth inhibition assay (absorbance readout)				
Incubation time	72 h	40 h	20 h	48 h
RZ' (n= 240 wells)	0.80 ± 0.05	0.75 ± 0.01	0.77 ± 0.05	0.81 ± 0.03
S/B (n= 240 wells)	48.95 ± 10.10	53.05 ± 5.50	57.71 ± 7.04	54.21 ± 5.89
IC₅₀ AmB (µg/mL)	0.45 (0.33- 0.60)	1.25 (1.12- 1.33)	6.77 (6.11- 7.51)	4.51 (4.33- 4.69)
Viability inhibition assay (fluorescence readout)				
Incubation time (resazurin)	5 - 15 min	3 h	2 h	1 h 30 min
RZ' (n= 240 wells)	0.94 ± 0.03	0.91 ± 0.01	0.94 ± 0.01	0.95 ± 0.01
S/B (n= 240 wells)	24.98 ± 4.90	17.01 ± 1.35	17.54 ± 1.76	13.62 ± 1.65
IC₅₀ of AmB (µg/mL)	0.27 (0.25-0.30)	1.21 (1.19-1.23)	6.75 (6.41-7.12)	5.38 (5.30-5.46)

3.5. *Fusarium proliferatum* Microdilution Assay

The antifungal assay against *F. proliferatum* was also developed following the same steps. For the absorbance-based assay, no significant differences were observed in the RZ' value using both conidia concentrations (5×10⁵ and 1×10⁶ conidia/mL) (0.72 for both). However, 1×10⁶ conidia/mL provided a clear increase in the S/B values (from 14.49 to 59.06). The optimal time for the incubation of assay plates was 20 h due to the faster growth rate of this strain, with RZ' = 0.77 ± 0.05 and S/B = 57.71 ± 7.04. After 2 h of incubation with resazurin, the fluorescence readouts provided the most robust values, where the QC parameters were RZ' = 0.94 ± 0.01 and S/B = 17.54 ± 1.76. Tolerance to DMSO by *F. proliferatum* showed a normal rate of conidia germination up to 4% DMSO. *F. proliferatum* is the most resistant strain of the panel to AmB. IC₅₀s were determined for both readouts in a DRC starting at 100 µg/mL with eight-point 1:2 serial dilutions to 0.78 µg/mL; the IC₅₀s for absorbance and fluorescence were 6.77 µg/mL (6.11–7.51 µg/mL) and 6.75 µg/mL (6.41–7.12 µg/mL), respectively (Table 4).

3.6. *Magnaporthe grisea* Microdilution Assay

No significant differences were observed in the RZ' and S/B values when two concentrations of conidia/mL were compared in the development of the *M. grisea* antifungal assay. The main difference was the time required to complete the resazurin reduction process (more than 3 h for 5×10⁵ conidia/mL). Therefore, 1×10⁶ conidia/mL was selected as the concentration for the *M.*

grisea inoculum. In this set-up, the assay plates were incubated for 48 h to ensure higher QC parameters for the absorbance readouts ($RZ' = 0.81 \pm 0.03$ and $S/B = 54.21 \pm 5.89$) and for 1 h and 30 min with resazurin for the fluorescence-based viability assay ($RZ' = 0.95 \pm 0.01$ and $S/B = 13.62 \pm 1.65$). DMSO-tolerance curves showed that *M. grisea* can accept up to 2% DMSO final concentration before conidia germination is affected. The best DRC for the standard AmB started at a final concentration of 50 $\mu\text{g/mL}$ with eight-point 1:2 serial dilutions to 0.39 $\mu\text{g/mL}$; the $IC_{50} = 4.51$ $\mu\text{g/mL}$ (4.33–4.69 $\mu\text{g/mL}$) for the absorbance readouts and 5.38 $\mu\text{g/mL}$ (5.30–5.46 $\mu\text{g/mL}$) for the fluorescence readouts (Table 4).

3.7. Sensitivity and Resistance to Antifungal Standards

The antifungal potential of 40 known fungicide agents was evaluated using both agar and microdilution methods (Table 5). Compound stocks were prepared at 1 mg/mL in 100% DMSO, from which 2 μL was diluted to a final assay volume of 100 μL to avoid the inhibitory effects of the solvent. The four phytopathogens were resistant to benalaxyl, cytochalasin, dimethomorph, ethaboxam, flutianil, iprovalicarb, mandipropamid, metalaxyl, radicol, and validamycin at the maximum assay concentrations. The remaining 30 standards with inhibitory effects against one or more phytopathogens of the panel were then titrated in DRC using both methodologies (agar-based and microdilution assays). The standard curves of the compounds started at 20 $\mu\text{g/mL}$ (final assay concentration) with 10-point 1:2 serial dilutions to 0.04 $\mu\text{g/mL}$. The Minimal Inhibitory Concentration (MIC) for the agar-based assays was determined to be the lowest concentration that generated an inhibition zone (halo diameter > 5 mm), and IC_{50} was determined to be the concentration responsible for 50% of the inhibition in the microdilution assays. Both values were used to confirm the antifungal activity of the different chemical classes of the compounds and were compared with previously described data (Table 5).

Azoxystrobin, benomyl, cycloheximide, cyprodinil, difeconazole, ferbam, fludioxonil, mandestrobin, mefentrifluconazole, metconazole, pydiflumetofen, pyraclostrobin, thiabendazole, trifloxystrobin, and triflumizole presented a broad antifungal spectrum against the four phytopathogens. In general, strobirulins (azoxystrobin, mandestrobin, pyraclostrobin, and trifloxystrobin) were the most effective agents. This group of compounds are inhibitors of cellular respiration through the complex III *cytochrome bc1* (ubiquinone oxidase) Qo site [42]. They have an extended antifungal spectrum on many filamentous fungi and are considered the most important agricultural fungicide group. Within this chemical class, pyraclostrobin was the most active compound among the standards, with MIC and IC_{50} values consistently low for the four phytopathogens (Table 5), in agreement with previous reports [43,44].

The most relevant chemical classes in use were triazoles, imidazoles, and benzimidazoles, which were effective against more than one plant pathogen. The most active triazoles were metconazole, difeconazole, and mefentrifluconazole, inhibiting the four strains. Metconazole required the lowest concentration to inhibit fungal development in both assay methods (agar and microdilution), mainly against *F. proliferatum* (MIC 31.25 $\mu\text{g/mL}$ and $IC_{50} < 0.04$ $\mu\text{g/mL}$), confirming its reported potential to control the Fusarium head blight of wheat (FHB) [45,46]. The remaining five triazoles provided broad activity profiles with some specificities between the two assay methods. Cyproconazole, flutriafol, and tetraconazole were totally inactive against *M. grisea*, while

fenbuconazole and itraconazole only showed very poor inhibitory effects against *F. proliferatum*, suggesting that higher concentrations of the compounds may be required to reach the MIC and IC₅₀ values.

Both imidazoles (triflumizole and fenamidone) presented two different activity patterns. Triflumizole was more effective, with significantly lower MIC and IC₅₀ values for the four phytopathogens (in line with the broad antifungal spectrum reported in the literature and its effects on mycelial growth, spore germination, and germ tube elongation) [47]. Fenamidone, a very effective fungicide for *Oomycete* diseases such as downy mildew and certain leaf spot diseases [48], also showed inhibitory effects against *C. acutatum* and *M. grisea*. Finally, the benzimidazoles thiabendazol and benomyl, which affect the polymerization of β -tubulin and have been reported as fungicides for the control of the *Fusarium* species of a variety of crops [49], also exhibited inhibitory activity on other species, such as *B. cinerea*, *C. acutatum*, and *M. grisea*.

Other interesting antifungal agents tested were those that affect the synthesis of proteins. Among them, cycloheximide was the most active one, exhibiting inhibition of the four phytopathogens with both assay methodologies, which confirmed its previously reported antifungal potential [50]. Cyprodinil showed higher inhibitory activity against *B. cinerea* in particular, with MIC (7.81 $\mu\text{g/mL}$) and IC₅₀ values (0.06 $\mu\text{g/mL}$ for the absorbance readouts and 0.29 $\mu\text{g/mL}$ for the fluorescence readouts) that were significantly lower than those obtained for the other pathogens. This higher potency might be explained by cyprodinil's mode of action, as it inhibits the biosynthesis of methionine, which affects the secretion of hydrolytic enzymes and is related to the mechanism of pathogenesis of *B. cinerea* [51]. Finally, in this group, the nucleosidic Natural Products tunicamycin and tubercidin, produced by *Streptomyces* species and previously reported to have antifungal activity against various human and plant pathogens [52,53], showed high specificity against *B. cinerea* and *C. acutatum*, an activity not reported to date.

Inhibitors of cellular respiration through the complex II succinate dehydrogenase (SDHI) were very effective with respect to controlling the *B. cinerea* strain. Within this group, pydiflumetofen was the most effective at inhibiting the four phytopathogens in both methodologies, well in line with previous reports of its broad antifungal spectrum [54,55]. Fluopyram and isofetamid showed a more specific activity profile, being fluopyram more active against *F. proliferatum* and isofetamid more active against *M. grisea*. Boscalid was highly and specifically active against the germination and viability of *B. cinerea*, with IC₅₀ values of 0.33 $\mu\text{g/mL}$ (absorbance) and 0.70 $\mu\text{g/mL}$ (fluorescence), in agreement with previous reported data in growth inhibition tests (0.7 $\mu\text{g/mL}$ to inhibit 50% of mycelial growth) [56,57]. *C. acutatum* resistance to this chemical class can be explained by previous reports of a natural resistance in different *Colletotrichum* species to SDHI fungicides [58,59].

Fludioxonil and cyclosporin A, with similar modes of action affecting signal transduction, have also been described for the control of different pathogens. Fludioxonil confirmed its broad antifungal spectrum, being more effective against *B. cinerea*. Several in vitro and field studies have determined this compound to be one of the most effective fungicides for the control of this phytopathogen through the inhibition of mycelial growth, germination, and conidiation [57]. Cyclosporin A (previously reported to have antifungal properties against *Candida* species) also showed inhibitory

effects on *B. cinerea* and weak activity against *C. acutatum* [60,61], activities that have never been reported.

The last four antifungal standards belong to diverse chemical classes and present different modes of action. The picolinamide class is represented by fenpicoxamid, a semisynthetic modification of the natural compound UK-2A [62,63]. This fungicide, mainly used in cereals for the control of *Z. tritici*, was also active against *B. cinerea* and *M. grisea*. The dithio-carbamate ferbam, which has been described as a multi-site contact inhibitor for several phytopathogens [42,64,65], demonstrated activity against the four tested strains. Finally, cerulenin, a natural compound extensively studied for its antifungal potential through the inhibition of fatty acid biosynthesis, presented a lack of activity against most of the phytopathogens that could be correlated to its limited activity to yeasts and dimorphic fungi [66,67].

Therefore, the results obtained with the forty tested compounds validated the optimized assay conditions for the four phytopathogens. The developed HTS platform can characterize the activity of a wide diversity of synthetic and natural antifungal compounds and identify the known and new sensitivities and resistances of these four relevant phytopathogens.

3.8. Antifungal Potential of Microbial Extract Libraries

A proof of concept (POC) piloting HTS approach was also used with a small subset of 2400 microbial Natural Product extracts from the MEDINA Library. Extracts at 2xWBE (Whole Broth Equivalent) in 20% DMSO were screened at a final 1:10 dilution to avoid any inhibitory effects derived from the DMSO concentrations against the four pathogens. The antifungal activity observed in the agar-based assays was determined by measuring the diameter and turbidity of the inhibition zones (mm) when diameters were larger than 5 mm. Following this 5 mm cut-off, we obtained screening hit-rates ranging from 0.50% for *C. acutatum*, 1.88% for *F. proliferatum*, and 1.92% for *B. cinerea* to 2.13% for *M. grisea*.

The antifungal activity was determined in microdilution assays as the percentage of inhibition (% INH), calculated for both the absorbance and fluorescence data. Figure 7a,b show a symmetrical and normal distribution around 0% INH of activity observed in the *B. cinerea* assay, indicating a low interference of the samples with both readouts. However, slight differences were observed between the activity distributions in the absorbance and fluorescence data. Statistical analysis showed that boxplots significantly highlighted the hit populations to the upper quartile, corresponding to a % INH > 60% for absorbance (Figure 7a) and a % INH > 35% for fluorescence (Figure 7b). Absorbance readouts provided greater dispersion in comparison to fluorescence due to the higher coefficient of variation of absorbance (CV = 14.87) compared to fluorescence (CV = 2.36). This could be explained by the fact that some extracts may promote phytopathogen growth, generating higher absorbance values, and this phytopathogen growth is minimized by the fluorescence of resazurin. Moreover, the fluorescence assay showed larger *z'* scores that better separated the active samples from the general inactive population, also indicating more robust data. However, fluorescence readouts can be easily affected by certain sample components and/or their pH, which interferes with resazurin, generating false-positive signals. This effect can sometimes be challenging for the identification of active samples. Therefore, a hit selection criterion should only consider those extracts which are

active in both assays. In this sense, only samples that inhibit fungal growth and also affect cell viability were selected. The implementation of these criteria resulted in hit rates of 0.71% for *C. acutatum*, 1.04% for *F. proliferatum*, 1.50% for *B. cinerea*, and 2.63% for *M. grisea*.

In general, we have shown that the developed protocols ensure a rapid and efficient HTS platform that allows for the profiling of the antifungal properties of a broad variety of samples (from synthetic to Natural Product compounds and extracts) using different assay methodologies (agar-based and liquid microdilution assays) for the high-quality selection of new potential inhibitors of the most relevant phytopathogens, namely *Botrytis cinerea*, *Colletotrichum acutatum*, *Fusarium proliferatum*, and *Magnaporthe grisea*.

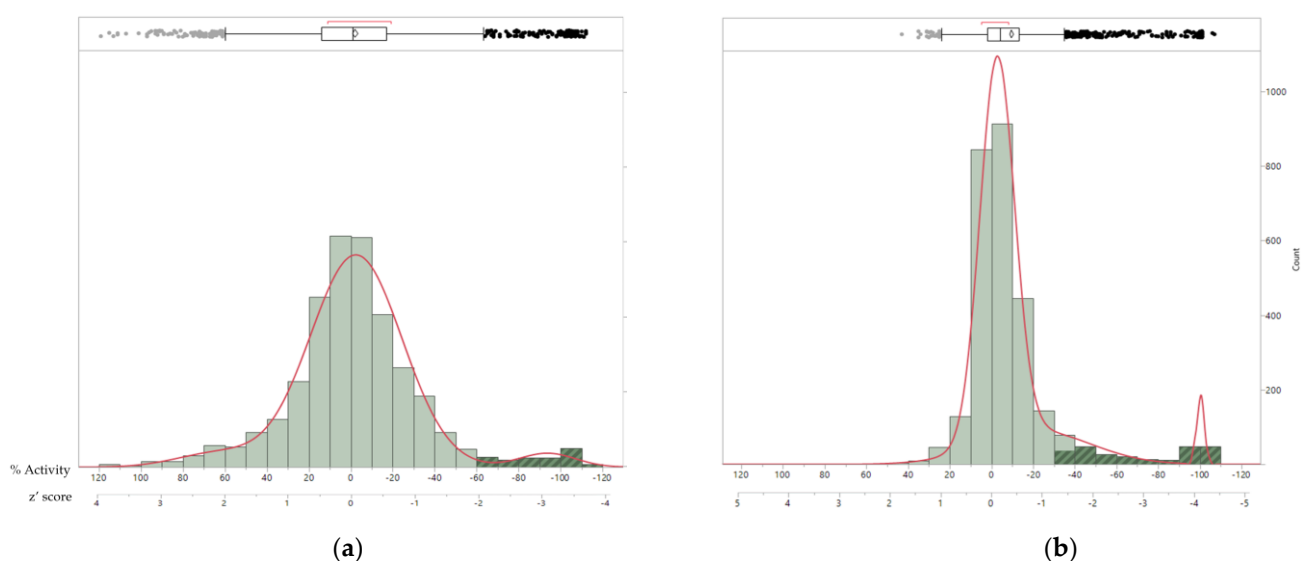


Figure 7. Population distribution histogram (bin size = 20%) of the antifungal activities of the 2400 microbial extracts tested against *B. cinerea*: **(a)** absorbance readouts and **(b)** fluorescence readouts. Distribution is represented according to the activity scale (% INH) and z' score scale. Hit populations in the upper quartile of the boxplot are highlighted in dark green.

Chapter 3

Table 5. *In vitro* activity of 40 commercial antifungal agents against *B. cinerea*, *C. acutatum*, *F. proliferatum*, and *M. grisea*. MIC values (µg/mL) correspond with the minimal concentration that inhibits fungal growth in the agar-based assay, and IC₅₀ values (µg/mL) indicate the necessary concentration to inhibit 50% of conidia germination (Abs; absorbance readout) and cell viability (Flu; fluorescence readout); both parameters were obtained based on their DRC. The values in parenthesis correspond to confidence intervals of 95%. No activity detected at the maximal tested concentration is indicated as ‘i’ for ‘inactive’.

Chemical Class	Compound	Mode of action/ Target site	<i>Botrytis cinerea</i>			<i>Colletotrichum acutatum</i>			<i>Fusarium proliferatum</i>			<i>Magnaporthe grisea</i>		
			Agar MIC	Abs IC ₅₀	Flu IC ₅₀	Agar MIC	Abs IC ₅₀	Flu IC ₅₀	Agar MIC	Abs IC ₅₀	Flu IC ₅₀	Agar MIC	Abs IC ₅₀	Flu IC ₅₀
Acylalanines	benalaxyl	nucleic acids metabolism/ RNA polymerase I	i	i	i	i	i	i	i	i	i	i	i	i
	metalaxyl		i	i	i	i	i	i	i	i	i	i	i	i
Anilino-pyrimidines	cyprodinil	protein synthesis	7.81	0.06 (0.05-0.07)	0.29 (0.24-0.35)	15.63	> 20	14.99 (11.69-19.20)	i	8.28 (7.12-9.62)	14.33 (13.88-15.35)	i	16.02 (13.11-19.57)	> 20
Benzimidazoles	benomyl	cytoskeleton and motor proteins/Tubulin	62.5	0.06 (0.05-0.07)	0.06 (0.05-0.06)	125	0.35 (0.33-0.38)	0.46 (0.43-0.49)	500	0.98 (0.88-1.09)	0.95 (0.88-1.03)	1000	1.64 (1.51-1.78)	1.33 (1.29-1.37)
	thiabendazole		250	0.24 (0.21-0.28)	0.25 (0.21-0.30)	62.5	10.71 (9.66-11.87)	> 20	1000	2.15 (1.95-2.36)	1.99 (1.84-2.15)	-	18.57 (17.86-19.31)	16.39 (16.04-16.75)
Cinnamic acid amides	dimethomorph	cell wall biosynthesis/ cellulose synthase	i	i	i	i	i	i	i	i	i	i	i	i
Cyano-methylene thiazolidines	flutianil	unknown	i	i	i	i	i	i	i	i	i	i	i	i
Cyclic nonribosomal peptides	cyclosporin A	signal transduction	125	1.27 (0.92-1.74)	2.20 (1.66-2.93)	i	3.87 (3.198-4.70)	10.84 (10.27-11.44)	i	i	i	i	i	i
Dicarboximide	cycloheximide	protein synthesis	250	8.96 (7.27-11.05)	4.91 (4.05-5.96)	250	0.57 (0.49-0.66)	1.67 (1.53-1.82)	125	1.29 (1.07-1.56)	1.21 (1.11-1.31)	250	7.94 (7.44-8.48)	5.07 (4.90-5.25)
Dithio-carbamates	ferbam	multi-site contact	250	0.30 (0.28-0.32)	0.37 (0.36-0.38)	62.5	0.24 (0.22-0.25)	0.66 (0.63-0.70)	125	1.23 (1.08-1.41)	1.84 (1.75-1.94)	i	0.45 (0.43-0.47)	0.28 (0.28-0.29)
Ethylamino- thiazolecarboxamide	ethaboxam	cytoskeleton and motor proteins/tubulin	i	i	i	i	i	i	i	i	i	i	i	i
Glucopyranosyl antibiotics	validamycin	unknown/trehalase	i	i	i	i	i	i	i	i	i	i	i	i
Imidazolone	triflumizole	sterol biosynthesis/ C14-demethylase (erg11/cyp51)	62.5	< 0.04	< 0.04	15.63	< 0.04	< 0.04	7.81	0.26 (0.22-0.32)	0.28 (0.23-0.35)	31.25	0.05 (0.04-0.06)	< 0.04
	fenamidone	respiration/complex III: cyt bc1 at Qo site (cytb gene)	i	i	i	500	11.33 (10.25-12.51)	> 20	i	i	i	500	9.45 (8.79-10.16)	1.94 (1.85-2.02)
Macrocyclic	radicicol	histidine kinase/Hsp90	i	i	i	i	i	i	i	i	i	i	i	i
Mandelic acid amides	mandipropamid	cell wall biosynthesis/ cellulose synthase	i	i	i	i	i	i	i	i	i	i	i	i
Monocarboxylic acid amide	cerulenin	fatty acid biosynthesis/ b-ketoacyl-acyl carrier protein synthase	i	i	i	i	6.70 (5.64-7.96)	11.98 (11.47-12.51)	i	i	i	i	i	i
Mycotoxin	cytochalasin B	Cell division	i	i	i	i	i	i	i	i	i	i	i	i
N-methoxy-(phenylethyl)- pyrazolecarboxamides	pydiflumetofen	respiration/complex II: succinate-dehydrogenase	15.63	0.07 (0.07-0.08)	0.12 (0.11-0.13)	i	6.32 (5.32-7.50)	2.08 (1.89-2.29)	15.63	< 0.04	< 0.04	15.62	0.14 (0.11-0.18)	< 0.04

Table 5. Cont.

Chemical Class	Compound	Mode of action/ Target site	<i>Botrytis cinerea</i>			<i>Colletotrichum acutatum</i>			<i>Fusarium proliferatum</i>			<i>Magnaporthe grisea</i>		
			Agar MIC	Abs IC ₅₀	Flu IC ₅₀	Agar MIC	Abs IC ₅₀	Flu IC ₅₀	Agar MIC	Abs IC ₅₀	Flu IC ₅₀	Agar MIC	Abs IC ₅₀	Flu IC ₅₀
Nucleoside	tubercidin	protein synthesis	<i>i</i>	<i>i</i>	<i>i</i>	<i>i</i>	12.25 (9.69-15.49)	> 20	<i>i</i>	<i>i</i>	<i>i</i>	<i>i</i>	<i>i</i>	<i>i</i>
	tunicamycin		125	2.62 (1.79-3.84)	2.55 (2.34-2.77)	500	4.05 (3.55-4.63)	6.71 (5.26-7.20)	<i>i</i>	<i>i</i>	<i>i</i>	<i>i</i>	<i>i</i>	<i>i</i>
Phenyl-oxo-ethylthiophene amide	isofetamid	respiration/complex II: succinate-dehydrogenase	31.25	0.16 (0.13-0.19)	0.40 (0.34-0.45)	<i>i</i>	<i>i</i>	<i>i</i>	<i>i</i>	14.00 (10.95-17.91)	19.94 (16.92-23.50)	62.5	1.49 (1.26-1.77)	0.23 (0.21-0.26)
Phenylpyrroles	fludioxonil	signal transduction/ MAP/Histidine Kinase (os-2, HOG1)	62.5	< 0.04	0.07 (0.07-0.07)	31.25	0.07 (0.07-0.07)	0.07 (0.07-0.07)	31.25	0.09 (0.09-0.11)	< 0.04	125	0.22 (0.21-0.24)	0.09 (0.09-0.09)
Picolinamides	fenpicoxamid	respiration/complex III: cyt bc1 at Qi site	62.5	0.07 (0.06-0.08)	0.43 (0.32-0.57)	15.63	<i>i</i>	<i>i</i>	<i>i</i>	<i>i</i>	<i>i</i>	62.5	2.04 (1.61-2.59)	0.40 (0.39-0.42)
Pyridinecarboxamides	boscalid	respiration/complex II: succinate-dehydrogenase	125	0.33 (0.30-0.36)	0.70 (0.65-0.74)	<i>i</i>	<i>i</i>	<i>i</i>	<i>i</i>	<i>i</i>	<i>i</i>	<i>i</i>	<i>i</i>	<i>i</i>
Pyridinyl-ethylbenzamides	fluopyram		125	0.28 (0.25-0.32)	1.27 (1.17-1.37)	<i>i</i>	<i>i</i>	<i>i</i>	<i>i</i>	5.77 (4.08-8.15)	12.24 (10.49-14.28)	<i>i</i>	> 20	17.28 (16.02-18.64)
Strobirulin	azoxystrobin	respiration/complex III: cyt. bc1 at Qo site (cyt b gene)	250	0.06 (0.06-0.07)	0.06 (0.05-0.07)	62.5	0.05 (0.04-0.05)	0.09 (0.09-0.09)	31.25	0.39 (0.32-0.49)	0.22 (0.19-0.26)	62.5	0.10 (0.09-0.11)	0.08 (0.07-0.08)
	mandestrobin		250	< 0.04	0.78 (0.69-0.87)	250	0.12 (0.11-0.13)	0.08 (0.08-0.09)	31.25	0.12 (0.11-0.13)	0.04 (0.04-0.05)	500	2.27 (2.07-2.50)	0.82 (0.79-0.85)
	pyraclostrobin		31.25	< 0.04	0.07 (0.05-0.09)	3.91	< 0.04	< 0.04	7.81	0.06 (0.05-0.07)	< 0.04	1.95	< 0.04	< 0.04
	trifloxystrobin		31.25	0.88 (0.51-1.50)	1.99 (1.66-2.40)	7.81	6.41 (5.83-7.05)	6.43 (6.06-6.81)	7.81	7.23 (6.44-8.12)	7.79 (6.59-9.21)	3.90	1.83 (1.52-2.20)	1.59 (1.49-1.70)
Triazoles	cyproconazole	sterol biosynthesis/ C14-demethylase (erg11/cyp51)	500	0.34 (0.27-0.43)	0.39 (0.35-0.44)	62.5	0.68 (0.61-0.76)	2.08 (1.93-2.22)	<i>i</i>	1.76 (1.17-2.64)	1.58 (1.37-1.81)	<i>i</i>	<i>i</i>	<i>i</i>
	difenoconazole		250	0.44 (0.39-0.49)	0.81 (0.67-0.97)	250	0.16 (0.14-0.17)	0.61 (0.56-0.67)	125	0.70 (0.52-0.96)	0.38 (0.32-0.45)	1000	11.89 (11.34-12.47)	7.78 (7.34-8.25)
	fenbuconazole		500	0.20 (0.18-0.22)	0.43 (0.38-0.49)	<i>i</i>	0.23 (0.20-0.27)	0.58 (0.52-0.64)	<i>i</i>	1.82 (1.41-2.37)	1.39 (1.15-1.67)	<i>i</i>	<i>i</i>	<i>i</i>
	itraconazole		62.5	0.31 (0.19-0.51)	0.31 (0.29-0.33)	62.5	0.12 (0.11-0.13)	0.63 (0.58-0.70)	62.5	0.53 (0.41-0.68)	0.74 (0.62-0.87)	<i>i</i>	<i>i</i>	<i>i</i>
	mefentrifluconazole		250	0.07 (0.06-0.08)	0.11 (0.10-0.12)	62.5	0.11 (0.09-0.12)	0.28 (0.23-0.34)	1000	0.55 (0.42-0.71)	0.22 (0.20-0.25)	1000	<i>i</i>	<i>i</i>
	metconazole		250	0.06 (0.05-0.05)	0.10 (0.09-0.11)	62.5	< 0.04	0.05 (0.05-0.06)	31.25	< 0.04	< 0.04	500	4.15 (3.86-4.47)	4.16 (3.91-4.41)
	tetraconazole		<i>i</i>	12.52 (7.73-20.29)	5.40 (4.96-5.88)	<i>i</i>	1.30 (0.97-1.75)	3.16 (2.89-3.46)	<i>i</i>	8.02 (6.26-10.29)	9.07 (8.29-9.92)	<i>i</i>	<i>i</i>	<i>i</i>
	flutriafol		<i>i</i>	11.02 (9.69-12.55)	> 20	<i>i</i>	6.82 (6.26-7.43)	6.48 (6.16-6.82)	<i>i</i>	3.19 (2.79-3.64)	3.38 (3.09-3.70)	<i>i</i>	<i>i</i>	<i>i</i>
Valinamide carbamates	iprovalicarb	cell wall biosynthesis/ cellulose synthase	<i>i</i>	<i>i</i>	<i>i</i>	<i>i</i>	<i>i</i>	<i>i</i>	<i>i</i>	<i>i</i>	<i>i</i>	<i>i</i>	<i>i</i>	<i>i</i>

4. Conclusions

In this work, two HTS methodologies have been developed and validated to evaluate the antifungal effects of a large diversity of samples, pure compounds, and complex mixtures against four important fungal phytopathogens. The described approach can be applied for the development of new protocols for antifungal assays with additional strains. On the one hand, the previously developed agar-based assay allows us to fix some of the problems related to manual agar tests, mainly regarding the time, the throughput of the assay, and the required sample volume. On the other hand, the microdilution method provides more information about the antifungal effects of samples as it can differentiate the inhibition of fungal growth (absorbance readouts) and cell viability (fluorescence readouts) within the same assay. Furthermore, this methodology is even more time-efficient, requires a lower quantity of fungal conidia, and has the potential to be scaled up to the 384-well format, allowing for the screening of a higher number of samples.

Both assay methods were validated using a large selection of synthetic and natural antifungal compounds covering a broad variety of modes of action. The MIC and IC₅₀ values reported in the literature were in agreement with the results obtained using both assay set-ups (agar-based and microdilution assays), detecting activities at very low concentrations (<0.04 µg/mL). In addition and as previously reported, some differences were observed in the activities from agar and microdilution methods, revealing the importance of using both methodologies in the characterization of new antifungal agents. In general, both assay set-ups can identify hits according to their potency, which may result in more activity in one set-up than in the other due to the differential diffusion between the samples on the agar set-up, differential fungal growth rates, fungal physiology in the assay conditions, and/or specificity on their mechanisms of action. Therefore, future screening strategies to identify new fungicides should include both methodologies in order to collect more reliable data regarding the antifungal potential of sample libraries.

Finally, the POC piloting screening of a subset of 2400 Natural Product extracts validated the use of this HTS assay platform for the evaluation of sample libraries to identify new antifungal agents. Future studies will focus on the characterization of the chemical diversity of new bioactive metabolites detected in this preliminary screening and extending the use of the HTS phytopathogen platform for the discovery of new biocontrol products in plant protection.

References

1. Cattò, C.; de Vincenti, L.; Borgonovo, G.; Bassoli, A.; Marai, S.; Villa, F.; Cappitelli, F.; Saracchi, M. Sub-lethal concentrations of *Perilla frutescens* essential oils affect phytopathogenic fungal biofilms. *J. Environ. Manag.* 2019, *245*, 264–272. [[Google Scholar](#)] [[CrossRef](#)]
2. Iftikhar, S.; Vigne, A.; Sepulveda-Diaz, J.E. Droplet-based microfluidics platform for antifungal analysis against filamentous fungi. *Sci. Rep.* 2021, *11*, 22998. [[Google Scholar](#)] [[CrossRef](#)] [[PubMed](#)]
3. Adnan, M.; Islam, W.; Shabbir, A.; Khan, K.A.; Ghramh, H.A.; Huang, Z.; Chen, H.Y.H.; Lu, G.D. Plant defense against fungal pathogens by antagonistic fungi with *Trichoderma* in focus. *Microb. Pathog.* 2019, *129*, 7–18. [[Google Scholar](#)] [[PubMed](#)]
4. Dean, R.; Van Kan, J.A.; Pretorius, Z.A.; Hammond-Kosack, K.E.; Di Pietro, A.; Spanu, P.D.; Rudd, J.J.; Dickman, M.; Kahmann, R.; Ellis, J.; et al. The Top 10 fungal pathogens in molecular plant pathology. *Mol. Plant Pathol.* 2012, *13*, 414–430. [[Google Scholar](#)] [[CrossRef](#)]
5. Viaud, M.C.; Balhadère, P.; Talbot, N.J. A *Magnaporthe grisea* cyclophilin acts as a virulence determinant during plant infection. *Plant Cell* 2002, *14*, 917–930. [[Google Scholar](#)] [[CrossRef](#)]
6. Kohli, M.M.; Mehta, Y.R.; Guzman, E.; de Viedma, L.; Cubilla, L.E. Pyricularia blast—A threat to wheat cultivation. *Czech J. Genet. Plant Breed.* 2011, *47*, S130–S134. [[Google Scholar](#)]
7. Koeck, M.; Hardham, A.; Dodds, P.N. The role of effectors of biotrophic and hemibiotrophic fungi in infection. *Cell Microbiol.* 2011, *13*, 1849–1857. [[Google Scholar](#)] [[CrossRef](#)]
8. Wang, Q.; Tao, S.; Dubé, C.; Tury, E.; Hao, Y.J.; Zhang, S.; Zhao, M.; Wu, W.; Khanizadeh, S. Postharvest changes in the total phenolic content, antioxidant capacity and L-phenylalanine ammonia-lyase activity of strawberries inoculated with *Botrytis*. *J. Plant Stud.* 2012, *1*, 11–18. [[Google Scholar](#)] [[CrossRef](#)]
9. Soylu, E.M.; Kurt, Ş.; Soylu, S. In vitro and in vivo antifungal activities of the essential oils of various plants against tomato grey mould disease agent *Botrytis cinerea*. *Int. J. Food Microbiol.* 2010, *143*, 183–189. [[Google Scholar](#)] [[CrossRef](#)]
10. Couderchet, M. Benefits and problems of fungicide control of *Botrytis cinerea* in vineyards of Champagne. *Vitis* 2003, *42*, 165–171. [[Google Scholar](#)]
11. Arias, M.M.; Leandro, L.F.; Munkvold, G.P. Aggressiveness of *Fusarium* species and impact of root infection on growth and yield of soybeans. *Phytopathology* 2013, *103*, 822–832. [[Google Scholar](#)] [[CrossRef](#)]
12. Lalošević, M.; Jevtić, R.; Župunski, V.; Maširević, S.; Orbović, B. Virulence structure of the wheat powdery mildew population in Serbia. *Agronomy* 2022, *12*, 45. [[Google Scholar](#)] [[CrossRef](#)]
13. Cacciola, S.O.; Faedda, R.; Sinatra, F.; Agosteo, G.; Schena, L.; Frisullo, S.; Lio, G.M.D.S. Olive anthracnose. *J. Plant Pathol.* 2012, *94*, 29–44. Available online: <https://www.jstor.org/stable/45156006> (accessed on 27 July 2023).

14. Gang, G.H.; Cho, H.J.; Kim, H.S.; Kwack, Y.B.; Kwak, Y.S. Analysis of fungicide sensitivity and genetic diversity among *Colletotrichum* species in sweet persimmon. *Plant Pathol. J.* 2015, 31, 115. [[Google Scholar](#)] [[CrossRef](#)] [[PubMed](#)]
15. Da Silva, L.L.; Moreno, H.L.A.; Correia, H.L.N.; Santana, M.F.; de Queiroz, M.V. *Colletotrichum*: Species complexes, lifestyle, and peculiarities of some sources of genetic variability. *Appl. Microbiol. Biot.* 2020, 104, 1891–1904. [[Google Scholar](#)] [[CrossRef](#)]
16. Gonçalves, D.C.; Ribeiro, W.R.; Gonçalves, D.C.; Menini, L.; Costa, H. Recent advances and future perspective of essential oils in control *Colletotrichum* spp.: A sustainable alternative in postharvest treatment of fruits. *Food Res. Int.* 2021, 150, 110758. [[Google Scholar](#)] [[CrossRef](#)] [[PubMed](#)]
17. Méndez-Morán, L.; Reynaga-Peña, C.G.; Springer, P.S.; Ruiz-Herrera, J. *Ustilago maydis* infection of the nonnatural host *Arabidopsis thaliana*. *Mycology* 2005, 95, 480–488. [[Google Scholar](#)]
18. Lawrence, G.J.; Dodds, P.N.; Ellis, J.G. Rust of flax and linseed caused by *Melampsora lini*. *Mol. Plant Pathol.* 2007, 8, 349–364. [[Google Scholar](#)] [[CrossRef](#)]
19. Brauer, V.S.; Rezende, C.P.; Pessoni, A.M.; De Paula, R.G.; Rangappa, K.S.; Nayaka, S.C.; Gupta, V.K.; Almeida, F. Antifungal agents in agriculture: Friends and foes of public health. *Biomolecules* 2019, 9, 521. [[Google Scholar](#)] [[CrossRef](#)]
20. Lucas, J.A. Chapter One—Fungi, Food Crops, and Biosecurity: Advances and Challenges. In *Advances in Food Security and Sustainability*; Barling, D., Ed.; Elsevier: Amsterdam, The Netherlands, 2017; Volume 2, pp. 1–40. [[Google Scholar](#)] [[CrossRef](#)]
21. Pretty, J.; Bharucha, Z.P. Integrated pest management for sustainable intensification of agriculture in Asia and Africa. *Insects* 2015, 6, 152–182. [[Google Scholar](#)] [[CrossRef](#)]
22. Meela, M.M.; Mdee, L.K.; Masoko, P.; Eloff, J.N. Acetone leaf extracts of seven invasive weeds have promising activity against eight important plant fungal pathogens. *S. Afr. J. Bot.* 2019, 121, 442–446. [[Google Scholar](#)] [[CrossRef](#)]
23. Rampersad, S.N. A rapid colorimetric microtiter bioassay to evaluate fungicide sensitivity among *Verticillium dahliae* isolates. *Plant Dis.* 2011, 95, 248–255. [[Google Scholar](#)] [[CrossRef](#)] [[PubMed](#)]
24. Chadha, S.; Kale, S.P. Simple fluorescence-based high throughput cell viability assay for filamentous fungi. *Lett. Appl. Microbiol.* 2015, 61, 238–244. [[Google Scholar](#)] [[CrossRef](#)]
25. Serrano, R.; González-Menéndez, V.; Rodríguez, L.; Martín, J.; Tormo, J.R.; Genilloud, O. Co-culturing of fungal strains against *Botrytis cinerea* as a model for the induction of chemical diversity and therapeutic agents. *Front. Microbiol.* 2017, 8, 649. [[Google Scholar](#)] [[CrossRef](#)]
26. Santra, H.K.; Banerjee, D. Natural Products as fungicide and their role in Crop Protection. In *Natural Bioactive Products in Sustainable Agriculture*; Springer: Singapore, 2020; pp. 131–219. [[Google Scholar](#)] [[CrossRef](#)]
27. Kumar, S.; Singh, A. Biopesticides: Present status and the future prospects. *J. Biofertil. Biopestic.* 2015, 6, e129. [[Google Scholar](#)] [[CrossRef](#)]

28. Sayyed, R.Z.; Patel, P.R. Biocontrol potential of siderophore producing heavy metal resistant *Alcaligenes* sp. and *Pseudomonas aeruginosa* RZS3 vis-à-vis Organophosphorus Fungicide. *Indian J. Microbiol.* 2011, 51, 266–272. [[Google Scholar](#)] [[CrossRef](#)] [[PubMed](#)]
29. González-Menéndez, V.; Asensio, F.; Moreno, C.; de Pedro, N.; Monteiro, M.C.; de la Cruz, M.; Vicente, F.; Bills, G.F.; Reyes, F.; Genilloud, O.; et al. Assessing the effects of adsorptive polymeric resin additions on fungal secondary metabolite chemical diversity. *Mycology* 2014, 5, 179–191. [[Google Scholar](#)] [[CrossRef](#)]
30. Chen, C.; Long, L.; Zhang, F.; Chen, Q.; Chen, C.; Yu, X.; Liu, Q.; Bao, J.; Long, Z. Antifungal activity, main active components and mechanism of Curcuma longa extract against *Fusarium graminearum*. *PLoS ONE* 2018, 13, e0194284. [[Google Scholar](#)] [[CrossRef](#)]
31. Monteiro, M.C.; de La Cruz, M.; Cantizani, J.; Moreno, C.; Tormo, J.R.; Mellado, E.; De Lucas, J.R.; Asensio, F.; Valiente, V.; Brakhage, A.A.; et al. A new approach to drug discovery: High-throughput screening of microbial natural extracts against *Aspergillus fumigatus* using resazurin. *J. Biomol. Screen.* 2012, 17, 542–549. [[Google Scholar](#)] [[CrossRef](#)]
32. Vega, B.; Liberti, D.; Harmon, P.F.; Dewdney, M.M. A rapid resazurin-based microtiter assay to evaluate Qol sensitivity for *Alternaria alternata* isolates and their molecular characterization. *Plant Dis.* 2012, 96, 1262–1270. [[Google Scholar](#)] [[CrossRef](#)]
33. Santos, D.A.; Hamdan, J.S. Evaluation of broth microdilution antifungal susceptibility testing conditions for *Trichophyton rubrum*. *J. Clin. Microbiol.* 2005, 43, 1917–1920. [[Google Scholar](#)] [[CrossRef](#)] [[PubMed](#)]
34. De La Cruz, M.; Martín, J.; González-Menéndez, V.; Pérez-Victoria, I.; Moreno, C.; Tormo, J.R.; EL Aouad, N.; Guarro, J.; Vicente, F.; Reyes, F.; et al. Chemical and physical modulation of antibiotic activity in *Emericella* species. *Chem. Biodivers.* 2012, 9, 1095–1113. [[Google Scholar](#)] [[CrossRef](#)] [[PubMed](#)]
35. Thevissen, K.; Terras, F.R.G.; Broekaert, W. Permeabilization of fungal membranes by plant defensins inhibits fungal growth. *Appl. Environ. Microbiol.* 1999, 65, 5451–5458. [[Google Scholar](#)] [[CrossRef](#)] [[PubMed](#)]
36. Pelloux-Prayer, A.; Priem, B.; Joseleau, J. Kinetic evaluation of conidial germination of *Botrytis cinerea* by a spectrofluorometric method. *Mycol. Res.* 1998, 102, 320–322. [[Google Scholar](#)] [[CrossRef](#)]
37. Franche, A.; Imbs, C.; Fayeulle, A.; Merlier, F.; Billamboz, M.; Léonard, E. Zinc-mediated reactions on salicylaldehyde for *Botrytis cinerea* control. *Chin. Chem. Lett.* 2020, 31, 706–710. [[Google Scholar](#)] [[CrossRef](#)]
38. Chutrakul, C.; Khaokhajorn, P.; Auncharoen, P.; Boonruengprapa, T.; Mongkolporn, O. The potential of a fluorescent-based approach for bioassay of antifungal agents against chili anthracnose disease in Thailand. *Biosci. Biotechnol. Biochem.* 2013, 77, 259–265. [[Google Scholar](#)] [[CrossRef](#)]
39. Chutrakul, C.; Boonruangprapa, T.; Suvannakad, R.; Isaka, M.; Sirithunya, P.; Toojinda, T.; Kirtikara, K. Ascherxanthone B from *Aschersonia luteola*, a new antifungal compound active against rice blast pathogen *Magnaporthe grisea*. *J. Appl. Microbiol.* 2009, 107, 1624–1631. [[Google Scholar](#)] [[CrossRef](#)]

40. Alastruey-Izquierdo, A.; Cuenca-Estrella, M.; Monzón, A.; Mellado, E.; Rodríguez-Tudela, J.L. Antifungal susceptibility profile of clinical *Fusarium* spp. isolates identified by molecular methods. *J. Antimicrob. Chemother.* 2008, *61*, 805–809. [[Google Scholar](#)] [[CrossRef](#)]
41. Gray, K.C.; Palacios, D.S.; Dailey, I.; Endo, M.M.; Uno, B.E.; Wilcock, B.C.; Burke, M.D. Amphotericin primarily kills yeast by simply binding ergosterol. *Proc. Natl. Acad. Sci. USA* 2012, *109*, 2234–2239. [[Google Scholar](#)] [[CrossRef](#)]
42. Fungicide Resistance Action Committee. FRAC Code List ©* 2022: Fungal Control Agents Sorted by Cross-Resistance Pattern and Mode of Action (Including Coding for FRAC Groups on Product Labels). Available online: https://www.frac.info/docs/default-source/publications/frac-code-list/frac-code-list-2022--final.pdf?sfvrsn=b6024e9a_2 (accessed on 1 June 2023).
43. Mondal, S.N.; Bhatia, A.; Shilts, T.; Timmer, L.W. Baseline sensitivities of fungal pathogens of fruit and foliage of *Citrus* to Azoxystrobin, Pyraclostrobin, and Fenbuconazole. *Plant Dis.* 2005, *89*, 1186–1194. [[Google Scholar](#)] [[CrossRef](#)]
44. Piccirillo, G.; Carrieri, R.; Polizzi, G.; Azzaro, A.; Lahoz, E.; Fernández-Ortuño, D.; Vitale, A. In vitro and in vivo activity of QoI fungicides against *Colletotrichum gloeosporioides* causing fruit anthracnose in *Citrus sinensis*. *Sci. Hortic.* 2018, *236*, 90–95. [[Google Scholar](#)] [[CrossRef](#)]
45. Grayson, B.T.; Boyd, S.L.; Sampson, A.J.; Drummond, J.N.; Walter, D. Effect of adjuvants on the performance of the new cereal fungicide, metconazole. I glasshouse trials. *Pestic. Sci.* 1995, *45*, 153–160. [[Google Scholar](#)] [[CrossRef](#)]
46. Pirgozliev, S.R.; Edwards, S.G.; Hare, M.C.; Jenkinson, P. Effect of dose rate of Azoxystrobin and Metconazole on the development of Fusarium Head Blight and the accumulation of Deoxynivalenol (DON) in wheat grain. *Eur. J. Plant Pathol.* 2002, *108*, 469–478. [[Google Scholar](#)] [[CrossRef](#)]
47. Song, Y.; Xu, D.; Lu, H.; He, L.; Chen, L.; Shao, J.; Xu, C.; Mu, W.; Liu, F. Baseline sensitivity and efficacy of the sterol biosynthesis inhibitor triflumizole against *Botrytis cinerea*. *Australas. Plant Pathol.* 2015, *45*, 65–72. [[Google Scholar](#)] [[CrossRef](#)]
48. Angioni, A.; Porcua, L.; Dedola, F. Determination of famoxadone, fenamidone, fenhexamid and iprodione residues in greenhouse tomatoes. *Pest. Manag. Sci.* 2012, *68*, 543–547. [[Google Scholar](#)] [[CrossRef](#)]
49. Zhou, Y.; Xu, J.; Zhu, Y.; Duan, Y.; Zhou, M. Mechanism of action of the benzimidazole fungicide on *Fusarium graminearum*: Interfering with polymerization of monomeric tubulin but not polymerized microtubule. *Phytopathology* 2016, *106*, 807–813. [[Google Scholar](#)] [[CrossRef](#)]
50. Prakash, O.; Kumar, R.; Parkash, V. Synthesis and antifungal activity of some new 3-hydroxy-2-(1-phenyl-3-aryl-4-pyrazolyl) chromones. *Eur. J. Med. Chem.* 2008, *43*, 435–440. [[Google Scholar](#)] [[CrossRef](#)]
51. Petsikos-Panayotarou, N.; Markellou, E.; Kalamarakis, A.E.; Kyriakopoulou, D.; Malathrakis, N.E. In vitro and in vivo activity of Cyprodinil and Pyrimethanil on *Botrytis cinerea* isolates resistant to other Botryticides and selection for resistance to Pyrimethanil in a greenhouse population in Greece. *Eur. J. Plant Pathol.* 2003, *109*, 173–182. [[Google Scholar](#)] [[CrossRef](#)]

52. Kim, B.S.; Byung Byung, K.H. Microbial Fungicides in the Control of Plant Diseases. *J. Phytopathol.* 2007, *155*, 641–653. [[Google Scholar](#)] [[CrossRef](#)]
53. Yang, F.; Gritsenko, V.; Futterman, Y.S.; Gao, L.; Zhen, C.; Lu, H.; Jiang, Y.Y.; Bermanb, J. Tunicamycin potentiates antifungal drug tolerance via aneuploidy in *Candida albicans*. *mBio* 2021, *12*, e02272-21. [[Google Scholar](#)] [[CrossRef](#)]
54. Di, S.; Cang, T.; Liu, Z.; Xie, Y.; Zhao, H.; Qi, P.; Wang, Z.; Xu, H.; Wang, X. Comprehensive evaluation of chiral pydiflumetofen from the perspective of reducing environmental risks. *Sci. Total Environ.* 2022, *826*, 154033. [[Google Scholar](#)] [[CrossRef](#)] [[PubMed](#)]
55. Liu, S.; Ma, J.; Jiang, B.; Yang, G.; Guo, M. Functional characterization of MoSdhB in conferring resistance to pydiflumetofen in blast fungus *Magnaporthe oryzae*. *Pest. Manag. Sci.* 2022, *78*, 4018–4027. [[Google Scholar](#)] [[CrossRef](#)]
56. Amiri, A.; Heath, S.M.; Peres, N.A. Resistance to fluopyram, fluxapyroxad and penthiopyrad in *Botrytis cinerea* from strawberry. *Plant Dis.* 2013, *98*, 532–539. [[Google Scholar](#)] [[CrossRef](#)] [[PubMed](#)]
57. Kim, J.O.; Shin, J.H.; Gumilang, A.; Chung, K.; Choi, K.Y.; Kim, K.S. Effectiveness of different classes of fungicides on *Botrytis cinerea* causing gray mold on fruit and vegetables. *Plan. Pathol. J.* 2016, *32*, 570–574. [[Google Scholar](#)] [[CrossRef](#)] [[PubMed](#)]
58. Ishii, H.; Zhen, F.; Hu, M.; Li, X.; Schnabel, G. Efficacy of SDHI fungicides, including benzovindiflupyr, against *Colletotrichum* species. *Pest. Manag. Sci.* 2016, *72*, 1844–1853. [[Google Scholar](#)] [[CrossRef](#)]
59. Oliveira, M.S.; Cordova, L.G.; Peres, N.A. Efficacy and baseline sensitivity of Succinate-Dehydrogenase-Inhibitor fungicides for management of *Colletotrichum* crown rot of strawberry. *Plant Dis.* 2020, *104*, 2860–2865. [[Google Scholar](#)] [[CrossRef](#)]
60. Li, Y.; Sun, S.; Guo, Q.; Ma, L.; Shi, C.; Su, L.; Li, H. In vitro interaction between azoles and cyclosporin A against clinical isolates of *Candida albicans* determined by the checkerboard method and time-kill curves. *J. Antimicrob. Chemother.* 2008, *61*, 577–585. [[Google Scholar](#)] [[CrossRef](#)]
61. Cordeiro, R.A.; Macedo, R.B.; Teixeira, C.E.C.; Marques, F.J.F.; Bandeira, T.J.P.G.; Moreira, J.L.B.; Brilhante, R.S.N.; Rocha, M.F.G.; Sidrim, J.J.C. The calcineurin inhibitor cyclosporin A exhibits synergism with antifungals against *Candida parapsilosis* species complex. *J. Med. Microbiol.* 2014, *63*, 936–944. [[Google Scholar](#)] [[CrossRef](#)]
62. Owen, W.J.; Yao, C.; Myung, K.; Kemmitt, G.; Leader, A.; Meyer, K.G.; Bowling, A.J.; Slanec, T.; Kramer, V.J. Biological characterization of fenpicoxamid, a new fungicide with utility in cereals and other crops. *Pest. Manag. Sci.* 2017, *73*, 2005–2016. [[Google Scholar](#)] [[CrossRef](#)]
63. Loiseleur, O. Natural products in the discovery of agrochemicals. *Chimia* 2017, *71*, 810–822. [[Google Scholar](#)] [[CrossRef](#)]
64. Malik, A.K. Determination of the fungicide ferbam in wheat grains after adsorption onto microcrystalline naphthalene. *J. AOAC Int.* 2000, *83*, 971–976. [[Google Scholar](#)] [[PubMed](#)]
65. Rathore, H.S.; Ishratullah, K.; Varshney, C.; Varshney, G.; Mojumdar, S.C. Fungicidal and bactericidal activity of metal diethyldithiocarbamate fungicides. *Synthesis and characterization. J. Therm. Anal. Calorim.* 2008, *94*, 75–81. [[Google Scholar](#)] [[CrossRef](#)]

Chapter 3

66. Omura, S. The antibiotic cerulenin, a novel tool for biochemistry as an inhibitor of fatty acid synthesis. *Bacteriol. Rev.* 1976, *40*, 681–697. [[Google Scholar](#)] [[CrossRef](#)] [[PubMed](#)]
67. Bills, G.F.; Platas, G.; Gams, W. Conspecificity of the cerulenin and helvolic acid producing *Cephalosporium caerulens*, and the hypocrealean fungus *Sarocladium oryzae*. *Mycol. Res.* 2004, *108*, 1291–1300. [[Google Scholar](#)] [[CrossRef](#)]

Chapter 4

Leaf-litter-associated fungi from South Africa to control fungal plant pathogens

Rachel Serrano, Víctor González-Menéndez, Ignacio Pérez-Victoria, Isabel Sánchez, Clara Toro, Thomas A. Mackenzie, Jesús Martín, José R. Tormo, Olga Genilloud

Scientific Reports, 2025

(submitted)

JCR 3.8, Q1, total journal citations 734947

Abstract

Fungal genomes encode a huge biosynthetic potential to produce a wide diversity of chemical structures with valuable biological activities, remaining silent or under-expressed with standard laboratory conditions. Fungal Natural Products provide numerous environmentally friendly properties that make them an attractive alternative to the use of synthetic pesticides for the control and management of fungal diseases in plants. The main goal of this study was to explore and characterize leaf-litter-associated fungi from South Africa for the discovery of new bio-fungicides. For this purpose, a subset of 232 fungal strains were selected from the MEDINA Fungal Collection and were taxonomically classified. Molecular and phylogenetic analyses revealed a great richness and complexity in leaf-litter-associated fungi from endemic plants of South Africa, one of the worldwide biodiversity “hotspots”. Then, a specifically designed OSMAC approach, with five different fermentation media and the addition of SAHA, was employed to explore their biosynthetic capacity to produce bioactive secondary metabolites. The antifungal activity of 2,362 fungal extracts was assessed against four relevant fungal phytopathogens using a recently developed HTS platform. The presence of SAHA during fungal fermentations in specific formulation media generated considerable changes in the metabolomic profiles that clearly influencing the diversity and quantity of metabolites. This differential metabolite production also affected the activity hit-rates, that increased the number of active extracts against *B. cinerea* and *M. grisea*. As a proof of concept, the addition of SAHA to BRFT medium during fermentation of *Libertasomyces aloeticus* CF-168990 led to the discovery of the novel molecule libertamide $C_{16}H_{27}NO_2$, which showed a great potential to control the growth of *Zymoseptoria tritici*, the causal agent of septoria leaf blotch. Therefore, leaf-litter from South Africa proven to be a valuable source of undescribed fungal species with a considerable biosynthetic potential, that provided several promising candidates for the discovery of possible new natural fungicides.

Keywords: fungal strains, leaf-litter, phytopathogens, fungicides, Natural Products, secondary metabolites

1. Introduction

Plant pathogens are the most important cause of crop losses in agriculture worldwide. Fungal phytopathogens exhibit a broad range of host plants, leading to devastating ecological and economic damages (Jayawardena et al., 2021; Pandit et al., 2022; Riseh et al., 2022). Among the most significant genera of fungal phytopathogens are *Magnaporthe*, *Botrytis*, *Puccinia*, *Fusarium*, *Blumeria*, *Zymoseptoria*, *Colletotrichum*, *Ustilago* and *Melampsora*, which are included in the top ten of the most problematic phytopathogenic fungi (Dean et al., 2012). The preferred strategies to control and manage these fungal diseases involve the use of chemical pesticides. Nowadays, synthetic fungicides are widely employed due to their efficiency in controlling fungal infections and their critical role in preventing the spread of diseases. However, excessive use of these agrochemicals can lead to severe negative impact on both environmental and human health (Pandit et al., 2022; Riseh et al., 2022). Moreover, the application of chemical pesticides is strictly regulated to guarantee the quality and safety of agricultural products. Therefore, there is an urgent need to

develop a new effective generation of fungicides from natural sources that can contribute to crop protection for a more sustainable agriculture.

Microbial Natural Products are considered a valuable source of novel bioactive molecules with a wide range of applications in medicine, food industry and agriculture (Atanasov et al., 2021; Riedling et al., 2024). They exhibit important properties such as biodegradability, low toxicity, biocompatibility and a large variety of modes of action, which make them a viable alternative for the control and the management of plant diseases (Pandit et al., 2022; Santra & Banerjee, 2020). In particular, fungi have been extensively explored for the discovery of new bioactive compounds due to their huge biosynthetic capability encoded in their genome (Riedling et al., 2024; Xue et al., 2023). Numerous fungal secondary metabolites have been identified as potential biopesticides, mostly belonging to phenolic, terpenoid and alkaloid chemical classes (Pandit et al., 2022; Santra & Banerjee, 2020). Griseofulvin and dechlorogriseofulvin, isolated from various species of fungi including endophytic strains of *Penicillium canescens* and *Xylaria* sp., demonstrated strong inhibitory effects against relevant phytopathogens such as *Botrytis cinerea*, *Blumeria graminis*, *Colletotrichum orbiculare*, *Corticium sasakii*, *Didymella bryoniae*, *Magnaporthe grisea*, *Sclerotinia sclerotiorum* (Park et al., 2005; Wang et al., 2010). Similarly, compounds such as sterols have shown antifungal activity on *Bipolaris sorokiniana*, a common root rot pathogen of wheat and barley crops (Lu et al., 2000). Additionally, epoxycytochalasin H and cytochalasins N and H were obtained from the endophyte *Phomopsis* sp. and exhibited a strong inhibition of *Bipolaris sorokiniana*, *B. maydi*, *Botrytis cinerea*, *Rhizoctonia cerealis*, *Sclerotinia sclerotiorum* and *Fusarium oxysporum* (Jing et al., 2011). Finally, bioactive compounds strobirulins, first identified by Anke et al., 1977 from culture of the basidiomycete *Strobilurus tenacellus*, have played a key role in the development of the β -methoxyacrylate class of relevant agricultural fungicides (Niego et al., 2023).

Fungi are ubiquitous microorganisms than can colonize multiple ecosystems (Bills & Gloer, 2016; Niego et al., 2023). Specifically, in terrestrial habitats fungi play an important role in carbon and nutrient cycling through the decomposition of organic material. The process of leaf-litter decomposition is a highly complex process that required the presence of a large number of diverse microorganisms, where fungi are an essential element because of their ability to degrade recalcitrant components present in leaf-litter matter such as cellulose, lignin and suberin (Foster et al., 2022; Grossman et al., 2020; Voříšková & Baldrian, 2013). Consequently, communities associated with leaf-litter harbour a significant number of rare and unique species (Crous et al., 2006; Foster et al., 2022; Voříšková & Baldrian, 2013). The fungal community associated with leaf-litter is dominated by *Ascomycota* phylum, followed by *Basidiomycota*, especially saprotrophic cord-forming fungi, both considered to possess the richest secondary metabolic potential (Bills & Gloer, 2016). Several previous works have studied the biodiversity of leaf-litter fungi in South Africa, mainly focused on fungi associated with *Proteaceae* (proteas) and *Restionaceae* (restios). South Africa is considered one of the biodiversity “hotspots”, including areas such as the Cape Floral Kingdom that is the smallest and most biodiverse biome, dominated by endemic plants (Crous et al., 2006; Mamathaba et al., 2022; Goldblatt & Manning, 2000). In this context, South Africa provides unique and valuable conditions to develop a highly diverse leaf-litter material.

Despite the high fungal biosynthetic capability to produce a large variety of bioactive Natural Products, this potential remains mostly unknown and silent under traditional fermentation conditions. OSMAC (One Strain Many Compounds) is a culture-based approach commonly applied

to fungal strains for enhancing secondary metabolite expression under laboratory conditions. This approach involves the use of multiple nutritional and cultivation conditions such as the use of different media (carbon and nitrogen sources), variations in shaking and aeration, modifications of pH levels and temperature, as well as the addition of epigenetic modifiers (Abdelwahab et al., 2018; Gakuubi et al., 2022; Serrano et al., 2021; Wei et al., 2021; Xue et al., 2023). On the one hand, numerous reports have demonstrated the importance of media composition to induce the production of fungal secondary metabolites. Previous studies with a nutritional array revealed that the solid-state-fermentation (SSF) using a rice-based medium provided the most complex and diverse metabolite profiles (Serrano et al., 2021; Song et al., 2023; Wei et al., 2021). On the other hand, epigenetic modifiers were also effectively activating silent biosynthetic pathways during fungal fermentations (Beau et al., 2012; Du et al., 2014; Gubiani et al., 2017; Gupta et al., 2020; Henrikson et al., 2009; Pillay et al., 2022; Xue et al., 2023; Zhang et al., 2019). More specifically, suberoylanilide hydroxamic acid (SAHA) is considered the most widely used histone deacetylase modifier for the induction of the secondary metabolite production in fungi (Xue et al., 2023; Zhang et al., 2019).

In our previous work published by Serrano et al., in 2021, it was confirmed that variations in the medium composition and the addition of SAHA had a significant impact on the metabolomic profiles of a broad diversity of leaf-litter-associated fungal strains. For this purpose, a specific OSMAC approach was designed where each fungal strain (n=232) was cultured in 10 different fermentation conditions, including four liquid submerged fermentation media (SmF) LSFM, MCKX, SMK-II, YES and one solid-state fermentation (SSF) BRFT medium, in presence and absence of SAHA, generating a library of 2,362 crude extracts that contained the largest diversity of secondary metabolites produced by these leaf-litter-associated fungi. Therefore, the primary objectives of this study have been to taxonomically characterize in detail this group of 232 fungal strains isolated from leaf-litter collected in South Africa, and to evaluate their potential to control fungal phytopathogens). The assessment of their bioactivity on a High-throughput Screening (HTS) assay panel against four relevant fungal phytopathogens (*Botrytis cinerea*, *Colletotrichum acutatum*, *Fusarium proliferatum*, and *Magnaporthe grisea*), has allowed us to identify and characterize here the most interesting antifungal extracts and their bioactive secondary metabolites.

2. Results

2.1. Biodiversity of the fungal population

The selected 232 fungal strains isolated from leaf-litter collected in South Africa was obtained from MEDINA´s Fungal Collection. Their phylogenetic analysis combined with Blast identification using ITS1-5.8-ITS2 and 28S rDNA revealed the full characterization in 11 different fungal classes, 33 orders, 81 families and more than 158 genera. *Pleosporales* (n=94), followed by *Helotiales* (n=25), *Hypocreales* (n=12) *Chaetothyriales* (n=9) and *Xylariales* (n=8) were the most represented orders. The remaining 61 fungal strains were distributed among 27 different orders. Within the most abundant order *Pleosporales*, fungal strains were categorized in 59 genera from 23 families, being *Didymellaceae* (n=20), *Phaeosphaeriaceae* (n=15), *Didymosphaeriaceae* (n=8) and *Cucurbitariaceae* (n=7) the most representative families. From the total 158 different genera

included in the study, 112 were represented by only one species, suggesting a high taxonomic diversity of leaf-litter-associated fungi (see full list in Supplementary Information, Table S1).

Furthermore, the molecular identification highlighted a large number of strains whose ITS rDNA sequences showed similarities lower than 95% with any previously published sequences in public databases. A total of 64 strains (28%) were classified as tentative new species that will be described in future works (Figure 1 and Table S1). For example, *Acrospermum* sp. CF-166111 isolated from leaf-litter of mountain fynbos of *Protea repens*, *Corticium* sp. CF-166036 from mountain fynbos *Protea laurifolia*, *Tremateia* sp. CF-168994 from coastal fynbos *Diosma subulata*, *Scolecobasidium* sp. CF-164484 from coastal fynbos *Chrysanthemoides monilifera*, *Neoanthostomella* sp. CF-164451 from coastal fynbos *Sideroxylon inerme*, *Alfoldia* sp. CF-169033 from lowland fynbos *Rafnia* cf. *triflora* and *Tarchonanthus camphorates*, *Melnikomyces* sp. CF-164291 from leaf-litter of culm restio or *Clavulina* sp. CF-164389 from leaf-litter of wild olive, are some of these strains remarked as potentially novel species.

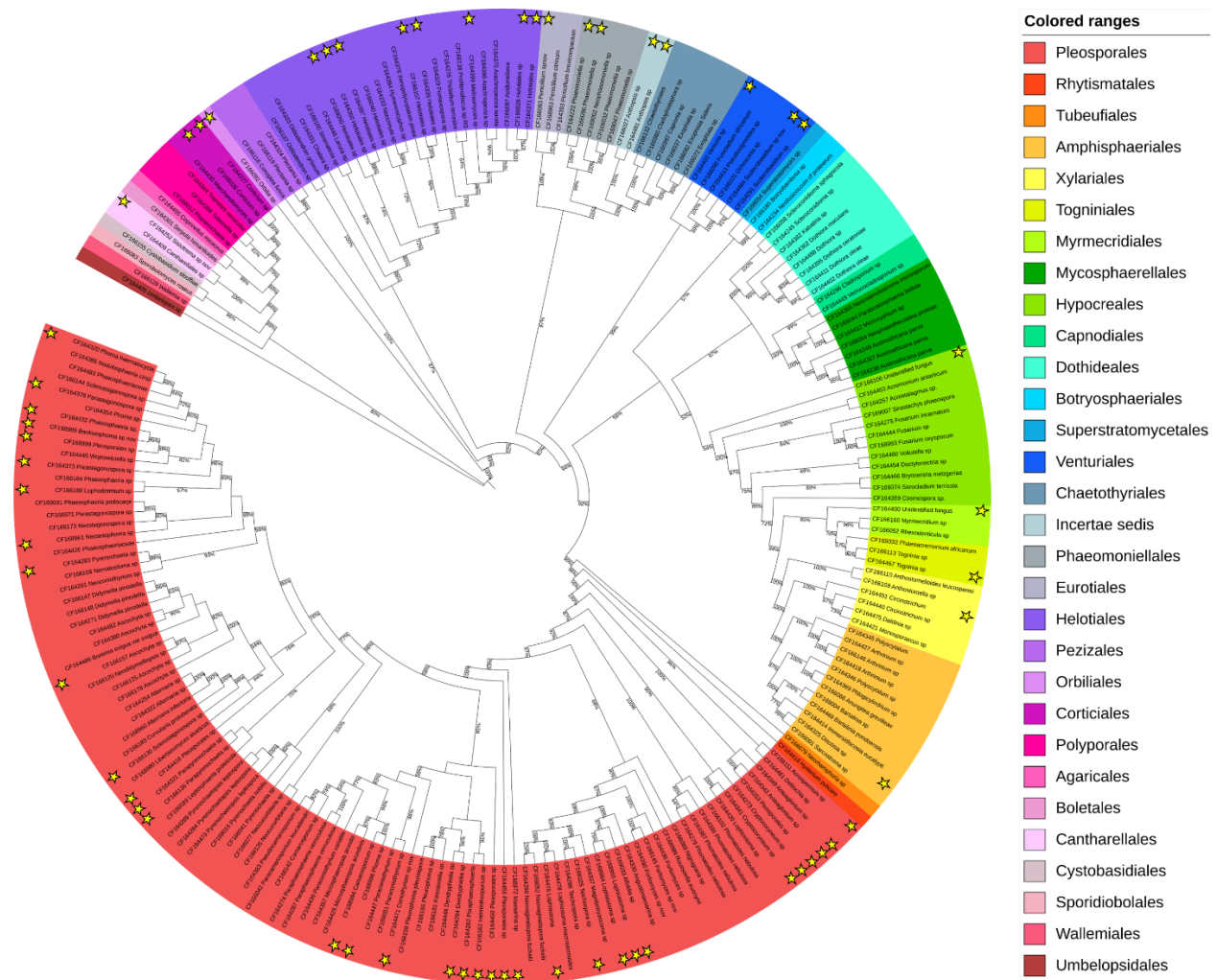


Figure 1. Phylogenetic tree based on maximum likelihood for 28S rDNA sequences of leaf-litter-associated fungi from South Africa. Major taxonomic orders are labelled using differential colour coding. Clade maximum likelihood bootstrap values are indicated on the branches (>50%). Yellow stars highlight the potential new species.

2.2. HTS Platform activity characterization against fungal phytopathogens

The previously generated 2,362 extract library was assessed in a primary screening on an HTS platform against four phytopathogens selected according to their impact on global agriculture. To assess the bioactivity of each fungal extract, absorbance and fluorescence data were used to determine the percentage of inhibition (% INH). Instead of selecting extracts that inhibited more than 50% of conidial germination, we further analyzed the activity distribution using a robust statistical criterium for the hit selection. The distribution of active extracts was evaluated with JMP® software to test the normality of data and identify possible outliers as potential hits. The distribution of the hits population for each phytopathogen is represented in Figure 2.

2.2.1 *Botrytis cinerea* microdilution assay. Fungal extracts were tested against *B. cinerea*, responsible of gray mold disease in several important crops. Activity based on absorbance and fluorescence data are represented in two different histograms (Figures 2a-b). Both readouts exhibited a symmetrical and normal distribution, as indicated the boxplots with central values around 0% INH and zero z' score. In addition, graphics display a wide bell-shaped distribution, reflecting a high variability in the activity data. Despite this dispersion in data, the activity distribution allowed the differentiation of hits from the population. Statistical analysis showed extracts with % INH > -53% (z' score > -1.5) as outliers in the upper quartile from absorbance data (Figure 2a, black dots at the upper-right) and % INH > -41% (z' score > -1.5) for fluorescence (Figure 2b), highlighting them as the hit population. The criterion for hit selection was stringent to prioritize high-quality hits, where only extracts with activity greater than -53% INH in both readouts were considered hits. Based on this criterion, a total of 113 active extracts (4.78% hit-rate) from 60 fungal strains were identified as hits against *B. cinerea*.

2.2.2. *Colletotrichum acutatum* microdilution assay. The HTS platform also included the evaluation of the antifungal potential of the extract library against *C. acutatum*, the causative pathogen of anthracnose disease. Statistical analysis of antifungal activity showed a normal distribution of the data, with the absorbance boxplot slightly shifted to the left (non-activity/overgrowth), but distribution was normalized with z' score transformation around zero (Figure 2c). Histograms exhibited extracts with % INH > -16% in the upper quartile of both boxplots (z' score > -1.5 for absorbance and z' score > -0.75 for fluorescence), corresponding to the outlier populations (Figures 2c-d). However, this percentage of inhibition was very low and insufficient to select the most potent active extracts. Therefore, a more stringent hit-selection criterion was applied with a cut-off of 50% INH and z' scores > -2 for both readouts, allowing to identify the upper quartile outliers as hits from the normal population. This second criterion aimed to prioritize the selection of highly active candidates, resulting in only 29 active extracts (1.23% hit-rate) that corresponded to 12 fungal strains.

2.2.3. *Fusarium proliferatum* microdilution assay. Activity distribution against *F. proliferatum*, a pathogen associated with the dry rot of garlic bulb, showed again a symmetrical bell-shaped curve indicating a normal distribution of data. Figure 2e shows the absorbance boxplot with a leftward shift for activity axis, suggesting the overgrowth of this phytopathogen. Data were also normalized by z' score as previously shown in the *C. acutatum* assay. However, fluorescence-based activity

showed clustered data around 0% INH and zero z' score (Figure 2f). The outlier population was highlighted from % INH > -13.92% (z' score > -1.25) for absorbance and % INH > -16.61% (z' score > -0.75) for fluorescence. Despite this distribution, the hit selection criteria remained stringent as previously performed for *C. acutatum*, where only extracts with more than 50% of inhibition were considered hits (upper quartile outliers), resulting in the selection of 36 active extracts (1.52% hit-rate) corresponding to 13 fungal strains.

2.2.4. *Magnaporthe grisea* microdilution assay. The microdilution assay against *M. grisea* CF-105765, the causative agent of rice blast disease, revealed a unique pattern of antifungal activity with a non-symmetrical distribution in both assay readouts. On the one hand, fluorescence data distribution showed a short interquartile (length of the box), indicating small data variations, but two hit populations were highlighted in the upper quartile (binormal distribution) (Figure S1). On the other hand, absorbance data did not follow a normal distribution, exhibiting a large bell-shaped curve that extended from -100% to 100% of activity (Figure S1a) and prevented discrimination of hits. When active extracts with more than 50% INH were selected, a high number of hits ($n=420$, 17.78% hit-rate) were identified. This hit population was studied in detail and most of active extracts corresponded to BRFT fermentations ($n=202$), which were further analyzed by Mass Spectrometry. When these extracts in BRFT were not considered in the activity distribution, the new activity histograms showed a normal and symmetrical distribution with two hit populations (Figures 2g-h). The first group of active extracts supported by absorbance and fluorescence data was prioritized as containing the most potent hits. This selection corresponded to activities higher than -87% INH in both assays (z' score > -2.25 for absorbance and z' score > -3.5 for fluorescence). Following this criterium, 41 active extracts (1.74% hit-rate) from 18 fungal strains were identified as hits, which were explained by the presence of known bioactive metabolites in subsequent dereplication. This second outlier hit population was further studied to identify potentially new antifungal molecules. The fluorescence-based activity boxplot highlighted this second population of outliers (Figure 2h), despite they were not statistically distinguished from the mean population observed with absorbance data (Figure 2g). This hit population included a total of 213 extracts (9.02% hit-rate) with more than 50% of inhibition of *M. grisea*. This activity group corresponded to fermentations of 82 fungal strains in more than one condition, being 32 strains common to other phytopathogens.

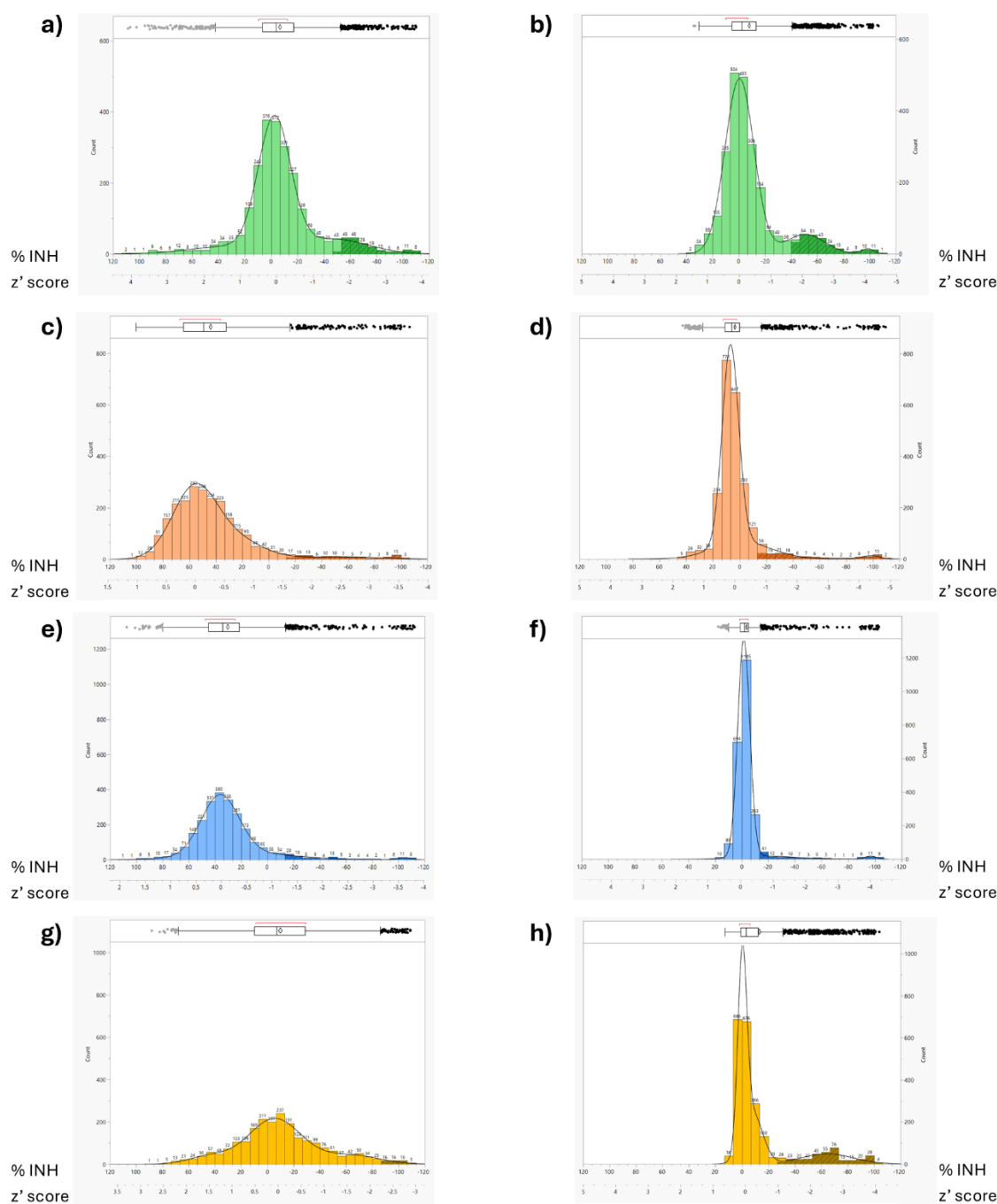


Figure 2. Distribution of antifungal activity based on absorbance (left column) and fluorescence data (right column) against (a-b) *Botrytis cinerea* B05.10, (c-d) *Colletotrichum acutatum* CF-137177, (e-f) *Fusarium proliferatum* CBS 115.97 and (g-h) *Magnaporthe grisea* CF-105765. The x-axis shows the range of percentage of inhibition and the corresponding z' score values, while the y-axis shows the frequency of occurrences.

2.3. Chemical dereplication of active extracts

The screening campaign against the four phytopathogens resulted in a total of 340 active extracts, which were selected for a deeper chemical dereplication of known active compounds. The combined analysis with LC-LRMS and LC-HRMS identified a total of 95 known molecules with a broad chemical diversity in 187 active extracts corresponding to 68 strains (Figure 3). The distribution of the dereplicated molecules revealed that 64 compounds were detected in single strains, whereas 31 were common to more than one strain. The most frequently dereplicated molecules were stemphytoxin I, preussomerin B, palmarumycin C₁₅, palmarumycin C₁₆ and mellein. In general, palmarumycins were the most represented family of bioactive compounds, including palmarumycin B₁, B₉, C₁₂, C₁₃, C₁₅ and C₁₆, described as phytotoxic, antimicrobial, and cytotoxic compounds. Among all dereplicated compounds, six were only detected in fermentations with SAHA: 7-chloro-6-methoxymellein, cinatrin C₁/C₂/C₃, cordycerebroside A/B, funicone, nomofungin and quinolactacin A₂. N-deoxyakanthomycin and exophillic acid were the unique molecules found in fermentations without SAHA that generated antifungal activity. The remaining active molecules were detected in fermentations with and without SAHA.

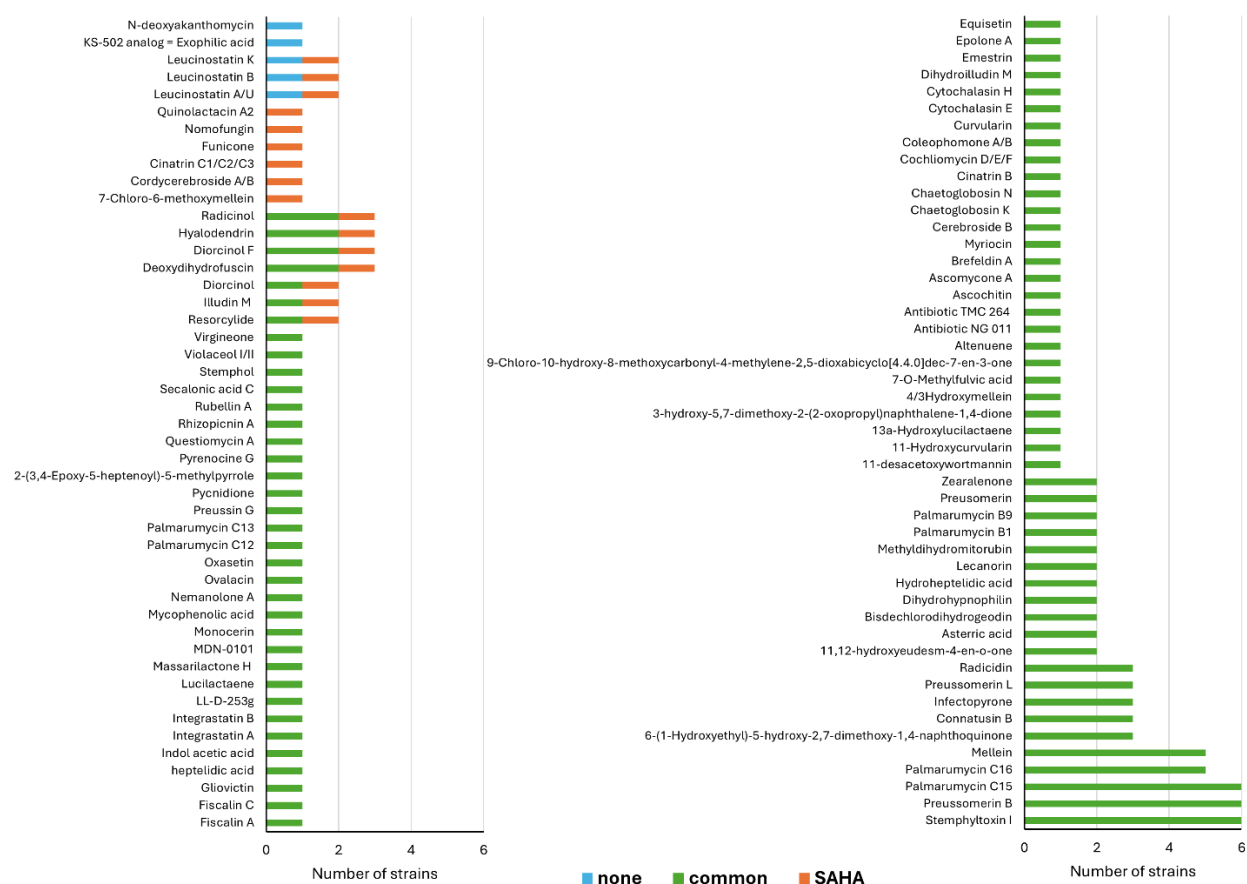


Figure 3. Dereplicated molecules by LC-LRMS and LC-HRMS analyses in only the active extracts from leaf-litter-associated fungi. Compounds are shown according to their production in absence of SAHA (blue), in presence of SAHA (orange) and produced in both conditions (green), tentatively supporting the observed activity.

2.4. Differential induction of antifungal activities

The hit population of 340 active extracts from 117 fungal strains obtained from the HTS Platform were distributed according to their fermentation conditions where they were originally obtained (Figures 4 and Table S2). Figure 4a shows the distribution of the active extracts based on the fermentation media, being the solid medium BRFT the most productive to generate activity against *B. cinerea* and *C. acutatum*. In contrast, for *F. proliferatum* and *M. grisea* the best fermentation media to obtain bioactivities were the liquid conditions LSFM and SMK-II, respectively. Additionally, the influence of SAHA on the bioactivity rates was also evaluated (Figure 4b). The addition of SAHA during fungal fermentations clearly increased the number of active extracts against *B. cinerea* and *M. grisea*. However, the opposite effect was observed for *C. acutatum* and *F. proliferatum*, where fermentations with SAHA provided fewer number of active extracts.

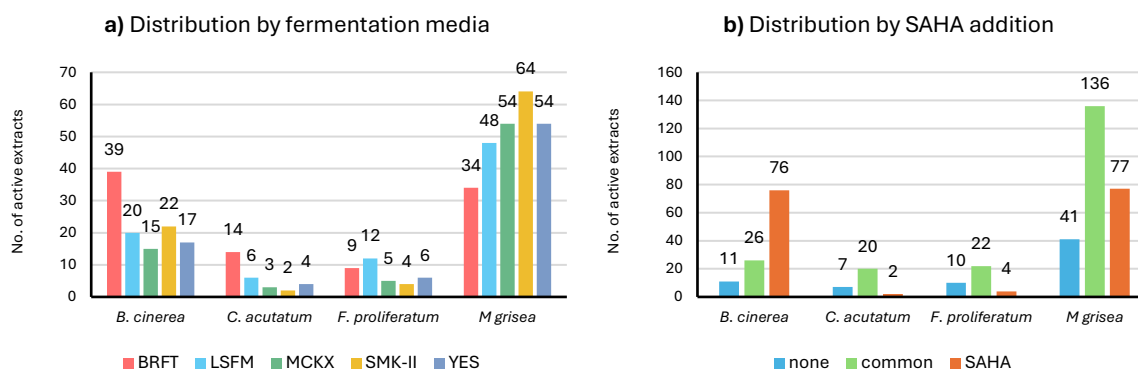


Figure 4. Distribution of active extracts against each phytopathogen according to the culture conditions; **(a)** fermentation medium and **(b)** the presence or absence of SAHA during the fermentation process. none = fermentations without SAHA were active, common = fermentations with and without SAHA were active, SAHA = fermentations in presence of SAHA was the active one.

2.4.1. Differential metabolite production in the presence of SAHA. The addition of SAHA during fungal fermentations promoted important changes in the activity phytopathogen hit-rates. For example, the number of active extracts against *B. cinerea* increased from 11 hits in non-supplemented fermentations to 76 hits in presence of SAHA (Figure 4b). To characterize in detail these differences observed in presence and absence of SAHA, the chemical profiles of hits where SAHA induced a new antifungal activity were compared to identify differential metabolite productions. This evaluation revealed two different categories based on the effect of SAHA on the secondary metabolite profiles:

(i) Fungal fermentations with clear enhancement in the production levels of specific compounds in the presence of SAHA: Upon chemical analysis, the activity of 27 active extracts could be explained by the effect of SAHA to increase the production levels of known bioactive metabolites. Figures 5a-d and Table 1 show some interesting examples with significant modulation of specific metabolites that correlated to the antifungal activity observed against phytopathogens.

The strain *Curvularia protuberata* CF-166183 produced 11-hydroxycurvularin, resorcylic acid and curvularin in BRFT medium, but the production levels of these three compounds were enhanced in the presence of SAHA (Figure 5a). Another example is the increase of peak area of bisdechlorodihydrogeodin and asteric acid when *Oidiodendron* sp. CF-166187 was grown in BRFT with SAHA (Figure 5b). The strain *Pyrenochaetopsis leptospora* CF-164269 doubled the production of stemphylytoxin I in YES medium with SAHA (Figure 5c). Moreover, *Forliomyces* sp. CF-164290 showed an improvement in the production of ascomycone A during its fermentation in YES medium with SAHA (Figure 5d).

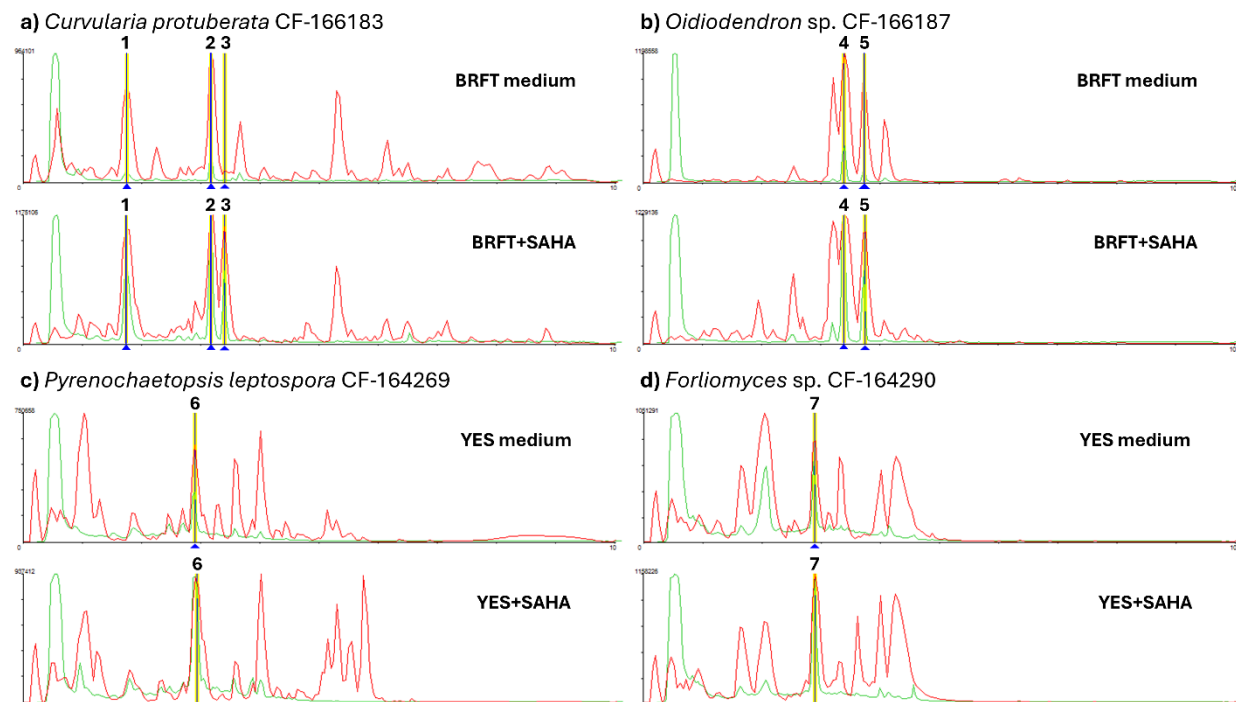


Figure 5. Examples of LC-HRMS profiles of active extracts where SAHA addition generated an enhancement in production levels of bioactive metabolites. HPLC/UV at 210 nm normalized profiles in green and HPLC/HR-MS normalized profiles in red. Indicated peaks highlighted in yellow.

Table 1. MS comparison of production levels of known active metabolites in absence and presence of SAHA.

Peak number	Compound name	Molecular formula	Accurate mass	Retention time	Peak area in BRFT	Peak area in BRFT+SAHA
1	11-hydroxycurvularin	C ₁₆ H ₂₀ O ₆	308.1257	1.76	15,290,921	25,862,301
2	resorcylic acid	C ₁₆ H ₁₈ O ₅	290.1152	3.18	15,392,816	20,242,995
3	curvularin	C ₁₆ H ₂₀ O ₅	292.1312	3.40	1,397,442	17,717,421
4	bisdechlorodihydrogeodin	C ₁₇ H ₁₆ O ₇	332.0896	3.39	19,428,975	25,949,254
5	asteric acid	C ₁₇ H ₁₆ O ₈	330.0746	3.73	19,142,264	32,233,012
6	stemphylytoxin III	C ₂₀ H ₁₂ O ₆	348.0636	2.92	12,839,908	24,041,106
7	ascomycone A	C ₁₆ H ₁₄ O ₆	302.0796	2.90	21,484,759	37,395,496

(ii) **Bioactive compounds that were only produced in the presence of SAHA:** The addition of SAHA during fungal fermentations also modified the secondary metabolite profiles of some strains, promoting the production of unique molecules (Figures 6a-d & Table 2). For example, the production of 7-chloro-6-methoxymellein by *Pseudocoleophoma* sp. CF-164448 was only observed in the presence of SAHA. Figure 6a shows the LC-HRMS profiles of this strain in LSFM medium, highlighting a small peak at 4.26 min (peak number 9) that corresponds to this antifungal compound that is only detected in LSFM with SAHA. Additionally, this molecule was also detected in the fermentation of the same strain in BRFT with SAHA, which also showed inhibitory effects on the germination of *B. cinerea* and *M. grisea* conidia (data not shown). Another example is the strain *Sarcostroma* sp. CF-166091, that produced only in BRFT with SAHA two bioactive metabolites hyalodendrin and diorcinol (Figure 6b), which generated the inhibition of *B. cinerea*. Moreover, the antifungal activity detected in the strain *Pyrenochaeta nobilis* CF-169016 in BRFT with SAHA corresponded to the induction of infectopyrone in the presence of SAHA (Figure 6c). Finally, the strain *Desertiserpentica* sp. CF-164476 showed significant differential chemical and bioactivity profiles due to the SAHA addition. In figure 6d the profile from the BRFT fermentation extract highlighted the production of N-deoxyakanthomycin, whereas the addition of SAHA in the same medium induced the production of the cytotoxic molecule illudin M.

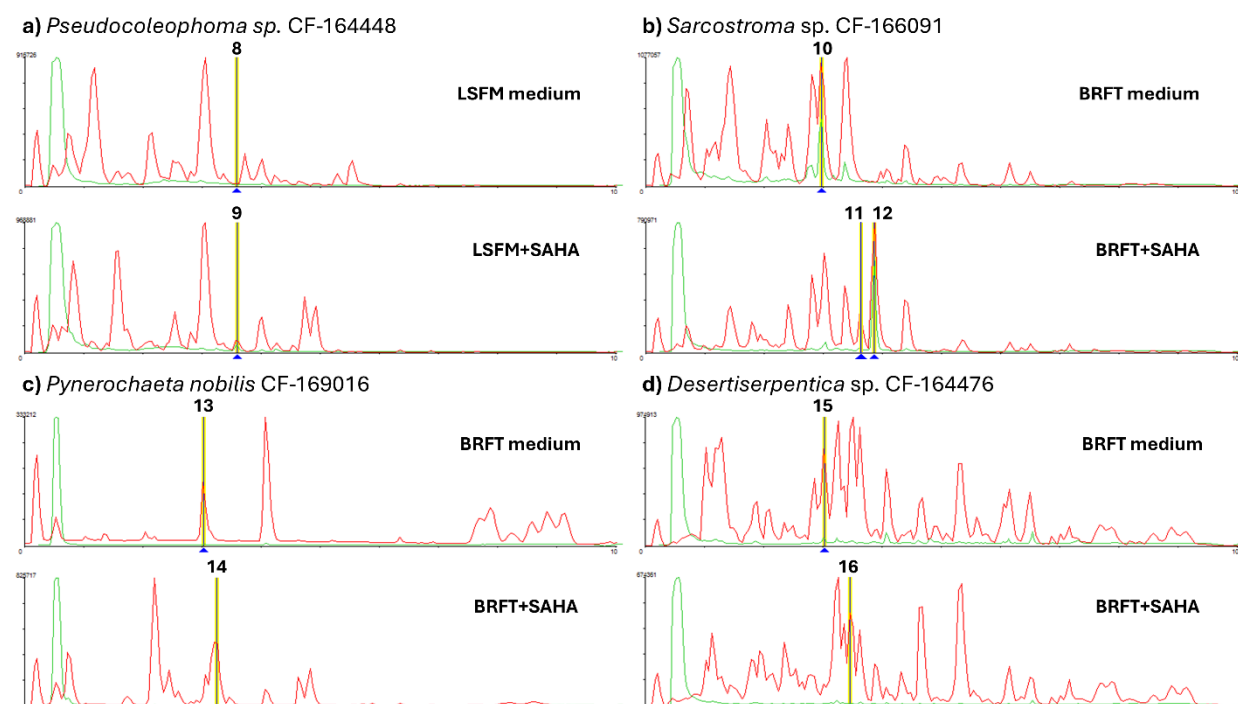


Figure 6. Examples of LC-HRMS profiles of active extracts where SAHA addition induced the expression of unique bioactive metabolites. HPLC/UV at 210 nm normalized profiles in green and HPLC/HR-MS normalized profiles in red. Indicated peaks highlighted in yellow.

Table 2. Examples of induced bioactive metabolites by the presence of SAHA during fungal fermentations

Peak number	Compound name	Molecular formula	Accurate mass	Retention time	Fermentation condition
8	undetermined	-	222.1612	4.42	BRFT
9	7-chloro-6-methoxymellein	C ₁₁ H ₁₁ ClO ₄	242.0346	4.26	BRFT+SAHA
10	undetermined	C ₁₅ H ₁₈ O ₅	278.1152	2.97	BRFT
11	hyalodendrin	C ₁₄ H ₁₆ N ₂ O ₃ S ₂	260.1158	3.62	BRFT+SAHA
12	diorcinol	C ₁₄ H ₁₄ O ₃	230.0943	3.86	BRFT+SAHA
13	undetermined	C ₁₅ H ₁₈ N ₂ O ₃	306.1033	3.02	BRFT
14	infectopyrone	C ₁₄ H ₁₆ O ₅	264.0989	3.24	BRFT+SAHA
15	N-deoxykanthomycin	C ₁₆ H ₂₅ NO ₃	279.1832	3.02	BRFT
16	illudin M	C ₁₅ H ₂₀ O ₃	248.1401	3.45	BRFT+SAHA

2.4.2. Differential metabolite production by fermentation medium. Variations in carbon and nitrogen sources during fermentation process also significantly influenced the expression of bioactive secondary metabolites. All the tested fermentation media ensured the production of specific activities against the four phytopathogens. For example, the active extracts against *B. cinerea* included fermentations in the five media: BRFT (n=39), SMK-II (n=22), LSFM (n=20), YES (n=17) and MCKX (n=15) (Figure S2). Similar results were obtained for *C. acutatum* active extracts. However, the ranking clearly changed in the *F. proliferatum* screening, where, on the contrary, the most productive conditions for the production of activities were LSFM (n=12), being followed by BRFT (n=9), YES (n=6), MCKX (n=5) and SMK-II (n=4). Finally, non-significant differences were found between the fermentation media in the case of active extracts against *M. grisea*.

A relevant example of this differential metabolite production according to the nutritional arrays is the strain *Chalara* sp. CF-164331. Figure 7 shows the LC-HRMS profiles of this strain grown in six fermentation conditions, which were active against *M. grisea*. On the one hand, two related unidentified molecules C₁₃H₁₃ClO₆ and C₁₃H₁₃ClO₅ were detected in all the conditions but with different production levels. A significant increase in the peak areas was observed in their production in LSFM medium with and without SAHA. On the other hand, fermentations of the same strain in SMK-II medium (both with and without SAHA) produced additionally the macrocyclic mycotoxin emestrin. Moreover, the production of this compound was enhanced by the addition of SAHA, that consequently increased the inhibitory effects of this extract. Finally, fermentations in BRFT medium changed again the chemical profiles, inducing the production of two additional metabolites (C₁₉H₂₃N₅O₅ and C₁₈H₂₄O₈) that might be related to its activity against *M. grisea*.

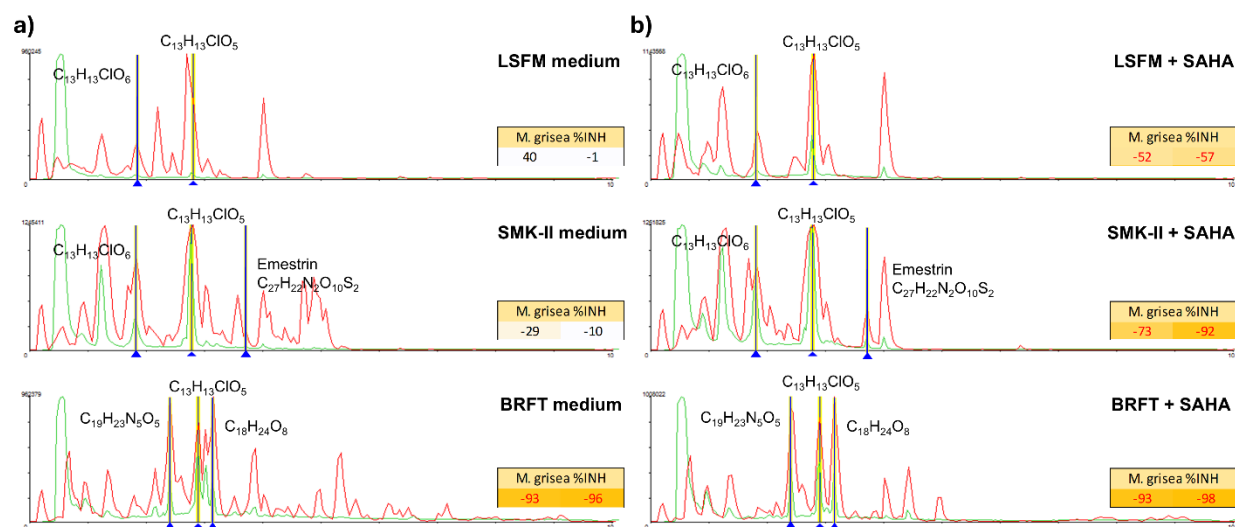


Figure 7. Comparative analysis of LC-HRMS profiles produced by fermentations of the strain *Chalara* sp. CF-164331 in three different media **(a)** in the absence of SAHA and **(b)** in the presence of SAHA. HPLC/UV at 210 nm profiles in green and HPLC/HR-MS profiles in red.

2.5. Production of selected activities in fungal fermentations

Many active extracts were not dereplicated and/or the identified known compounds did not support the antifungal activity they presented. The 11 most potent extracts were prioritized for scaled-up growth and fractionation, and a detailed study of their chemical composition was performed. The strains were grown under the original fermentation conditions using both EPA vials and flask formats to generate enough material for a first deconvolution of their components.

In some cases, the scaled-up growth or the fractionation enrichment allowed to identify the presence of known bioactive compounds not previously detected in the original active extracts because of their low production. This included the antibiotic L-783277 by the strain *Neoconiothyrium* sp. CF-164281, antibiotic AS-2077715 by *Scleroconidioma sphagnicola* CF-166058 and gliovictin and hyalodendrin by the strain *Alfoldia* sp. CF-168984. Furthermore, the extracts of the strain *Equiseticola* sp. CF-164483 in BRFT, SMK-II and YES media in the presence of SAHA inhibited *B. cinerea* and *M. grisea*. Dereplication analysis could not identify any bioactive molecules that explained this differential bioactivity. Therefore, new scaled-up fermentations and subsequent bio-guided fractionation steps were required to identify a family of aspochalasins related compounds ($C_{24}H_{37}NO_4$ & $C_{24}H_{35}NO_3$) which were identified as responsible for the antifungal activity detected in different fractions. Further analyses will be required to isolate and purify these peaks in order to determine their structures and to characterize their biological activity against the fungal phytopathogens.

Another interesting hit analyzed in detail was the strain *Anthosthomelloides leucospermi* CF-166110, that showed activity against *M. grisea* and *B. cinerea*, both in MCKX and SMK-II media with SAHA. In addition to the presence of cytochalasin H in the extracts, chemical dereplication showed more complex metabolite profiles, as shown for the semipreparative HPLC profiles from fermentations in SMK-II in absence and presence of SAHA (Figure S3). The addition of the epigenetic

Chapter 4

elicitor clearly influenced the production of different peaks related to the family of cytochalasins. Moreover, the activity bio-guided fractionation showed that different cytochalasins were associated with the inhibition of *M. grisea*, as did ternantin for the *B. cinerea* inhibition. Similarly, the related strain *Anthostomella* sp. CF-166109 showed very similar HPLC profiles where the presence of cytochalasins, heptelidic acid, anhydrosepedonin and ternatin were also identified.

The potent activity of the strain *Ramusculicola* sp. CF-166025 against *M. grisea* when cultured in SMK-II with SAHA was found to be associated, after a bio-guided fractionation, to a family of compounds with molecular formulae $C_{17}H_{22}O_4$ and $C_{17}H_{22}O_3$, not detected in the absence of SAHA, as well as the enhancement of the production levels of $C_{17}H_{20}O_3$, $C_{17}H_{22}O_3$ and $C_{17}H_{22}O_2$ (Figure S4). Further analyses are required to purify and elucidate the structure of this family of potential new antifungal molecules.

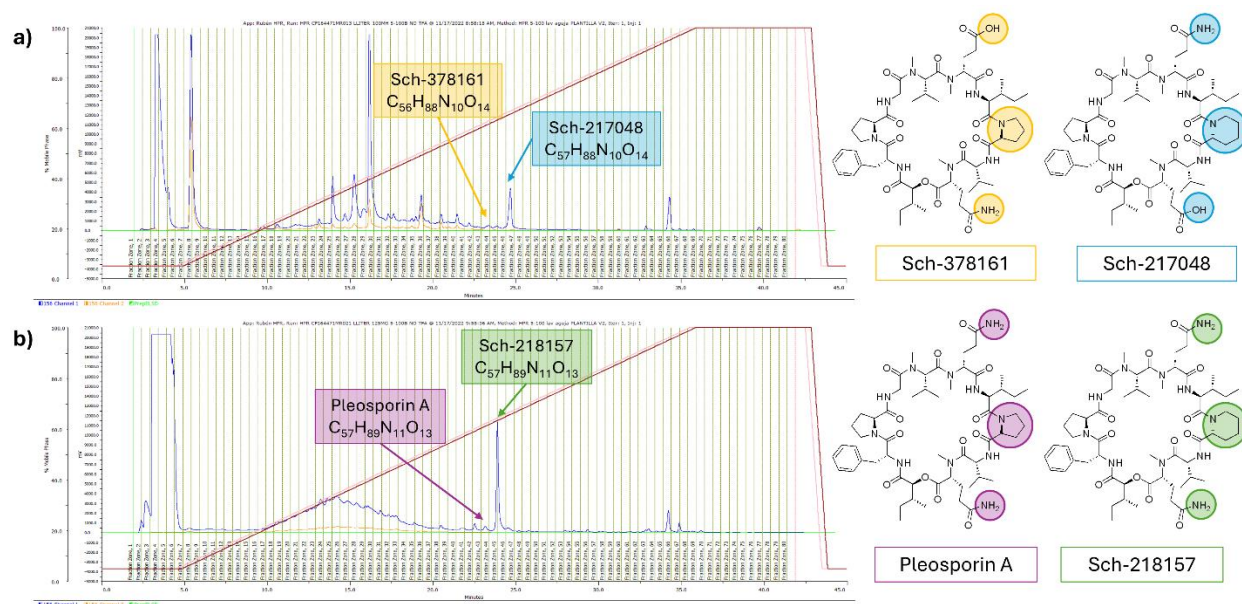


Figure 8. HPLC profiles of the strain *Coniothyrium* sp. CF-164471 when grown in MCKX medium (a) in absence and (b) in presence of SAHA. Preparative HPLC/UV at 210 nm fractionation profiles in blue, 280 nm in orange and B gradient (5-100% ACN/H₂O) in red.

The strain *Coniothyrium* sp. CF-164471 produced an inhibitory activity against *B. cinerea* when grown in MCKX with SAHA, but any known molecule could be identified to support this activity. The HPLC preparative fractionations of its scaled-up fermentations with and without the epigenetic elicitor revealed a clear modulation of the metabolite profiles. The strain produced a family of bioactive compounds Sch-217048, Sch-218157, Sch-378161 and pleosporin A with different production levels (Figure 8). The fractionation HPLC profiles showed that Sch-378161 (fractions 44 and 45) and Sch-217048 (fraction 47) were produced in MCKX, whereas in the presence of SAHA, related but different compounds are produced: pleosporin A (fraction 44) and Sch-218157 (fractions 45 and 46). All four compounds were purified and tested against the panel of

phytopathogens, but IC_{50} values could only be calculated for Sch-218157, showing a poor inhibition of *B. cinerea* with $IC_{50}=111.6 \mu\text{g/mL}$ in fluorescence-based assay. This inhibitory activity was not confirmed in absorbance-based assay due to the low potency of the growth inhibition. The other three compounds showed $IC_{50} > 160 \mu\text{g/mL}$ against all the phytopathogens tested.

2.6. Discovery of the antifungal libertamide

The strain *Libertasomyces aloeticus* CF-168990 showed specific inhibition of *B. cinerea* in the original extracts from MCKX and BRFT fermentations only with SAHA. Any known compound could be dereplicated in its crude library extracts. The scaled-up growth of the strain in flasks, after confirmation of the activity and further bioassay guided fractionation, LC-DAD-HRMS analysis and NMR spectroscopy, identified a compound of molecular formula $C_{16}H_{27}NO_2$ ($[M+H]^+$ at m/z 266.2119) associated with a new antifungal compound, that we named libertamide (Figure 9, S5-S15 and Table S3). This compound was produced in scaled-up fermentation in flasks with MCKX and BRFT (both with and without SAHA), but with different production yields: 9.9 mg in MXCK medium (production yield of 188 mg/L), 11.2 mg in MCKX+SAHA (production yield of 229 mg/L), 11.8 mg in BRFT medium (production yield of 303 mg/L) and 13.1 mg in BRFT+SAHA (production yield of 395 mg/L). Once this new compound was identified, the presence of libertamide was confirmed in all the inactive extracts obtained without SAHA, but in lower concentrations compared to the active extracts obtained with SAHA.

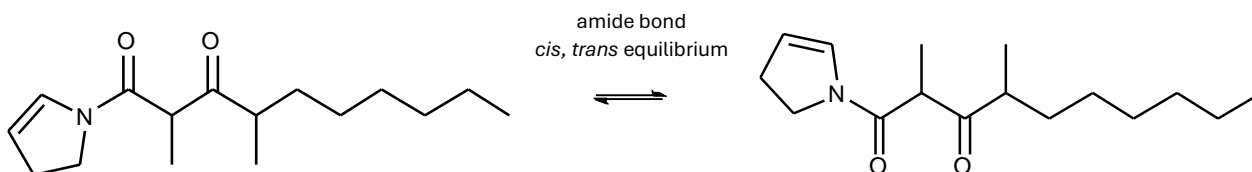


Figure 9. Structure of libertamide $C_{16}H_{27}NO_2$ in its amide bond *cis/trans* equilibrium.

The antifungal activity profile of libertamide was evaluated against a wider panel of seven phytopathogenic strains. Dose-response curves (DRC) were performed at concentrations ranging from $160 \mu\text{g/mL}$ to $0.31 \mu\text{g/mL}$ and IC_{50} were determined. The most potent activity was obtained against the phytopathogen *Zymoseptoria tritici* CBS 115943, with values ranging from $0.91 \mu\text{g/mL}$ for the absorbance-based assay to $1.30 \mu\text{g/mL}$ for the fluorescence-based assay (Table 3, Figure S16). Additionally, the cytotoxicity in the HepG2 cell line was determined from a DRC starting at $40 \mu\text{g/mL}$, that showed $ED_{50} = 25.77 \mu\text{g/mL}$ (Table 3, Figure S17). Concentrations from 2 to $20 \mu\text{g/mL}$ of libertamide exhibited high inhibition on *Z. tritici* without any cytotoxic effect. The antifungal potential against human pathogens was also evaluated for *Aspergillus fumigatus*, *Candida albicans* and *Cryptococcus neoformans*, but all minimal inhibitory concentrations were higher than $160 \mu\text{g/mL}$ (data not shown).

Table 3. Antifungal activity of libertamide based on IC₅₀ (µg/mL) against a panel of relevant phytopathogens and cytotoxicity evaluation based on ED₅₀ (µg/mL).

Phytopathogen strain	IC ₅₀ (µg/mL)	
	Absorbance-based assay	Fluorescence-based assay
<i>Zymoseptoria tritici</i> CBS 115943	0.91 ± 0.12	1.30 ± 0.01
<i>Botrytis cinerea</i> B05.10	34.05 ± 4.06	49.74 ± 3.87
<i>Verticillium dahliae</i> CBS 717.96	31.83 ± 3.03	24.80 ± 3.18
<i>Colletotrichum acutatum</i> CF-137177	36.33 ± 1.09	41.08 ± 1.77
<i>Fusarium oxysporum</i> sbssp. <i>cubense</i> CBS 102025	61.80 ± 4.15	51.29 ± 7.20
<i>Magnaporthe grisea</i> CF-105765	67.81 ± 3.25	84.60 ± 0.80
<i>Fusarium proliferatum</i> CBS 115.97	120.43 ± 4.84	136.50 ± 7.55
Human cancer cell line	ED ₅₀ (µg/mL)	
	MTT-based assay	
HepG2 cell line	25.14 ± 2.45	

3. Discussion

Decomposer fungal communities associated with leaf-litter have been extensively studied because of their remarkable biodiversity. They include a high proportion of unique and rare species playing essential ecological roles (Crous et al., 2006; Foster et al., 2022; Voříšková & Baldrian, 2013). These fungal species contribute significantly to the decomposition of organic matter, a crucial process for nutrient cycling in terrestrial ecosystems (Grossman et al., 2020). One of the objectives of this study was to explore and characterize in detail the antifungal potential of a highly diverse group of fungal strains isolated from leaf-litter collected in various habitats across South Africa. The phylogenetic analysis combined with molecular identification allowed to improve the previously published taxonomic classification of 232 fungal strains. *Ascomycota* was the most abundant phylum (93.10%), in line with the reported prevalence of ascomycetes in this habitat, most probably due to their capacity to degrade complex plant components (Bills & Gloer, 2016; Tedersoo et al., 2014). The high number of taxonomic classes, orders, families and genera characterized confirmed the complexity and richness of fungal communities associated with this environment (Crous et al., 2006; Foster et al., 2022; Voříšková & Baldrian, 2013). In addition, molecular identification techniques such as DNA barcoding and phylogenetic analysis revealed that a significant number of strains (64 strains, 28%) could be potential undescribed species (Tabla S1). Further morphological studies and phylogenetic analyses will be required to determine the taxonomic position of these newly discovered taxa. These findings have confirmed the huge potential of leaf-litter-associated communities as an excellent source of novel and unique fungal strains, in particular the leaf-litter from South African endemic plants belonging to *Proteaceae* and *Restionaceae* families (Crous et

al., 2006; Foster et al., 2022; Goldblatt & Manning, 2000; Tedersoo et al., 2014; Voříšková & Baldrian, 2013).

The discovery of new fungal species presents an opportunity to access to undescribed biosynthetic potential that might lead to the discovery of novel bioactive compounds. Fungal genomes contain numerous gene clusters that encode valuable information for the biosynthesis of bioactive metabolites, usually silent under standard laboratory production conditions (Pandit et al., 2022; Riedling et al., 2024; Santra & Banerjee, 2020; Xue et al., 2023). Therefore, the development of new strategies to activate the expression of unexplored compounds is required. For this purpose, a specific OSMAC approach has been previously performed to maximize the metabolite production of this fungal population (Serrano et al., 2021). The selected 232 strains were then cultured in a nutritional array that included four liquid fermentation media (LSFM, MCKX, SMK-II and YES) and one solid-state fermentation (BRFT), all in presence and absence of the epigenetic elicitor SAHA, described in Serrano et al., 2021.

The recently developed HTS assay platform for the discovery of phytopathogen inhibitors (Serrano et al., 2023) allowed us the evaluation of the antifungal potential of this library of 2,362 fungal extracts. The screening campaign was carried out against *Botrytis cinerea*, *Colletotrichum acutatum*, *Fusarium proliferatum* and *Magnaporthe grisea*, four relevant fungal phytopathogens with a considerable impact in global economy (Dean et al., 2012; Jayawardena et al., 2021; Pandit et al., 2022; Riseh et al., 2022). HTS platform profiling allowed the identification of bioactive extracts and prioritized hit populations with high antifungal potential. Hit selection is frequently performed by applying a cut-off of 50% of inhibition, nevertheless we further analyzed the activity distributions to identify outlier hits populations based on statistical criteria. High bioactivity hit-rates were obtained, being *M. grisea* the most sensitive phytopathogen (10.75% of hit-rate), followed by *B. cinerea* (4.78%), while *F. proliferatum* and *C. acutatum* were the most resistant strains with 1.52% and 1.23% of hit-rates respectively. Despite *M. grisea* microdilution assay provided the highest number of hits, many of them were associated with interferences due to the presence of fatty acids in extracts produced in the solid medium BRFT. The detailed LC-HRMS analysis of the composition of these active extracts identified different fatty acids such as linoleic acid, linolenic acid, 11-hydroxylinolenic acid, 1-linolenoyl-sn-glycerol, 1-monolinolein and 1-oleoyl-sn-glycerol. The antimicrobial properties of fatty acids such as linoleic acid, linolenic acid and monolinolenins have already been reported and might support these results observed in *M. grisea* (Huang et al., 2010; Kusumah et al., 2020).

Overall, from the 340 active extracts obtained in the screening, 187 hits were supported by the presence of 95 known bioactive compounds. The deeper dereplication study by low- and high-resolution mass spectrometry analyses (LC-LRMS and LC-HRMS respectively) allowed to correlate 60 of the previously dereplicated molecules (Serrano et al., 2021) as potential responsible for the antifungal activity, and to identify 35 additional already known bioactive molecules. These results confirmed the antifungal biosynthetic potential encoded in the fungal genomes of leaf-litter related strains (Pandit et al., 2022; Santra & Banerjee, 2020). Therefore, fungal communities associated with leaf-litter are not only the origin of a great biodiversity of strains, but also a relevant source of bioactive compounds with potential to control fungal plant pathogens.

Moreover, dereplication analyses facilitated the deprioritization of the hits whose activity could be associated with known bioactive compounds. For *B. cinerea*, 86 extracts from the 113 hits contained known bioactive compounds, resulting in the prioritization of 27 active extracts as possible sources of novel antifungal metabolites. Similarly, three hits from the 29 active extracts against *C. acutatum* and only one hit from the 36 active extracts against *F. proliferatum* were selected for further studies. The strain *Alfoldia* sp. CF-168984, a potential undescribed species within the genus *Alfoldia*, was the unique hit against *F. proliferatum* producing tentative new bioactive molecules. However, a detailed study involving the bio-guided fractionation from a new scaled-up growth of this strain in flasks allowed to determine the production of gliovictin and hyalodendrin. Both compounds belonging to the class of epidithiodioxopiperazines are described in literature with a broad-spectrum of activity as antimicrobial and cytotoxic agents, that supported the phytopathogen inhibition profile observed (Müllbacher & Eichner, 1984; Rightsel et al., 1964; Stillwell et al., 1974; Strunz et al., 1973). Furthermore, dereplication analyses were fundamental in *M. grisea* results due to the large number of active extracts obtained, which were quickly reduced by the identification of known bioactive molecules explaining the inhibitions to 104 active extracts that were studied as a potential source of undescribed antifungal metabolites. Therefore, the combination of LC-LRMS and LC-HRMS analyses confirmed once again the relevance of the dereplication in hit selection steps, in order to focus only on the isolation of novel bioactive molecules (Flores-Bocanegra et al., 2022; Pérez-Victoria et al., 2016; Wolfender et al., 2019).

The hit populations were further studied to evaluate the effect of both culture-based approaches (medium composition and SAHA) in the production of bioactive metabolites. On the one hand, the medium composition played a crucial role on the production bioactive molecules. As previously described in Serrano et al., 2021, fungal fermentations in a rice-based medium provided more complex metabolite profiles than submerged fermentations in liquid media. This chemical richness obtained in solid-state culture conditions could explain the high number of active extracts obtained in BRFT medium against *B. cinerea* and *C. acutatum*, being both assays independent on the presence or absence of fatty acids in this medium. However, in the *F. proliferatum* and *M. grisea* screenings, the most productive media were LSFM and SMK-II, respectively. The taxonomic distribution of active strains was dominated by the order *Pleosporales* against the four phytopathogens, in line with the initial distribution of the studied leaf-litter fungal population. Moreover, the high diversity of the selected fungal population made it challenging to identify a single medium as the optimal condition, resulting this aspect specific for each taxonomic group. For example, the strain *Chalara* sp. CF-164331 demonstrated how changes in the medium formulation can modulate the chemical production and therefore its biological activity. LC-HRMS profiles showed a differential production of two related potentially new molecules ($C_{13}H_{13}ClO_6$ and $C_{13}H_{13}ClO_5$) in LSFM, SMK-II and BRFT fermentations, enhanced by the presence of SAHA, that was also reflected on the inhibition percentages of *M. grisea* (Figure 7). Moreover, this strain selectively produced the mycotoxin emestrin only in the SMK-II medium, confirming previously described biosynthetic potential of species of *Chalara* sp. (Adpressa et al., 2017). This example confirmed that changes in carbon and nitrogen sources clearly influenced the induction of certain metabolites and that the discovery of bioactive compounds is highly dependent on fungal potential where multiple media production conditions are required to exploit these resources (González-Menéndez et al., 2014; Serrano et al., 2021; Song et al., 2023; Wei et al., 2021).

Fermentations in MCKX and YES media also provided active extracts from various fungal strains, being great candidates to improve the production levels of specific compounds. However, both formulations were not identified as the best culture condition due to overlapped results with other fermentation conditions. Therefore, none of the culture media included in this OSMAC approach should be discarded for leaf-litter strains because all of them produced unique hits, although BRFT, LSFM and SMK-II media could be prioritized being the most productive culture conditions to ensure antifungal activities against *B. cinerea*, *C. acutatum*, *F. proliferatum* and *M. grisea*.

On the other hand, the incorporation of the histone deacetylase inhibitor SAHA significantly influenced the bioactivity rates. The addition of SAHA during fungal fermentations improved the overall hit-rate against *B. cinerea* and *M. grisea*, increasing the number of active extracts. SAHA has been extensively used in literature to alter the expression of silent or under-expressed biosynthetic gene clusters, leading the modulation of metabolite productions (Beau et al., 2012; Du et al., 2014; Gubiani et al., 2017; Henrikson et al., 2009; Xue et al., 2023; Zhang et al., 2019). To characterize the influence of SAHA on biological activity, LC-HRMS profiles of hits were compared in presence and absence of the epigenetic elicitor. The analysis revealed that SAHA enhanced both the diversity and the relative amounts of some bioactive metabolites, supporting the differential bioactivity profiles observed. The potential new species of *Coniothyrium* CF-164471 is an example of induction of two bioactive compounds that were only produced in presence of SAHA (Pleosporin A and Sch-218157), with activity against *B. cinerea*. Meanwhile, *Anthosthomelloides leucospermi* CF-166110 showed clear enhancements of production levels of cytochalasins, that increased the inhibition of *M. grisea*. In this study, the most predominant effect induced by SAHA was the improved production of specific bioactive compounds, that allowed the access to a variety of fungal metabolites typically produced in minimal quantities under non-supplemented conditions, where their potential activity remains underestimated.

Despite the lack of a universal optimal fermentation condition that ensures the expression of all the biosynthetic potential of fungi, SAHA addition to a specific formulation medium can enhance its general fungal metabolite production. A proof of concept was the production of the new antifungal agent libertamide ($C_{16}H_{27}NO_2$) by the strain *Libertasomyces aloeticus* CF-168990. The addition of SAHA to BRFT medium specifically increased by two-fold the production levels of this molecule. *Libertasomyces* is a genus described by Crous in 2016 from samples collected in the west coast of Cape Town, South Africa, that involves four species *L. aloeticus*, *L. myopori*, *L. platani* and *L. quercus* (Crous et al., 2019; Crous, et al., 2016a; Crous, et al., 2016b; Crous & Groenewald, 2017). Our strain *L. aloeticus* CF-168990, isolated from leaf-litter of the coastal fynbos *Diosma subulate*, shows 99.31% of similarity with ITS sequences of the holotype CBS 145558, isolated from leaves of *Aloe* collected in South Africa (Crous et al., 2019). To date, the family of libertalides A-N were the only bioactive molecules produced by a *Libertasomyces* strain, described with immunomodulatory activity (Chen et al., 2022; Sun et al., 2017). Libertamide, is structurally different from libertalides, as well as in its biological activity as antifungal agent. The novel molecule libertamide was initially identified as inhibitor of *B. cinerea*, but IC_{50} and ED_{50} for HepG2 human cell line showed close values, indicating that the dose to inhibit the 50% of this phytopathogen has cytotoxic effects. However, a significant difference was obtained when the molecule was tested against *Zymoseptoria tritici*, with IC_{50} 28 times lower than ED_{50} for HepG2 (Figures S16-S17). These results support the

potential use of the strain *Libertasomyces aloeticus* CF-168990 and the novel compound libertamide as a biocontrol agent of the septoria leaf blotch caused by *Z. tritici*.

Numerous reports have been focused on the ability of SAHA to modulate the expression of secondary metabolites in single fungal strains (Beau et al., 2012; Du et al., 2014; Gubiani et al., 2017; Henrikson et al., 2009; Zhang et al., 2019). However, our results from a wide diverse population of 232 fungal strains demonstrated that the addition of SAHA maximizes the biosynthetic potential of the general population. This enhancement was not only observed in individual strains, but also across the majority of the taxonomically diverse leaf-litter fungal population studied. Hence, the epigenetic manipulation using SAHA represents a suitable method to generate diverse libraries for the discovery of new bioactive metabolites. Nevertheless, the opposite effects observed for *C. acutatum* and *F. proliferatum* screenings highlighted the variability in the responses of fungi to SAHA addition for the production of antifungals, indicating that its impact on the metabolomic profile could be production-strain specific, and medium or target dependent.

4. Material and methods

4.1. Fungal strain characterization

Fungal strains were initially characterized by their morphological structures developed on different agar media (YM, CMA, OAT). Subsequently, genomic DNA extraction, PCR amplification and DNA sequencing were performed as previously described Gonzalez-Menendez et al., 2017. rDNA sequences of the complete ITS1-5.8S-ITS2-28S region or independent ITS and partial 28S were compared with sequences at GenBank®, the NITE Biological Resource Center (<http://www.nbrc.nite.go.jp>) and CBS strain database (<http://www.westerdijkinstituut.nl>) by using the BLAST® application. ITS sequences that showed similarity higher than 98% were considered within the same genera and higher than 99% within the same species. However, when similarity between ITS sequences were lower than 95%, the corresponding strains were classified as potential new species.

Moreover, a Bayesian analysis with MrBayes 3.01 using the Markov Chain Monte Carlo (MCMC) approach was applied with the partial sequences of 28S gen. Additionally, Maximum Likelihood method (ML) and ultrafast bootstrap support values for phylogenetic trees were assessed calculating 1,000 replicates with IQ-TREE software (González-Menéndez et al., 2018; Nguyen et al., 2015).

4.2. Bioactivity evaluation

The antifungal activity of the previously generated library of 2,362 fungal extracts by Serrano et al., in 2021, was characterized against four relevant fungal phytopathogenic fungal strains: *Botrytis cinerea* B05.10, *Colletotrichum acutatum* CF-137177, *Fusarium proliferatum* CBS 115.97 and *Magnaporthe grisea* CF-105765. The primary screening campaign was performed with the described High-Throughput Screening Platform with these strains (Serrano et al., 2023). Absorbance and

fluorescence raw data were used to calculate biological activity via the Genedata Screener® software (Genedata AG, Basel, Switzerland). Additional statistical analysis using JMP® software was applied to distribute and categorize the activity populations.

The described HTS liquid methodology was also applied with different fungal phytopathogens such as *Fusarium oxysporum* sbsp. *cubense* CBS 102025, *Verticillium dahliae* CBS 717. 96 and *Zymoseptoria tritici* CBS 115943, in order to characterize the antifungal activity of the new compound. Moreover, cytotoxicity of the compound was evaluated against the HepG2 cell line (hepatocellular carcinoma, ATCC HB8065) by a MTT reduction colorimetric assay.

4.3. Chemical dereplication of bioactive extracts

The active extracts were analysed by Liquid Chromatography Mass Spectrometry (LC-MS) for the identification of known secondary metabolites. Low resolution LC-MS profiles (UV signal, retention time, and fragmentation patterns) were compared with MEDINA's internal database of known Natural Products (Pérez-Victoria et al., 2016). Extracts without LC-LRMS dereplication match were further analysed by high resolution LC-MS (retention time and accurate mass) for tentative identification of molecular formula to search in the commercial Chapman & Hall Dictionary of Natural Products (CRC Press "Dictionary of Natural Products on USB, ver.30.2") and Natural Products Atlas (Pérez-Victoria, 2024; van Santen et al., 2022). Finally, confirmation by LC-ESI-HRMS/MS fragmentation was needed in specific cases.

4.4. Isolation of bioactive compounds

Antifungal extracts of interest were selected for scaled-up growth fermentation to obtain higher amounts of material to perform bio-guided purification processes. Active fungal strains were cultivated under the same fermentation conditions where they showed antifungal activity scaling-up using two flasks containing 100 mL of the specific medium in presence and absence of SAHA (100 µM) and two EPA vials with 10 mL to replicate the original fermentation conditions. Fermentations were extracted with equal volume of acetone or methyl-ethyl-ketone (MEK) (depending on the fermentation medium and original sample preparation) under continuous shaking at 220rpm for 1h. The mycelium was then pelleted by centrifugation and the supernatant (400 mL) was concentrated under a stream of nitrogen.

Preparative reverse phase HPLC fractionation (Agilent™ Zorbax® SB-C8, 22 × 250 mm, 7 µm; 20 mL min⁻¹, UV detection at 210 nm) was performed with custom linear gradients of acetonitrile in water over 37 min. Subsequent semipreparative fractionations (Agilent™ Zorbax® SB-C8, 9.4 × 250 mm, 5 µm; 3.6 mL min⁻¹, UV detection at 210 nm) with specific linear gradients of acetonitrile in water without TFA were required to obtain pure compounds. LC-HRMS and NMR spectroscopy were employed in purity confirmation over 90% and structure elucidation of purified compounds.

5. Conclusions

In summary, this study represents the first systematic exploration of leaf-litter-associated fungi for the discovery of novel compounds to control fungal plant pathogens. Fungal isolates from leaf-litter resulted to be a valuable source of potential undescribed species with great biosynthetic capability. The OSMAC approach including nutritional arrays and the epigenetic elicitor SAHA, previously described to activate this metabolomic potential, has been confirmed here to produce numerous bioactive molecules against the four fungal phytopathogens. Every medium formulation included in the OSMAC study provided a high number of unique hits, resulting optimal for the discovery of antifungal compounds. The addition of SAHA to fungal fermentations clearly influenced the general diversity and quantity of metabolite production, but did not increase the hit-rates on finding antifungals against the four phytopathogens. Therefore, it is difficult to propose a single fermentation condition of the proposed as the optimal one to exploit the fungal biosynthetic potential of leaf- litter. Nevertheless, the combination of both culture-based approaches proven to be an effective strategy for the discovery of new bioactive molecules.

Furthermore, the novel molecule libertamide $C_{16}H_{27}NO_2$ is the first secondary metabolite isolated from *Libertasomyces aloeticus* with antifungal properties to inhibit fungal phytopathogens, specifically *Z. tritici*. This molecule was produced by the strain *L. aloeticus* CF-168990, but the activity was initially only produced in the presence of SAHA, being a clear example of the relevance of optimizing fermentation processes to maximize chemical production. Finally, further studies will be required to fully characterize the additional undescribed metabolites identified in this study with potential valuable applications in the field as fungicide agents.

References

- Abdelwahab, M. F., Kurtán, T., Mándi, A., Müller, W. E. G., Fouad, M. A., Kamel, M. S., Liu, Z., Ebrahim, W., Daletos, G., & Proksch, P. (2018). Induced secondary metabolites from the endophytic fungus *Aspergillus versicolor* through bacterial co-culture and OSMAC approaches. *Tetrahedron Letters*, 59(27), 2647–2652. <https://doi.org/10.1016/j.tetlet.2018.05.067>
- Adressa, D. A., Stalheim, K. J., Proteau, P. J., & Loesgen, S. (2017). Unexpected Biotransformation of the HDAC Inhibitor Vorinostat Yields Aniline-Containing Fungal Metabolites. *ACS Chemical Biology*, 12(7), 1842–1847. <https://doi.org/10.1021/acscchembio.7b00268>
- Atanasov, A. G., Zotchev, S. B., Dirsch, V. M., & Supuran, C. T. (2021). Natural products in drug discovery: advances and opportunities. *Nature Reviews Drug Discovery*, 20(3), 200–216. <https://doi.org/10.1038/s41573-020-00114-z>
- Beau, J., Mahid, N., Burda, W. N., Harrington, L., Shaw, L. N., Mutka, T., Kyle, D. E., Barisic, B., Van Olphen, A., & Baker, B. J. (2012). Epigenetic Tailoring for the Production of Anti-Infective Cytosporones from the Marine Fungus *Leucostoma persoonii*. *Marine Drugs*, 10(4), 762–774. <https://doi.org/10.3390/md10040762>
- Bills, G. F., Dombrowski, A. W., & Goetz, M. A. (2012). The “FERMEX” Method for Metabolite-Enriched Fungal Extracts (pp. 79–96). https://doi.org/10.1007/978-1-62703-122-6_5
- Bills, G. F., & Gloer, J. B. (2016). Biologically Active Secondary Metabolites from the Fungi. *Microbiology Spectrum*, 4(6). <https://doi.org/10.1128/microbiolspec.FUNK-0009-2016>
- Chen, Y., Pang, X., He, Y., Lin, X., Zhou, X., Liu, Y., & Yang, B. (2022). Secondary Metabolites from Coral-Associated Fungi: Source, Chemistry and Bioactivities. *Journal of Fungi*, 8(10), 1043. <https://doi.org/10.3390/jof8101043>
- Crous, P. W., Carnegie, A. J., Wingfield, M. J., Sharma, R., Mughini, G., Noordeloos, M. E., Santini, A., Shouche, Y. S., Bezerra, J. D. P., Dima, B., Guarnaccia, V., Imrefi, I., Jurjević, Ž., Knapp, D. G., Kovács, G. M., Magistà, D., Perrone, G., Rămă, T., Rebriev, Y. A., ... Groenewald, J. Z. (2019). Fungal Planet description sheets: 868–950. *Persoonia - Molecular Phylogeny and Evolution of Fungi*, 42(1), 291–473. <https://doi.org/10.3767/persoonia.2019.42.11>
- Crous, P. W., & Groenewald, J. Z. (2017). The Genera of Fungi — G 4: Camarosporium and Dothiora. *IMA Fungus*, 8(1), 131–152. <https://doi.org/10.5598/imafungus.2017.08.01.10>
- Crous, P. W., Rong, I. H., Wood, A., Lee, S., Glen, H., Botha, W., Slippers, B., de Beer, W. Z., Wingfield, M. J., & Hawksworth, D. L. (2006). How many species of fungi are there at the tip of Africa? *Studies in Mycology*, 55, 13–33. <https://doi.org/10.3114/sim.55.1.13>
- Crous, P. W., Wingfield, M. J., Burgess, T. I., Hardy, G. E. St. J., Crane, C., Barrett, S., Cano-Lira, J. F., Leroux, J. J., Thangavel, R., Guarro, J., Stchigel, A. M., Martín, M. P., Alfredo, D. S., Barber, P. A., Barreto, R. W., Baseia, I. G., Cano-Canals, J., Cheewangkoon, R., Ferreira, R. J., ... Stephenson, S. L. (2016). Fungal Planet description sheets: 469–557. *Persoonia - Molecular Phylogeny and Evolution of Fungi*, 37(1), 218–403. <https://doi.org/10.3767/003158516X694499>
- Crous, P. W., Wingfield, M. J., Richardson, D. M., Leroux, J. J., Strasberg, D., Edwards, J., Roets, F., Hubka, V., Taylor, P. W. J., Heykoop, M., Martín, M. P., Moreno, G., Sutton, D. A., Wiederhold, N. P., Barnes, C. W., Carlavilla, J. R., Gené, J., Giraldo, A., Guarnaccia, V., ... Groenewald, J. Z. (2016).

- Fungal Planet description sheets: 400–468. *Persoonia - Molecular Phylogeny and Evolution of Fungi*, 36(1), 316–458. <https://doi.org/10.3767/003158516X692185>
- Dean, R., Van Kan, J. A. L., Pretorius, Z. A., Hammond-Kosack, K. E., Di Pietro, A., Spanu, P. D., Rudd, J. J., Dickman, M., Kahmann, R., Ellis, J., & Foster, G. D. (2012). The Top 10 fungal pathogens in molecular plant pathology. *Molecular Plant Pathology*, 13(4), 414–430. <https://doi.org/10.1111/J.1364-3703.2011.00783.X>
- Flores-Bocanegra, L., Al Subeh, Z. Y., Egan, J. M., El-Elmat, T., Raja, H. A., Burdette, J. E., Pearce, C. J., Linington, R. G., & Oberlies, N. H. (2022). Dereplication of Fungal Metabolites by NMR-Based Compound Networking Using MADByTE. *Journal of Natural Products*, 85(3), 614–624. <https://doi.org/10.1021/acs.jnatprod.1c00841>
- Foster, R., Hartikainen, H., Hall, A., & Bass, D. (2022). Diversity and Phylogeny of Novel Cord-Forming Fungi from Borneo. *Microorganisms*, 10(2), 239. <https://doi.org/10.3390/microorganisms10020239>
- Gakuubi, M. M., Ching, K. C., Munusamy, M., Wibowo, M., Liang, Z.-X., Kanagasundaram, Y., & Ng, S. B. (2022). Enhancing the Discovery of Bioactive Secondary Metabolites From Fungal Endophytes Using Chemical Elicitation and Variation of Fermentation Media. *Frontiers in Microbiology*, 13. <https://doi.org/10.3389/fmicb.2022.898976>
- Gao, Y., Wang, L., Kalscheuer, R., Liu, Z., & Proksch, P. (2020). Antifungal polyketide derivatives from the endophytic fungus *Aplosporella javeedii*. *Bioorganic & Medicinal Chemistry*, 28(10), 115456. <https://doi.org/10.1016/j.bmc.2020.115456>
- Goldblatt, P. & Manning, J. (2000). *Cape plants: a conspectus of the Cape flora of South Africa* (National Botanical Institute, Ed.; Strelitzia, Vol. 9).
- González-Menéndez, V., Asensio, F., Moreno, C., de Pedro, N., Monteiro, M. C., de la Cruz, M., Vicente, F., Bills, G. F., Reyes, F., Genilloud, O., & Tormo, J. R. (2014). Assessing the effects of adsorptive polymeric resin additions on fungal secondary metabolite chemical diversity. *Mycology*, 5(3), 179–191. <https://doi.org/10.1080/21501203.2014.942406>
- González-Menéndez, V., Crespo, G., de Pedro, N., Diaz, C., Martín, J., Serrano, R., Mackenzie, T. A., Justicia, C., González-Tejero, M. R., Casares, M., Vicente, F., Reyes, F., Tormo, J. R., & Genilloud, O. (2018). Fungal endophytes from arid areas of Andalusia: high potential sources for antifungal and antitumoral agents. *Scientific Reports*, 8(1), 9729. <https://doi.org/10.1038/s41598-018-28192-5>
- Gonzalez-Menendez, V., Martin, J., Siles, J. A., Gonzalez-Tejero, M. R., Reyes, F., Platas, G., Tormo, J. R., & Genilloud, O. (2017). Biodiversity and chemotaxonomy of *Preussia* isolates from the Iberian Peninsula. *Mycological Progress*, 16(7), 713–728. <https://doi.org/10.1007/s11557-017-1305-1>
- González-Menéndez, V., Pérez-Bonilla, M., Pérez-Victoria, I., Martín, J., Muñoz, F., Reyes, F., Tormo, J., & Genilloud, O. (2016). Multicomponent Analysis of the Differential Induction of Secondary Metabolite Profiles in Fungal Endophytes. *Molecules*, 21(2), 234. <https://doi.org/10.3390/molecules21020234>
- Grossman, J. J., Cavender-Bares, J., & Hobbie, S. E. (2020). Functional diversity of leaf litter mixtures slows decomposition of labile but not recalcitrant carbon over two years. *Ecological Monographs*, 90(3). <https://doi.org/10.1002/ecm.1407>
- Gubiani, J. R., Wijeratne, E. M. K., Shi, T., Araujo, A. R., Arnold, A. E., Chapman, E., & Gunatilaka, A. A. L. (2017). An epigenetic modifier induces production of (10' S)-verruculide B, an inhibitor of

- protein tyrosine phosphatases by *Phoma* sp. nov. LG0217, a fungal endophyte of *Parkinsonia microphylla*. *Bioorganic & Medicinal Chemistry*, 25(6), 1860–1866. <https://doi.org/10.1016/j.bmc.2017.01.048>
- Gupta, S., Kulkarni, M. G., White, J. F., & Van Staden, J. (2020). Epigenetic-based developments in the field of plant endophytic fungi. *South African Journal of Botany*, 134, 394–400. <https://doi.org/10.1016/j.sajb.2020.07.019>
- Henrikson, J. C., Hoover, A. R., Joyner, P. M., & Cichewicz, R. H. (2009). A chemical epigenetics approach for engineering the in situ biosynthesis of a cryptic natural product from *Aspergillus niger*. *Org. Biomol. Chem.*, 7(3), 435–438. <https://doi.org/10.1039/B819208A>
- Huang, C. B., George, B., & Ebersole, J. L. (2010). Antimicrobial activity of n-6, n-7 and n-9 fatty acids and their esters for oral microorganisms. *Archives of Oral Biology*, 55(8), 555–560. <https://doi.org/10.1016/j.archoralbio.2010.05.009>
- Jayawardena, R. S., Hyde, K. D., de Farias, A. R. G., Bhunjun, C. S., Fernandez, H. S., Manamgoda, D. S., Udayanga, D., Herath, I. S., Thambugala, K. M., Manawasinghe, I. S., Gajanayake, A. J., Samarakoon, B. C., Bundhun, D., Gomdola, D., Huanraluek, N., Sun, Y., Tang, X., Promputtha, I., & Thines, M. (2021). What is a species in fungal plant pathogens? *Fungal Diversity*, 109(1), 239–266. <https://doi.org/10.1007/s13225-021-00484-8>
- Jing, F., Yang, Z., Hai Feng, L., Yong Hao, Y., & Jian Hua, G. (2011). Antifungal metabolites from *Phomopsis* sp. By254, an endophytic fungus in *Gossypium hirsutum*. *African Journal of Microbiology Research*, 5(10), 1231–1236. <https://doi.org/10.5897/AJMR11.272>
- Kusumah, D., Wakui, M., Murakami, M., Xie, X., Yukihito, K., & Maeda, I. (2020). Linoleic acid, α -linolenic acid, and monolinolenins as antibacterial substances in the heat-processed soybean fermented with *Rhizopus oligosporus*. *Bioscience, Biotechnology, and Biochemistry*, 84(6), 1285–1290. <https://doi.org/10.1080/09168451.2020.1731299>
- Lu, H., Zou, W. X., Meng, J. C., Hu, J., & Tan, R. X. (2000). New bioactive metabolites produced by *Colletotrichum* sp., an endophytic fungus in *Artemisia annua*. *Plant Science*, 151(1), 67–73. [https://doi.org/10.1016/S0168-9452\(99\)00199-5](https://doi.org/10.1016/S0168-9452(99)00199-5)
- Mamathaba, M. P., Yessoufou, K., & Moteetee, A. (2022). What Does It Take to Further Our Knowledge of Plant Diversity in the Megadiverse South Africa? *Diversity*, 14(9), 748. <https://doi.org/10.3390/d14090748>
- Müllbacher, A., & Eichner, R. D. (1984). Immunosuppression in vitro by a metabolite of a human pathogenic fungus. *Proceedings of the National Academy of Sciences*, 81(12), 3835–3837. <https://doi.org/10.1073/pnas.81.12.3835>
- Nguyen, L.-T., Schmidt, H. A., von Haeseler, A., & Minh, B. Q. (2015). IQ-TREE: A Fast and Effective Stochastic Algorithm for Estimating Maximum-Likelihood Phylogenies. *Molecular Biology and Evolution*, 32(1), 268–274. <https://doi.org/10.1093/molbev/msu300>
- Niego, A. G. T., Lambert, C., Mortimer, P., Thongklang, N., Rapior, S., Grosse, M., Schrey, H., Charria-Girón, E., Walker, A., Hyde, K. D., & Stadler, M. (2023). The contribution of fungi to the global economy. *Fungal Diversity*, 121(1), 95–137. <https://doi.org/10.1007/s13225-023-00520-9>
- Pandit, M. A., Kumar, J., Gulati, S., Bhandari, N., Mehta, P., Katyal, R., Rawat, C. D., Mishra, V., & Kaur, J. (2022). Major Biological Control Strategies for Plant Pathogens. *Pathogens*, 11(2), 273. <https://doi.org/10.3390/pathogens11020273>

- Pérez-Victoria, I. (2024). Natural Products Dereplication: Databases and Analytical Methods (pp. 1–56). https://doi.org/10.1007/978-3-031-59567-7_1
- Pérez-Victoria, I., Martín, J., & Reyes, F. (2016). Combined LC/UV/MS and NMR Strategies for the Dereplication of Marine Natural Products. *Planta Medica*, 82(09/10), 857–871. <https://doi.org/10.1055/s-0042-101763>
- Pillay, L. C., Nekati, L., Makhwitine, P. J., & Ndlovu, S. I. (2022). Epigenetic Activation of Silent Biosynthetic Gene Clusters in Endophytic Fungi Using Small Molecular Modifiers. *Frontiers in Microbiology*, 13. <https://doi.org/10.3389/fmicb.2022.815008>
- Riedling, O., Walker, A. S., & Rokas, A. (2024). Predicting fungal secondary metabolite activity from biosynthetic gene cluster data using machine learning. *Microbiology Spectrum*, 12(2). <https://doi.org/10.1128/spectrum.03400-23>
- Rightsel, W. A., Schneider, H. G., Sloan, B. J., Graf, P. R., Miller, F. A., Bartz, Q. R., Ehrlich, J., & Dixon, G. J. (1964). Antiviral Activity of Gliotoxin and Gliotoxin Acetate. *Nature*, 204(4965), 1333–1334. <https://doi.org/10.1038/2041333b0>
- Riseh, R. S., Hassanisaadi, M., Vatankhah, M., Babaki, S. A., & Barka, E. A. (2022). Chitosan as a potential natural compound to manage plant diseases. *International Journal of Biological Macromolecules*, 220, 998–1009. <https://doi.org/10.1016/j.ijbiomac.2022.08.109>
- Santra, H. K., & Banerjee, D. (2020). Natural Products as Fungicide and Their Role in Crop Protection. In *Natural Bioactive Products in Sustainable Agriculture* (pp. 131–219). Springer Singapore. https://doi.org/10.1007/978-981-15-3024-1_9
- Serrano, R., González-Menéndez, V., Martínez, G., Toro, C., Martín, J., Genilloud, O., & Tormo, J. R. (2021). Metabolomic Analysis of The Chemical Diversity of South Africa Leaf Litter Fungal Species Using an Epigenetic Culture-Based Approach. *Molecules*, 26(14), 4262. <https://doi.org/10.3390/molecules26144262>
- Serrano, R., González-Menéndez, V., Tormo, J. R., & Genilloud, O. (2023). Development and Validation of a HTS Platform for the Discovery of New Antifungal Agents against Four Relevant Fungal Phytopathogens. *Journal of Fungi*, 9(9), 883. <https://doi.org/10.3390/jof9090883>
- Song, Z., Sun, Y. J., Xu, S., Li, G., Yuan, C., & Zhou, K. (2023). Secondary metabolites from the Endophytic fungi *Fusarium decemcellulare* F25 and their antifungal activities. *Frontiers in Microbiology*, 14. <https://doi.org/10.3389/fmicb.2023.1127971>
- Stillwell, M. A., Magasi, L. P., & Strunz, G. M. (1974). Production, isolation, and antimicrobial activity of hyalodendrin, a new antibiotic produced by a species of *Hyalodendron*. *Canadian Journal of Microbiology*, 20(5), 759–764. <https://doi.org/10.1139/m74-116>
- Strunz, G. M., Kakushima, M., Stillwell, M. A., & Heissner, C. J. (1973). Hyalodendrin: a new fungitoxic epidithiodioxopiperazine produced by a *Hyalodendron* species. *Journal of the Chemical Society, Perkin Transactions 1*, 2600. <https://doi.org/10.1039/p19730002600>
- Sun, Y.-Z., Kurtán, T., Mándi, A., Tang, H., Chou, Y., Soong, K., Su, L., Sun, P., Zhuang, C.-L., & Zhang, W. (2017). Immunomodulatory Polyketides from a *Phoma* -like Fungus Isolated from a Soft Coral. *Journal of Natural Products*, 80(11), 2930–2940. <https://doi.org/10.1021/acs.jnatprod.7b00463>
- Tedersoo, L., Bahram, M., Pölme, S., Kõljalg, U., Yorou, N. S., Wijesundera, R., Ruiz, L. V., Vasco-Palacios, A. M., Thu, P. Q., Suija, A., Smith, M. E., Sharp, C., Saluveer, E., Saitta, A., Rosas, M., Riit,

- T., Ratkowsky, D., Pritsch, K., Põldmaa, K., ... Abarenkov, K. (2014). Global diversity and geography of soil fungi. *Science*, 346(6213). <https://doi.org/10.1126/science.1256688>
- van Santen, J. A., Poynton, E. F., Iskakova, D., McMann, E., Alsup, T. A., Clark, T. N., Fergusson, C. H., Fewer, D. P., Hughes, A. H., McCadden, C. A., Parra, J., Soldatou, S., Rudolf, J. D., Janssen, E. M.-L., Duncan, K. R., & Linington, R. G. (2022). The Natural Products Atlas 2.0: a database of microbially-derived natural products. *Nucleic Acids Research*, 50(D1), D1317–D1323. <https://doi.org/10.1093/nar/gkab941>
- Voříšková, J., & Baldrian, P. (2013). Fungal community on decomposing leaf litter undergoes rapid successional changes. *The ISME Journal*, 7(3), 477–486. <https://doi.org/10.1038/ismej.2012.116>
- Wang, J., Lin, W., Wray, V., Lai, D., & Proksch, P. (2013). Induced production of depsipeptides by co-culturing *Fusarium tricinctum* and *Fusarium begoniae*. *Tetrahedron Letters*, 54(20), 2492–2496. <https://doi.org/10.1016/j.tetlet.2013.03.005>
- Wang, Y., Wang, G., Wang, L., Xu, X., Xia, J., Huang, X., Wu, Y., & Zhang, C. (2010). [Isolation and identification of an endophytic fungus of *Polygonatum cyrtoneura* and its antifungal metabolites]. *Wei Sheng Wu Xue Bao = Acta Microbiologica Sinica*, 50(8), 1036–1043.
- Wei, Q., Bai, J., Yan, D., Bao, X., Li, W., Liu, B., Zhang, D., Qi, X., Yu, D., & Hu, Y. (2021). Genome mining combined metabolic shunting and OSMAC strategy of an endophytic fungus leads to the production of diverse natural products. *Acta Pharmaceutica Sinica B*, 11(2), 572–587. <https://doi.org/10.1016/j.apsb.2020.07.020>
- Wolfender, J., Allard, P., Kubo, M., & Queiroz, E. F. (2019). Metabolomics Strategies for the Dereplication of Polyphenols and Other Metabolites in Complex Natural Extracts. In *Recent Advances in Polyphenol Research* (pp. 183–205). Wiley. <https://doi.org/10.1002/9781119427896.ch7>
- Zhang, S., Fang, H., Yin, C., Wei, C., Hu, J., & Zhang, Y. (2019). Antimicrobial Metabolites Produced by *Penicillium mallochii* CCH01 Isolated From the Gut of *Ectropis oblique*, Cultivated in the Presence of a Histone Deacetylase Inhibitor. *Frontiers in Microbiology*, 10. <https://doi.org/10.3389/fmicb.2019.02186>

IV. General Discussion

Plant pathogens are the most important cause of crop losses in agriculture worldwide. Fungal phytopathogens can infect a broad range of host plants, leading to considerable ecological and economic damage (Jayawardena et al., 2021; Pandit et al., 2022; Riseh et al., 2022). The preferred method to mitigate these devastating losses is the use of synthetic agrochemical agents, but their application results in significant environmental challenges. There is an urgent need to develop new and eco-friendly alternatives for safe control and management of plant diseases. Biocontrol strategies with Natural Products (NPs) are potential alternatives that involved the use of microbial strains and their antagonistic activity through the production of bioactive metabolites and/or enzymes to suppress the growth of plant pathogens (Khan et al., 2021). Microorganisms have contributed significantly to the development of numerous natural antifungal agents for the management of plant diseases. Fungi are considered a prolific source of structurally diverse and biologically active Secondary Metabolites (SMs) (Atanasov et al., 2021; Flores-Bocanegra et al., 2022; Gakuubi et al., 2022; González-Menéndez et al., 2018; Niego et al., 2023; Riedling et al., 2024; Xue et al., 2023). However, most of their biosynthetic gene clusters (BGCs) remain silent or poorly expressed under standard laboratory conditions. Approaches such as the exploration of new taxonomic species, variations in culture medium compositions, co-cultivation with different microorganisms or the use of epigenetic elicitors, have proven to be effective in the expression of cryptic biosynthetic pathways (Abdelwahab et al., 2018; Hautbergue et al., 2018). This study aims to evaluate some of these strategies across a wide biodiversity of fungal strains, with the objective of expanding the expression of their biosynthetic chemical potential to discover novel fungicide agents against relevant fungal phytopathogens.

Microorganisms typically co-exist within communities where they are in constant interactions with a wide variety of organisms. These interactions play a crucial role in communication or competition within the environment microbiome that clearly influence the growth, morphology and development of microorganisms (Bertrand et al., 2014). Numerous reports have demonstrated how microbial interactions can modulate fungal metabolism through the activation of complex regulatory signalling cascades and triggering specific biosynthetic pathways (Abdelwahab et al., 2018; Bertrand et al., 2014; Guo et al., 2024). These natural interactions can be artificially mimicked in the laboratory by co-culturing techniques where microorganisms are challenged to grow together. Microbial interactions between co-cultured strains could generate specific signals that determine important alterations in metabolomic expression, resulting in the production of SMs as defense or competition (Schulz et al., 2015). The first specific objective of this work focused on the agar-based co-cultivation of a wide diverse fungal population against the phytopathogen *Botrytis cinerea*, in order to study the ability of this fungus to trigger the production of novel bioactive SMs in the general fungal population.

Microbial interactions between fungi or between fungi and bacteria have been extensively studied for the induction of SMs production (Keller et al., 2005; Scherlach & Hertweck, 2009b). In this work, the strain ***B. cinerea* CBS 102414** was selected as a model strain to induce the production of new SMs. *B. cinerea* is responsible for grey mold disease, that promotes severe damage and losses in a variety of crops during both pre- and post-harvesting steps (Dean et al., 2012; Wang et al., 2012). The selection of this phytopathogenic fungus was due to its large distribution in the environment and its fast growth rate in agar plates, that makes it ideal for a rapid identification of antagonisms by co-culturing. The highly diverse 762 fungal strains selected from the MEDINA Fungal Collection,

included isolates from numerous geographical origins and environments to ensure a highly biodiverse population. The studied group included fungi from soil, leaf-litter, rhizosphere, plant endophytes and epiphytes, lichens, and marine sources, among other origins. Given that the main goal was to identify antagonists of fungal phytopathogens, strains from environments related to agricultural crops were prioritized such as soils (n=138), leaf-litter (n=187) and plants (n=281), ecosystems where possible interactions with phytopathogens are often found. Strains had been isolated from samples collected in four climatic regions including: a) temperate areas as broad as Argentina, Japan, New Zealand, Republic of Georgia and western Europe, b) arid climate zones from areas of Australia, Chile, Arizona (USA) and Almeria (Spain), c) tropical forests in Africa, Indic Ocean, Central and South America, and d) Mediterranean ecosystems from Southern Europe and South Africa. Moreover, morphological and molecular analyses based on ITS1-5.8S-ITS2 and 28S rDNA genes confirmed that the selected fungal population harboured a high taxonomic diversity.

Co-cultures of the fungal strains with *B. cinerea* in Petri dishes required incubations of 10 days, the time required by the pathogen to grow and invade the whole surface of the control plate. From the 762 studied strains, 93 showed a clear inhibition of the phytopathogen growth (12.21% hit-rate). These inhibitory strains were similarly distributed within the different climatic and ecological groups, being leaf-litter fungi the largest group of active strains against *B. cinerea* (n=33). However, this habitat could not be identified as the optimal source of antagonists of the phytopathogen given the different distribution of the initial strain population among the ecological groups. Therefore, detailed studies had to be carried out later with a different group of leaf-litter-associated fungi to assess its real potential against fungal phytopathogens. Furthermore, as results of the interaction, the morphology of *B. cinerea* exhibited considerable changes in the colony front that affected the texture and color of its mycelium (Chapter 1, Figure 1). These morphological changes are related with the activation of different BGCs, hence with a valuable modulation of their metabolic activity (Bertrand et al., 2014; Selegato & Castro-Gamboa, 2023). Then, the molecules responsible for the inhibition could be accumulating in this inhibition area between both fungi.

For better characterization of the 93 positive antagonisms and to determine changes in the metabolite patterns in the zones of inhibition, these zones between both inhibitor and phytopathogen were extracted separately and analyzed by Mass Spectrometry (MS). For this purpose, two areas in the co-culture plates were extracted to identify the diffusion of molecules or signals in each positive antagonism (Chapter 1, Figure 2): i) the clear **inhibition zone** corresponding to the area between both co-cultured strains, lacking fungal growth, and ii) the **front of the colony of *B. cinerea*** which was inhibited, to evaluate the response of the phytopathogen to the interaction. The analysis of these two different co-culture extracts from each positive antagonism allowed to differentiate tentatively if the metabolites or signals were produced by the strains inhibiting the phytopathogen, or by *B. cinerea* as a mechanism of defense, based on the diffusion gradient. Additionally, the analysis of the extracts of the axenic cultures of the 93 antagonistic strains and the phytopathogen separately, allowed the comparison of their chemical composition.

Dereplication analyses detected the presence of several known bioactive molecules that were produced constitutively by 25 of the antagonistic strains. Molecules such as *integrastin* B, *palmarumycin* C₁₅, *australifungin*, *equisetin*, *cordyol* C, *illudin* C₃ and *7-chloro-6-methoxymellein* were detected in both mono- and co-culture plates, independently of the microbial interactions. Most of these compounds are antifungal metabolites produced by a variety of fungal strains and

might explain the inhibition of *B. cinerea*. Other known molecules such as *11-hydroxy-dehydro-botrydienol*, *botrytisic acid A* and *B*, *dehydro-botrydienol*, *3-hydroxy-4-oxocyclofarnesa-2,5,7,9-tetraen-11,8-olide*, *norbotrydialone acetate*, *botrydialenol phytotoxin*, *10-oxo-dehydro-dihydro-botrydial*, *hydrated-botryenalol* and *dehydro-botrydienal* were detected only in co-culture extracts, more specifically in the front of the inhibited mycelium of the phytopathogen (Chapter 1, Figure 4). These molecules are described in the literature as toxins produced by *B. cinerea*, and they could represent a possible defense response of the phytopathogen to the antagonistic strain. More interesting results were those obtained with certain bioactive metabolites only detected in the co-cultured plates, specifically in the inhibition zone, lacking any fungal growth. The induced compounds identified were *SNF 4794-7*, *mycorrhizin A*, *palmarumycins*, *preussomerins*, *penicillic acid* and *chaetoxanthone C*, which were originally described from a wide range of fungal taxa but never reported as metabolites produced by *B. cinerea*. Moreover, these compounds were spatially concentrated in the inhibition zone of co-culture plates, but were absent or in traces in the *B. cinerea* inhibited mycelia, so they could correspond to induced compounds produced by the antagonistic strain during microbial interaction with the phytopathogen. These findings revealed a clear bidirectional communication during co-culturing between both confronted strains. Fungal strains could attack the phytopathogen by the production of a wide diversity of bioactive molecules, and *B. cinerea* also could respond with the production of antimicrobial compounds such as the *botryanes* (Porquier et al., 2019).

Furthermore, in most of the co-culture extracts were not known active molecules identified, suggesting this fungal interaction to be a potential source of undescribed active metabolites, as shown in the analysis of the two fungal strains which exhibited significant metabolomic changes during their interactions with *B. cinerea*: *Phoma* sp. CF-090072 and *Skeletocutis amorphia* CF-190679 (Chapter 1, Figures 5G-H). The strain ***Phoma* sp. CF-090072** (isolated from a contaminated soil collected in Singapore) produced a multi-chlorinated family of four compounds that were not described in Dictionary of Natural Products (DNP). The production levels of the two potential new molecules ($C_{15}H_{13}ClO_5$ & $C_{15}H_{12}Cl_2O$) that were detected in both mono- and co-cultures, were clearly influenced by *B. cinerea* interactions. On the contrary, another two additional chlorinated molecules ($C_{20}H_{14}Cl_3O_5$ & $C_{19}H_{12}Cl_5O_3$) were only detected in the co-culturing extract. The strain ***Skeletocutis amorphia* CF-190679** (isolated from leaf-litter associated with palm crop in Guatemala), produced a possible new metabolite ($C_{23}H_{36}O_9$) when grown both in mono- and co-cultures, as well as a potential new compound ($C_{40}H_{62}O_{13}$), that was induced by interactions with *B. cinerea*. Both cases are examples supporting the hypothesis that interactions with *B. cinerea* can trigger the activation of silent BGCs involved in the production of new molecules. Therefore, co-culturing with the strain *B. cinerea* CBS 102414 has proved to be a valuable model system to enhance the biosynthetic potential of highly diverse fungi, and to screen for antagonistic strains as possible biocontrol agents.

The assay of the extract library obtained from the co-culture zones against a panel of human and plant pathogens has permitted to assess the presence of potentially new antifungal molecules. Various methods are available for screening the antimicrobial activity of samples under *in vitro* laboratory conditions. The disk-diffusion and agar dilution methods on Petri dishes are commonly used methods to evaluate the antifungal activity of extracts and compounds against phytopathogens (Huang et al., 2018; Jiménez et al., 2011; Yang et al., 2012). These manual assay

methods present limitations such as they are time-consuming, expensive, have poor reproducibility and require large quantity of sample. Therefore, new agar-based High-Throughput Screening (HTS) protocols were needed to be developed and validated for a rapid and robust screening using large sample libraries. For this purpose, an **agar-based HTS method** was optimized for plant pathogenic strains based on the previously described assay protocol for the human pathogen *Candida albicans* (de la Cruz et al., 2012). The antifungal panel included the three phytopathogens *Colletotrichum acutatum*, *Fusarium proliferatum* and *Magnaporthe grisea* because of their impact in global agriculture (Dean et al., 2012), and the two human pathogens *Aspergillus fumigatus* and *Candida albicans*, due to their high relevance in invasive infections (Garcia-Rubio et al., 2020). The HTS agar method developed in OmniTray® assay plates allowed to test 48 samples per plate (Annex Chapter 1, Figures S1-S3) including reference compounds for positive and negative controls. Moreover, the protocol required the setup in a liquid handling automated equipment such as a BiomekFX™ robot, combined to the use of an Image Analyzer® for an automatic readout, which significantly reduced both time and costs allowing the screening of higher number of samples. This agar-based HTS methodology is in fact applicable to many other different fungal strains, but it requires to generate an adequate number of conidia which is a limiting factor for certain species. For this reason, a specific optimization of fungal sporulation process was required with each phytopathogenic strain during the setup of the assay platform.

As many as 130 co-culture-derived extracts (corresponding to 86 antagonisms) were identified as active in the agar-based HTS assays, presenting a broad antifungal spectrum against the plant pathogens (69.90 % hit-rate). In contrast, only 24 extracts showed activity against the human pathogens (12.90 % hit-rate) (Chapter 1, Figure 3). The selection of *B. cinerea* as phytopathogen model for this co-culturing approach might be the reason for the high hit-rates of activities in these extracts against other phytopathogens, activities not observed against the human pathogens. Interactions with *B. cinerea* might induce the production of specific diverse chemical signals as a defense mechanism, focused on the inhibition of the phytopathogen growth. Similarly, Robbins et al., in 2016, revealed that a co-culture of an actinomycete strain and *Cryptococcus neoformans* led to the production of *ibomycin*, a potent antifungal active specifically against this human pathogen. Therefore, the selection of a human pathogen for a co-culture approach could trigger the possible induction of antifungals molecules with selective activity against human pathogens.

Finally, the newly developed HTS agar-based method provided an efficient tool to evaluate the antifungal potential of samples more efficiently, with higher reproducibility and robustness than traditional manual methods. Most of the co-culture extracts showed inhibitory effects on the phytopathogens of the panel, mainly against *Magnaporthe grisea* which was the most sensitive strain. Moreover, bioactive metabolites responsible for the inhibition of *B. cinerea* in co-culturing were extracted, and their activity could be also evaluated on other targets. These results demonstrate that *B. cinerea* inhibition is mediated by the production of antifungal metabolites, that in most cases are induced only in this condition. Therefore, we can confirm the effectiveness of the co-culturing method in activating the **expression of BGCs** encoding the biosynthesis of bioactive metabolites, which remain silent or poorly expressed when strains are not challenged in axenic cultures.

However, this technique also presented challenges related to its complexity, reproducibility, and scale-up (Guo et al., 2024). Co-cultivation is highly sensitive to variations in environmental

conditions, inoculum ratios or resource competitions that can affect the reproducibility of metabolite production and microbial interactions. The cases of the strains *Phoma* sp. CF-090072 and *Skeletocutis amorphia* CF-190679 have been two promising examples of inductions of novel bioactive molecules by co-culturing methods. However, maintaining the delicate balance of these microbial co-cultures and ensuring consistent metabolite production at larger scales presented significant challenges to purify enough quantities of compound for further chemical characterization and structural elucidation. Several subsequent efforts were made to optimize culture-based approaches and improve the production of higher titers of these potential novel compounds. Unfortunately, co-culture scale-up, variations in fermentation format or nutritional arrays of both strains were unfruitful to obtain enough amounts of these active compounds, which did not allow their chemical and biological characterization. Therefore, this lack of successful results after time-consuming experiments highlighted that the co-culturing technique stimulates the induction of new metabolites that, sometimes, are impossible to scale-up in quantities for a successful purification under laboratory conditions, confirming that new approaches are needed to solve this significant challenge.

Given these limitations of scale-up reproducibility associated with the agar co-culturing technique, a second methodology was explored with the aim of expanding the fungal chemical diversity and producing novel bioactive compounds. An important strategy to modulate the biosynthesis of novel metabolites involves modifications in culture environments mimicked by media formulations (Abdelwahab et al., 2018; Gakuubi et al., 2022; González-Menéndez et al., 2014; Wang et al., 2012; Xue et al., 2023). Therefore, specific nutritional arrays were designed to study the metabolomic potential in a new selection of fungi. For this experiment we targeted a new population of strains associated with leaf-litter to assess the potential of this very diverse fungal community to produce novel compounds. Leaf-litter is a complex environment where fungi interact with a wide range of organisms, which could additionally facilitate to find antagonists of plant pathogens. This habitat constitutes a well-studied environment that harbours a great biodiversity of decomposer microorganism responsible for the degradation of recalcitrant components from plants (Crous et al., 2006; Foster et al., 2022; Grossman et al., 2020). Furthermore, leaf-litter was the most active group against *B. cinerea* within the antagonistic strains (co-culturing approach).

This study was focused on a group of 400 fungal strains from the MEDINA Fungal Collection, isolated from **leaf-litter collected in South Africa**, considered one of the worldwide biodiversity “hotspots” (Crous et al., 2006; Mamathaba et al., 2022). An initial morphological identification of the strains allowed to avoid common ubiquitous saprophytic species such as *Cladosporium*, *Penicillium* and *Aspergillus*, as well as redundant strains from the same sources to ensure the broadest diversity of the fungal population. The selected subset of 232 fungal cultures with the widest morphological diversity was preliminary classified, based on the Blast analysis of 28S rDNA sequences, in four taxonomical ranks (class, order, family and genera) (Chapter 2). Then, an exhaustive taxonomic study by phylogenetic analyses combined with Blast using ITS1-5.8-ITS2 rDNA sequences was performed to improve the initial classification (Chapter 4). This exhaustive taxonomic analysis highlighted the wide diversity of the studied fungal population, confirming the reported complexity and richness of the fungal communities associated with leaf-litter matter, and specifically from endemic plants of South Africa, already reported in literature (Crous et al., 2006; Foster et al., 2022; Goldblatt & Manning, 2000; Voříšková & Baldrian, 2013). Furthermore, the molecular identification

highlighted 64 strains (28%) whose ITS rDNA sequences showed similarities lower than 95% with any previously available sequences in public databases, as potential new species that are currently being studied and will be described in future works (Chapter 4, Figure 1; Annex Chapter 4, Table S1). The discovery of new fungal species presents an excellent opportunity to access to new biosynthetic potential.

Fungal genomes encode valuable information for the discovery of novel bioactive compounds, but usually remain silent under standard laboratory conditions (Pandit et al., 2022; Riedling et al., 2024). Therefore, a specific culture-based approach was designed to address these limitations, and each fungal strain was cultured in four **liquid fermentation media (SmF)** (LSFM, MCKX, SMK-II and YES media) and one **solid-state fermentation (SSF)** condition (BRFT medium) to maximize the chances for inducing the production of new secondary metabolites. Among the SmF, the media LSFM and YES were selected due to their reported ability to improve the metabolite production in fungal fermentations (González-Menéndez et al., 2014, 2016). Alternatively, the media MCKX and SMK-II were specifically formulated for this leaf-litter fungal population. The MCKX medium has a rich base formulation with mannitol and yeast extract as carbon and nitrogen sources, ingredients used in MMK2, another previously described production medium (González-Menéndez et al., 2014, 2016), as well as xylose, commonly found in leaf-litter environments from plant cell walls. Different carbon and nitrogen sources were selected for the medium SMK-II, such as soluble starch, maltose and soybean flour, also reported to be components of successful formulations for bioactive metabolite production (González-Menéndez et al., 2014, 2016). This fermentation medium was supplemented with L-proline, an amino acid that has been reported to be crucial in the production of the antifungal compound *pneumocandin* by *Glarea lozoyensis* (Petersen et al., 2001). Murashige and Skoog salts, widely used for plant cultures, were added to both new media to stimulate the growth and development of fungal strains able to metabolize leaf-litter components. Finally, the medium BRFT containing brown rice as carbon source and yeast extract as nitrogen source, was introduced as the SSF condition to produce broader diversity of chemical profiles compared to liquid media, as previously reported for many other fungal species (Bills et al., 2012; Gao et al., 2020; Song et al., 2023; Wei et al., 2021). In addition, all these fermentation conditions were evaluated in presence and absence of the **epigenetic elicitor suberoylanilide hydroxamic acid (SAHA)**, one of the most frequently used histone deacetylase (HDAC) inhibitors for inducing the production of several bioactive metabolites in elicitation studies (Beau et al., 2012; Gubiani et al., 2017; Henrikson et al., 2009; J. Sun et al., 2012; Xue et al., 2023; Zhang et al., 2019; Zhao et al., 2018; Zhu et al., 2019). The incorporation of the epigenetic elicitor into the OSMAC (One Strain Many Compounds) approach might additionally improve the chemical diversity produced by the nutritional array, with the aim to discovery of new bioactive compounds.

Several of the fungal strains studied showed differential patterns in their macromorphology (Chapter 2, Figures 1a-b), which might be evidences of modulation in the expression of certain BGCs, as a response to alterations in the environment. The use of two extraction solvents for the fermentation broths from the liquid and solid media ensured an efficient extraction of SMs (Bills et al., 2008, 2012; González-Menéndez et al., 2014, 2016; Peláez et al., 2000). The chemical composition of the resulting 2,362 fungal extracts was analyzed by Liquid Chromatography Low Resolution Mass Spectrometry (LC-LRMS) and **MASS Studio 2.3 software** in **untargeted metabolomics**. This analysis allowed to statistically compare the [rt-*m/z*] chemical components

among the samples for assessing the influence of the tested culture conditions on the induction of new chemical diversity and on the relative amounts of each metabolite produced (García & Tormo, 2003; González-Menéndez et al., 2014; Martínez et al., 2017; Tormo et al., 2003).

On the one hand, MASS Studio revealed that the **SSF in BRFT medium** ensures the highest number of the global and unique chemical components, compared to the panel of four SmF (Chapter 2, Figure 2). Previous studies reported that fungal strains grown in SSF generally exhibit more complex metabolite profiles than the same strains when grown in SmF (Bader et al., 2021; Bigelis et al., 2006; Bills et al., 2012; Webb & Manan, 2017). The use of SSF with fungi might bring them closer to the growth conditions of their natural habitats, offering potential benefits for the microbial cultivation and metabolite production (Bills et al., 2012; Webb & Manan, 2017). Monaghan et al., in 1995, clustered the metabolite production of *Nodulisporium* sp. in three different SSF, distant to the four SmF. In addition, several new fungal metabolites have been produced in rice-based medium with different nutrient formulations, such as *cladosins A-E* by *Cladosporium sphaerospermum* (Wu et al., 2014) two *xanthone* derivatives, two *phenolic bisabolene-type sesquiterpenes*, *scopulamide*, and *scopupyrone* from the marine-derived *Scopulariopsis* sp. (Elnaggar et al., 2016), and five new *polyketides* by the endophyte *Phomopsis* sp. Sh917 (Tang et al., 2017). However, we could not confirm if the medium BRFT was a successful formulation due to its nutrient composition or because it provides a solid support, and/or a synergy of both factors. Therefore, another SSF with different nutrient compositions should be included in future studies to compare with the medium BRFT. Furthermore, SmF media also showed effectiveness for inducing the production of a considerable range of unique metabolites. Fermentations in the media LSM and YES were the most productive conditions for generating global and unique chemical components, followed by the new MCKX and SMK-II media, although no significative differences were observed among the four SmF media (Chapter 2, Figure 2).

On the other hand, the **addition of SAHA** at different stages of the fermentation processes (both inoculum and production) in the five media, significantly increased the number of total and unique chemical components (Chapter 2, Figure 2). SAHA is the most used HDAC inhibitor due to its great ability to modulate the production of fungal SMs (Beau et al., 2012; Gubiani et al., 2017; Henrikson et al., 2009; Sun et al., 2012; Xue et al., 2023; Zhang et al., 2019; Zhao et al., 2018; Zhu et al., 2019), but its application to enhance broadly the chemical diversity on a wide diverse fungal population had never been analytically supported. Despite the differences between positive and negative ionization modes of MS and the similarities between histograms of retention times (Chapter 2, Figure 3), our results revealed that the addition of SAHA clearly improved the total number of exclusive chemical components across the whole fungal population studied. Dereplication analyses also confirmed these effects of SAHA on the metabolite production with the identification of 22 known compounds only in fermentation conditions supplemented with SAHA (Chapter 2, Figures 4 and 5).

Furthermore, MASS Studio 2.3 software was implemented to rank the 10 different fermentations conditions, from the best to the worst for inducing chemical diversity and relative amounts of each chemical component produced. According to this untargeted metabolomics method, fermentations in BRFT with and without SAHA were again the most productive conditions, followed by the four SmF conditions with SAHA (Chapter 2, Figure 6). These findings indicate that SmF conditions resulted in lower diversity and amounts of metabolites, although these four media were

successful formulations for this leaf-litter fungi because all of them were selected in the ranking as the best one for certain group of strains. More interestingly, the ranking highlighted that SAHA clearly influenced the production of SMs of the whole fungal population, because every medium with SAHA was ranked prior to its corresponding medium without the epigenetic elicitor. Additional chemometric analyses to compare the output from the different media were based on Dice (presence and absence of [rt- m/z]) and Pearson (area of [rt- m/z]) statistical similarity coefficients that clustered first the metabolomic profiles for the same fermentation media, being again BRFT the medium which provided the most different profiles (Chapter 2, Figure 9). Similarly, González-Menéndez et al. in 2014 studied the addition of adsorptive polymeric resins to fungal fermentations and concluded the addition of Diaion® and Amberlite® resins generated slightly lower variations in the chemical profiles than changes in the composition of culture media. Therefore, the optimization of the medium composition could be a more important factor, rather than the addition of epigenetic elicitors, to enhance the chemical diversity produced by widely diverse groups of fungi.

Due to the high taxonomic diversity of the studied fungal population, more specific analyses were applied on smaller homogeneous taxonomic subgroups. In general, BRFT fermentations (with and/or without SAHA) were the most productive for the orders *Pleosporales*, *Capnodiales*, *Xylariales*, *Helotiales* and *Chaetothyriales*, and the presence of SAHA clearly improved the chemical diversity. However, some interesting differences were observed among some groups (Chapter 2, Figure 7): fermentations of *Pleosporales*, *Capnodiales* and *Chaetothyriales* in YES with SAHA stood out as the most productive SmF condition, in line with the reported ability of this medium to produce a wide range of fungal metabolites (Bills et al., 2008; González-Menéndez et al., 2014, 2016); the order *Helotiales* also showed higher number of chemical components when grown in the new formulation SMK-II with SAHA, that could be related to the reported ability of these fungi to grow on maltose or the positive effects of L-proline addition on *Glarea lozoyensis* (*Helotiales*) (Knapp & Kovács, 2016; Petersen et al., 2001); meanwhile LSFM with SAHA was the best SmF condition for *Xylariales* and *Hypocreales*, confirming the reported success of this formulation to promote chemical changes during fungal fermentations (Bills et al., 2008; González-Menéndez et al., 2014, 2016). Furthermore, we studied the effects in the class *Agaricomycetes*, one of the most important groups of leaf-litter decomposers including unique fungal strains with high metabolic potential (Schneider et al., 2012). Among this subset, the addition of SAHA ensured an enhancement of the chemical diversity in BRFT, LSFM and MCKX media, in contrast to their same media without SAHA (Chapter 2, Figure 8).

The **targeted metabolomics** study with Liquid Chromatography High Resolution Mass Spectrometry (LC-HRMS) provided more complex information and allowed to identify three different **effects of SAHA on the metabolite production** for certain strains: (i) conditions where the addition of SAHA did not affect the metabolomic profiles, as the strains *Corticium* sp. CF-166036 and *Microxyphium* sp. CF-164412 in the medium BRFT; (ii) conditions with clear improvement in the production levels of given compounds in the presence of SAHA, such as the production of *radicidin* by *Microxyphium* sp. CF-164412 in LSFM medium (Chapter 2, Figure 12); and (iii) induction of compounds that only were produced in the presence of SAHA. This last effect could be represented by the induction of *terricolin*, *leucinostatins A* and *B*, and three unidentified m/z in fermentations of *Corticium* sp. CF-166036 with SAHA (Chapter 2, Figure 11), as well as the identification of *quinolactacin A₂* and a possible new metabolite only in fermentations of *Microxyphium* sp. CF-

164412 with SAHA (Chapter 2, Figure 12). This differential production correlated to Dice-UPGMA dendrograms (Chapter 2, Figure 10), where a specific isolated cluster was observed. Therefore, the LC-HRMS targeted metabolomics analyses of both cases demonstrated that the initial untargeted metabolomics by LC-LRMS provided a valuable and robust preliminary information about the metabolomic changes induced during fungal fermentations.

In summary, this study is the first systematic metabolomic analysis that has explored the effects of SAHA on such a broad taxonomically diverse group of fungal strains when cultured in solid and liquid conditions. Results confirmed that changes in the medium composition had a larger impact on their metabolome profiles than the addition of the elicitor SAHA. Moreover, this is the first chemometric confirmation that supports the solid fermentation in BRFT medium as the most productive formulation that generates greater metabolomic changes and relevant enhancements of SMs production. Results also supported the hypothesis that the addition of SAHA during fungal fermentations can determine substantial metabolomic changes on the chemical profiles for an entire fungal population, as well as within different taxonomic classes, orders or families.

Once the metabolomic analysis had revealed that nutritional arrays in the presence of SAHA generated a wide range of chemical components, further studies were subsequently performed to identify new antifungal agents among these components. The developed agar-based HTS improved many limitations associated with traditional agar tests, but it still exhibited disadvantages such as the restrictions in generating the quantity of conidia required for large scale campaigns, and difficulties in accurately determining the potency of compounds from the measurement of the zone of growth inhibition. Therefore, to respond to the large scale testing needs of a library of 2,362 extracts, microdilution methods were developed and validated for each target pathogen enabling the discovery of new antifungal agents. The **microdilution method** provides more information about the antifungal effects of a sample, as it can differentiate the inhibition of fungal growth (absorbance readouts) and cell viability (resazurin fluorescence readouts) within the same assay well. This methodology, performed in 96-well plates, is even more time and cost-efficient, requires a lower quantity of conidia, and has the potential to be scaled up to the 384-well format, which makes it ideal for large screening campaigns looking for new fungicide agents. Moreover, the development of a HTS method based on microdilution required statistical analyses and quality control parameters that increased the robustness of the results for large sets. For this purpose, a specialized evaluation of different medium formulations, inoculum concentrations, germination curves, tolerance to dimethyl-sulfoxide (DMSO), and Dose Response Curves (DRC) of the antifungal control *amphotericin B* were also performed, to establish the optimal assay conditions that allowed the highest reproducibility and robustness of data (Chapter 3, Figures 2-6 and Tables 3-4).

The selection of the target phytopathogenic strains was based on their scientific and economic importance reported in the top ten fungal phytopathogens (Dean et al., 2012). Thus, the strains *Colletotrichum acutatum* CF-137177, *Fusarium proliferatum* CBS 115.97 and *Magnaporthe grisea* CF-105765 were selected (same strains used in agar-based HTS). In the case of *Botrytis cinerea*, the strain B05.10 or CECT20754 was selected to optimize the assay conditions because of its greater sporulation rate, compared to the strain used for the co-culture approach (CBS 102414). In addition, *B. cinerea* B05.10 is a wild-type strain commonly used as a model for genomic and pathogenicity studies (Liu et al., 2023; Staats & van Kan, 2012). Once the optimal assay conditions were established for the four phytopathogens selected (Chapter 3, Table 4), a primary screening with **40**

known antifungal standards was performed to validate the assay parameters of both agar and microdilution HTS methods. The four phytopathogens were resistant to *benalaxyl*, *cytochalasin*, *dimethomorph*, *ethaboxam*, *flutianil*, *iprovalicarb*, *mandipropamid*, *metalaxyl*, *radicicol*, and *validamycin* at the maximum assay concentrations. However, the specificity of the remaining 30 standards was characterized by DRC (Chapter 3, Table 5). *Strobirulins*, *triazoles*, *imidazoles* and *benzimidazoles* were the most effective standards against the four phytopathogens through different modes of action, in line with their reported broad antifungal spectrum (FRAC Code List ©, 2022). Among them, *benzimidazoles*, *thiabendazol* and *benomyl* have been described for the control of *Fusarium* species (Zhou et al., 2016), however exhibited additional inhibitory activity against *B. cinerea*, *C. acutatum*, and *M. grisea*. Another interesting group of antifungal agents were those that affect the synthesis of proteins, where *cycloheximide* and *cyprodinil* confirmed their antifungal potential through the inhibition of the four phytopathogens with both assay methodologies (Prakash et al., 2008). In addition, the nucleosidic NPs *tunicamycin* and *tubercidin* showed high specificity against *B. cinerea* and *C. acutatum*, an activity not previously reported. *Cyclosporin A* was active against *B. cinerea* and weakly against *C. acutatum*, activities that had never been described, apart from its antifungal properties against *Candida* species (Cordeiro et al., 2014; Li et al., 2008). Finally, the natural compound *cerulenin* presented a lack of activity against most of the phytopathogens, what could be correlated to its reported limited activity to yeasts and dimorphic fungi (Bills et al., 2004; Omura, 1976).

Therefore, this HTS Platform characterized known and novel sensitivities and resistances of *B. cinerea*, *C. acutatum*, *F. proliferatum* and *M. grisea* to these 40 standards, using two different assay methodologies (agar-based and liquid microdilution assays). Despite that some differences were observed in the antifungal potency of some compounds, a high number of synthetic and natural fungicide compounds with a broad variety of modes of action were detected at very low concentrations (<0.04 µg/mL). These differences observed for certain fungi may be dependent on the differential diffusion of samples in media due to the chemical properties of the molecules, the specificity on their mechanisms of action and/or the differential fungal growth rates and physiologies, according to the two methodologies using in the assay setups. Therefore, the combination of both HTS methods could be applied in the characterization of novel fungicide agents in order to obtain more reliable data of their antifungal potential.

A proof of concept **piloting** was performed with a small subset of wide diverse 2,400 **microbial extracts** (1,200 actinomycete extracts and 1,200 fungal extracts) from the MEDINA Library, in order to validate the assay conditions for screening with NP Libraries. Microbial extracts containing 20% DMSO were tested at a final 1:10 dilution to avoid any inhibitory effects derived from the DMSO concentration on the plant pathogens. The antifungal activities obtained from agar-based assays were determined by measuring the diameter and turbidity of the inhibition zones (mm). However, the activities in microdilution assays, based on absorbance and fluorescence data, allowed further statistical analyses. Screening campaigns usually apply a 50% inhibition cut-off as initial selection criterion, but we further analyzed the activity population distributions to select and prioritize hits based also on statistical criteria. Activities based on absorbance and fluorescence data were represented in different histograms, where x-axis showed the range of percentage of inhibition and the corresponding statistical *z'* score values, while y-axis shows the frequency of occurrences (Chapter 3, Figure 7).

Statistical analyses allowed us to define a specific threshold of hit selection for each phytopathogen, in order to prioritize only high-quality bioactive hits. In the case of *B. cinerea*, both histograms showed slight differences between the distribution of data and their corresponding hit populations (Chapter 3, Figure 7). Absorbance data provided larger dispersion than fluorescence data due to a higher coefficient of variation, which might be explained by the overgrowth of the phytopathogen by the addition of certain extracts, generating higher absorbance values, which is minimized in the fluorescence readout. Moreover, the fluorescence assay showed larger z' scores, which better separated the active extracts from the general inactive population, indicating a more robust dataset. However, fluorescence readouts can be easily affected by the presence of colored or fluorescent molecules and/or variations in pH, which interferes with resazurin generating false-positive signals. NP extracts are typically complex mixtures of known and unknown molecules at different concentrations, and they tend to be rich in pan-assay interference compounds (PAINS) which can affect both cell viability and assay readouts (Wilson et al., 2020). This effect can sometimes challenge the identification of active samples. Therefore, a robust hit selection criterion should only consider those extracts which are active in both assays. Thus, only samples that inhibited fungal growth (absorbance) and also affected cell viability (fluorescence) were selected as hits. Therefore, the implementation of this phytopathogen HTS platform could be considered an efficient tool to explore broad microbial sample libraries, ensuring a high quality selection of new potential inhibitors of plant pathogens, facilitating the efficient discovery of the next-generation of fungicides for the biocontrol of *Botrytis cinerea*, *Colletotrichum acutatum*, *Fusarium proliferatum* and *Magnaporthe grisea*.

Subsequently, this HTS microdilution methodology for the discovery of phytopathogen inhibitors was applied to evaluate the potential antifungal activity of the previously enhanced **library of 2,362 leaf-litter fungal extracts** from the OSMAC approach (Chapter 2). Statistical analyses suggested specific hit selection criteria for each phytopathogen (Chapter 4, Figure 2). In *Botrytis cinerea* screening only extracts with activity higher than -53% INH in both methodologies (absorbance and fluorescence) were considered hits. In the case of *C. acutatum* and *F. proliferatum* the extracts with activity greater than -17% INH could be considered hits because of being statistically separated to the normal population. However, this percentage of inhibition was insufficient to select the most potent active extracts, then a second criterion of selection was applied, and only outliers in the upper quartile were considered hits. Finally, *M. grisea* was the most sensitive phytopathogen with the highest hit-rates, as previously observed in the agar-based HTS campaign (Chapter 1), with a unique pattern of activity distribution. A detailed study of hit populations identified most of these extracts corresponded to fermentations in the medium BRFT (n=202), that frequently contain diverse interfering fatty acids such as *linoleic acid*, *linolenic acid*, *11-hydroxylinolenic acid*, *1-linolenoyl-sn-glycerol*, *1-monolinolein* and *1-oleoyl-sn-glycerol*, reported to show unspecific inhibitory effects on fungal growth (Huang et al., 2010; Kusumah et al., 2020). Consequently, new histograms were generated without these extracts with high concentration of fatty acids (Chapter 4, Figures 2g-h), which allowed to prioritize two separated hit populations. The first group of actives, supported by absorbance and fluorescence data, contained the most potent hits (> -86% INH, n=41 active extracts) but no successful case for the discovery of novel metabolites were identified among them. Thus, a second hit population containing lower potency hits was selected and studied in detail (from -50 to -86% INH, n=213 active extracts).

In summary, this primary screening campaign provided a high number of active extracts (n=340) that were deeper analyzed chemically. **Dereplication analyses** identified 95 known bioactive molecules as potentially responsible for the antifungal activity observed in 187 of these active extracts. LC-LRMS and LC-HRMS analyses revealed a great diversity of chemical structures suggesting the high biosynthetic richness encoded in leaf-litter-associated fungi, where *stemphyllotoxin I*, *preussomerin B*, *palmarumycins C₁₅* and *C₁₆*, and *mellein*, described in DNP with a broad antifungal spectrum, were the most common dereplicated bioactive compounds (Chapter 4, Figure 3). Moreover, the identification of known bioactive molecules also facilitated the selection of the most interesting hits, to avoid redundancy and focus only on potentially novel antifungal molecules (Flores-Bocanegra et al., 2022; Pérez-Victoria et al., 2016; Wolfender et al., 2019). Dereplication was also an essential step for prioritization in *M. grisea* hits due to the large number of active extracts identified and the interferences with fatty acids.

In addition, active hit populations were further analyzed to address the influence of nutritional arrays and SAHA addition to promote **antifungal activity** against the fungal phytopathogens. On the one hand, previous results highlighted that the medium composition played a crucial role improving the metabolite production in fungi (Chapter 2), and this chemical diversity has clearly influenced the bioactivity profiles, as it has been shown later in Chapter 4. As previously mentioned, fungal fermentations in the medium BRFT provided more complex metabolite profiles than SmF, which can explain the high number of active extracts obtained from this SSF against *B. cinerea* and *C. acutatum* (Chapter 4, Figure 4a). However, in *F. proliferatum* and *M. grisea* screenings, the media that provided the highest number of hits were LSFM and SMK-II, respectively. These results made it challenging to determine a single medium as the optimal condition, in line with the results from untargeted metabolomics where the executed OSMAC approach was effective for inducing the production of general SMs, specifically molecules potentially active against *B. cinerea*, *C. acutatum*, *F. proliferatum* and *M. grisea*. On the other hand, we have also shown that the addition of SAHA significantly influenced the bioactivity rates. In general, the addition of SAHA during fungal fermentations improved the overall hit-rates against these fungal phytopathogens, in particular by increasing the number of active extracts against *B. cinerea* and *M. grisea* (Chapter 4, Figure 4b). LC-HRMS analyses revealed that SAHA enhanced both diversity and the amounts of certain bioactive metabolites (Chapter 4, Figures 5-7), what supported the differential bioactivity profiles observed. Furthermore, we have shown that the most predominant effects induced by SAHA were to increase the production levels of specific compounds, opening the access to the scale-up production of a variety of fungal metabolites that are typically produced in minimal quantities, where their potential activity remained hidden or underestimated.

Despite the lack of a universal optimal fermentation condition that ensured the expression of all the biosynthetic potential of fungi, SAHA addition to specific formulation medium can enhance the general fungal metabolite production. A proof of concept of this effect was the production of the new antifungal compound **libertamide (C₁₆H₂₇NO₂)** by the strain *Libertasomyces aloeticus* CF-168990, whose antifungal activity was initially detected only in the presence of SAHA. Moreover, the addition of SAHA to the medium BRFT during scaled-up growth specifically increased by two-fold the production levels of this molecule. To date, the family of *libertalides A-N* was the only described active molecules produced by *Libertasomyces* strains, as immunomodulatory agents (Chen et al., 2022; Sun et al., 2017). *Libertamide* is structurally related to *scalusamides* and different from

libertalides (Chapter 4, Figure 9; Annex Chapter 4, Figures S5-S15 and S18-S19), as well as its antifungal activity against fungal phytopathogens (Chapter 4, Table 3; Annex Chapter 4, Figures S16 and S17). These results supported the potential use of the strain *Libertasomyces aloeticus* CF-168990 and the novel compound *libertamide* as a biocontrol agent of the septoria leaf blotch caused by *Zymoseptoria tritici*.

The implementation of various culture-based techniques, such as co-cultivation, variations in media formulations, and the use of the epigenetic elicitor SAHA, has facilitated the elicitation of diverse biosynthetic pathways associated with the production of bioactive fungal SMs, which are usually silent or poorly expressed under standard laboratory conditions. Although fungal interactions during co-culturing techniques have proven to be efficient tools in inducing bioactive compounds, they also present challenges related to reproducibility and scalability which limited the characterization of promising antifungal new compounds. The incorporation of SAHA has enhanced the biosynthetic potential across a wide variety of fungal strains, increasing the general chemical diversity of bioactive metabolites. Furthermore, the use of SAHA has significantly improved the production levels of specific compounds, enabling the access to a variety of fungal SMs that are typically produced in minimal quantities under non-supplemented conditions. Nevertheless, the variability in responses of different fungi to the presence of SAHA suggests the need for a correct selection of specific strains and the **optimization of their medium compositions** for metabolite production.

This study also highlights the significance of integrating various culture-based approaches that include epigenetic elicitation to unlock the unexplored biosynthetic potential of fungal strains. Furthermore, the development of novel fungicides from microbial sources requires the implementation of innovative metabolomics tools to study the chemical diversity produced under different conditions, as well as the validation of HTS Platforms to characterize their activity profiles. The combination of all these analytical techniques not only allowed us to expand the chemical diversity encoded in fungal genomes, but also accelerated the discovery of new fungicides as effective biocontrol agents for a future sustainable agriculture.

V. Conclusions

- I. The strain *Botrytis cinerea* CBS 102414 is an effective model system to assess the antagonistic potential of a broad diversity of fungal strains as biocontrol agents, as well as to modulate the production of bioactive metabolites.
- II. Fungal interactions during co-culturing can activate specific biosynthetic pathways by the exchange of chemical signals, leading to the production of new bioactive secondary metabolites against fungal phytopathogens.
- III. Leaf-litter fungal communities from South Africa are a prolific source of new fungal species with a high biosynthetic potential to produce widely diverse secondary metabolites.
- IV. The optimization of nutritional arrays is an essential step for improving metabolite production in fungi, being solid-state fermentations the most productive conditions to increase the chemical diversity and the amounts of metabolites.
- V. The addition of the epigenetic elicitor suberoylanilide hydroxamic acid (SAHA) to fungal fermentations determines an efficient activation of silent biosynthetic pathways, resulting in a significant enhancement of the metabolite production of unique chemical components, offering the possibilities for discovering previously inaccessible compounds.
- VI. The development of a High-Throughput Screening (HTS) Platform offers an efficient evaluation of extensive synthetic and Natural Product Libraries of samples, for a rapid identification of inhibitors of fungal phytopathogens.
- VII. The implementations of the HTS Platform based on microdilution methods facilitates the large scale discovery of bioactive compounds with applications in agriculture for the control and management of plant diseases by fungal phytopathogens.
- VIII. The combination of specific culture-based approaches with innovative metabolomics and advanced HTS Platforms can expand the chemical diversity encoded in fungal genomes, and accelerate the discovery of new fungicides as shown with the novel compound *libertamide*, the first described antifungal compound produced by *Libertasomyces* spp.

VI. References

- Ababa, G. (2023). Biology, taxonomy, genetics, and management of *Zymoseptoria tritici*: the causal agent of wheat leaf blotch. *Mycology*, **14**(4), 292–315. <https://doi.org/10.1080/21501203.2023.2241492>
- Abdelwahab, M.F., Kurtán, T., Mándi, A., Müller, W.E.G., Fouad, M.A., Kamel, M.S., Liu, Z., Ebrahim, W., Daletos, G., & Proksch, P. (2018). Induced secondary metabolites from the endophytic fungus *Aspergillus versicolor* through bacterial co-culture and OSMAC approaches. *Tetrahedron Letters*, **59**(27), 2647–2652. <https://doi.org/10.1016/j.tetlet.2018.05.067>
- Adpressa, D.A., Stalheim, K.J., Proteau, P.J., & Loesgen, S. (2017). Unexpected Biotransformation of the HDAC Inhibitor Vorinostat Yields Aniline-Containing Fungal Metabolites. *ACS Chemical Biology*, **12**(7), 1842–1847. <https://doi.org/10.1021/acscchembio.7b00268>
- Alanzi, A., Elhawary, E.A., Ashour, M.L., & Moussa A.Y. (2023). *Aspergillus* co-cultures: A recent insight into their secondary metabolites and microbial interactions. *Archives of Pharmacal Research*, **46**, 273–298. <https://doi.org/10.1007/s12272-023-01442-5>
- Alarcon-Barrera, J.C., Kostidis, S., Ondo-Mendez, A., & Giera, M. (2022). Recent advances in metabolomics analysis for early drug development. *Drug Discovery Today*, **27**(6), 1763–1773. <https://doi.org/10.1016/j.drudis.2022.02.018>
- Arias, M.M.D., Leandro, L.F., & Munkvold, G.P. (2013). Aggressiveness of *Fusarium* Species and Impact of Root Infection on Growth and Yield of Soybeans. *Ecology and Epidemiology*, **103**(8), 822–832. <https://doi.org/10.1094/PHYTO-08-12-0207-R>
- Atanasov, A.G., Zotchev, S.B., Dirsch, V.M., & Supuran, C.T. (2021). Natural products in drug discovery: advances and opportunities. *Nature Reviews Drug Discovery*, **20**(3), 200–216. <https://doi.org/10.1038/s41573-020-00114-z>
- Bader, C.D., Haack, P.A., Panter, F., Krug, D., & Müller, R. (2021). Expanding the Scope of Detectable Microbial Natural Products by Complementary Analytical Methods and Cultivation Systems. *Journal of Natural Products*, **84**(2), 268–277. <https://doi.org/10.1021/acs.jnatprod.0c00942>
- Bader, J., Mast-Gerlach, E., Popović, M.K., Bajpai, R., & Stahl, U. (2010). Relevance of microbial coculture fermentations in biotechnology. *Journal of Applied Microbiology*, **109**(2), 371–387. <https://doi.org/10.1111/j.1365-2672.2009.04659.x>
- Bartlett, D.W., Clough, J.M., Godwin, J.R., Hall, A.A., Hamer, M., & Parr-Dobrzanski, B. (2002). The strobilurin fungicides. *Pest Management Science*, **58**(7), 649–662. <https://doi.org/10.1002/ps.520>
- Beau, J., Mahid, N., Burda, W.N., Harrington, L., Shaw, L.N., Mutka, T., Kyle, D.E., Barisic, B., Van Olphen, A., & Baker, B.J. (2012). Epigenetic Tailoring for the Production of Anti-Infective Cytosporones from the Marine Fungus *Leucostoma persoonii*. *Marine Drugs*, **10**(4), 762–774. <https://doi.org/10.3390/md10040762>
- Bérdy, J. (2012). Thoughts and facts about antibiotics: Where we are now and where we are heading. *The Journal of Antibiotics*, **65**(8), 385–395. <https://doi.org/10.1038/ja.2012.27>
- Bertrand, S., Bohni, N., Schnee, S., Schumpp, O., Gindro, K., & Wolfender, J.L. (2014). Metabolite induction via microorganism co-culture: A potential way to enhance chemical diversity for drug discovery. *Biotechnology Advances*, **32**(6), 1180–1204. <https://doi.org/10.1016/j.biotechadv.2014.03.001>
- Bigelis, R., He, H., Yang, H.Y., Chang, L.P., & Greenstein, M. (2006). Production of fungal antibiotics using polymeric solid supports in solid-state and liquid fermentation. *Journal of Industrial Microbiology & Biotechnology*, **33**(10), 815–826. <https://doi.org/10.1007/s10295-006-0126-z>

References

- Bills, G.F., Dombrowski, A.W., & Goetz, M.A. (2012). The “FERMEX” Method for Metabolite-Enriched Fungal Extracts. In: Keller, N., Turner, G. (eds) *Fungal Secondary Metabolism. Methods in Molecular Biology*, **vol 944**. Humana Press, Totowa, NJ. https://doi.org/10.1007/978-1-62703-122-6_5
- Bills, G.F., & Gloer, J.B. (2016). Biologically Active Secondary Metabolites from the Fungi. *Microbiology Spectrum*, **4**(6). <https://doi.org/10.1128/microbiolspec.FUNK-0009-2016>.
- Bills, G.F., Platas, G., Fillola, A., Jiménez, M.R., Collado, J., Vicente, F., Martín, J., González, A., Bur-Zimmermann, J., Tormo, J.R., & Peláez, F. (2008). Enhancement of antibiotic and secondary metabolite detection from filamentous fungi by growth on nutritional arrays. *Journal of Applied Microbiology*, **104**(6), 1644–1658. <https://doi.org/10.1111/j.1365-2672.2008.03735.x>
- Bills, G.F., Platas, G., & Gams, W. (2004). Conspecificity of the cerulenin and helvolic acid producing ‘*Cephalosporium caerulens*’, and the hypocrealean fungus *Sarocladium oryzae*. *Mycological Research*, **108**(11), 1291–1300. <https://doi.org/10.1017/S0953756204001297>
- Bills, G.F., & Polishook, J.D. (1994). Abundance and diversity of microfungi in leaf litter of a lowland rain forest in Costa Rica. *Mycologia*, **86**(2), 187–198. <https://doi.org/10.1080/00275514.1994.12026393>.
- Chadha, S., & Kale, S.P. (2015). Simple fluorescence-based high throughput cell viability assay for filamentous fungi. *Letters in Applied Microbiology*, **61**(3), 238–244. <https://doi.org/10.1111/lam.12460>
- Chen, M., Zhang, W., Shao, C.L., Chi, Z.M., & Wang, C.Y. (2016). DNA Methyltransferase Inhibitor Induced Fungal Biosynthetic Products: Diethylene Glycol Phthalate Ester Oligomers from the Marine-Derived Fungus *Cochliobolus lunatus*. *Marine Biotechnology*, **18**(3), 409–417. <https://doi.org/10.1007/s10126-016-9703-y>
- Chen, Y., Pang, X., He, Y., Lin, X., Zhou, X., Liu, Y., & Yang, B. (2022). Secondary Metabolites from Coral-Associated Fungi: Source, Chemistry and Bioactivities. *Journal of Fungi*, **8**(10), 1043. <https://doi.org/10.3390/jof8101043>
- Collado, J., Platas, G., Paulus, B., & Bills, G.F. (2007). High-throughput culturing of fungi from plant litter by a dilution-to-extinction technique. *FEMS Microbiology Ecology*, **60**(3), 521–533. <https://doi.org/10.1111/j.1574-6941.2007.00294.x>
- Cordeiro, R.A., Macedo, R.B., Teixeira, C.E.C., Marques, F.J.F., Bandeira, T.J.P.G., Moreira, J.L.B., Brilhante, R.S.N., Rocha, M.F.G., & Sidrim, J.J.C. (2014). The calcineurin inhibitor cyclosporin A exhibits synergism with antifungals against *Candida parapsilosis* species complex. *Journal of Medical Microbiology*, **63**(7), 936–944. <https://doi.org/10.1099/jmm.0.073478-0>
- Couderchet, M. (2003). Benefits and problems of fungicide control of *Botrytis cinerea* in vineyards of Champagne. *Vitis* **42**(4), 165–171. <https://doi.org/10.5073/vitis.2003.42.165-171>
- Crous, P.W., Carnegie, A.J., Wingfield, M.J., Sharma, R., Mughini, G., Noordeloos, M.E., Santini, A., Shouche, Y.S., Bezerra, J.D.P., Dima, B., Guarnaccia, V., Imrefi, I., Jurjević, Ž., Knapp, D.G., Kovács, G.M., Magistà, D., Perrone, G., Rämä, T., Rebriev, Y.A., ... Groenewald, J.Z. (2019). Fungal Planet description sheets: 868–950. *Persoonia - Molecular Phylogeny and Evolution of Fungi*, **42**(1), 291–473. <https://doi.org/10.3767/persoonia.2019.42.11>
- Crous, P.W., & Groenewald, J.Z. (2017). The Genera of Fungi — G 4: *Camarosporium* and *Dothiora*. *IMA Fungus*, **8**(1), 131–152. <https://doi.org/10.5598/imafungus.2017.08.01.10>

- Crous, P.W., Rong, I.H., Wood, A., Lee, S., Glen, H., Botha, W., Slippers, B., de Beer, W.Z., Wingfield, M.J., & Hawksworth, D.L. (2006). How many species of fungi are there at the tip of Africa? *Studies in Mycology*, **55**, 13–33. <https://doi.org/10.3114/sim.55.1.13>
- Crous, P.W., Wingfield, M.J., Burgess, T.I., Hardy, G.E. St. J., Crane, C., Barrett, S., Cano-Lira, J.F., Leroux, J.J., Thangavel, R., Guarro, J., Stchigel, A.M., Martín, M.P., Alfredo, D.S., Barber, P.A., Barreto, R.W., Baseia, I.G., Cano-Canals, J., Cheewangkoon, R., Ferreira, R.J., ... Stephenson, S.L. (2016). Fungal Planet description sheets: 469–557. *Persoonia - Molecular Phylogeny and Evolution of Fungi*, **37**(1), 218–403. <https://doi.org/10.3767/003158516X694499>
- Crous, P.W., Wingfield, M.J., Richardson, D.M., Leroux, J.J., Strasberg, D., Edwards, J., Roets, F., Hubka, V., Taylor, P.W.J., Heykoop, M., Martín, M.P., Moreno, G., Sutton, D.A., Wiederhold, N.P., Barnes, C.W., Carlavilla, J.R., Gené, J., Giraldo, A., Guarnaccia, V., ... Groenewald, J.Z. (2016). Fungal Planet description sheets: 400–468. *Persoonia - Molecular Phylogeny and Evolution of Fungi*, **36**(1), 316–458. <https://doi.org/10.3767/003158516X692185>
- da Silva, L.L., Moreno, H.L.A., Correia, H.L.N., Santana, M.F., & de Queiroz, M.V. (2020). *Colletotrichum*: species complexes, lifestyle, and peculiarities of some sources of genetic variability. *Applied Microbiology and Biotechnology*, **104**:5, 104(5), 1891–1904. <https://doi.org/10.1007/S00253-020-10363-Y>
- De La Cruz, M., Martín, J., González-Menéndez, V., Pérez-Victoria, I., Moreno, C., Tormo, J.R., El Aouad, N., Guarro, J., Vicente, F., Reyes, F., & Bills, G.F. (2012). Chemical and physical modulation of antibiotic activity in *Emericella* species. *Chemistry and Biodiversity*, **9**(6), 1095–1113. <https://doi.org/10.1002/CBDV.201100362>
- Dean, R., Van Kan, J.A.L., Pretorius, Z.A., Hammond-Kosack, K.E., Di Pietro, A., Spanu, P.D., Rudd, J.J., Dickman, M., Kahmann, R., Ellis, J., & Foster, G.D. (2012). The Top 10 fungal pathogens in molecular plant pathology. *Molecular Plant Pathology*, **13**(4), 414–430. <https://doi.org/10.1111/J.1364-3703.2011.00783.X>
- Du, L., King, J.B., & Cichewicz, R.H. (2014). Chlorinated Polyketide Obtained from a *Daldinia* sp. Treated with the Epigenetic Modifier Suberoylanilide Hydroxamic Acid. *Journal of Natural Products*, **77**(11), 2454–2458. <https://doi.org/10.1021/np500522z>
- Elnaggar, M.S., Ebada, S.S., Ashour, M.L., Ebrahim, W., Müller, W.E.G., Mándi, A., Kurtán, T., Singab, A., Lin, W., Liu, Z., & Proksch, P. (2016). Xanthones and sesquiterpene derivatives from a marine-derived fungus *Scopulariopsis* sp. *Tetrahedron*, **72**(19), 2411–2419. <https://doi.org/10.1016/j.tet.2016.03.073>
- Fillinger, S., & Elad Y. (2016). *Botrytis*-the fungus, the pathogen and its management in agricultural systems. Fillinger Sabine & Yigal Elad (eds). Springer International Publishing Switzerland. <https://doi.org/10.1007/978-3-319-23371-0>
- Flores-Bocanegra, L., Al Subeh, Z.Y., Egan, J.M., El-Elimat, T., Raja, H.A., Burdette, J.E., Pearce, C.J., Linington, R.G., & Oberlies, N.H. (2022). Dereplication of Fungal Metabolites by NMR-Based Compound Networking Using MADByTE. *Journal of Natural Products*, **85**(3), 614–624. <https://doi.org/10.1021/acs.jnatprod.1c00841>
- Foster, R., Hartikainen, H., Hall, A., & Bass, D. (2022). Diversity and Phylogeny of Novel Cord-Forming Fungi from Borneo. *Microorganisms*, **10**(2), 239. <https://doi.org/10.3390/microorganisms10020239>

References

- FRAC Code List^{®*} 2022: Fungal control agents sorted by cross-resistance pattern and mode of action (including coding for FRAC Groups on product labels). (2022). <https://www.frac.info/knowledge-database/downloads>
- Frąc, M., Hannula, S.E., Betka, M., & Jędryczka, M. (2018). Fungal Biodiversity and Their Role in Soil Health. *Frontiers in Microbiology*, **9**. <https://doi.org/10.3389/fmicb.2018.00707>
- Gakuubi, M.M., Ching, K.C., Munusamy, M., Wibowo, M., Liang, Z.X., Kanagasundaram, Y., & Ng, S.B. (2022). Enhancing the Discovery of Bioactive Secondary Metabolites From Fungal Endophytes Using Chemical Elicitation and Variation of Fermentation Media. *Frontiers in Microbiology*, **13**. <https://doi.org/10.3389/fmicb.2022.898976>
- Gao, Y., Wang, L., Kalscheuer, R., Liu, Z., & Proksch, P. (2020). Antifungal polyketide derivatives from the endophytic fungus *Aplosporella javeedii*. *Bioorganic & Medicinal Chemistry*, **28**(10), 115456. <https://doi.org/10.1016/j.bmc.2020.115456>
- García, J.B., & Tormo, J.R. (2003). HPLC Studio: A Novel Software Utility to Perform HPLC Chromatogram Comparison for Screening Purposes. *SLAS Discovery*, **8**(3), 305–315. <https://doi.org/10.1177/1087057103008003008>
- Garcia-Rubio, R., de Oliveira, H.C., Rivera, J., & Trevijano-Contador, N. (2020). The Fungal Cell Wall: *Candida*, *Cryptococcus*, and *Aspergillus* Species. *Frontiers in Microbiology*, **10**. <https://doi.org/10.3389/fmicb.2019.02993>
- Glare, T.R., Gwynn, R.L., & Moran-Diez, M.E. (2016). Development of Biopesticides and Future Opportunities. In: T. Glare & M. Mora-Diez (eds.), *Microbial-Based Biopesticides. Methods in Molecular Biology* (Vol. **1477**, pp. 211–221). https://doi.org/10.1007/978-1-4939-6367-6_16
- González-Menéndez, V., Asensio, F., Moreno, C., de Pedro, N., Monteiro, M.C., de la Cruz, M., Vicente, F., Bills, G.F., Reyes, F., Genilloud, O., & Tormo, J.R. (2014). Assessing the effects of adsorptive polymeric resin additions on fungal secondary metabolite chemical diversity. *Mycology*, **5**(3), 179–191. <https://doi.org/10.1080/21501203.2014.942406>
- González-Menéndez, V., Crespo, G., de Pedro, N., Diaz, C., Martín, J., Serrano, R., Mackenzie, T.A., Justicia, C., González-Tejero, M.R., Casares, M., Vicente, F., Reyes, F., Tormo, J.R., & Genilloud, O. (2018). Fungal endophytes from arid areas of Andalusia: high potential sources for antifungal and antitumoral agents. *Scientific Reports*, **8**(1), 9729. <https://doi.org/10.1038/s41598-018-28192-5>
- Gonzalez-Menéndez, V., Martin, J., Siles, J.A., Gonzalez-Tejero, M.R., Reyes, F., Platas, G., Tormo, J.R., & Genilloud, O. (2017). Biodiversity and chemotaxonomy of *Preussia* isolates from the Iberian Peninsula. *Mycological Progress*, **16**(7), 713–728. <https://doi.org/10.1007/s11557-017-1305-1>
- González-Menéndez, V., Pérez-Bonilla, M., Pérez-Victoria, I., Martín, J., Muñoz, F., Reyes, F., Tormo, J., & Genilloud, O. (2016). Multicomponent Analysis of the Differential Induction of Secondary Metabolite Profiles in Fungal Endophytes. *Molecules*, **21**(2), 234. <https://doi.org/10.3390/molecules21020234>
- Gouda, S., Das, G., Sen, S.K., Shin, H.S., & Patra, J.K. (2016). Endophytes: A Treasure House of Bioactive Compounds of Medicinal Importance. *Frontiers in Microbiology*, **7**. <https://doi.org/10.3389/fmicb.2016.01538>
- Grossman, J.J., Cavender-Bares, J., & Hobbie, S.E. (2020). Functional diversity of leaf litter mixtures slows decomposition of labile but not recalcitrant carbon over two years. *Ecological Monographs*, **90**(3). <https://doi.org/10.1002/ecm.1407>

- Gubiani, J.R., Wijeratne, E.M.K., Shi, T., Araujo, A.R., Arnold, A.E., Chapman, E., & Gunatilaka, A.A.L. (2017). An epigenetic modifier induces production of (10' S)-verruculide B, an inhibitor of protein tyrosine phosphatases by *Phoma* sp. nov. LG0217, a fungal endophyte of *Parkinsonia microphylla*. *Bioorganic & Medicinal Chemistry*, **25**(6), 1860–1866. <https://doi.org/10.1016/j.bmc.2017.01.048>
- Guo, L., Xi, B., & Lu, L. (2024). Strategies to enhance production of metabolites in microbial co-culture systems. *Bioresource Technology*, **406**, 131049. <https://doi.org/10.1016/j.biortech.2024.131049>
- Gupta, S., Kulkarni, M.G., White, J.F., & Van Staden, J. (2020). Epigenetic-based developments in the field of plant endophytic fungi. *South African Journal of Botany*, **134**, 394–400. <https://doi.org/10.1016/j.sajb.2020.07.019>
- Hautbergue, T., Jamin, E.L., Debrauwer, L., Puel, O., & Oswald, I.P. (2018). From genomics to metabolomics, moving toward an integrated strategy for the discovery of fungal secondary metabolites. *Natural Product Reports*, **35**(2), 147–173. <https://doi.org/10.1039/C7NP00032D>
- Hemphill, C.F.P., Sureechatchaiyan, P., Kassack, M.U., Orfali, R.S., Lin, W., Daletos, G., & Proksch, P. (2017). OSMAC approach leads to new fusarielin metabolites from *Fusarium tricinctum*. *The Journal of Antibiotics*, **70**(6), 726–732. <https://doi.org/10.1038/ja.2017.21>
- Henrikson, J.C., Hoover, A.R., Joyner, P.M., & Cichewicz, R.H. (2009). A chemical epigenetics approach for engineering the *in situ* biosynthesis of a cryptic natural product from *Aspergillus niger*. *Organic & Biomolecular Chemistry*, **7**(3), 435–438. <https://doi.org/10.1039/B819208A>
- Huang, C.B., George, B., & Ebersole, J.L. (2010). Antimicrobial activity of n-6, n-7 and n-9 fatty acids and their esters for oral microorganisms. *Archives of Oral Biology*, **55**(8), 555–560. <https://doi.org/10.1016/j.archoralbio.2010.05.009>
- Huang, R.H., Gou, J.Y., Zhao, D.L., Wang, D., Liu, J., Ma, G.Y., Li, Y.Q., & Zhang, C.S. (2018). Phytotoxicity and anti-phytopathogenic activities of marine-derived fungi and their secondary metabolites. *RSC Advances*, **8**(66), 37573–37580. <https://doi.org/10.1039/C8RA08047J>
- Izquierdo-García, L.F., González-Almario, A., Cotes, A.M., & Moreno-Velandia, C.A. (2020). *Trichoderma virens* Gl006 and *Bacillus velezensis* Bs006: a compatible interaction controlling *Fusarium* wilt of cape gooseberry. *Scientific Reports*, **10**(1), 6857. <https://doi.org/10.1038/s41598-020-63689-y>
- Jayawardena, R.S., Hyde, K.D., de Farias, A.R.G., Bhunjun, C.S., Fernandez, H.S., Manamgoda, D.S., Udayanga, D., Herath, I.S., Thambugala, K.M., Manawasinghe, I.S., Gajanayake, A.J., Samarakoon, B.C., Bundhun, D., Gomdola, D., Huanraluek, N., Sun, Y., Tang, X., Promputtha, I., & Thines, M. (2021). What is a species in fungal plant pathogens? *Fungal Diversity*, **109**(1), 239–266. <https://doi.org/10.1007/s13225-021-00484-8>
- Jiménez, E., Dorta, F., Medina, C., Ramírez, A., Ramírez, I., & Peña-Cortés, H. (2011). Anti-Phytopathogenic Activities of Macro-Algae Extracts. *Marine Drugs*, **9**(5), 739–756. <https://doi.org/10.3390/md9050739>
- Jing, F., Yang, Z., Hai-Feng, L., Yong-Hao, Y., & Jian-Hua, G. (2011). Antifungal metabolites from *Phomopsis* sp. By254, an endophytic fungus in *Gossypium hirsutum*. *African Journal of Microbiology Research*, **5**(10), 1231–1236. <https://doi.org/10.5897/AJMR11.272>
- Kang, D. (2011). Chemotaxonomy of *Trichoderma* spp. Using Mass Spectrometry-Based. *Journal of Microbiology and Biotechnology*, **21**(1), 5–13. <https://doi.org/10.4014/jmb.1008.08018>
- Katz, L., & Baltz, R.H. (2016). Natural product discovery: past, present, and future. *Journal of Industrial Microbiology and Biotechnology*, **43**(2–3), 155–176. <https://doi.org/10.1007/s10295-015-1723-5>

References

- Keller, N.P., Turner, G., & Bennett, J.W. (2005). Fungal secondary metabolism — from biochemistry to genomics. *Nature Reviews Microbiology*, **3**(12), 937–947. <https://doi.org/10.1038/nrmicro1286>
- Khan, M., Salman, M., Ahmad Jan, S., & Khan Shinwari, Z. (2021). Biological control of fungal phytopathogens: A comprehensive review based on *Bacillus* species. *MOJ Biology and Medicine*, **6**(2), 90–92. <https://doi.org/10.15406/mojbm.2021.06.00137>
- Knapp, D.G., & Kovács, G.M. (2016). Interspecific metabolic diversity of root-colonizing endophytic fungi revealed by enzyme activity tests. *FEMS Microbiology Ecology*, **92**(12), fiw190. <https://doi.org/10.1093/femsec/fiw190>
- Knowles, S.L., Raja, H.A., Roberts, C.D., & Oberlies, N.H. (2022). Fungal–fungal co-culture: a primer for generating chemical diversity. *Natural Product Reports*, **39**(8), 1557–1573. <https://doi.org/10.1039/D1NP00070E>
- Kohli, M.M., Mehta, Y.R., Guzman, E., De Viedma, L., & Cubilla, L.E. (2011). Pyricularia blast-a threat to wheat cultivation. *Czech Journal of Genetics and Plant Breeding*, **47**, 2011 (Special Issue): S130–S134. DOI: 10.17221/3267-CJGPB
- Kusumah, D., Wakui, M., Murakami, M., Xie, X., Yukihiro, K., & Maeda, I. (2020). Linoleic acid, α -linolenic acid, and monolinolenins as antibacterial substances in the heat-processed soybean fermented with *Rhizopus oligosporus*. *Bioscience, Biotechnology, and Biochemistry*, **84**(6), 1285–1290. <https://doi.org/10.1080/09168451.2020.1731299>
- Lalošević, M., Jevtić, R., Župunski, V., Maširević, S., & Orbović, B. (2021). Virulence Structure of the Wheat Powdery Mildew Population in Serbia. *Agronomy* **2022**, **Vol. 12**, Page 45, 12(1), 45. <https://doi.org/10.3390/AGRONOMY12010045>
- Lawrence, G.J., Dodds, P.N., & Ellis, J.G. (2007). Rust of flax and linseed caused by *Melampsora lini*. *Molecular Plant Pathology*, **8**(4), 349–364. <https://doi.org/10.1111/J.1364-3703.2007.00405.X>
- Lee, S., Mel'nik, V., Taylor, J.E., & Crous, P.W. (2004). Diversity of saprobic hyphomycetes on *Proteaceae* and *Restionaceae* from South Africa. *Fungal Diversity*, **17**, 91–114.
- Leiva-Mora, M., Capdesuñer, Y., Villalobos-Olivera, A., Moya-Jiménez, R., Saa, L. R., & Martínez-Montero, M. E. (2024). Uncovering the Mechanisms: The Role of Biotrophic Fungi in Activating or Suppressing Plant Defense Responses. *Journal of Fungi*, **10**(9), 635. <https://doi.org/10.3390/jof10090635>
- Leng, L., Li, W., Chen, J., Leng, S., Chen, J., Wei, L., Peng, H., Li, J., Zhou, W., Huang, H. (2021). Co-culture of fungi-microalgae consortium for wastewater treatment: A review. *Bioresource Technology*, **330**, 125008. <https://doi.org/10.1016/j.biortech.2021.125008>
- Li, G., Jian, T., Liu, X., Lv, Q., Zhang, G., & Ling, J. (2022). Application of Metabolomics in Fungal Research. *Molecules*, **27**(21), 7365. <https://doi.org/10.3390/molecules27217365>
- Li, Y., Sun, S., Guo, Q., Ma, L., Shi, C., Su, L., & Li, H. (2008). *In vitro* interaction between azoles and cyclosporin A against clinical isolates of *Candida albicans* determined by the checkerboard method and time-kill curves. *Journal of Antimicrobial Chemotherapy*, **61**(3), 577–585. <https://doi.org/10.1093/jac/dkm493>
- Liu, K., Liu, W., Huang, X., Liu, Y., Cui, X., Zhang, Z., Li, B., El-Mogy, M.M., Tian, S., & Chen, T. (2023). Identification of virulence-related proteins during *Botrytis cinerea* – fruit interaction at early phase. *Postharvest Biology and Technology*, **204**, 112443. <https://doi.org/10.1016/j.postharvbio.2023.112443>

- Lu, H., Zou, W. X., Meng, J.C., Hu, J., & Tan, R.X. (2000). New bioactive metabolites produced by *Colletotrichum* sp., an endophytic fungus in *Artemisia annua*. *Plant Science*, **151**(1), 67–73. [https://doi.org/10.1016/S0168-9452\(99\)00199-5](https://doi.org/10.1016/S0168-9452(99)00199-5)
- Mamathaba, M.P., Yessoufou, K., & Moteetee, A. (2022). What Does It Take to Further Our Knowledge of Plant Diversity in the Megadiverse South Africa? *Diversity*, **14**(9), 748. <https://doi.org/10.3390/d14090748>
- Martínez, G., González-Menéndez, V., Martín, J., Reyes, F., Genilloud, O., & Tormo, J.R. (2017). MASS Studio: A Novel Software Utility to Simplify LC-MS Analyses of Large Sets of Samples for Metabolomics. In: Rojas, I., Ortuño, F. (eds) Bioinformatics and Biomedical Engineering. IWBBIO 2017. *Lecture Notes in Computer Science*, vol **10208**. Springer, Cham. https://doi.org/10.1007/978-3-319-56148-6_20
- Mel'nik, V., Lee, S., Groenewald, J.Z. (Ewald), & Crous, P.W. (2004). New hyphomycetes from *Restionaceae* in fynbos: *Parasarcopodium ceratocaryi* gen. et sp. nov., and *Rhexodenticula elegiae* sp. nov. *Mycological Progress*, **3**(1), 19–28. <https://doi.org/10.1007/s11557-006-0072-1>
- Méndez-Morán, L., Reynaga-Peña, C.G., Springer, P.S., & Ruiz-Herrera, J. (2005). *Ustilago maydis* Infection of the Nonnatural Host *Arabidopsis thaliana*. *Mycology*, **95**(5), 480–488.
- Miethke, M., Pieroni, M., Weber, T., Brönstrup, M., Hammann, P., Halby, L., Arimondo, P.B., Glaser, P., Aigle, B., Bode, H.B., Moreira, R., Li, Y., Luzhetskyy, A., Medema, M.H., Pernodet, J.L., Stadler, M., Tormo, J.R., Genilloud, O., Truman, A.W., ... Müller, R. (2021). Towards the sustainable discovery and development of new antibiotics. *Nature Reviews Chemistry*, **5**(10), 726–749. <https://doi.org/10.1038/s41570-021-00313-1>
- Miura, D., Tanaka, H., & Wariishi, H. (2004). Metabolomic differential display analysis of the white-rot basidiomycete *Phanerochaete chrysosporium* grown under air and 100% oxygen. *FEMS Microbiology Letters*, **234**(1), 111–116. <https://doi.org/10.1111/j.1574-6968.2004.tb09521.x>
- Monaghan, R.L., Polishook, J.D., Pecore, V.J., Bills, G.F., Nallin-Omstead, M., & Streicher, S.L. (1995). Discovery of novel secondary metabolites from fungi—is it really a random walk through a random forest? *Canadian Journal of Botany*, **73**(S1), 925–931. <https://doi.org/10.1139/b95-340>
- Monteiro, M.C., De La Cruz, M., Cantizani, J., Moreno, C., Tormo, J.R., Mellado, E., De Lucas, J.R., Asensio, F., Valiente, V., Brakhage, A.A., Latgé, J.P., Genilloud, O., & Vicente, F. (2012). A new approach to drug discovery: high-throughput screening of microbial natural extracts against *Aspergillus fumigatus* using resazurin. *Journal of Biomolecular Screening*, **17**(4), 542–549. <https://doi.org/10.1177/1087057111433459>
- Moody, S.C. (2014). Microbial Co-Culture: Harnessing Intermicrobial Signaling for the Production of Novel Antimicrobials. *Future Microbiology*, **9**(5), 575–578. <https://doi.org/10.2217/fmb.14.25>
- Müllbacher, A., & Eichner, R.D. (1984). Immunosuppression in vitro by a metabolite of a human pathogenic fungus. *Proceedings of the National Academy of Sciences*, **81**(12), 3835–3837. <https://doi.org/10.1073/pnas.81.12.3835>
- Nguyen, L.T., Schmidt, H.A., von Haeseler, A., & Minh, B.Q. (2015). IQ-TREE: A Fast and Effective Stochastic Algorithm for Estimating Maximum-Likelihood Phylogenies. *Molecular Biology and Evolution*, **32**(1), 268–274. <https://doi.org/10.1093/molbev/msu300>

References

- Niego, A.G.T., Lambert, C., Mortimer, P., Thongklang, N., Rapior, S., Grosse, M., Schrey, H., Charria-Girón, E., Walker, A., Hyde, K.D., & Stadler, M. (2023). The contribution of fungi to the global economy. *Fungal Diversity*, **121**(1), 95–137. <https://doi.org/10.1007/s13225-023-00520-9>
- Nonaka, K., Abe, T., Iwatsuki, M., Mori, M., Yamamoto, T., Shiomi, K., Ômura, S., & Masuma, R. (2011). Enhancement of metabolites productivity of *Penicillium pinophilum* FKI-5653, by co-culture with *Trichoderma harzianum* FKI-5655. *The Journal of Antibiotics*, **64**(12), 769–774. <https://doi.org/10.1038/ja.2011.91>
- Oh, D.C., Kauffman, C.A., Jensen, P.R., & Fenical, W. (2007). Induced Production of Emericellamides A and B from the Marine-Derived Fungus *Emericella* sp. in Competing Co-culture. *Journal of Natural Products*, **70**(4), 515–520. <https://doi.org/10.1021/np060381f>
- Omura S. (1976). The Antibiotic Cerulenin, a Novel Tool for Biochemistry as an Inhibitor of Fatty Acid Synthesis. *American Society for Microbiology*, **40**(3).
- Pandit, M.A., Kumar, J., Gulati, S., Bhandari, N., Mehta, P., Katyal, R., Rawat, C.D., Mishra, V., & Kaur, J. (2022). Major Biological Control Strategies for Plant Pathogens. *Pathogens*, **11**(2), 273. <https://doi.org/10.3390/pathogens11020273>
- Paranagama, P.A., Wijeratne, E.M.K., & Gunatilaka, A.A.L. (2007). Uncovering Biosynthetic Potential of Plant-Associated Fungi: Effect of Culture Conditions on Metabolite Production by *Paraphaeosphaeria quadrisepata* and *Chaetomium chiversii*. *Journal of Natural Products*, **70**(12), 1939–1945. <https://doi.org/10.1021/np070504b>
- Park, J.H., Choi, G.J., Lee, S.W., Lee, H.B., Kim, K.M., Jung, H.S., Jang, K.S., Cho, K.Y., Kim, J.C. (2005). Griseofulvin from *Xylaria* sp. Strain F0010, an Endophytic Fungus of *Abies holophylla* and its Antifungal Activity Against Plant Pathogenic Fungi. *Journal of Microbiology and Biotechnology*, **15**, 1, 112–117.
- Pathogens, precipitation and produce prices. (2021). *Nature Climate Change*, **11**(8), 635–635. <https://doi.org/10.1038/s41558-021-01124-4>
- Peláez, F., Cabello, A., Platas, G., Díez, M.T., del Val, A.G., Basilio, A., Martán, I., Vicente, F., Bills, G.F., Giacobbe, R.A., Schwartz, R.E., Onishi, J.C., Meinz, M.S., Abruzzo, G.K., Flattery, A.M., Kong, L., & Kurtz, M.B. (2000). The Discovery of Enfumafungin, a Novel Antifungal Compound Produced by an Endophytic *Hormonema* Species Biological Activity and Taxonomy of the Producing Organisms. *Systematic and Applied Microbiology*, **23**(3), 333–343. [https://doi.org/10.1016/S0723-2020\(00\)80062-4](https://doi.org/10.1016/S0723-2020(00)80062-4)
- Pelloux-Prayer, A.L., Priem B., Joseleau J.P. (1998). Kinetic evaluation of conidial germination of *Botrytis cinerea* by a spectrofluorometric method. *Mycological Research*, **102**, Issue 3, Pages 320–322. <https://doi.org/10.1017/S095375629700511>
- Pérez-Victoria, I. (2024). Natural Products Dereplication: Databases and Analytical Methods. In: Kinghorn, A.D., Falk, H., Gibbons, S., Asakawa, Y., Liu, J.K., Dirsch, V.M. (eds) Progress in the Chemistry of Organic Natural Products 124. *Progress in the Chemistry of Organic Natural Products*, vol **124**. Springer, Cham. https://doi.org/10.1007/978-3-031-59567-7_1
- Pérez-Victoria, I., Martín, J., & Reyes, F. (2016). Combined LC/UV/MS and NMR Strategies for the Dereplication of Marine Natural Products. *Planta Medica*, **82**(09/10), 857–871. <https://doi.org/10.1055/s-0042-101763>

- Goldblatt, P., & Manning, J. (2000). Cape plants: a conspectus of the Cape flora of South Africa. National Botanical Institute, Ed.; *Strelitzia*, **Vol. 9**.
- Petersen, L.A., Hughes, D.L., Hughes, R., DiMichele, L., Salmon, P., & Connors, N. (2001). Effects of amino acid and trace element supplementation on pneumocandin production by *Glarea lozoyensis*: impact on titer, analogue levels, and the identification of new analogues of pneumocandin B0. *Journal of Industrial Microbiology and Biotechnology*, **26**(4), 216–221. <https://doi.org/10.1038/sj.jim.7000115>
- Pillay, L.C., Nekati, L., Makhwitine, P.J., & Ndlovu, S.I. (2022). Epigenetic Activation of Silent Biosynthetic Gene Clusters in Endophytic Fungi Using Small Molecular Modifiers. *Frontiers in Microbiology*, **13**. <https://doi.org/10.3389/fmicb.2022.815008>
- Porquier, A., Moraga, J., Morgant, G., Dalmais, B., Simon, A., Sghyer, H., Collado, I.G., & Viaud, M. (2019). Botcinic acid biosynthesis in *Botrytis cinerea* relies on a subtelomeric gene cluster surrounded by relics of transposons and is regulated by the Zn2Cys6 transcription factor BcBoa13. *Current Genetics*, **65**(4), 965–980. <https://doi.org/10.1007/s00294-019-00952-4>
- Prakash, O., Kumar, R., & Parkash, V. (2008). Synthesis and antifungal activity of some new 3-hydroxy-2-(1-phenyl-3-aryl-4-pyrazolyl) chromones. *European Journal of Medicinal Chemistry*, **43**(2), 435–440. <https://doi.org/10.1016/j.ejmech.2007.04.004>
- Rampersad, S.N. (2011). A rapid colorimetric microtiter bioassay to evaluate fungicide sensitivity among *Verticillium dahliae* isolates. *Plant Disease*, **95**(3), 248–255. <https://doi.org/10.1094/PDIS-10-10-0725>
- Reyes, F., Bills, G.F., & Durán-Patrón, R. (2022). Editorial: Strategies for the Discovery of Fungal Natural Products. *Frontiers in Microbiology*, **13**. <https://doi.org/10.3389/fmicb.2022.897756>
- Riedling, O., Walker, A.S., & Rokas, A. (2024). Predicting fungal secondary metabolite activity from biosynthetic gene cluster data using machine learning. *Microbiology Spectrum*, **12**(2). <https://doi.org/10.1128/spectrum.03400-23>
- Rightsel, W.A., Schneider, H.G., Sloan, B.J., Graf, P.R., Miller, F.A., Bartz, Q.R., Ehrlich, J., & Dixon, G.J. (1964). Antiviral Activity of Gliotoxin and Gliotoxin Acetate. *Nature*, **204**(4965), 1333–1334. <https://doi.org/10.1038/2041333b0>
- Riseh, R.S., Hassanisaadi, M., Vatankhah, M., Babaki, S.A., & Barka, E.A. (2022). Chitosan as a potential natural compound to manage plant diseases. *International Journal of Biological Macromolecules*, **220**, 998–1009. <https://doi.org/10.1016/j.ijbiomac.2022.08.109>
- Rokas, A., Mead, M.E., Steenwyk, J.L., Raja, H.A., Oberlies, N.H. (2022) Biosynthetic gene clusters and the evolution of fungal chemodiversity. *Natural Products Reports*, **37**(7), 868–878. doi: 10.1039/c9np00045c
- Robbins, N., Spitzer, M., Wang, W., Waglechner, N., Patel, D.J., O'Brien, J.S., Ejim, L., Ejim, O., Tyers, M., & Wright, G.D. (2016). Discovery of Ibomycin, a Complex Macrolactone that Exerts Antifungal Activity by Impeding Endocytic Trafficking and Membrane Function. *Cell Chemical Biology*, **23**(11), 1383–1394. <https://doi.org/10.1016/j.chembiol.2016.08.015>
- Robey, M.T., Caesar, L.K., Drott, M.T., Keller, N.P., & Kelleher, N.L. (2021). An interpreted atlas of biosynthetic gene clusters from 1,000 fungal genomes. *Proceedings of the National Academy of Sciences*, **118**(19). <https://doi.org/10.1073/pnas.2020230118>

References

- Rodrigo, S., García-Latorre, C., & Santamaria, O. (2021). Metabolites Produced by Fungi against Fungal Phytopathogens: Review, Implementation and Perspectives. *Plants*, **11**(1), 81. <https://doi.org/10.3390/plants11010081>
- Tormo, J.R., García, J. B., DeAntonio, M., Feliz, J., Mira, A., Díez, M. T., Hernández, P., & Peláez, F. (2003). A method for the selection of production media for actinomycete strains based on their metabolite HPLC profiles. *Journal of Industrial Microbiology and Biotechnology*, **30**(10), 582–588. <https://doi.org/10.1007/s10295-003-0084-7>
- Santra, H.K., & Banerjee, D. (2020). Natural Products as Fungicide and Their Role in Crop Protection. In Natural Bioactive Products in Sustainable Agriculture. In: Singh, J., Yadav, A. (eds) *Natural Bioactive Products in Sustainable Agriculture*. Springer, Singapore. https://doi.org/10.1007/978-981-15-3024-1_9
- Savary, S., Willocquet, L., Pethybridge, S.J., Esker, P., McRoberts, N., & Nelson, A. (2019). The global burden of pathogens and pests on major food crops. *Nature Ecology & Evolution*, **3**(3), 430–439. <https://doi.org/10.1038/s41559-018-0793-y>
- Scherlach, K., & Hertweck, C. (2006). Discovery of aspoquinolones A–D, prenylated quinoline-2-one alkaloids from *Aspergillus nidulans*, motivated by genome mining. *Organic & Biomolecular Chemistry*, **4**(18), 3517–3520. <https://doi.org/10.1039/B607011F>
- Scherlach, K., & Hertweck, C. (2009a). Triggering cryptic natural product biosynthesis in microorganisms. *Organic & Biomolecular Chemistry*, **7**(9), 1753. <https://doi.org/10.1039/b821578b>
- Schneider, T., Keiblinger, K.M., Schmid, E., Sterflinger-Gleixner, K., Ellersdorfer, G., Roschitzki, B., Richter, A., Eberl, L., Zechmeister-Boltenstern, S., & Riedel, K. (2012). Who is who in litter decomposition? Metaproteomics reveals major microbial players and their biogeochemical functions. *The ISME Journal*, **6**(9), 1749–1762. <https://doi.org/10.1038/ismej.2012.11>
- Schulz, B., Haas, C., Junker, N., & M. Schobert. (2015). Fungal Endophytes Are Involved in Multiple Balanced Antagonisms. *Current Science*, **109**(1), 39–45.
- Selegato, D.M., & Castro-Gamboa, I. (2023). Enhancing chemical and biological diversity by co-cultivation. *Frontiers in Microbiology*, **14**. <https://doi.org/10.3389/fmicb.2023.1117559>
- Sharma, I. (2021). Phytopathogenic fungi and their biocontrol applications. In Fungi Bio-Prospects in Sustainable Agriculture, Environment and Nano-Technology (pp. 155–188). Elsevier. <https://doi.org/10.1016/B978-0-12-821394-0.00007-X>
- Shwab, E.K., Bok, J.W., Tribus, M., Galehr, J., Graessle, S., & Keller, N.P. (2007). Histone Deacetylase Activity Regulates Chemical Diversity in *Aspergillus*. *Eukaryotic Cell*, **6**(9), 1656–1664. <https://doi.org/10.1128/EC.00186-07>
- Siless, G.E., Gallardo, G.L., Rodriguez, M.A., Rincón, Y.A., Godeas, A.M., & Cabrera, G.M. (2018). Metabolites from the Dark Septate Endophyte *Drechslera* sp. Evaluation by LC/MS and Principal Component Analysis of Culture Extracts with Histone Deacetylase Inhibitors. *Chemistry & Biodiversity*, **15**(8). <https://doi.org/10.1002/cbdv.201800133>
- Singh, S.B., Young, K., & Miesel, L. (2011). Screening strategies for discovery of antibacterial natural products. *Expert Review of Anti-Infective Therapy*, **9**(8), 589–613. <https://doi.org/10.1586/eri.11.81>
- Soliman, S.S. M., & Raizada, M.N. (2013). Interactions between Co-Habiting fungi Elicit Synthesis of Taxol from an Endophytic Fungus in Host Taxus Plants. *Frontiers in Microbiology*, **4**. <https://doi.org/10.3389/fmicb.2013.00003>

- Song, Z., Sun, Y.J., Xu, S., Li, G., Yuan, C., & Zhou, K. (2023). Secondary metabolites from the Endophytic fungi *Fusarium decemcellulare* F25 and their antifungal activities. *Frontiers in Microbiology*, **14**. <https://doi.org/10.3389/fmicb.2023.1127971>
- Späth, G., & Loiseleur, O. (2024). Chemical case studies from natural products of recent interest in the crop protection industry. *Natural Product Reports*, **41**(12), 1915–1938. <https://doi.org/10.1039/D4NP00035H>
- Staats, M., & van Kan, J.A.L. (2012). Genome Update of *Botrytis cinerea* Strains B05.10 and T4. *Eukaryotic Cell*, **11**(11), 1413–1414. <https://doi.org/10.1128/EC.00164-12>
- Stillwell, M.A., Magasi, L.P., & Strunz, G.M. (1974). Production, isolation, and antimicrobial activity of hyalodendrin, a new antibiotic produced by a species of *Hyalodendron*. *Canadian Journal of Microbiology*, **20**(5), 759–764. <https://doi.org/10.1139/m74-116>
- Strunz, G.M., Kakushima, M., Stillwell, M.A., & Heissner, C.J. (1973). Hyalodendrin: a new fungitoxic epidithiodioxopiperazine produced by a *Hyalodendron* species. *Journal of the Chemical Society, Perkin Transactions 1*, 2600. <https://doi.org/10.1039/p19730002600>
- Sun, J., Awakawa, T., Noguchi, H., & Abe, I. (2012). Induced production of mycotoxins in an endophytic fungus from the medicinal plant *Datura stramonium* L. *Bioorganic & Medicinal Chemistry Letters*, **22**(20), 6397–6400. <https://doi.org/10.1016/j.bmcl.2012.08.063>
- Sun, Y.Z., Kurtán, T., Mándi, A., Tang, H., Chou, Y., Soong, K., Su, L., Sun, P., Zhuang, C.L., & Zhang, W. (2017). Immunomodulatory Polyketides from a Phoma-like Fungus Isolated from a Soft Coral. *Journal of Natural Products*, **80**(11), 2930–2940. <https://doi.org/10.1021/acs.jnatprod.7b00463>
- Tang, J.W., Wang, W.G., Li, A., Yan, B.C., Chen, R., Li, X.N., Du, X., Sun, H.D., & Pu, J.X. (2017). Polyketides from the endophytic fungus *Phomopsis* sp. sh917 by using the one strain/many compounds strategy. *Tetrahedron*, **73**(26), 3577–3584. <https://doi.org/10.1016/j.tet.2017.02.019>
- Taylor, J.E., Lee, S., & Crous, P.W. (2001). Biodiversity in the Cape Floral Kingdom: fungi occurring on *Proteaceae*. *Mycological Research*, **105**(12), 1480–1484. <https://doi.org/10.1017/S0953756201004944>
- Tedersoo, L., Bahram, M., Põlme, S., Kõljalg, U., Yorou, N. S., Wijesundera, R., Ruiz, L.V., Vasco-Palacios, A.M., Thu, P.Q., Suija, A., Smith, M.E., Sharp, C., Saluveer, E., Saitta, A., Rosas, M., Riit, T., Ratkowsky, D., Pritsch, K., Põldmaa, K., ... Abarenkov, K. (2014). Global diversity and geography of soil fungi. *Science*, **346**(6213). <https://doi.org/10.1126/science.1256688>
- Thambugala, K.M., Daranagama, D.A., Phillips, A.J.L., Kannangara, S.D., Promputtha, I. (2020). Fungi vs. Fungi in Biocontrol: An Overview of Fungal Antagonists Applied Against Fungal Plant Pathogens. *Frontiers in Cell Infection Microbiology*, **30**(10), 604923. doi: 10.3389/fcimb.2020.604923
- Toghueo, R.M.K., Sahal, D., & Boyom, F.F. (2020). Recent advances in inducing endophytic fungal specialized metabolites using small molecule elicitors including epigenetic modifiers. *Phytochemistry*, **174**, 112338. <https://doi.org/10.1016/j.phytochem.2020.112338>
- Tsuda, M., Sasaki, M., Mugishima, T., Komatsu, K., Sone, T., Tanaka, M., Mikami, Y., & Kobayashi, J. (2005). Scalusamides A–C, New Pyrrolidine Alkaloids from the Marine-Derived Fungus *Penicillium citrinum*. *Journal of Natural Products*, **68**(2), 273–276. <https://doi.org/10.1021/np049661q>
- Ul-Hassan, S.R., Strobel, G.A., Booth, E., Knighton, B., Floerchinger, C., & Sears, J. (2012). Modulation of volatile organic compound formation in the Mycodiesel-producing endophyte *Hypoxylon* sp. CI-4. *Microbiology*, **158**(2), 465–473. <https://doi.org/10.1099/mic.0.054643-0>

References

- van Santen, J.A., Poynton, E.F., Iskakova, D., McMan, E., Alsup, T.A., Clark, T.N., Fergusson, C.H., Fewer, D.P., Hughes, A.H., McCadden, C.A., Parra, J., Soldatou, S., Rudolf, J.D., Janssen, E.M.L., Duncan, K.R., & Linington, R.G. (2022). The Natural Products Atlas 2.0: a database of microbially-derived natural products. *Nucleic Acids Research*, **50**(D1), D1317–D1323. <https://doi.org/10.1093/nar/gkab941>
- Vega, B., Liberti, D., Harmon, P.F., & Dewdney, M.M. (2012). A Rapid Resazurin-Based Microtiter Assay to Evaluate QoI Sensitivity for *Alternaria alternata* Isolates and Their Molecular Characterization. *Plant Disease*, **96**(9), 1262–1270. <https://doi.org/10.1094/PDIS-12-11-1037-RE>
- Voříšková, J., & Baldrian, P. (2013). Fungal community on decomposing leaf litter undergoes rapid successional changes. *The ISME Journal*, **7**(3), 477–486. <https://doi.org/10.1038/ismej.2012.116>
- Wang, J., Lin, W., Wray, V., Lai, D., & Proksch, P. (2013). Induced production of depsipeptides by co-culturing *Fusarium tricinctum* and *Fusarium begoniae*. *Tetrahedron Letters*, **54**(20), 2492–2496. <https://doi.org/10.1016/j.tetlet.2013.03.005>
- Wang, Q., Tao, S., Dubé, C., Tury, E., Hao, Y.J., Zhang, S., Zhao, M., Wu, W., & Khanizadeh, S. (2012). Postharvest Changes in the Total Phenolic Content, Antioxidant Capacity and L-Phenylalanine Ammonia-Lyase Activity of Strawberries Inoculated with *Botrytis cinerea*. *Journal of Plant Studies*, **1**(2). <https://doi.org/10.5539/jps.v1n2p11>
- Wang, Y., Wang, G., Wang, L., Xu, X., Xia, J., Huang, X., Wu, Y., & Zhang, C. (2010). Isolation and identification of an endophytic fungus of *Polygonatum cyrtoneura* and its antifungal metabolites. *Wei Sheng Wu Xue Bao = Acta Microbiologica Sinica*, **50**(8), 1036–1043.
- Webb, C., & Manan, M.A. (2017). Design Aspects of Solid State Fermentation as Applied to Microbial Bioprocessing. *Journal of Applied Biotechnology & Bioengineering*, **4**(1). <https://doi.org/10.15406/jabb.2017.04.00094>
- Wei, Q., Bai, J., Yan, D., Bao, X., Li, W., Liu, B., Zhang, D., Qi, X., Yu, D., & Hu, Y. (2021). Genome mining combined metabolic shunting and OSMAC strategy of an endophytic fungus leads to the production of diverse natural products. *Acta Pharmaceutica Sinica B*, **11**(2), 572–587. <https://doi.org/10.1016/j.apsb.2020.07.020>
- Wiemann, P., Willmann, A., Straeten, M., Kleigrew, K., Beyer, M., Humpf, H., & Tudzynski, B. (2009). Biosynthesis of the red pigment bikaverin in *Fusarium fujikuroi*: genes, their function and regulation. *Molecular Microbiology*, **72**(4), 931–946. <https://doi.org/10.1111/j.1365-2958.2009.06695.x>
- Wilson, B.A.P., Thornburg, C.C., Henrich, C.J., Grkovic, T., & O’Keefe, B.R. (2020). Creating and screening natural product libraries. *Natural Product Reports*, **37**(7), 893–918. <https://doi.org/10.1039/C9NP00068B>
- Wolfender, J., Allard, P., Kubo, M., & Queiroz, E.F. (2019). Metabolomics Strategies for the Dereplication of Polyphenols and Other Metabolites in Complex Natural Extracts. In: Heidi Halbwirth, Karl Stich, Véronique Cheynier, Stéphane Quideau (eds.). *Recent Advances in Polyphenol Research* (pp. 183–205). Wiley. <https://doi.org/10.1002/9781119427896.ch7>
- Wu, G., Sun, X., Yu, G., Wang, W., Zhu, T., Gu, Q., & Li, D. (2014). Cladosins A–E, Hybrid Polyketides from a Deep-Sea-Derived Fungus, *Cladosporium sphaerospermum*. *Journal of Natural Products*, **77**(2), 270–275. <https://doi.org/10.1021/np400833x>

- Xu, K., Li, X.Q., Zhao, D.L., & Zhang, P. (2021). Antifungal Secondary Metabolites Produced by the Fungal Endophytes: Chemical Diversity and Potential Use in the Development of Biopesticides. *Frontiers in Microbiology*, **12**. <https://doi.org/10.3389/fmicb.2021.689527>
- Xue, M., Hou, X., Fu, J., Zhang, J., Wang, J., Zhao, Z., Xu, D., Lai, D., & Zhou, L. (2023). Recent Advances in Search of Bioactive Secondary Metabolites from Fungi Triggered by Chemical Epigenetic Modifiers. *Journal of Fungi*, **9**(2), 172. <https://doi.org/10.3390/jof9020172>
- Yang, X.J., Miao, F., Yao, Y., Cao, F.J., Yang, R., Ma, Y.N., Qin, B.F., & Zhou, L. (2012). *In Vitro* Antifungal Activity of Sanguinarine and Chelerythrine Derivatives against Phytopathogenic Fungi. *Molecules*, **17**(11), 13026–13035. <https://doi.org/10.3390/molecules171113026>
- Zabalgoeazcoa, I. (2008). Fungal endophytes and their interaction with plant pathogens: a review. *Spanish Journal of Agricultural Research*, **6**, 138–146. <https://doi.org/10.5424/sjar/200806S1-382>
- Zaker, M. (2016). Natural Plant Products as Eco-friendly Fungicides for Plant Diseases Control- A Review. *The Agriculturists*, **14**(1), 134–141. <https://doi.org/10.3329/agric.v14i1.29111>
- Zhang, S., Fang, H., Yin, C., Wei, C., Hu, J., & Zhang, Y. (2019). Antimicrobial Metabolites Produced by *Penicillium mallochii* CCH01 Isolated From the Gut of *Ectropis oblique*, Cultivated in the Presence of a Histone Deacetylase Inhibitor. *Frontiers in Microbiology*, **10**. <https://doi.org/10.3389/fmicb.2019.02186>
- Zhang, S., Shi, G., Xu, X., Guo, X., Li, S., Li, Z., Wu, Q., & Yin, W.B. (2024). Global Analysis of Natural Products Biosynthetic Diversity Encoded in Fungal Genomes. *Journal of Fungi*, **10**(9), 653. <https://doi.org/10.3390/jof10090653>
- Zhao, M., Yuan, L.Y., Guo, D.L., Ye, Y., Da-Wa, Z.M., Wang, X.L., Ma, F.W., Chen, L., Gu, Y.C., Ding, L.S., & Zhou, Y. (2018). Bioactive halogenated dihydroisocoumarins produced by the endophytic fungus *Lachnum palmae* isolated from *Przewalskia tangutica*. *Phytochemistry*, **148**, 97–103. <https://doi.org/10.1016/j.phytochem.2018.01.018>
- Zhou, Y., Xu, J., Zhu, Y., Duan, Y., & Zhou, M. (2016). Mechanism of Action of the Benzimidazole Fungicide on *Fusarium graminearum*: Interfering with Polymerization of Monomeric Tubulin But Not Polymerized Microtubule. *Phytopathology*, **106**(8), 807–813. <https://doi.org/10.1094/PHYTO-08-15-0186-R>
- Zhu, J.X., Ding, L., & He, S. (2019). Discovery of a new biphenyl derivative by epigenetic manipulation of marine-derived fungus *Aspergillus versicolor*. *Natural Product Research*, **33**(8), 1191–1195. <https://doi.org/10.1080/14786419.2018.1465423>

VII. Annexes

NNEX CHAPTER 1. Co-Culturing of fungal strains against *Botrytis cinerea* as a model for the induction of chemical diversity and therapeutic agents.

Table S1. Results of antifungal activity and cytotoxicity on HepG2 cell line of the co-culture extract library. The antifungal activity against the three phytopathogens and the two human pathogens is indicated as the diameter of the inhibition halo (mm), and the cytotoxicity as percentage of cell growth inhibition (% INH) compared to standards.

Compound ID	Description	LCMS GOLD	<i>C. acutatum</i>	<i>F. proliferatum</i>	<i>M. grisea</i>	<i>C. albicans</i>	<i>A. fumigatus</i>	Hep-G2
			Halo (mm)	Halo (mm)	Halo (mm)	Halo (mm)	Halo (mm)	% INH (24h)
C?-292032-a01-MO001-EC01	Control		0	0	0	0	0	113.91
C?-295211-a02-MO002-EC01	Control		0	0	0	0	0	48.98
CF-086331-a06-MO001-EC01	Axenic	gliotoxin	7.6	0	0	0	0	-96.92
CF-086331-a06-MO002-EC01	Axenic	gliotoxin	5.6	0	0	0	0	-85.12
CBS 102414/CF-086331-a03	Inhibition zone		0	0	6.7	0	0	-17.50
CBS 102414/CF-086331-a03	Inhibited mycelium		0	0	0	0	0	1.18
CF-090071-a05-MO001-EC01	Axenic		0	0	0	0	0	26.49
CF-090071-a05-MO002-EC01	Axenic		0	0	0	0	0	30.02
CBS 102414/CF-090071-a03	Inhibition zone		0	6.6	5.5	0	0	78.28
CBS 102414/CF-090071-a03	Inhibited mycelium		0	6.6	0	0	0	101.28
CF-090072-a04-MO001-EC01	Axenic		0	0	0	0	0	22.96
CF-090072-a04-MO002-EC01	Axenic		0	0	0	0	0	34.36
CBS 102414/CF-090072-a03	Inhibition zone		0	0	6.4	0	0	58.52
CBS 102414/CF-090072-a03	Inhibited mycelium		0	0	0	0	0	75.90
CF-090127-a02-MO002-EC01	Axenic	violaceol I/ II	0	0	0	0	0	2.27
CF-090127-a02-MO003-EC01	Axenic	violaceol I/ II	0	0	0	0	0	11.86
CBS 102414/CF-090127-a03	Inhibition zone		0	0	6.1	0	0	29.92
CBS 102414/CF-090127-a03	Inhibited mycelium		0	0	0	0	0	74.07
CF-090258-a07-MO001-EC01	Axenic		0	0	0	0	0	31.23
CF-090258-a07-MO002-EC01	Axenic		0	0	0	0	0	17.10
CBS 102414/CF-090258-a03	Inhibition zone		0	0	0	0	0	4.61
CBS 102414/CF-090258-a03	Inhibited mycelium		4.9	0	0	0	0	-66.78
CF-090378-a06-MO001-EC01	Axenic		0	0	0	0	0	22.65
CF-090378-a06-MO002-EC01	Axenic		0	0	0	0	0	28.91
CBS 102414/CF-090378-a05	Inhibition zone		0	0	6.9	0	0	90.79
CBS 102414/CF-090378-a05	Inhibited mycelium		0	0	0	0	0	61.79
CF-091927-a05-MO001-EC01	Axenic		0	0	0	0	0	3.56
CF-091927-a05-MO002-EC01	Axenic		0	0	0	0	0	-7.51
CBS 102414/CF-091927-a03	Inhibition zone		0	0	0	0	0	-27.30
CBS 102414/CF-091927-a03	Inhibited mycelium		0	0	6.4	0	0	20.64
CF-092670-a04-MO001-EC01	Axenic		0	0	0	0	0	25.68
CF-092670-a04-MO002-EC01	Axenic		0	0	0	0	0	40.41
CBS 102414/CF-092670-a03	Inhibition zone		0	0	0	0	0	-90.79
CBS 102414/CF-092670-a03	Inhibited mycelium		0	0	6.7	0	0	-95.10
CF-095017-a04-MO001-EC01	Axenic		0	0	0	0	0	25.88
CF-095017-a04-MO002-EC01	Axenic		0	0	0	0	0	19.42

Annexes

CBS 102414/CF-095017-a03	Inhibition zone		0	0	0	0	0	66.75
CBS 102414/CF-095017-a03	Inhibited mycelium		0	0	7.2	0	0	-95.36
CF-096730-a08-MO001-EC01	Axenic		0	0	0	0	0	0.05
CF-096730-a08-MO002-EC01	Axenic		0	0	0	0	0	19.53
CBS 102414/CF-096730-a06	Inhibition zone		0	0	0	0	0	9.01
CBS 102414/CF-096730-a06	Inhibited mycelium		5.6	0	6.3	0	0	-23.07
CF-108442-a04-MO001-EC01	Axenic		0	0	0	0	0	7.11
CF-108442-a04-MO002-EC01	Axenic		0	0	0	0	0	-5.70
CBS 102414/CF-108442-a03	Inhibition zone		6.2	6.9	6.8	0	0	-40.10
CBS 102414/CF-108442-a03	Inhibited mycelium		0	0	5.9	0	0	-42.19
CF-109100-a04-MO001-EC01	Axenic		0	0	0	0	0	15.78
CF-109100-a04-MO002-EC01	Axenic		0	0	0	0	0	23.79
CBS 102414/CF-109100-a03	Inhibition zone		0	0	6.3	0	0	-23.91
CBS 102414/CF-109100-a03	Inhibited mycelium		0	0	0	0	0	-14.63
CF-109684-a10-MO001-EC01	Axenic	gliotoxin	6.5	6.3	6.4	0	0	-99.95
CF-109684-a10-MO002-EC01	Axenic	gliotoxin	5.5	0	0	0	0	-89.96
CBS 102414/CF-109684-a07	Inhibition zone		0	0	6.5	0	0	-47.55
CBS 102414/CF-109684-a07	Inhibited mycelium		0	0	0	0	0	-36.19
CF-110925-a04-MO001-EC01	Axenic		0	0	0	0	0	23.97
CF-110925-a04-MO002-EC01	Axenic		0	0	0	0	0	19.53
CBS 102414/CF-110925-a03	Inhibition zone		0	0	6.3	0	0	44.94
CBS 102414/CF-110925-a03	Inhibited mycelium		0	0	0	0	0	-34.49
CF-111323-a04-MO001-EC01	Axenic	cyclosporin A	0	0	0	0	0	17.81
CF-111323-a04-MO002-EC01	Axenic		0	0	0	0	0	13.37
CBS 102414/CF-111323-a03	Inhibition zone		0	5.7	6.7	0	0	2.77
CBS 102414/CF-111323-a03	Inhibited mycelium		5.4	7.9	7.4	0	0	-94.75
CF-114839-a05-MO001-EC01	Axenic		5.9	0	5	0	0	-92.08
CF-114839-a05-MO002-EC01	Axenic		0	0	6.5	0	0	-78.46
CBS 102414/CF-114839-a03	Inhibition zone		0	0	5.5	0	0	-20.64
CBS 102414/CF-114839-a03	Inhibited mycelium		0	0	0	0	0	-15.68
CF-116114-a05-MO001-EC01	Axenic		0	0	0	0	0	12.97
CF-116114-a05-MO002-EC01	Axenic		0	0	0	0	0	30.93
CBS 102414/CF-116114-a04	Inhibition zone		0	0	0	0	0	29.17
CBS 102414/CF-116114-a04	Inhibited mycelium		0	0	0	0	0	56.56
CF-116317-a04-MO001-EC01	Axenic		6.5	6.3	6.1	0	0	-94.40
CF-116317-a04-MO002-EC01	Axenic		0	0	6.7	0	0	-94.30
CBS 102414/CF-116317-a03	Inhibition zone		0	0	0	0	0	-98.76
CBS 102414/CF-116317-a03	Inhibited mycelium		0	0	7.4	0	0	-99.93
CF-116676-a10-MO001-EC01	Axenic	preussomerins A, B and L	7.1	7.5	6.7	7.7	10.2	-100.05
CF-116676-a10-MO002-EC01	Axenic	preussomerins A, B and L	7.2	7.1	7.5	7.3	10.3	-99.95
CBS 102414/CF-116676-a07	Inhibition zone	palmarumycin C15, preussomerins B and F	6.1	7.5	9.8	0	10.7	-99.54
CBS 102414/CF-116676-a07	Inhibited mycelium	palmarumycin C15, preussomerins B and F	7	7	6.3	0	7.9	-99.67
CF-116728-a04-MO001-EC01	Axenic		0	0	0	0	0	-100.05
CF-116728-a04-MO002-EC01	Axenic		0	0	0	0	0	-90.16
CBS 102414/CF-116728-a03	Inhibition zone		5.6	6.2	8.7	0	0	-99.54
CBS 102414/CF-116728-a03	Inhibited mycelium		6.1	6.6	5.6	0	0	-93.14
CF-116869-a04-MO001-EC01	Axenic		0	0	0	0	0	40.82
CF-116869-a04-MO002-EC01	Axenic		0	0	0	0	0	37.69
CBS 102414/CF-116869-a03	Inhibition zone		0	0	0	0	0	32.29
CBS 102414/CF-116869-a03	Inhibited mycelium		6.4	6.1	6.3	0	0	-29.74
CF-118005-a04-MO001-EC01	Axenic		0	0	8.3	0	0	20.74

CF-118005-a04-MO002-EC01	Axenic		6.5	0	6.8	0	0	23.56
CBS 102414/CF-118005-a03	Inhibition zone		5.9	7.5	0	0	8.9	-97.98
CBS 102414/CF-118005-a03	Inhibited mycelium		7.3	7.9	6.1	0	7.5	-98.24
CF-118101-a05-MO001-EC01	Axenic		0	0	0	0	0	-17.00
CF-118101-a05-MO002-EC01	Axenic		0	0	0	0	0	-12.26
CBS 102414/CF-118101-a04	Inhibition zone		0	0	6.5	0	0	-22.60
CBS 102414/CF-118101-a04	Inhibited mycelium		0	0	0	0	0	-20.25
CF-153629-a03-MO001-EC01	Axenic		0	0	0	0	0	-7.11
CF-153629-a03-MO002-EC01	Axenic		0	0	0	0	0	-1.56
CBS 102414/CF-153629-a02	Inhibition zone		6.3	0	0	0	0	0.92
CBS 102414/CF-153629-a02	Inhibited mycelium		0	0	0	0	0	-49.04
CF-160675-a04-MO001-EC01	Axenic		0	0	0	0	0	9.13
CF-160675-a04-MO002-EC01	Axenic		0	0	0	0	0	29.52
CBS 102414/CF-160675-a03	Inhibition zone		0	0	0	0	0	82.40
CBS 102414/CF-160675-a03	Inhibited mycelium		0	0	10	0	0	17.67
CF-164326-a07-MO001-EC01	Axenic	preussomerins B and L	5.9	7.1	6	0	9.2	-95.41
CF-164326-a07-MO002-EC01	Axenic	preussomerins B and L	0	0	0	0	0	-71.49
CBS 102414/CF-164326-a04	Inhibition zone	preussomerin B	6	0	6.1	0	0	-84.39
CBS 102414/CF-164326-a04	Inhibited mycelium	preussomerin B	0	0	0	0	0	-84.00
CF-175615-a05-MO001-EC01	Axenic	preussomerin L	7.3	7.1	6.4	0	9.7	-98.44
CF-175615-a05-MO002-EC01	Axenic	preussomerins A and L	6.7	7	6.8	0	8.8	-97.83
CBS 102414/CF-175615-a03	Inhibition zone	preussomerins B and F	7.3	7	7	0	9	-98.89
CBS 102414/CF-175615-a03	Inhibited mycelium	preussomerins B and F	6.6	7.8	7.2	0	8	-98.89
CF-175637-a05-MO001-EC01	Axenic	preussomerin L	7.4	7.1	7.2	9.8	10.8	-99.85
CF-175637-a05-MO002-EC01	Axenic	preussomerin L	6.5	7.7	6.5	0	9	-93.59
CBS 102414/CF-175637-a03	Inhibition zone	palmarumycin C15, preussomerins B and F	7.2	8.3	6.5	0	7.7	-49.61
CBS 102414/CF-175637-a03	Inhibited mycelium	palmarumycin C15, preussomerins B and F	7.3	7.5	6.1	0	8.2	-98.01
CF-176883-a05-MO001-EC01	Axenic		0	0	0	0	0	-4.59
CF-176883-a05-MO002-EC01	Axenic		0	0	0	0	0	27.70
CBS 102414/CF-176883-a03	Inhibition zone		7	6.4	5.5	0	0	-80.41
CBS 102414/CF-176883-a03	Inhibited mycelium		7	6.9	7	0	0	-96.03
CF-177133-a05-MO001-EC01	Axenic		0	0	6.6	0	0	17.20
CF-177133-a05-MO002-EC01	Axenic		0	0	0	0	0	6.41
CBS 102414/CF-177133-a03	Inhibition zone		6.1	6.3	6.3	0	0	-96.03
CBS 102414/CF-177133-a03	Inhibited mycelium		6.7	7.3	6	0	0	-97.30
CF-179292-a05-MO001-EC01	Axenic		6.2	0	0	0	0	-0.66
CF-179292-a05-MO002-EC01	Axenic		0	0	0	0	0	9.43
CBS 102414/CF-179292-a02	Inhibition zone		0	0	6	0	0	24.69
CBS 102414/CF-179292-a02	Inhibited mycelium		0	0	0	0	0	-14.11
CF-182855-a07-MO001-EC01	Axenic		0	0	0	0	0	11.65
CF-182855-a07-MO002-EC01	Axenic		0	0	0	0	0	24.57
CBS 102414/CF-182855-a04	Inhibition zone	equisetin	0	0	6.1	0	0	12.70
CBS 102414/CF-182855-a04	Inhibited mycelium	equisetin	0	0	0	0	0	-9.01
CF-183032-a05-MO001-EC01	Axenic	preussomerins A and L	6.4	6.7	6.3	0	7.8	-94.40
CF-183032-a05-MO002-EC01	Axenic	preussomerins A and L	0	6.2	6.7	0	0	-70.18
CBS 102414/CF-183032-a03	Inhibition zone	preussomerins B and F	7.5	6.7	0	0	6	-76.68
CBS 102414/CF-183032-a03	Inhibited mycelium	preussomerin F	6.6	6.9	6.8	0	6.9	-82.82
CF-183212-a07-MO001-EC01	Axenic		0	0	0	0	0	-20.03
CF-183212-a07-MO002-EC01	Axenic		0	0	0	0	0	15.39
CBS 102414/CF-183212-a04	Inhibition zone		6.3	6.6	7.4	6.2	0	-97.71
CBS 102414/CF-183212-a04	Inhibited mycelium		6	6.7	7.1	0	0	-95.23

Annexes

CF-185390-a05-MO001-EC01	Axenic		0	0	0	0	0	-9.13
CF-185390-a05-MO002-EC01	Axenic		0	0	0	0	0	-9.94
CBS 102414/CF-185390-a03	Inhibition zone	verscenoside C	0	0	0	0	0	47.76
CBS 102414/CF-185390-a03	Inhibited mycelium	verscenoside C	0	0	0	0	0	10.01
CF-185391-a05-MO001-EC01	Axenic		0	0	0	0	0	-7.72
CF-185391-a05-MO002-EC01	Axenic		0	0	0	0	0	12.97
CBS 102414/CF-185391-a03	Inhibition zone		6.1	0	6.6	0	0	-92.62
CBS 102414/CF-185391-a03	Inhibited mycelium		5	6.9	7.1	0	0	-91.84
CF-185405-a06-MO001-EC01	Axenic	preussomerin L	6.5	6.9	5.9	0	11.3	-99.04
CF-185405-a06-MO002-EC01	Axenic	preussomerin L	5.8	6.1	6.9	0	8.1	-94.80
CBS 102414/CF-185405-a04	Inhibition zone	preussomerin F	7.1	7.3	7.6	0	10.8	-99.28
CBS 102414/CF-185405-a04	Inhibited mycelium	preussomerins B and F	6.5	7.4	7.8	0	10.1	-99.93
CF-185415-a07-MO001-EC01	Axenic	preussomerins A, B and L	7.1	8.4	8.2	8.8	14.9	-99.75
CF-185415-a07-MO002-EC01	Axenic	preussomerins A, B and L	5.1	7.3	6.7	0	10.3	-98.23
CBS 102414/CF-185415-a05	Inhibition zone	preussomerins B and F	6.5	7.4	6.2	0	8.8	-98.44
CBS 102414/CF-185415-a05	Inhibited mycelium	preussomerins B and F	6.7	7.5	6.2	0	9.6	-95.17
CF-185600-a05-MO001-EC01	Axenic	preussomerin L	0	6.5	6	0	9.2	-93.09
CF-185600-a05-MO002-EC01	Axenic	preussomerin L	0	7	6.9	0	9.2	-90.97
CBS 102414/CF-185600-a03	Inhibition zone		6.5	5.7	6.1	0	0	-67.02
CBS 102414/CF-185600-a03	Inhibited mycelium	preussomerin F	6.7	6.9	6.8	0	8.2	-99.41
CF-185603-a08-MO001-EC01	Axenic	preussomerin L	6.2	7.1	6.4	0	8.4	-96.42
CF-185603-a08-MO002-EC01	Axenic	preussomerin L	0	6.8	6.8	0	5.9	-86.73
CBS 102414/CF-185603-a03	Inhibition zone	preussomerin F	6.8	6.8	7.1	0	7.1	-79.69
CBS 102414/CF-185603-a03	Inhibited mycelium	preussomerin F	7.1	7.4	0	0	8.4	-94.06
CF-185636-a05-MO001-EC01	Axenic	$C_{20}H_{14}O_4 + C_{20}H_{16}O_5$	6.6	6.6	6	0	0	-99.85
CF-185636-a05-MO002-EC01	Axenic	$C_{20}H_{14}O_4 + C_{20}H_{16}O_5$	0	6.1	6.2	0	0	-99.95
CBS 102414/CF-185636-a03	Inhibition zone	$C_{20}H_{14}O_4 + C_{20}H_{16}O_5$	6.8	6.7	6.6	0	0	-98.86
CBS 102414/CF-185636-a03	Inhibited mycelium	$C_{20}H_{14}O_4 + C_{20}H_{16}O_5$	6.5	0	0	0	0	-63.95
CF-185650-a05-MO001-EC01	Axenic	preussomerin L	5.9	6.3	7.2	0	7.8	-82.09
CF-185650-a05-MO002-EC01	Axenic		0	0	0	0	0	-41.32
CBS 102414/CF-185650-a03	Inhibition zone	palmarumycin C15, preussomerin F	7.3	6.6	0	0	11	-95.03
CBS 102414/CF-185650-a03	Inhibited mycelium	preussomerin F	6.9	8	6.6	0	8.4	-93.47
CF-185653-a06-MO001-EC01	Axenic	cercosporamide	0	0	0	0	0	-10.71
CF-185653-a06-MO002-EC01	Axenic	cercosporamide	0	0	0	0	0	17.33
CBS 102414/CF-185653-a03	Inhibition zone		6.4	0	5.7	0	0	-91.20
CBS 102414/CF-185653-a03	Inhibited mycelium		0	0	0	0	0	-54.15
CF-185670-a05-MO001-EC01	Axenic		0	0	0	0	0	4.29
CF-185670-a05-MO002-EC01	Axenic		0	0	0	0	0	13.50
CBS 102414/CF-185670-a03	Inhibition zone		0	0	7.2	0	0	4.96
CBS 102414/CF-185670-a03	Inhibited mycelium		0	0	0	0	0	27.30
CF-187233-a05-MO001-EC01	Axenic		0	0	0	0	0	-15.57
CF-187233-a05-MO002-EC01	Axenic		0	0	0	0	0	12.88
CBS 102414/CF-187233-a03	Inhibition zone		0	0	0	0	0	52.87
CBS 102414/CF-187233-a03	Inhibited mycelium		6.4	6.2	5.3	5.1	0	12.56
CF-187272-a06-MO001-EC01	Axenic	palmarumycin C15, preussomerins A, F and L	5.5	6.6	7.1	7.2	9.2	-99.69
CF-187272-a06-MO002-EC01	Axenic	preussomerin L	6.2	6.3	7	0	8.4	-99.17
CBS 102414/CF-187272-a04	Inhibition zone	palmarumycin C15, preussomerin A	7	7.2	6.4	0	9	-97.59
CBS 102414/CF-187272-a04	Inhibited mycelium	palmarumycin C15, preussomerin F	7.4	7.4	0	0	7.3	-94.32
CF-187525-a05-MO001-EC01	Axenic		0	0	0	0	0	13.09
CF-187525-a05-MO002-EC01	Axenic		0	0	0	0	0	35.64
CBS 102414/CF-187525-a03	Inhibition zone		0	0	0	0	0	19.26

CBS 102414/CF-187525-a03	Inhibited mycelium		0	0	6	0	0	-17.04
CF-187689-a05-MO001-EC01	Axenic		0	0	0	0	0	-99.59
CF-187689-a05-MO002-EC01	Axenic		0	0	0	0	0	-97.72
CBS 102414/CF-187689-a03	Inhibition zone		0	0	6.1	0	0	19.46
CBS 102414/CF-187689-a03	Inhibited mycelium		0	0	0	0	0	-21.95
CF-187925-a05-MO001-EC01	Axenic	palmarumycin C15, preussomerins A, B, F & L	6.2	7.3	6.6	0	6.8	-99.59
CF-187925-a05-MO002-EC01	Axenic	palmarumycin C15, preussomerins A, B & F	0	7	0	0	0	-97.21
CBS 102414/CF-187925-a03	Inhibition zone		0	0	0	0	0	3.79
CBS 102414/CF-187925-a03	Inhibited mycelium	preussomerins B and F	0	0	7.4	0	0	-12.67
CF-189741-a06-MO001-EC01	Axenic	mycorrhizin A	5.2	5.9	5.7	0	7	-99.48
CF-189741-a06-MO002-EC01	Axenic	mycorrhizin A	0	0	0	0	0	-19.09
CBS 102414/CF-189741-a03	Inhibition zone	mycorrhizin A	9.5	8.5	9.3	7.9	9.4	-99.41
CBS 102414/CF-189741-a03	Inhibited mycelium	mycorrhizin A	8.5	7.9	8.3	7.3	8.4	-99.26
CF-190679-a05-MO001-EC01	Axenic		0	0	0	0	0	-5.74
CF-190679-a05-MO002-EC01	Axenic		0	0	0	0	0	14.64
CBS 102414/CF-190679-a03	Inhibition zone		0	6.7	0	0	0	-99.67
CBS 102414/CF-190679-a03	Inhibited mycelium		0	0	7.9	0	0	37.62
CF-191074-a06-MO001-EC01	Axenic	preussomerins B, F and L	6.4	7.6	6.1	0	8.4	-100.00
CF-191074-a06-MO002-EC01	Axenic	preussomerins A, B and L	6.9	6.2	6	0	7.7	-99.90
CBS 102414/CF-191074-a04	Inhibition zone	preussomerins B and F	6.5	7.8	0	0	8.3	-96.41
CBS 102414/CF-191074-a04	Inhibited mycelium	preussomerins B and F	6.4	7.2	6.5	0	6.1	-99.15
CF-191080-a04-MO001-EC01	Axenic	preussomerins A, B and L	6.5	7.9	6.3	0	10.7	-99.69
CF-191080-a04-MO002-EC01	Axenic	preussomerins A, B and L	6.6	7.6	6.7	0	8.3	-99.59
CBS 102414/CF-191080-a03	Inhibition zone	preussomerins B and F	6.8	6.9	0	0	6.6	-98.76
CBS 102414/CF-191080-a03	Inhibited mycelium	preussomerins B and F	0	0	6.7	0	0	-99.93
CF-192432-a06-MO001-EC01	Axenic	preussomerins A and L	6.1	8.3	6.6	0	8.7	-93.17
CF-192432-a06-MO002-EC01	Axenic	preussomerins A, B and L	6.5	6.2	7.1	0	9.5	-96.38
CBS 102414/CF-192432-a04	Inhibition zone	palmarumycin C15	6.2	5.9	5.1	0	7.9	-99.26
CBS 102414/CF-192432-a04	Inhibited mycelium	palmarumycin C15	6	6.5	5.7	0	8	-99.41
CF-192817-a07-MO001-EC01	Axenic		6.7	0	7.1	0	0	-55.61
CF-192817-a07-MO002-EC01	Axenic		0	0	0	0	0	-2.43
CBS 102414/CF-192817-a03	Inhibition zone		0	0	6.8	0	0	75.90
CBS 102414/CF-192817-a03	Inhibited mycelium		0	0	0	0	0	15.55
CF-192842-a05-MO001-EC01	Axenic		0	0	0	0	0	27.06
CF-192842-a05-MO002-EC01	Axenic		5.7	0	0	0	0	29.33
CBS 102414/CF-192842-a03	Inhibition zone		5.8	6.6	6.3	0	0	-95.23
CBS 102414/CF-192842-a03	Inhibited mycelium		0	0	0	0	0	-18.29
CF-195204-a05-MO001-EC01	Axenic		0	0	0	0	0	49.09
CF-195204-a05-MO002-EC01	Axenic		0	0	0	0	0	35.75
CBS 102414/CF-195204-a03	Inhibition zone		0	0	6.8	0	0	29.39
CBS 102414/CF-195204-a03	Inhibited mycelium		0	6.9	6.4	0	0	-67.15
CF-195236-a04-MO001-EC01	Axenic	mycophenolic acid	5.8	5.9	5.4	0	0	-25.71
CF-195236-a04-MO002-EC01	Axenic	mycophenolic acid	0	0	0	0	0	20.43
CBS 102414/CF-195236-a03	Inhibition zone		0	0	5	0	0	-26.67
CBS 102414/CF-195236-a03	Inhibited mycelium		0	0	0	0	0	19.26
CF-197986-a06-MO001-EC01	Axenic	palmarumycin C15, preussomerins A, B, F & L	6.7	7.5	5.8	8.4	9.7	-100.00
CF-197986-a06-MO002-EC01	Axenic	palmarumycin C15, preussomerins A, B and L	6.9	7.9	6.8	7.8	10.1	-99.90
CBS 102414/CF-197986-a05	Inhibition zone	preussomerin B	6.1	7.4	6.9	0	9.9	-99.15
CBS 102414/CF-197986-a05	Inhibited mycelium	preussomerin B	5.8	7.6	0	0	7.9	-99.54
CF-199866-a06-MO001-EC01	Axenic	palmarumycin C15, preussomerins A and L	5.9	6.3	6.4	0	8.9	-95.76
CF-199866-a06-MO002-EC01	Axenic	palmarumycin C15, preussomerins A and L	6.4	6.9	6.7	0	8	-95.55

Annexes

CBS 102414/CF-199866-a04	Inhibition zone	preussomerin F	6.3	6.8	0	0	8.6	-71.06
CBS 102414/CF-199866-a04	Inhibited mycelium	palmarumycin C15, preussomerins B and F	7.4	7.1	6.6	0	8.3	-97.32
CF-200182-a06-MO001-EC01	Axenic		0	0	0	0	0	11.74
CF-200182-a06-MO002-EC01	Axenic		0	0	0	0	0	28.71
CBS 102414/CF-200182-a03	Inhibition zone		0	7.4	5.3	0	0	-46.07
CBS 102414/CF-200182-a03	Inhibited mycelium		6.1	6	7	0	0	-99.56
CF-204001-a05-MO001-EC01	Axenic		0	0	0	0	0	5.85
CF-204001-a05-MO002-EC01	Axenic		0	0	0	0	0	5.23
CBS 102414/CF-204001-a03	Inhibition zone		0	0	0	0	0	60.09
CBS 102414/CF-204001-a03	Inhibited mycelium		0	0	8.2	0	0	36.84
CF-204100-a04-MO001-EC01	Axenic		0	0	0	0	0	3.16
CF-204100-a04-MO002-EC01	Axenic		4.9	0	0	0	0	12.47
CBS 102414/CF-204100-a03	Inhibition zone		0	0	0	0	0	74.07
CBS 102414/CF-204100-a03	Inhibited mycelium		0	7.4	6.8	0	0	-16.85
CF-204209-a04-MO001-EC01	Axenic	trichothecin	7.2	7	6.8	0	7	-28.71
CF-204209-a04-MO002-EC01	Axenic	trichothecin	6.2	7.8	7.2	0	0	-38.75
CBS 102414/CF-204209-a03	Inhibition zone	tricothecin	7.7	6.1	9.6	7.6	8.1	4.96
CBS 102414/CF-204209-a03	Inhibited mycelium	tricothecin	7.7	7.5	7	7.2	6.9	-5.49
CF-208279-a06-MO001-EC01	Axenic		0	0	0	0	0	11.54
CF-208279-a06-MO002-EC01	Axenic		0	0	0	0	0	22.09
CBS 102414/CF-208279-a03	Inhibition zone		0	0	6.5	0	0	-33.71
CBS 102414/CF-208279-a03	Inhibited mycelium		6.4	6.5	6.7	0	0	-99.43
CF-209171-a09-MO001-EC01	Axenic		0	0	0	0	0	2.33
CF-209171-a09-MO002-EC01	Axenic		0	0	0	0	0	13.09
CBS 102414/CF-209171-a07	Inhibition zone		0	0	6	0	0	-31.11
CBS 102414/CF-209171-a07	Inhibited mycelium		5	6.1	6	0	0	-84.00
CF-209253-a05-MO001-EC01	Axenic		0	0	0	0	0	-17.02
CF-209253-a05-MO002-EC01	Axenic		0	0	0	0	0	-5.95
CBS 102414/CF-209253-a03	Inhibition zone		0	0	6.3	0	0	82.81
CBS 102414/CF-209253-a03	Inhibited mycelium		0	0	0	0	0	20.59
CF-209628-a03-MO001-EC01	Axenic		0	0	0	0	0	25.30
CF-209628-a03-MO002-EC01	Axenic		0	0	0	0	0	16.92
CBS 102414/CF-209628-a02	Inhibition zone		0	0	0	0	0	17.96
CBS 102414/CF-209628-a02	Inhibited mycelium		0	0	0	0	0	17.81
CF-210766-a05-MO001-EC01	Axenic		0	0	0	0	0	12.05
CF-210766-a05-MO002-EC01	Axenic		0	0	0	0	0	17.12
CBS 102414/CF-210766-a03	Inhibition zone	verscenoside C	0	6.5	5.4	0	0	-59.83
CBS 102414/CF-210766-a03	Inhibited mycelium	verscenoside C	0	0	0	0	0	-16.25
CF-213368-a04-MO001-EC01	Axenic		0	0	0	0	0	-47.44
CF-213368-a04-MO002-EC01	Axenic		0	0	0	0	0	-38.44
CBS 102414/CF-213368-a03	Inhibition zone		0	0	6.1	0	0	-24.44
CBS 102414/CF-213368-a03	Inhibited mycelium		0	0	0	0	0	-9.04
CF-213376-a04-MO001-EC01	Axenic		0	0	0	0	0	-19.40
CF-213376-a04-MO002-EC01	Axenic		0	0	0	0	0	5.54
CBS 102414/CF-213376-a03	Inhibition zone		0	0	0	0	0	36.83
CBS 102414/CF-213376-a03	Inhibited mycelium		0	0	0	0	0	22.07
CF-214807-a04-MO001-EC01	Axenic		0	0	0	0	0	5.12
CF-214807-a04-MO002-EC01	Axenic		0	0	0	0	0	6.88
CBS 102414/CF-214807-a03	Inhibition zone		0	0	0	0	0	93.19
CBS 102414/CF-214807-a03	Inhibited mycelium		0	0	7.4	0	0	-10.37
CF-215288-a07-MO001-EC01	Axenic		4.7	0	0	0	0	10.50

CF-215288-a07-MO002-EC01	Axenic		0	0	0	0	0	-2.74
CBS 102414/CF-215288-a03	Inhibition zone		7.6	6.5	8.9	6.6	7.5	14.55
CBS 102414/CF-215288-a03	Inhibited mycelium		7	6.5	11.7	4.8	0	-17.96
CF-223912-a07-MO001-EC01	Axenic	preussomerins B and L	5.5	7.9	6.8	7.7	12.8	-99.79
CF-223912-a07-MO002-EC01	Axenic	preussomerin L	6.2	7.9	7.1	6.5	10.5	-98.65
CBS 102414/CF-223912-a06	Inhibition zone	palmarumycin C15, preussomerin F	8.1	7.9	11.2	9	17.8	-98.44
CBS 102414/CF-223912-a06	Inhibited mycelium	palmarumycin C15, preussomerin F	6.5	8.1	10.1	9.7	14.5	-95.32
CF-246868-a06-MO001-EC01	Axenic	palmarumycin C15, preussomerin L	0	7.1	6.7	0	7.5	-86.86
CF-246868-a06-MO002-EC01	Axenic	palmarumycin C15, preussomerin L	0	7.5	7.4	0	7.8	-83.65
CBS 102414/CF-246868-a05	Inhibition zone	palmarumycin C15, preussomerin L	6.8	7.1	6.6	0	8.8	-95.46
CBS 102414/CF-246868-a05	Inhibited mycelium	palmarumycin C15, preussomerin L	5.8	8.6	6.8	0	9.1	-96.74
CF-255912-a03-MO001-EC01	Axenic		0	0	0	0	0	7.09
CF-255912-a03-MO002-EC01	Axenic		0	0	0	0	0	19.19
CBS 102414/CF-255912-a02	Inhibition zone		0	0	0	0	0	46.77
CBS 102414/CF-255912-a02	Inhibited mycelium		0	0	0	0	0	34.28
CF-257866-a04-MO001-EC01	Axenic	7-chloro-6-methoxymellein	0	0	0	0	0	-17.85
CF-257866-a04-MO002-EC01	Axenic	7-chloro-6-methoxymellein	0	0	0	0	0	-2.22
CBS 102414/CF-257866-a03	Inhibition zone		0	0	0	0	0	56.15
CBS 102414/CF-257866-a03	Inhibited mycelium		0	0	7.8	0	0	32.59
CF-258646-a03-MO001-EC01	Axenic		0	0	0	0	0	9.26
CF-258646-a03-MO002-EC01	Axenic		0	0	0	0	0	-2.95
CBS 102414/CF-258646-a02	Inhibition zone		0	0	5.7	0	0	2.22
CBS 102414/CF-258646-a02	Inhibited mycelium		4.9	7.1	6.2	0	0	-78.81
CF-258778-a04-MO001-EC01	Axenic	palmarumycin C15, preussomerin B	0	0	0	0	0	-99.79
CF-258778-a04-MO002-EC01	Axenic	palmarumycin C15, preussomerin B	0	0	0	0	0	-96.48
CBS 102414/CF-258778-a03	Inhibition zone	preussomerins B and F	6.1	5.8	6.2	0	7.2	-98.44
CBS 102414/CF-258778-a03	Inhibited mycelium	preussomerins B and F	5.2	7.2	6.4	0	0	-98.86
CF-258809-a04-MO001-EC01	Axenic		0	0	0	0	0	-26.44
CF-258809-a04-MO002-EC01	Axenic		0	0	0	0	0	4.19
CBS 102414/CF-258809-a03	Inhibition zone		0	0	0	0	0	43.79
CBS 102414/CF-258809-a03	Inhibited mycelium		0	0	0	0	0	78.00
CF-260282-a06-MO001-EC01	Axenic		0	0	0	0	0	10.19
CF-260282-a06-MO002-EC01	Axenic		0	0	0	0	0	11.54
CBS 102414/CF-260282-a04	Inhibition zone	preussomerins B and F	6.3	6.8	0	0	0	-85.24
CBS 102414/CF-260282-a04	Inhibited mycelium	preussomerins B and F	6.1	7.2	0	0	7.9	-96.59
CF-260308-a04-MO001-EC01	Axenic		0	0	0	0	0	-10.81
CF-260308-a04-MO002-EC01	Axenic		0	0	0	0	0	3.88
CBS 102414/CF-260308-a02	Inhibition zone		6.4	5.7	6.2	0	0	-99.01
CBS 102414/CF-260308-a02	Inhibited mycelium		6.1	7.1	6.5	0	0	-89.21
CF-262323-a04-MO001-EC01	Axenic		0	0	0	0	0	-30.41
CF-262323-a04-MO002-EC01	Axenic		0	0	0	0	0	13.36
CBS 102414/CF-262323-a03	Inhibition zone		6.8	6.3	6.8	0	0	1.92
CBS 102414/CF-262323-a03	Inhibited mycelium		0	0	6.9	0	0	-11.57
CF-267373-a04-MO001-EC01	Axenic		0	0	0	0	0	39.06
CF-267373-a04-MO002-EC01	Axenic		0	0	0	0	0	39.95
CBS 102414/CF-267373-a03	Inhibition zone		6.8	0	7.4	0	0	-21.22
CBS 102414/CF-267373-a03	Inhibited mycelium		6.3	7.2	6	0	0	-94.46
CF-268679-a03-MO001-EC01	Axenic		5.7	0	0	7.6	0	48.73
CF-268679-a03-MO002-EC01	Axenic		0	0	0	6.1	0	43.13
CBS 102414/CF-268679-a02	Inhibition zone		0	0	0	0	0	94.75
CBS 102414/CF-268679-a02	Inhibited mycelium		0	0	0	0	0	95.74

Annexes

CF-268787-a04-MO001-EC01	Axenic		0	0	0	0	0	11.32
CF-268787-a04-MO002-EC01	Axenic		0	0	0	0	0	28.50
CBS 102414/CF-268787-a03	Inhibition zone		6.3	7.6	6.3	0	8.7	-98.58
CBS 102414/CF-268787-a03	Inhibited mycelium		6.6	6.9	5.8	0	0	-98.86
CF-268841-a04-MO001-EC01	Axenic	globosuxanthone A	0	0	0	0	0	-48.85
CF-268841-a04-MO002-EC01	Axenic	globosuxanthone A	0	0	0	0	0	-21.63
CBS 102414/CF-268841-a03	Inhibition zone	globosuxanthone A	6.5	6.8	6.9	0	0	-99.57
CBS 102414/CF-268841-a03	Inhibited mycelium	globosuxanthone A	7	6.7	0	0	0	-99.57
CF-269659-a05-MO001-EC01	Axenic	palmarumycin C15, preussomerins B and L	0	0	0	0	0	-89.44
CF-269659-a05-MO002-EC01	Axenic	palmarumycin C15, preussomerins B and L	0	0	6.9	0	0	-95.17
CBS 102414/CF-269659-a04	Inhibition zone	palmarumycin C15, preussomerin B	0	0	0	0	0	-69.06
CBS 102414/CF-269659-a04	Inhibited mycelium	preussomerins B and F	6.4	8	8.2	0	0	-97.73
CF-269692-a05-MO001-EC01	Axenic		0	0	5.7	0	0	-93.89
CF-269692-a05-MO002-EC01	Axenic		0	0	0	0	0	36.77
CBS 102414/CF-269692-a04	Inhibition zone		5.5	6.9	6.6	0	0	-99.15
CBS 102414/CF-269692-a04	Inhibited mycelium		5.8	6.7	5.5	0	0	-68.06
CF-277042-a05-MO001-EC01	Axenic		0	0	0	0	0	40.46
CF-277042-a05-MO002-EC01	Axenic		0	0	0	0	0	23.92
CBS 102414/CF-277042-a04	Inhibition zone		0	0	0	0	0	14.69
CBS 102414/CF-277042-a04	Inhibited mycelium		0	0	0	0	0	31.58
CF-284867-a05-MO001-EC01	Axenic	griseofulvin	0	0	0	0	0	-81.93
CF-284867-a05-MO002-EC01	Axenic	griseofulvin	0	0	0	0	0	-87.91
CBS 102414/CF-284867-a02	Inhibition zone	griseofulvin	0	0	7.2	0	0	17.63
CBS 102414/CF-284867-a02	Inhibited mycelium	griseofulvin	0	0	0	0	0	5.63
CF-285353-a07-MO001-EC01	Axenic		0	0	0	0	0	28.75
CF-285353-a07-MO002-EC01	Axenic		0	0	0	0	0	29.13
CBS 102414/CF-285353-a06	Inhibition zone		0	0	6.1	0	0	95.26
CBS 102414/CF-285353-a06	Inhibited mycelium		0	0	0	0	0	25.93
CF-288225-a03-MO001-EC01	Axenic		0	0	0	0	11.9	60.43
CF-288225-a03-MO002-EC01	Axenic		0	0	0	0	0	47.96
CBS 102414/CF-288225-a02	Inhibition zone		0	7.3	6.6	0	0	-24.59
CBS 102414/CF-288225-a02	Inhibited mycelium		5.6	7	6.8	0	0	-94.37

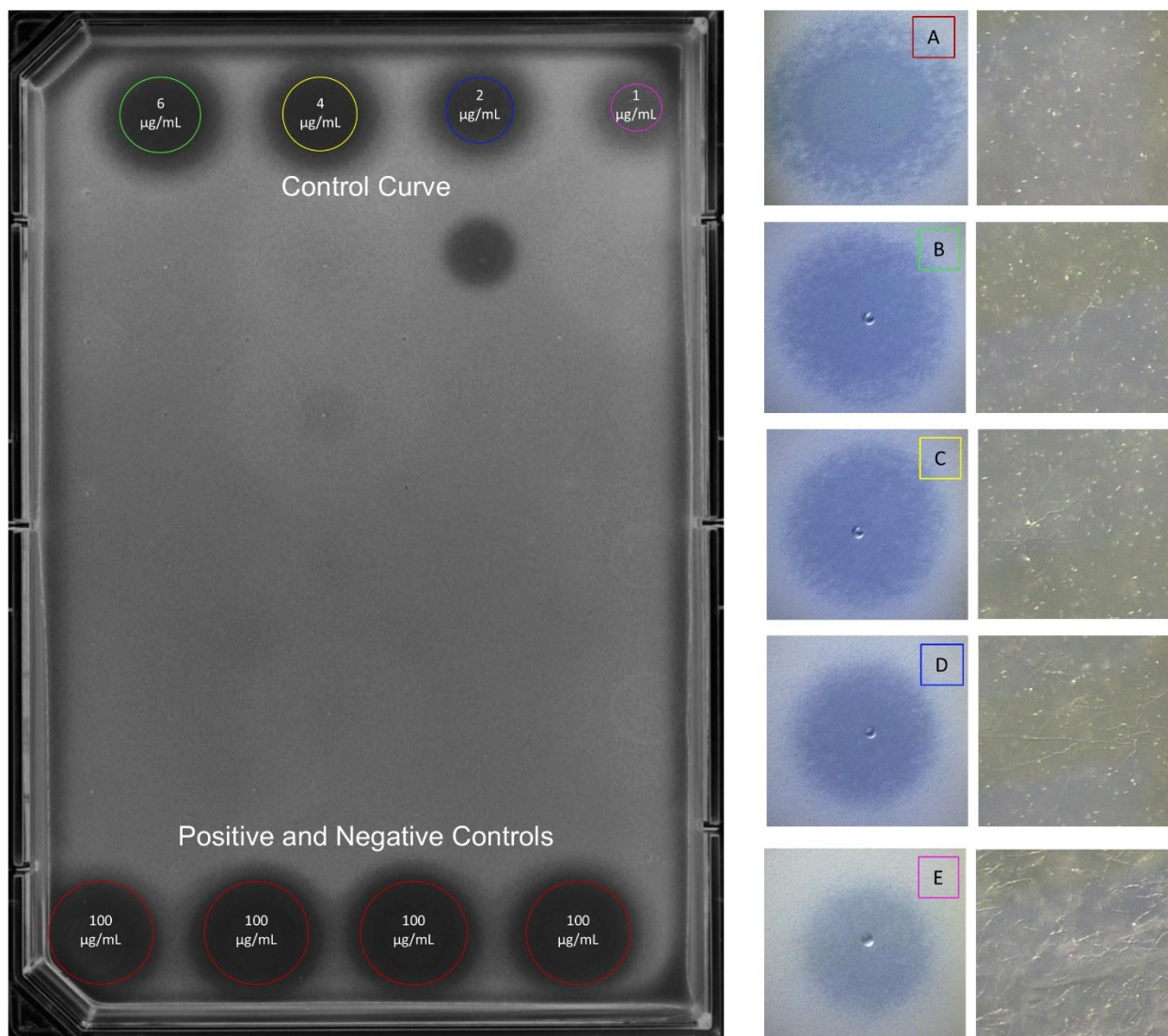


Figure S1. Plate design and categories of inhibition halos (A-E) in an assay plate of the agar-based HTS method for the identification of antifungals effective against *Colletotrichum acutatum*.

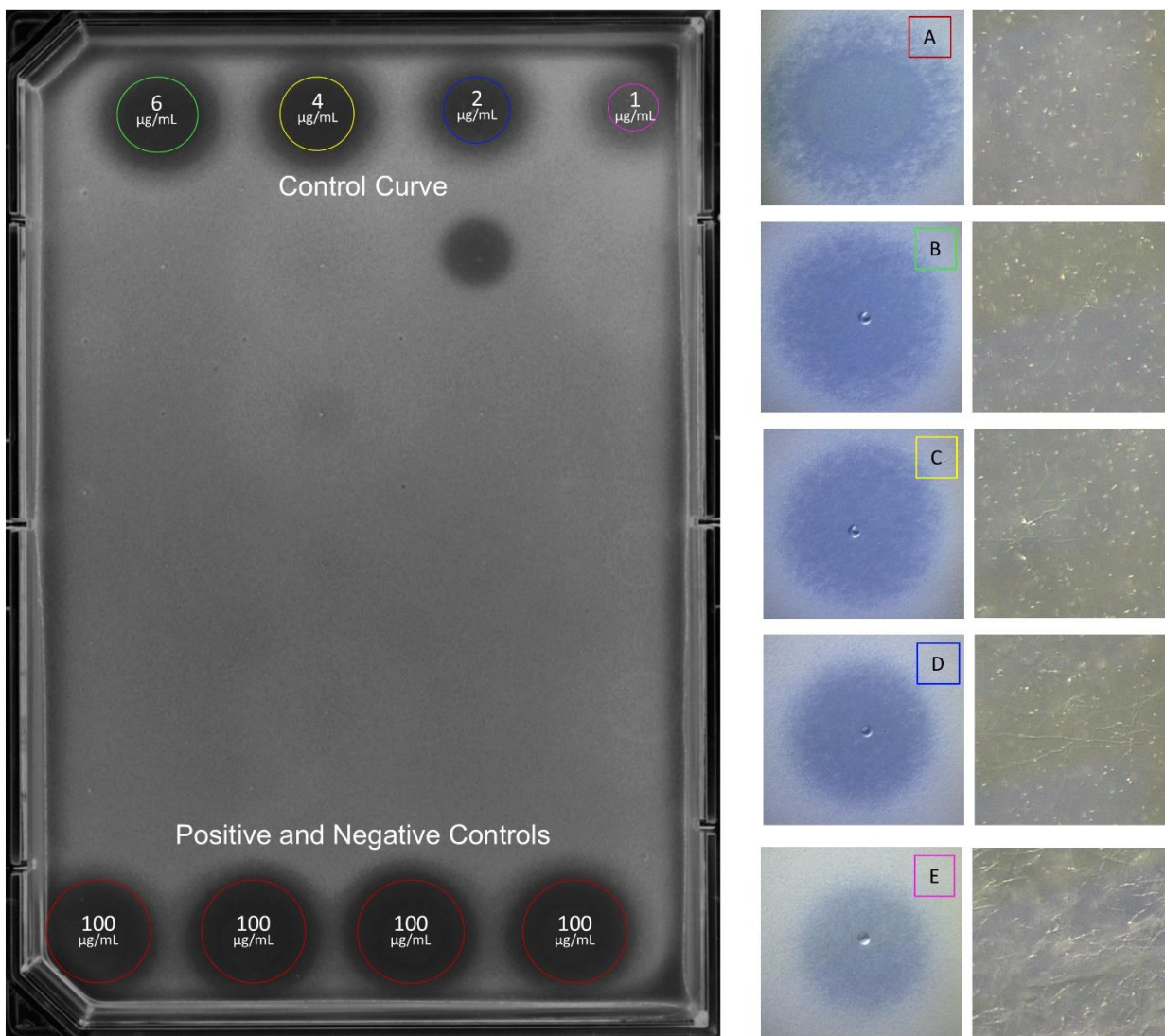


Figure S2. Plate design and categories of inhibition halos (A-E) in an assay plate of the agar-based HTS method for the identification of antifungals effective against *Fusarium proliferatum*.

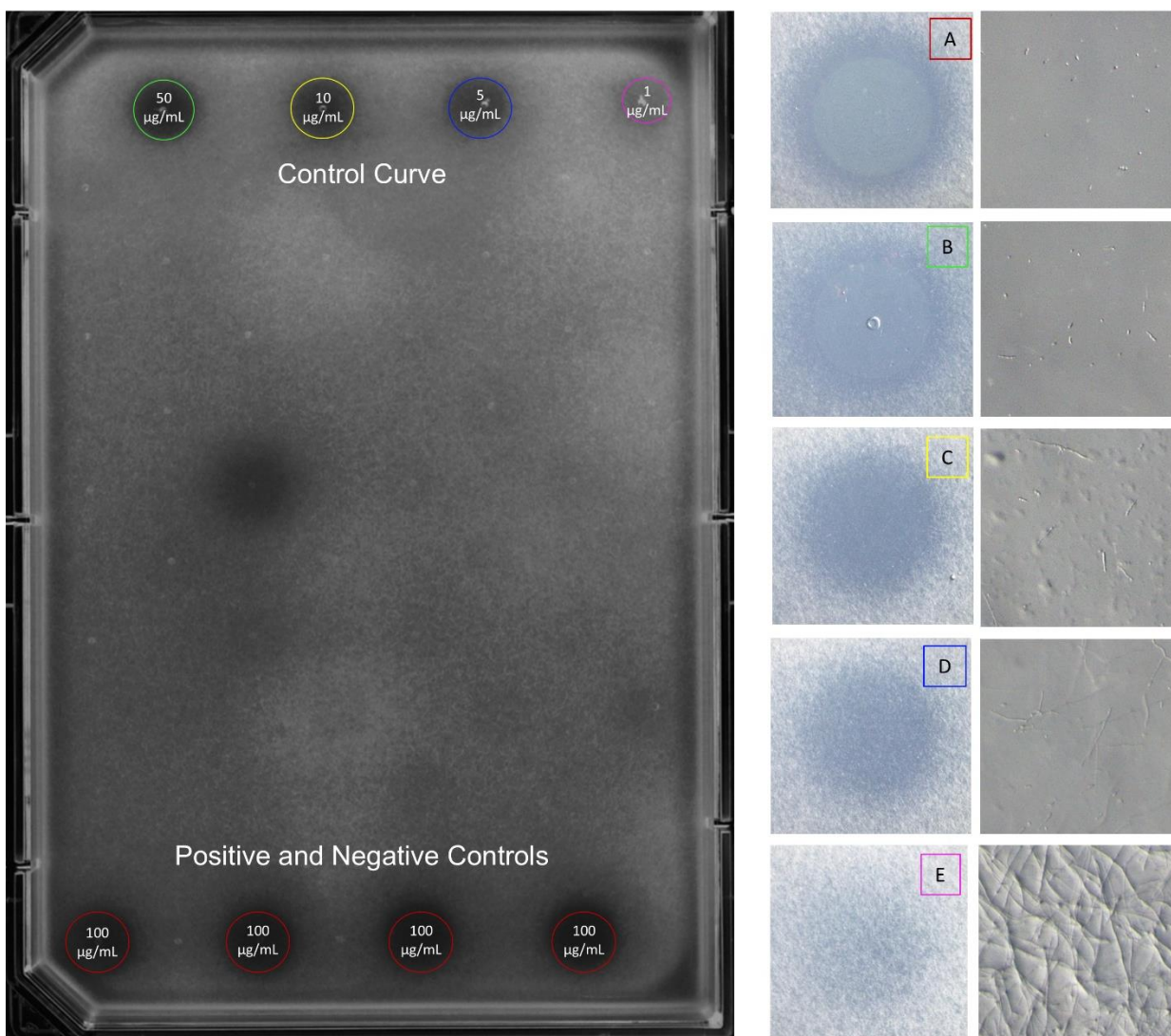


Figure S3. Plate design and categories of inhibition halos (A-E) in an assay plate of the agar-based HTS method for the identification of antifungals effective against *Magnaporthe grisea*.

ANNEX CHAPTER 2. Metabolomic analysis of the chemical diversity of leaf litter fungal species using an epigenetic culture-based approach.

Table S1. Taxonomic classification of the selected 232 fungal strains isolated from leaf litter of different local plants collected in South Africa across classes, orders, families and genus. Highlighted in bold the subsets studied in detail.

Class	Tax Order	Family	Genus	Origin	Dereplicated known metabolites
Agaricomycetes	<i>Corticiales</i>	<i>Corticiaceae</i>	<i>Corticium</i> (n=2)	<i>Protea laurifolia</i> and <i>P. repens</i>	connatusin B, Leucinostatin A and B, Terricolin
			<i>Marchandiomyces</i>	<i>Thamnochortus</i> sp.	
	<i>Cantharellales</i>	<i>Hydnaceae</i>	<i>Sistotrema</i>	<i>Protea repens</i>	
		<i>Tulasnellaceae</i>	<i>Tulasnella</i>	Culm restio	
		<i>Incertae sedis</i>	<i>Chantharealles</i>	<i>Olea europaea</i> sbsp <i>africana</i>	
	<i>Polyporales</i>	<i>Phanerochaetaceae</i>	<i>Phanerochaete</i>	<i>Rafnia</i> cf. <i>triflora</i> and <i>Tarchonanthus camphorates</i>	
		<i>Polyporaceae</i>	<i>Trametes</i>	Oak tree <i>Quercus</i> sp.	
	<i>Agaricales</i>	<i>Physalacriaceae</i>	<i>Cryptomarasmius</i>	<i>Protea repens</i>	Diorcinol
		<i>Psathyrellaceae</i>	<i>Coprinellus</i>	<i>Sideroxylon inerme</i>	
	<i>Boetales</i>	<i>Serpulaceae</i>	<i>Serpula</i>	<i>Brabejum stellatifolium</i>	
Dothideomycetes	<i>Pleosporales</i>	<i>Didymellaceae</i>	<i>Ascochyta</i> (n=5)	<i>Olea europaea</i> sbsp <i>africana</i>	Brefeldin A, Gliovictin, Indoleacetic acid, Leptosin I and C, Massarigenin A, Ovalacin, Palmarumycin C11 and C12
			<i>Boeremia</i>	<i>Chrysanthemoides monilifera</i>	
			<i>Didymella</i> (n=3)	<i>Elegia capensis</i> and culm restio	
			<i>Neodidymelliopsis</i>	<i>Protea repens</i>	
			<i>Phoma</i> (n=5)	<i>Protea repens</i> and culm restio	Cordylol C, Lecanorin, Phomalairdenone
		<i>Phaeosphaeriaceae</i>	<i>Banksiophoma</i>	Restio cf. <i>multiflorus</i>	Aposphaerin C
			<i>Neosetophoma</i>	Fynbos of restios	
			<i>Neostagonospora</i>	Fynbos of restios	Resorcylicide
			<i>Nodulosphaeria</i>	<i>Olea europaea</i> sbsp <i>africana</i>	Dehydromassarilactone D, Integrastatin B, Nemanolone A, Palmarumycin B1
			<i>Parastagonospora</i> (n=3)	<i>Olea europaea</i> sbsp <i>africana</i>	Cordylol C, Dihydrohypnophilin, Stagonolide F and C/G
			<i>Phaeosphaeria</i> (n=4)	<i>Olea europaea</i> sbsp <i>africana</i>	Dihydrohypnophilin, Mellein, 2-(3,4-Epoxy-5-heptenoyl)-5-methylpyrrole, Phaeosphaerin A and C, 11,12-hydroxyeudesm-4-en-3-one
			<i>Sclerostagonospora</i> (n=2)	<i>Elegia capensis</i>	Resorcylicide, Zearalenone, 2-(3,4-Epoxy-5-heptenoyl)-5-methylpyrrole)

			<i>Unidentified Phaeosphaeriaceae</i> (n=2)	<i>Olea europaea</i> sbsp <i>africana</i>	Infectopyrone, Penicillimide
Dothideomycetes	Pleosporales	Phaeosphaeriaceae	<i>Wojnowiciella</i>	<i>Carpobrotus edulis</i>	Bisdechlorodihydrogeodin, Pycnidione
		Cucurbitariaceae	<i>Neocucurbitaria</i> (n=2)	<i>Protea laurifolia</i>	Infectopyrone, 6-(1,2-Dihydroxypropyl)-4-hydroxy-3-(1-oxobutyl)-2H-pyran-2-one
			<i>Pyrenochaeta</i> (n=2)	Culm restio	Indoleacetic acid, Infectopyrone
			<i>Pyrenochaetopsis</i> (n=3)	<i>Chrysanthemoides monilifera</i> and culm restio	Preussomerin L
		Didymosphaeriaceae	<i>Didymosphaeria</i>	<i>Protea laurifolia</i>	Connatusin B, Diorcinol F, Deoxydihydrofusicin
			<i>Paracamarosporium</i>	<i>Protea laurifolia</i>	
			<i>Paraconiothyrium</i> (n=2)	<i>Protea laurifolia</i>	Emodin, Globosuxanthone A, Dihydroglobosuxanthone A
			<i>Paraphaeosphaeria</i> (n=2)	<i>Protea laurifolia</i>	Cordylol C
			<i>Pseudocamarosporium</i>	<i>Olea europaea</i> sbsp <i>africana</i>	Deoxydihydrofusicin
		Massarinaceae	<i>Helminthosporium</i>	Fynbos of restios	
			<i>Lophiostoma</i> (n=2)	Culm restio	Indoleacetic acid, Preussomerin A and B, Palmarumycin B1, C15 and C16
			<i>Massarina</i>	Restio cf. <i>multiflorus</i>	Dehydromassarilactone D, Infectopyrone, Pyronecine G
			<i>Vaginatipora</i> (n=2)	Culm restio	Equisetin, Oxasetin
		Teichosporaceae	<i>Teichospora</i> (n=3)	Culm restio	
			<i>Teichosporaceae</i>	Culm restio	
		Coniothyriaceae	<i>Coniothyrium</i> (n=3)	<i>Sideroxylon inerme</i> and culm restio	
		Pleosporaceae	<i>Alternaria</i> (n=3)	<i>Protea repens</i>	Alternariol, 9-O-Methylalternariol, Altenusin, Altenuic acid, Dihydroaltenuene A, Infectopyrone, 7-O-Methylfulvic acid, Pyrenocine G, Violaceol
		Sporormiaceae	<i>Forliomyces</i> (n=3)	<i>Elegia capensis</i> and culm restio	Mellein
		Amorosiaceae	<i>Alfoldia</i>	<i>Rafnia</i> cf. <i>triflora</i> and <i>Tarchonanthus camphorates</i>	
			<i>Angustimassarina</i>	Oak tree <i>Quercus</i> sp.	Rugulosin
		Anteagloniaceae	<i>Anteaglonium</i> (n=2)	Oak tree <i>Quercus</i> sp.	Ascochital
		Cryptocoryneaceae	<i>Cryptocoryneum</i> (n=2)	Culm restio	Palmarumycin B1, C15 and C16, Preussomerin B
		Microsphaeropsidaceae	<i>Microsphaeropsis</i> (n=2)	<i>Thamnochortus</i> sp.	
		Biatrisporaceae	<i>Nigrograna</i>	<i>Protea repens</i>	
		Delitschiaceae	<i>Delitschia</i>	<i>Sideroxylon inerme</i>	
Dothideomycetes	Pleosporales	Hermatomyetaceae	<i>Hermatomyces</i>	<i>Protea repens</i>	MDN-0104, Mycophenolic acid, Rubellin A
		Lentitheciaceae	<i>Keissleriella</i>	Fynbos of restios	
		Leptosphaeriaceae	<i>Leptosphaeria</i>	<i>Protea laurifolia</i>	Leptosphaeric acid

Annexes

		<i>Libertasomycetaceae</i>	<i>Libertasomyces</i>	<i>Diosma subulata</i>	Akanthomycin
		<i>Roussoellaceae</i>	<i>Roussoella</i>	<i>Diosma subulata</i>	PF 1140
		<i>Thyridariaceae</i>	<i>Lophiostoma</i>	Culm restio	Bipolaride B, Oxasetin
		<i>Torulaceae</i>	<i>Dendryphiella</i>	Culm restio	
		<i>Incertae sedis</i>	<i>Parapyrenochaeta</i>	<i>Elegia capensis</i>	Infectopyrone
			<i>Unidentified Pleosporales</i> (n=8)	Culm restio	Dehydromassarilactone D, Dihydrohypnophilin, Diorcinol F, Indoleacetic acid, Lecanorin, Pyrenocine G, Radicinin, Deoxyradicinin, Radicinol
	Capnodiales	<i>Teratosphaeriaceae</i>	<i>Austroafricana</i> (n=3)	<i>Olea europaea</i> sbsp <i>africana</i> and <i>Protea repens</i>	
			<i>Neocatenulostroma</i>	Oak tree <i>Quercus</i> sp.	
			<i>Neophaeothecoidea</i>	<i>Protea laurifolia</i>	
			<i>Parateratosphaeria</i>	<i>Rafnia</i> cf. <i>triflora</i> and <i>Tarchonanthus camphorates</i>	
		<i>Cladosporiaceae</i>	<i>Cladosporium</i>	Culm restio	
			<i>Verrucocladosporium</i>	<i>Carpobrotus edulis</i>	
	<i>Dothideales</i>	<i>Dothioraceae</i>	<i>Dothiora</i> (n=3)	Oak tree <i>Quercus</i> sp.	Coriolide, Coleophomone A/B, Lecanorin, Ovalacin
			<i>Kabatina</i>	Culm restio	Palmarumycin C12
		<i>Saccotheciaceae</i>	<i>Dothichiza</i>	Oak tree <i>Quercus</i> sp.	Monocerin
	<i>Botryosphaeriales</i>	<i>Botryosphaeriaceae</i>	<i>Neofusicoccum</i>	<i>Protea repens</i>	O-Methyldihydrobotrydial
		<i>Incertae sedis</i>	<i>Camarosporium</i> (n=2)	<i>Diosma subulata</i> and <i>Elegia capensis</i>	Cordylol C and E, Deoxydihydrofusicin Lecanorin
	<i>Venturiales</i>	<i>Venturiaceae</i>	<i>Anungitea</i>	<i>Protea laurifolia</i>	Secalonic acid C
			<i>Venturia</i>	<i>Olea europaea</i> sbsp <i>africana</i>	
	<i>Hysteriales</i>	<i>Hysteriaceae</i>	<i>Hysterium</i>	<i>Thamnochortus</i> sp.	
	<i>Superstratomyces</i>	<i>Superstratomycetaceae</i>	<i>Superstratomyces</i>	<i>Protea laurifolia</i>	
	<i>Tubeufiales</i>	<i>Incertae sedis</i>	<i>Neorhamphoria</i>	<i>Protea laurifolia</i>	
	<i>Incertae sedis</i>	<i>Pseudoperisporiaceae</i>	<i>Nematostoma</i>	<i>Protea repens</i>	
		<i>Incertae sedis</i>	<i>Pyrenochaeta</i>	Culm restio	Infectopyrone
			<i>Scleroconidioma</i> (n=2)	<i>Protea laurifolia</i> and <i>P. repens</i>	Antibiotic AS 2077715
Leotiomyces	Helotiales	<i>Arachnopezizaceae</i>	<i>Arachnopeziza</i> (n=2)	<i>Olea europaea</i> sbsp <i>africana</i>	Altersolanol G, Citreoviridin, Citrinin, Cytochalasin F/B, Radicinin, Rhacodione B, Graphislactone E acetone adduct
Leotiomyces	Helotiales	<i>Discinellaceae</i>	<i>Fontanospora</i>	<i>Brabejum stellatifolium</i>	Virgineone
		<i>Hamatocanthoscyphaceae</i>	<i>Chalara</i>	Oak tree <i>Quercus</i> sp.	
		<i>Hamatocanthoscyphaceae</i>	<i>Xenopolyscytalum</i>	<i>Olea europaea</i> sbsp <i>africana</i>	Rhacodione B

		<i>Helotiaceae</i>	<i>Hymenoscyphus</i>	<i>Olea europaea</i> sbsp <i>africana</i>	
			<i>Lanzia</i>	<i>Carpobrotus edulis</i>	
		<i>Hyaloscyphaceae</i>	<i>Meliniomyces</i>	Oak tree <i>Quercus</i> sp.	
		<i>Loramycetaceae</i>	<i>Acidomelania</i>	<i>Protea repens</i>	Citrinin
		<i>Mollisiaceae</i>	<i>Mollisia</i>	<i>Protea repens</i>	
		<i>Sclerotiniaceae</i>	<i>Stromatinia</i>	Fynbos of restios	
		<i>Solenopeziaceae</i>	<i>Tetracladium</i>	Culm restio	
		<i>Incertae sedis</i>	<i>Phialea</i>	<i>Protea laurifolia</i>	
			Unidentified <i>Helotiales</i> (n=6)	<i>Protea laurifolia</i> , <i>P. repens</i> , Oak tree <i>Quercus</i> sp., <i>Olea europaea</i> sbsp <i>africana</i>	Citrinin
	<i>Rhytismatales</i>	<i>Calloriaceae</i>	<i>Dactylaria</i> (n=2)	<i>Protea repens</i> and culm restio	PF 1140
		<i>Rhytismataceae</i>	<i>Lophodermium</i>	Fynbos of restios	
	<i>Erysiphales</i>	<i>Amorphothecaceae</i>	<i>Oidiodendron</i> (n=2)	Oak tree <i>Quercus</i> sp.	Asterric acid, Bisdechlorodihydrogeodin, 4/3-hydroxymellein, Dehydromassarilactone D, Deoxydihydrofusicin, Diorcinol F, Epicoccone, Fusicinarin, Trichothecinol A
	<i>Incertae sedis</i>	<i>Neocrinulaceae</i>	<i>Neocrinula</i>	<i>Protea repens</i>	
		<i>Incertae sedis</i>	<i>Coleophoma</i> (n=2)	<i>Protea repens</i> and <i>Olea europaea</i> sbsp <i>africana</i>	
		<i>Calloriaceae</i>	<i>Meliniomyces</i>	<i>Olea europaea</i> sbsp <i>africana</i>	Brefeldin A
Sordariomycetes	Hypocreales	<i>Nectriaceae</i>	<i>Cosmospora</i>	Oak tree <i>Quercus</i> sp.	Cephalochromin, Diorcinol F, Ustilaginoidin A and J
			<i>Dactylonectria</i>	<i>Sideroxylon inerme</i>	
			<i>Fusarium</i> (n=3)	Culm restio	Beauvericin, Dehydrofusaric acid, 5,6-Dehydrozearelenone, Equisetin, Lucilactaene, 6-Methoxyvestitol, Trichosetin
			<i>Fusicladium</i>	Culm restio	
			<i>Volutella</i>	<i>Sideroxylon inerme</i>	
		<i>Bionectriaceae</i>	<i>Bryocentria</i>	<i>Sideroxylon inerme</i>	
		<i>Hypocreaceae</i>	<i>Acrostalagmus</i>	<i>Protea repens</i>	Exophilic acid, Melinacidin II
		<i>Stachybotryaceae</i>	<i>Sirastachys</i>	<i>Rafnia</i> cf. <i>triflora</i> and <i>Tarchonanthus camphorates</i>	Mellein
		<i>Incertae sedis</i>	<i>Acremonium</i>	<i>Protea repens</i>	Deoxydihydrofusicin
			<i>Sarocladium</i>	<i>Protea laurifolia</i>	
	Sordariomycetes	Xylariales	<i>Xylariaceae</i>	<i>Anthostomella</i> (n=2)	<i>Sideroxylon inerme</i>
<i>Anthostomelloides</i>				<i>Protea repens</i>	Cytochalasin K and H, Heptelidic acid, Hydroheptelidic acid, Ternatin
<i>Circinotrichum</i> (n=2)				<i>Carpobrotus edulis</i> and <i>Sideroxylon inerme</i>	Antibiotic TMC 264, Cinatrin B, Connatusin B, Rhizopicnin A

Annexes

		<i>Diatrypaceae</i>	<i>Monosporascus</i>	<i>Thamnochortus</i> sp.	4-Hydroxy-5-methylmellein
		<i>Hypoxylaceae</i>	<i>Daldinia</i>	<i>Sideroxylon inerme</i>	Indoleacetic acid
		<i>Incertae sedis</i>	<i>Pleurophoma</i>	Fynbos of restios	
	<i>Amphisphaeriales</i>	<i>Bartaliniaceae</i>	<i>Bartalinea</i> (n=2)	<i>Diosma subulata</i> and <i>Sideroxylon inerme</i>	Lecanorin, Mellein, 4/3-hydroxymellein, N-deoxykanthomycin
		<i>Amphisphaeriaceae</i>	<i>Immersidiscosia</i>	<i>Olea europaea</i> sbsp <i>africana</i>	Antibiotic TMC 264, Secalonic acid C, Ulocladol
		<i>Discosiaceae</i>	<i>Discosia</i>	<i>Brabejum stellatifolium</i>	Naematolin, Photinide A
		<i>Phlogicylindriaceae</i>	<i>Phlogicylindrium</i>	<i>Olea europaea</i> sbsp <i>africana</i>	
		<i>Sporocadaceae</i>	<i>Sarcostroma</i>	<i>Protea repens</i>	Diorcinol, Nemanolone A
	<i>Togniniales</i>	<i>Togniniaceae</i>	<i>Phaeoacremonium</i>	<i>Rafnia</i> cf. <i>triflora</i> and <i>Tarchonanthus camphorates</i>	Desferriacetulfusigen
			<i>Togninia</i>	<i>Protea repens</i>	
	<i>Myrmecridiales</i>	<i>Incertae sedis</i>	<i>Myrmecridium</i>	Fynbos of restios	
	<i>Sordariales</i>	<i>Incertae sedis</i>	<i>Unidentified Sordariales</i>	<i>Olea europaea</i> sbsp <i>africana</i>	
	<i>Incertae sedis</i>	<i>Apiosporaceae</i>	<i>Arthrinium</i> (n=3)	<i>Thamnochortus</i> sp. and <i>Elegia capensis</i>	Alternariol, Brefeldin A, Cordyol C, Cytochalasin K, N-Hydroxyapiosporamide,
		<i>Incertae sedis</i>	<i>Pleurophoma</i>	Fynbos of restios	
Eurotiomycetes	Chaetothyriales	<i>Herpotrichiellaceae</i>	<i>Capronia</i>	<i>Diosma subulata</i>	Exophilic acid
			<i>Cladophialophora</i>	<i>Protea laurifolia</i>	Mellein
			<i>Exophiala</i> (n=3)	<i>Protea laurifolia</i>	
		<i>Coccodiniaceae</i>	<i>Microxiphium</i>	<i>Olea europaea</i> sbsp <i>africana</i>	Quinolactacin A2, Radicidin
		<i>Incertae sedis</i>	<i>Unidentified Chaetothyriales</i>	<i>Elegia capensis</i>	
	<i>Eurotiales</i>	<i>Aspergillaceae</i>	<i>Penicillium</i> (n=4)	<i>Protea laurifolia</i>	Antibiotic NG 011, Secalonic acid C, Chaetoglobosin P/N and K/L
	<i>Phaeomoniellales</i>	<i>Phaeomoniellaceae</i>	<i>Phaeomoniella</i> (n=2)	<i>Protea laurifolia</i>	
			<i>Unidentified Phaeomoniellales</i>	<i>Protea laurifolia</i>	Cerebroside C, Coriolide, Lecanorin
		<i>Celotheliaceae</i>	<i>Neophaeomoniella</i>	<i>Diosma subulata</i>	
<i>Pezizomycetes</i>	<i>Pezizales</i>	<i>Sarcosomataceae</i>	<i>Conoplea</i>	<i>Protea repens</i>	
<i>Pezizomycetes</i>	<i>Pezizales</i>	<i>Sarcosomataceae</i>	<i>Plectania</i> (n=2)	<i>Brabejum stellatifolium</i> and <i>Protea repens</i>	Isogaliellalactone
<i>Cystobasidiomycetes</i>	<i>Cystobasidiales</i>	<i>Cystobasidiaceae</i>	<i>Cystobasidium</i>	<i>Elegia capensis</i>	Citrinin
<i>Umbelopsidomycetes</i>	<i>Umbelopsidales</i>	<i>Umbelopsidaceae</i>	<i>Umbelopsis</i>	<i>Olea europaea</i> sbsp <i>africana</i>	
<i>Wallemiomycetes</i>	<i>Wallemiales</i>	<i>Wallemiaceae</i>	<i>Wallemia</i>	<i>Protea repens</i>	
<i>Microbotryomycetes</i>	<i>Sporidiobolales</i>	<i>Sporidiobolaceae</i>	<i>Sporobolomyces</i>	<i>Protea laurifolia</i>	
<i>Orbiliomycetes</i>	<i>Orbiliales</i>	<i>Orbiliaceae</i>	<i>Orbilia</i>	<i>Protea repens</i>	
<i>Incertae sedis</i>	<i>Incertae sedis</i>	<i>Incertae sedis</i>	<i>Anthopsis</i> (n=2)	<i>Chrysanthemoides monilifera</i>	
			<i>Ochroconis</i>	<i>Protea repens</i>	

			<i>Polyscytalum</i> (n=2)	Oak tree <i>Quercus</i> sp.	Mellein, 4/3Hydroxymellein
			<i>Pseudosigmoidea</i>	Oak tree <i>Quercus</i> sp.	
			<i>Rhexodenticula</i>	<i>Protea laurifolia</i>	
			<i>Unidentified</i> (n=10)	Fynbos of restios, <i>Chrysanthemoides monilifera</i> , <i>Elegia capensis</i> , <i>Protea repens</i> , <i>Olea europaea sbsp africana</i>	Connatusin B, N-deoxyakanthomycin, 11-Hydroxycurvularin, MDN-0101 [42], Nemanolone A, Pandangolide 2, Preussomerin L, Questiomycin A, Resorcylicide

ANNEX CHAPTER 4. Leaf-litter-associated fungi from South Africa to control fungal plant pathogens.**Table S1.** List of 232 fungal strains included in the phylogenetic analysis (possible new species are in bold).

Name	Genus	Species	Family	Order	Class	Sequence	% Similarity	GenBank No. of the highest score
CF-166111	AcrospERMum	sp.	AcrospERMaceae	AcrospERMales	Dothideomycetes	ITS	95	MK562005.1
CF-166079	<i>Bezerromyces</i>	sp.	<i>Bezerromycetaceae</i>	<i>Bezerromycetales</i>	<i>Dothideomycetes</i>	ITS	96	NR_173042.1
CF-166185	<i>Botryobambusa</i>	sp.	<i>Botryosphaeriaceae</i>	<i>Botryosphaeriales</i>	<i>Dothideomycetes</i>	28S	98	JX646809.1
CF-164395	<i>Dothiora</i>	<i>ceratoniae</i>	<i>Botryosphaeriaceae</i>	<i>Botryosphaeriales</i>	<i>Dothideomycetes</i>	ITS	99	KU728500.1
CF-164488	<i>Dothiora</i>	<i>coronillae</i>	<i>Botryosphaeriaceae</i>	<i>Botryosphaeriales</i>	<i>Dothideomycetes</i>	ITS	100	NR_157481.1
CF-164362	<i>Dothiora</i>	<i>maculans</i>	<i>Botryosphaeriaceae</i>	<i>Botryosphaeriales</i>	<i>Dothideomycetes</i>	ITS	100	MH860981.1
CF-164411	<i>Dothiora</i>	<i>oleae</i>	<i>Botryosphaeriaceae</i>	<i>Botryosphaeriales</i>	<i>Dothideomycetes</i>	ITS	99	KU728509.1
CF-164402	<i>Dothiora</i>	<i>oleae</i>	<i>Botryosphaeriaceae</i>	<i>Botryosphaeriales</i>	<i>Dothideomycetes</i>	ITS	100	KU728509.1
CF-164234	<i>Neofusicoccum</i>	<i>protearum</i>	<i>Botryosphaeriaceae</i>	<i>Botryosphaeriales</i>	<i>Dothideomycetes</i>	ITS	100	FJ150698.1
CF-164296	<i>Cladosporium</i>	sp.	<i>Cladosporiaceae</i>	<i>Capnodiales</i>	<i>Dothideomycetes</i>	ITS	100	MF473180.1/OR243761.1
CF-164449	<i>Verrucocladosporium</i>	<i>carpobroti</i>	<i>Cladosporiaceae</i>	<i>Capnodiales</i>	<i>Dothideomycetes</i>	ITS	100	MW175354.1
CF-164382	<i>Dothidea</i>	<i>eucalypti</i>	<i>Dothideaceae</i>	<i>Dothideales</i>	<i>Dothideomycetes</i>	ITS	99	NR_156390.1
CF-164419	<i>Hysterium</i>	<i>pulicare</i>	<i>Hysteriaceae</i>	<i>Hysteriales</i>	<i>Dothideomycetes</i>	ITS+28S	100	EU552137
CF-164367	<i>Austroafricana</i>	<i>parva</i>	<i>Teratosphaeriaceae</i>	<i>Mycosphaerellales</i>	<i>Dothideomycetes</i>	28S	100	EU707874.1
CF-164249	<i>Austroafricana</i>	<i>parva</i>	<i>Teratosphaeriaceae</i>	<i>Mycosphaerellales</i>	<i>Dothideomycetes</i>	ITS+28S	100	EU707874.1
CF-164238	<i>Austroafricana</i>	<i>parva</i>	<i>Teratosphaeriaceae</i>	<i>Mycosphaerellales</i>	<i>Dothideomycetes</i>	ITS+28S	100	EU707874.1
CF-164355	<i>Neocatenulostroma</i>	<i>microsporum</i>	<i>Teratosphaeriaceae</i>	<i>Mycosphaerellales</i>	<i>Dothideomycetes</i>	ITS+28s	100	EU167572.1
CF-166084	<i>Neophaeothecoidea</i>	<i>protea</i>	<i>Teratosphaeriaceae</i>	<i>Mycosphaerellales</i>	<i>Dothideomycetes</i>	ITS	99	NR_157417.1
CF-169044	<i>Parateratosphaeria</i>	<i>bellula</i>	<i>Teratosphaeriaceae</i>	<i>Mycosphaerellales</i>	<i>Dothideomycetes</i>	ITS+28S	99	EU019301.2
CF-169033	Alfoldia	sp.	Amorosiaceae	Pleosporales	Dothideomycetes	ITS	95	NR_171211.1
CF-168984	Alfoldia	sp.	Amorosiaceae	Pleosporales	Dothideomycetes	ITS	95	NR_171211.1
CF-164330	<i>Angustimassarina</i>	sp.	<i>Amorosiaceae</i>	<i>Pleosporales</i>	<i>Dothideomycetes</i>	ITS	100	KY548099.1
CF-164349	Anteaglonium	sp.	Anteagloniaceae	Pleosporales	Dothideomycetes	28S	100	GQ221876.1
CF-164342	Anteaglonium	sp.	Anteagloniaceae	Pleosporales	Dothideomycetes	28S	97	MH866969.1
CF-164236	Flammeascoma	sp.	Anteagloniaceae	Pleosporales	Dothideomycetes	ITS	99	MN598923.1
CF-164471	Coniothyrium	sp.	Coniothyriaceae	Pleosporales	Dothideomycetes	ITS	96	OP597892.1
CF-164281	<i>Neoconiothyrium</i>	sp.	<i>Coniothyriaceae</i>	<i>Pleosporales</i>	<i>Dothideomycetes</i>	ITS	96	MH858605.1
CF-164273	Cryptocoryneum	sp.	Cryptocoryneaceae	Pleosporales	Dothideomycetes	ITS	93	NR_153938.1
CF-164341	Cryptocoryneum	sp.	Cryptocoryneaceae	Pleosporales	Dothideomycetes	ITS	95	NR_153935.1
CF-166041	<i>Pyrenochaeta</i>	<i>pinicola</i>	<i>Cucurbitariaceae</i>	<i>Pleosporales</i>	<i>Dothideomycetes</i>	ITS	99	KJ869152.1

CF-166077	<i>Pyrenochaeta</i>	sp.	<i>Cucurbitariaceae</i>	<i>Pleosporales</i>	<i>Dothideomycetes</i>	ITS	96	NR_155692.1
CF-164283	<i>Pyrenochaeta</i>	sp.	<i>Cucurbitariaceae</i>	<i>Pleosporales</i>	<i>Dothideomycetes</i>	ITS	100	UDB05787168
CF-164479	<i>Pyrenochaetopsis</i>	<i>leptospora</i>	<i>Cucurbitariaceae</i>	<i>Pleosporales</i>	<i>Dothideomycetes</i>	ITS+28S	100	MF785793.1
CF-164284	<i>Pyrenochaetopsis</i>	<i>leptospora</i>	<i>Cucurbitariaceae</i>	<i>Pleosporales</i>	<i>Dothideomycetes</i>	ITS+28S	100	MF785793.1
CF-164269	<i>Pyrenochaetopsis</i>	<i>leptospora</i>	<i>Cucurbitariaceae</i>	<i>Pleosporales</i>	<i>Dothideomycetes</i>	ITS+28S	100	MF785793.1
CF-166135	<i>Pyricularia</i>	<i>caricis</i>	<i>Cucurbitariaceae</i>	<i>Pleosporales</i>	<i>Dothideomycetes</i>	ITS	100	MK432729.1
CF-164461	<i>Delitschia</i>	<i>chaetomioides</i>	<i>Delitschiaceae</i>	<i>Pleosporales</i>	<i>Dothideomycetes</i>	28S	99	MK347981.1
CF-166157	<i>Ascochyta</i>	sp	<i>Didymellaceae</i>	<i>Pleosporales</i>	<i>Dothideomycetes</i>	ITS	99	MG065764.1
CF-166125	<i>Ascochyta</i>	sp.	<i>Didymellaceae</i>	<i>Pleosporales</i>	<i>Dothideomycetes</i>	ITS+28S	98	EU167557.1/EU167559.1
CF-164482	<i>Ascochyta</i>	sp.	<i>Didymellaceae</i>	<i>Pleosporales</i>	<i>Dothideomycetes</i>	ITS+28S	99	EU167575.1
CF-164486	<i>Boeremia</i>	<i>exigua</i>	<i>Didymellaceae</i>	<i>Pleosporales</i>	<i>Dothideomycetes</i>	ITS+28S	100	EU167567.1
CF-164354	<i>Coniothyrium</i>	sp.	<i>Didymellaceae</i>	<i>Pleosporales</i>	<i>Dothideomycetes</i>	ITS	97	OP179019.1
CF-166148	<i>Didymella</i>	<i>pinodella</i>	<i>Didymellaceae</i>	<i>Pleosporales</i>	<i>Dothideomycetes</i>	ITS+28S	99	EU167565.1
CF-166147	<i>Didymella</i>	<i>pinodella</i>	<i>Didymellaceae</i>	<i>Pleosporales</i>	<i>Dothideomycetes</i>	ITS+28S	99	EU167565.1
CF-164271	<i>Didymella</i>	<i>pinodella</i>	<i>Didymellaceae</i>	<i>Pleosporales</i>	<i>Dothideomycetes</i>	ITS+28S	99	EU167565.1
CF-164380	<i>Microphaeropsis</i>	<i>proteae</i>	<i>Didymellaceae</i>	<i>Pleosporales</i>	<i>Dothideomycetes</i>	ITS	99	JN712495.1
CF-166120	<i>Neodidymelliopsis</i>	sp.	<i>Didymellaceae</i>	<i>Pleosporales</i>	<i>Dothideomycetes</i>	ITS+28S	100	MG065745.1
CF-164320	<i>Ophiobolus</i>	sp.	<i>Didymellaceae</i>	<i>Pleosporales</i>	<i>Dothideomycetes</i>	ITS	94	OM337541.1
CF-168996	<i>Phoma</i>	sp.	<i>Didymellaceae</i>	<i>Pleosporales</i>	<i>Dothideomycetes</i>	ITS	93	KY484798.1
CF-166102	<i>Phomatodes</i>	<i>nebulosa</i>	<i>Didymellaceae</i>	<i>Pleosporales</i>	<i>Dothideomycetes</i>	ITS+28S	99	EU552151.1
CF-164387	<i>Phomatodes</i>	<i>nebulosa</i>	<i>Didymellaceae</i>	<i>Pleosporales</i>	<i>Dothideomycetes</i>	ITS+28S	99	EU552151.1
CF-164386	<i>Phomatodes</i>	<i>nebulosa</i>	<i>Didymellaceae</i>	<i>Pleosporales</i>	<i>Dothideomycetes</i>	ITS+28S	99	EU552151.1
CF-164279	<i>Phomatodes</i>	<i>nebulosa</i>	<i>Didymellaceae</i>	<i>Pleosporales</i>	<i>Dothideomycetes</i>	ITS+28S	100	EU552151.1
CF-166178	<i>Pseudoascochyta</i>	sp.	<i>Didymellaceae</i>	<i>Pleosporales</i>	<i>Dothideomycetes</i>	ITS	99	NR_158274.1/NR_158273.1
CF-169051	<i>Chromolaenicola</i>	sp.	<i>Didymosphaeriaceae</i>	<i>Pleosporales</i>	<i>Dothideomycetes</i>	ITS	99	MT310601.1
CF-164447	<i>Chromolaenicola</i>	sp.	<i>Didymosphaeriaceae</i>	<i>Pleosporales</i>	<i>Dothideomycetes</i>	ITS	99	MT310601.1
CF-164439	<i>Didymosphaeria</i>	<i>variabile</i>	<i>Didymosphaeriaceae</i>	<i>Pleosporales</i>	<i>Dothideomycetes</i>	ITS+28S	100	JX496118.1
CF-166042	<i>Paracamarosporium</i>	<i>leucadendri</i>	<i>Didymosphaeriaceae</i>	<i>Pleosporales</i>	<i>Dothideomycetes</i>	ITS+28S	100	EU552106.1
CF-166142	<i>Paraconiothyrium</i>	<i>brasiliense</i>	<i>Didymosphaeriaceae</i>	<i>Pleosporales</i>	<i>Dothideomycetes</i>	ITS	99	JX496083.1
CF-164287	<i>Paraphaeosphaeria</i>	<i>parmeliae</i>	<i>Didymosphaeriaceae</i>	<i>Pleosporales</i>	<i>Dothideomycetes</i>	ITS	100	NR_137955.1
CF-164274	<i>Paraphaeosphaeria</i>	<i>verruculosa</i>	<i>Didymosphaeriaceae</i>	<i>Pleosporales</i>	<i>Dothideomycetes</i>	ITS	100	NR_137955.1
CF-164383	<i>Pseudocamarosporium</i>	<i>brabeji</i>	<i>Didymosphaeriaceae</i>	<i>Pleosporales</i>	<i>Dothideomycetes</i>	ITS+28S	99	EU552105.1
CF-164282	<i>Fuscostagonospora</i>	sp.	<i>Fuscostagonosporaceae</i>	<i>Pleosporales</i>	<i>Dothideomycetes</i>	ITS	93	NR_153964.1
CF-166162	<i>Fuscostagonospora</i>	sp.	<i>Fuscostagonosporaceae</i>	<i>Pleosporales</i>	<i>Dothideomycetes</i>	ITS	93	NR_163359.1
CF-166181	<i>Keissleriella</i>	sp.	<i>Lentitheciaceae</i>	<i>Pleosporales</i>	<i>Dothideomycetes</i>	ITS	98	KJ869112.1/NR_171713.1
CF-166029	<i>Leptosphaeria</i>	<i>proteicola</i>	<i>Leptosphaeriaceae</i>	<i>Pleosporales</i>	<i>Dothideomycetes</i>	ITS	100	JQ044439.1
CF-168990	<i>Libertasomyces</i>	<i>aloeticus</i>	<i>Libertasomycetaceae</i>	<i>Pleosporales</i>	<i>Dothideomycetes</i>	ITS	99	NR_165566.1
CF-164420	<i>Atrocalyx</i>	<i>nordicus</i>	<i>Lophiotremataceae</i>	<i>Pleosporales</i>	<i>Dothideomycetes</i>	ITS	99	NR_172997.1

Annexes

CF-164476	<i>Desertiserpentica</i>	sp.	<i>Lophiostomataceae</i>	<i>Pleosporales</i>	<i>Dothideomycetes</i>	ITS	95	NR_173310.1
CF-168965	<i>Lophiostoma</i>	sp.	<i>Lophiostomaceae</i>	<i>Pleosporales</i>	<i>Dothideomycetes</i>	ITS	90	MZ492968.1
CF-168972	<i>Massarina</i>	sp.	<i>Massarinaceae</i>	<i>Pleosporales</i>	<i>Dothideomycetes</i>	ITS	90	KU314982.1
CF-169052	<i>Vaginatispora</i>	<i>fuckelii</i>	<i>Massarinaceae</i>	<i>Pleosporales</i>	<i>Dothideomycetes</i>	ITS	100	EU552139.1
CF-164298	<i>Vaginatispora</i>	<i>fuckelii</i>	<i>Massarinaceae</i>	<i>Pleosporales</i>	<i>Dothideomycetes</i>	ITS	100	EU552139.1
CF-164425	<i>Microsphaeropsis</i>	<i>arundinis</i>	<i>Didymellaceae</i>	<i>Pleosporales</i>	<i>Dothideomycetes</i>	ITS	100	MZ771279.1
CF-164357	<i>Microsphaeropsis</i>	<i>arundinis</i>	<i>Didymellaceae</i>	<i>Pleosporales</i>	<i>Dothideomycetes</i>	ITS	100	MZ771279.1
CF-166088	<i>Nigrograna</i>	sp.	<i>Nigrogranaceae</i>	<i>Pleosporales</i>	<i>Dothideomycetes</i>	ITS	96	KX650556.1
CF-168985	<i>Banksiophoma</i>	sp.	<i>Phaeosphaeriaceae</i>	<i>Pleosporales</i>	<i>Dothideomycetes</i>	ITS	95	NR_153651.1
CF-164432	<i>Banksiophoma</i>	sp.	<i>Phaeosphaeriaceae</i>	<i>Pleosporales</i>	<i>Dothideomycetes</i>	ITS	95	NR_153651.1
CF-164483	<i>Equiseticola</i>	sp.	<i>Phaeosphaeriaceae</i>	<i>Pleosporales</i>	<i>Dothideomycetes</i>	28S	98	NG_059249.1
CF-166144	<i>Juncaceicola</i>	sp.	<i>Phaeosphaeriaceae</i>	<i>Pleosporales</i>	<i>Dothideomycetes</i>	ITS	98	NR_189996.1
CF-168961	<i>Neosetophoma</i>	sp.	<i>Phaeosphaeriaceae</i>	<i>Pleosporales</i>	<i>Dothideomycetes</i>	ITS	94	NR_185358.1
CF-166173	<i>Neostagonospora</i>	sp.	<i>Phaeosphaeriaceae</i>	<i>Pleosporales</i>	<i>Dothideomycetes</i>	ITS	99	MK595557.1
CF-166164	<i>Neostagonospora</i>	sp.	<i>Phaeosphaeriaceae</i>	<i>Pleosporales</i>	<i>Dothideomycetes</i>	ITS	98	NR_156265.1
CF-164385	<i>Nodulosphaeria</i>	<i>cirsi</i>	<i>Phaeosphaeriaceae</i>	<i>Pleosporales</i>	<i>Dothideomycetes</i>	ITS	100	KM014664.1
CF-168971	<i>Phaeosphaeria</i>	sp.	<i>Phaeosphaeriaceae</i>	<i>Pleosporales</i>	<i>Dothideomycetes</i>	ITS	97	NR_156608.1
CF-169031	<i>Phaeosphaeria</i>	<i>podocarpi</i>	<i>Phaeosphaeriaceae</i>	<i>Pleosporales</i>	<i>Dothideomycetes</i>	ITS	99	NR_137933.1
CF-169011	<i>Phaeosphaeria</i>	sp.	<i>Phaeosphaeriaceae</i>	<i>Pleosporales</i>	<i>Dothideomycetes</i>	ITS	93	OP596147.1
CF-164378	<i>Sclerostagonospora</i>	sp.	<i>Phaeosphaeriaceae</i>	<i>Pleosporales</i>	<i>Dothideomycetes</i>	ITS	95	JX517283.1/MH864458.1
CF-164373	<i>Sclerostagonospora</i>	sp.	<i>Phaeosphaeriaceae</i>	<i>Pleosporales</i>	<i>Dothideomycetes</i>	ITS	95	JX517283.1/MH864458.1
CF-166130	<i>Sclerostagonospora</i>	sp.	<i>Phaeosphaeriaceae</i>	<i>Pleosporales</i>	<i>Dothideomycetes</i>	ITS	91	JX517283.1
CF-164426	<i>Stagonospora</i>	sp.	<i>Phaeosphaeriaceae</i>	<i>Pleosporales</i>	<i>Dothideomycetes</i>	ITS	98	JX981494.1
CF-164445	<i>Wojnowiciella</i>	<i>dactylidis</i>	<i>Phaeosphaeriaceae</i>	<i>Pleosporales</i>	<i>Dothideomycetes</i>	ITS	99	MK442631.1
CF-168960	<i>Alternaria</i>	<i>infectoria</i>	<i>Pleosporaceae</i>	<i>Pleosporales</i>	<i>Dothideomycetes</i>	ITS	99	AY154690.1
CF-164322	<i>Alternaria</i>	<i>infectoria</i>	<i>Pleosporaceae</i>	<i>Pleosporales</i>	<i>Dothideomycetes</i>	ITS	99	AY154690.1
CF-164254	<i>Alternaria</i>	sp.	<i>Pleosporaceae</i>	<i>Pleosporales</i>	<i>Dothideomycetes</i>	ITS+28S	98	MK828116.1
CF-166183	<i>Curvularia</i>	<i>protuberata</i>	<i>Pleosporaceae</i>	<i>Pleosporales</i>	<i>Dothideomycetes</i>	ITS	100	KT012657.1
CF-168989	<i>Roussoella</i>	<i>euonymi</i>	<i>Roussoellaceae</i>	<i>Pleosporales</i>	<i>Dothideomycetes</i>	ITS	100	MH864531.1
CF-164438	<i>Fortiomyces</i>	sp.	<i>Sporormiaceae</i>	<i>Pleosporales</i>	<i>Dothideomycetes</i>	ITS+28S	96	NR_154006.1
CF-166145	<i>Fortiomyces</i>	sp.	<i>Sporormiaceae</i>	<i>Pleosporales</i>	<i>Dothideomycetes</i>	ITS+28S	96	NR_154006.1
CF-164290	<i>Fortiomyces</i>	sp.	<i>Sporormiaceae</i>	<i>Pleosporales</i>	<i>Dothideomycetes</i>	ITS+28S	96	NR_154006.1
CF-164337	<i>Magnibotryascoma</i>	<i>mali</i>	<i>Teichosporaceae</i>	<i>Pleosporales</i>	<i>Dothideomycetes</i>	ITS	99	ON811501.1
CF-166025	<i>Ramusculicola</i>	sp.	<i>Teichosporaceae</i>	<i>Pleosporales</i>	<i>Dothideomycetes</i>	ITS	95	NR_170816.1
CF-164286	<i>Teichospora</i>	sp.	<i>Teichosporaceae</i>	<i>Pleosporales</i>	<i>Dothideomycetes</i>	ITS	98	NR_154656.1
CF-166140	<i>Teichospora</i>	sp.	<i>Teichosporaceae</i>	<i>Pleosporales</i>	<i>Dothideomycetes</i>	ITS	95	MW269313.1
CF-164478	<i>Thyridaria</i>	<i>macrostromoides</i>	<i>Thyridariaceae</i>	<i>Pleosporales</i>	<i>Dothideomycetes</i>	ITS+28S	100	EU552157.1
CF-166136	<i>Parapyrenochaeta</i>	sp.	<i>Incertae sedis</i>	<i>Pleosporales</i>	<i>Dothideomycetes</i>	ITS	94	NR155674.1

CF-164294	<i>Pleosporales</i>	sp.	<i>Incertae sedis</i>	<i>Pleosporales</i>	<i>Dothideomycetes</i>	28S	97	JF449883.1
CF-168999	<i>Pleosporales</i>	sp.	<i>Incertae sedis</i>	<i>Pleosporales</i>	<i>Dothideomycetes</i>	ITS	92	OM670119.1
CF-164456	<i>Pleosporales</i>	sp.	<i>Incertae sedis</i>	<i>Pleosporales</i>	<i>Dothideomycetes</i>	ITS	99	KR909157.1
CF-164416	<i>Pleosporales</i>	sp.	<i>Incertae sedis</i>	<i>Pleosporales</i>	<i>Dothideomycetes</i>	ITS	95	AB986465.1
CF-164321	<i>Pleosporales</i>	sp.	<i>Incertae sedis</i>	<i>Pleosporales</i>	<i>Dothideomycetes</i>	ITS	99	FJ552933.1
CF-164253	<i>Pleosporales</i>	sp.	<i>Incertae sedis</i>	<i>Pleosporales</i>	<i>Dothideomycetes</i>	ITS	92	KU204434.1
CF-164448	<i>Pseudocoleophoma</i>	sp.	<i>Incertae sedis</i>	<i>Pleosporales</i>	<i>Dothideomycetes</i>	ITS	98	LC765163.1
CF-166054	<i>Superstratomyces</i>	sp.	<i>Superstratomycetaceae</i>	<i>Superstratomycetales</i>	<i>Dothideomycetes</i>	ITS	97	NR_152544.1
CF-166090	<i>Sympoventuria</i>	<i>africanum</i>	<i>Sympoventuriaceae</i>	<i>Venturiales</i>	<i>Dothideomycetes</i>	ITS	99	EU035424.1
CF-166066	<i>Anungitea</i>	<i>grevilleae</i>	<i>Venturiaceae</i>	<i>Venturiales</i>	<i>Dothideomycetes</i>	ITS	100	KX228252.1
CF-164403	<i>Venturia</i>	sp.	<i>Venturiaceae</i>	<i>Venturiales</i>	<i>Dothideomycetes</i>	ITS	86	EU035464.1
CF-164450	<i>Pleomonodictys</i>	sp.	<i>Pleomonodictydaceae</i>	<i>Incertae sedis</i>	<i>Dothideomycetes</i>	ITS	90	NR_154369.1
CF-166108	<i>Nematostoma</i>	sp.	<i>Pseudoperisporiaceae</i>	<i>Incertae sedis</i>	<i>Dothideomycetes</i>	ITS	97	MT547815.1
CF-166106	<i>Pseudoarthrographis</i>	sp.	<i>Incertae sedis</i>	<i>Incertae sedis</i>	<i>Dothideomycetes</i>	ITS	89	NR_160349.1
CF-169016	<i>Pyrenochaeta</i>	<i>nobilis</i>	<i>Incertae sedis</i>	<i>Incertae sedis</i>	<i>Dothideomycetes</i>	ITS	100	MF795792.1
CF-166058	<i>Scleroconidioma</i>	<i>sphagnicola</i>	<i>Incertae sedis</i>	<i>Incertae sedis</i>	<i>Dothideomycetes</i>	ITS	100	DQ182416.1
CF-164245	<i>Scleroconidioma</i>	<i>sphagnicola</i>	<i>Incertae sedis</i>	<i>Incertae sedis</i>	<i>Dothideomycetes</i>	ITS	100	DQ182416.1
CF-168994	<i>Tremateia</i>	sp.	<i>Incertae sedis</i>	<i>Incertae sedis</i>	<i>Dothideomycetes</i>	ITS	93	NR_168867.1
CF-164481	<i>Cyphellophora</i>	sp.	<i>Cyphellophoraceae</i>	<i>Chaetothyriales</i>	<i>Eurotiomycetes</i>	ITS	90	NR_163356.1
CF-166027	<i>Cyphellophora</i>	sp.	<i>Cyphellophoraceae</i>	<i>Chaetothyriales</i>	<i>Eurotiomycetes</i>	28S	98	NR_153555.1
CF-168997	<i>Capronia</i>	<i>coronata</i>	<i>Herpotrichiellaceae</i>	<i>Chaetothyriales</i>	<i>Eurotiomycetes</i>	ITS+28s	100	AF050242.1
CF-166132	<i>Cladophialophora</i>	sp.	<i>Herpotrichiellaceae</i>	<i>Chaetothyriales</i>	<i>Eurotiomycetes</i>	ITS	98	OQ913855.1
CF-166060	<i>Cladophialophora</i>	sp.	<i>Herpotrichiellaceae</i>	<i>Chaetothyriales</i>	<i>Eurotiomycetes</i>	ITS	98	OP437822.1
CF-166072	<i>Exophiala</i>	sp.	<i>Herpotrichiellaceae</i>	<i>Chaetothyriales</i>	<i>Eurotiomycetes</i>	ITS	98	OW988156.1
CF-166037	<i>Exophiala</i>	sp.	<i>Herpotrichiellaceae</i>	<i>Chaetothyriales</i>	<i>Eurotiomycetes</i>	ITS	96	OW988156.1
CF-164291	<i>Melnikomyces</i>	sp.	<i>Incertae sedis</i>	<i>Chaetothyriales</i>	<i>Eurotiomycetes</i>	ITS	88	NR_166358.1
CF-166082	<i>Phaeoannellomyces</i>	<i>elegans</i>	<i>Incertae sedis</i>	<i>Chaetothyriales</i>	<i>Eurotiomycetes</i>	ITS	100	MZ956802.1
CF-164393	<i>Penicillium</i>	<i>brevicompactum</i>	<i>Aspergillaceae</i>	<i>Eurotiales</i>	<i>Eurotiomycetes</i>	ITS	100	PP165506.1
CF-166063	<i>Penicillium</i>	sp.	<i>Aspergillaceae</i>	<i>Eurotiales</i>	<i>Eurotiomycetes</i>	ITS	95	NR_103667.2
CF-169047	<i>Neophaeomoniella</i>	sp.	<i>Celotheliaceae</i>	<i>Phaeomoniellales</i>	<i>Eurotiomycetes</i>	ITS	97	GQ153127.1/MZ127178.1
CF-169002	<i>Neophaeomoniella</i>	<i>zymoides</i>	<i>Celotheliaceae</i>	<i>Phaeomoniellales</i>	<i>Eurotiomycetes</i>	28S	99	GQ153127.1/MZ127178.1
CF-166032	<i>Neophaeomoniella</i>	sp.	<i>Celotheliaceae</i>	<i>Phaeomoniellales</i>	<i>Eurotiomycetes</i>	ITS	98	GQ153127.1
CF-166096	<i>Phaeomoniella</i>	sp.	<i>Celotheliaceae</i>	<i>Phaeomoniellales</i>	<i>Eurotiomycetes</i>	ITS	85	KX901894.1
CF-164222	<i>Phaeomoniella</i>	sp.	<i>Celotheliaceae</i>	<i>Phaeomoniellales</i>	<i>Eurotiomycetes</i>	ITS	86	KX901894.1
CF-164398	<i>Arachnopeziza</i>	sp.	<i>Arachnopezizaceae</i>	<i>Helotiales</i>	<i>Leotiomycetes</i>	ITS	98	OM951264.1
CF-164375	<i>Arachnopeziza</i>	<i>aurata</i>	<i>Arachnopezizaceae</i>	<i>Helotiales</i>	<i>Leotiomycetes</i>	ITS	100	MH558278.1
CF-166089	<i>Coleophoma</i>	sp.	<i>Dermateaceae</i>	<i>Helotiales</i>	<i>Leotiomycetes</i>	ITS	98	MK762611.1
CF-164376	<i>Xenopolyscytalum</i>	<i>pinia</i>	<i>Hamatocanthoscyphaceae</i>	<i>Helotiales</i>	<i>Leotiomycetes</i>	ITS	100	NR_156543.1

Annexes

CF-164399	<i>Hymenoscyphus</i>	sp.	<i>Helotiaceae</i>	<i>Helotiales</i>	<i>Leotiomyces</i>	ITS	97	FJ827234.1
CF-166138	<i>Proliferodiscus</i>	sp.	<i>Lachnaceae</i>	<i>Helotiales</i>	<i>Leotiomyces</i>	ITS	99	LC438558.1
CF-164261	<i>Mollisia</i>	<i>novobrunsvicensis</i>	<i>Mollisiaceae</i>	<i>Helotiales</i>	<i>Leotiomyces</i>	ITS	100	MT026439.1
CF-166097	<i>Mollisia</i>	<i>panicicola</i>	<i>Mollisiaceae</i>	<i>Helotiales</i>	<i>Leotiomyces</i>	28S	99	KF874621.1
CF-166187	<i>Oidiodendron</i>	sp.	<i>Myxotrichaceae</i>	<i>Helotiales</i>	<i>Leotiomyces</i>	ITS	99	MH864648.1
CF-164333	<i>Oidiodendron</i>	<i>tenuissimum</i>	<i>Myxotrichaceae</i>	<i>Helotiales</i>	<i>Leotiomyces</i>	ITS	99	MH864345.1
CF-164233	<i>Neocrinula</i>	<i>lambertiae</i>	<i>Neocrinulaceae</i>	<i>Helotiales</i>	<i>Leotiomyces</i>	ITS	99	MG386049.1
CF-164331	<i>Chalara</i>	sp.	<i>Pezizellaceae</i>	<i>Helotiales</i>	<i>Leotiomyces</i>	ITS	99	FR66723.1
CF-164384	<i>Nagrajchalara</i>	sp.	<i>Pezizellaceae</i>	<i>Helotiales</i>	<i>Leotiomyces</i>	ITS	96	OQ145667.1
CF-166040	<i>Nagrajchalara</i>	sp.	<i>Pezizellaceae</i>	<i>Helotiales</i>	<i>Leotiomyces</i>	ITS	96	OQ145679.1
CF-164446	<i>Lanzia</i>	<i>griselinia</i>	<i>Rutstroemiaceae</i>	<i>Helotiales</i>	<i>Leotiomyces</i>	ITS	99	MH003473.1
CF-166180	<i>Stromatinia</i>	sp.	<i>Sclerotiniaceae</i>	<i>Helotiales</i>	<i>Leotiomyces</i>	ITS	97	MH856286.1
CF-164276	<i>Tetracladium</i>	<i>terrestre</i>	<i>Solenopezaceae</i>	<i>Helotiales</i>	<i>Leotiomyces</i>	ITS	100	NR_160144
CF-164329	<i>Tricladium</i>	<i>attenuatum</i>	<i>Tricladaceae</i>	<i>Helotiales</i>	<i>Leotiomyces</i>	ITS	99	MH860241.1
CF-164338	<i>Helotiales</i>	sp.	<i>Incertae sedis</i>	<i>Helotiales</i>	<i>Leotiomyces</i>	ITS	97	MG707591.1
CF-169050	<i>Helotiales</i>	sp.	<i>Incertae sedis</i>	<i>Helotiales</i>	<i>Leotiomyces</i>	ITS	96	HE605242.1
CF-166107	<i>Helotiales</i>	sp.	<i>Incertae sedis</i>	<i>Helotiales</i>	<i>Leotiomyces</i>	ITS	98	MG707591.1
CF-166028	<i>Helotiales</i>	sp.	<i>Incertae sedis</i>	<i>Helotiales</i>	<i>Leotiomyces</i>	ITS	98	KY654691.1
CF-164397	<i>Helotiales</i>	sp.	<i>Incertae sedis</i>	<i>Helotiales</i>	<i>Leotiomyces</i>	ITS	91	FJ378851.1
CF-164371	<i>Helotiales</i>	sp.	<i>Incertae sedis</i>	<i>Helotiales</i>	<i>Leotiomyces</i>	ITS	98	KY654691.1
CF-164350	<i>Helotiales</i>	sp.	<i>Incertae sedis</i>	<i>Helotiales</i>	<i>Leotiomyces</i>	ITS	98	JF519573.1
CF-166188	<i>Lophodermium</i>	sp.	<i>Rhytismataceae</i>	<i>Rhytismatales</i>	<i>Leotiomyces</i>	ITS	95	EU520183.1
CF-166092	<i>Arthrobotrys</i>	sp.	<i>Orbiliaceae</i>	<i>Orbiliales</i>	<i>Orbiliomyces</i>	ITS	87	NR_175054.1
CF-166116	<i>Conoplea</i>	<i>fusca</i>	<i>Sarcosomataceae</i>	<i>Pezizales</i>	<i>Pezizomyces</i>	ITS+28S	100	EU552114.1
CF-166119	<i>Plectania</i>	sp.	<i>Sarcosomataceae</i>	<i>Pezizales</i>	<i>Pezizomyces</i>	ITS	98	OL653020.1
CF-164324	<i>Plectania</i>	sp.	<i>Sarcosomataceae</i>	<i>Pezizales</i>	<i>Pezizomyces</i>	ITS	98	OL653020.1
CF-164414	<i>Immersidiscosia</i>	<i>eucalypti</i>	<i>Amphisphaeriaceae</i>	<i>Amphisphaeriales</i>	<i>Sordariomyces</i>	ITS	100	AB594790.1
CF-169004	<i>Bartalinia</i>	<i>lateralis</i>	<i>Bartaliniaceae</i>	<i>Amphisphaeriales</i>	<i>Sordariomyces</i>	ITS	100	NR_161087.1
CF-164469	<i>Bartalinia</i>	<i>pondoensis</i>	<i>Bartaliniaceae</i>	<i>Amphisphaeriales</i>	<i>Sordariomyces</i>	ITS	100	NR_153599.1
CF-164325	<i>Discosia</i>	sp.	<i>Discosiaceae</i>	<i>Amphisphaeriales</i>	<i>Sordariomyces</i>	ITS	100	AB594784.1
CF-164369	<i>Phlogicylindrium</i>	sp.	<i>Phlogicylindriaceae</i>	<i>Amphisphaeriales</i>	<i>Sordariomyces</i>	28S	99	KJ869176.1
CF-166091	<i>Sarcostroma</i>	sp.	<i>Sporocadaceae</i>	<i>Amphisphaeriales</i>	<i>Sordariomyces</i>	ITS	98	EU552155.1
CF-164412	<i>Phialemonium</i>	<i>inflatum</i>	<i>Cephalothecaceae</i>	<i>Cephalothecales</i>	<i>Sordariomyces</i>	ITS	100	NR_165996.1
CF-164345	<i>Cylindrium</i>	sp.	<i>Cylindriaceae</i>	<i>Hypocreales</i>	<i>Sordariomyces</i>	ITS	98	MT223792.1
CF-164257	<i>Acrostalagus</i>	<i>luteoalbus</i>	<i>Hypocreaceae</i>	<i>Hypocreales</i>	<i>Sordariomyces</i>	ITS	100	OW987052.1
CF-164359	<i>Cosmospora</i>	sp.	<i>Nectriaceae</i>	<i>Hypocreales</i>	<i>Sordariomyces</i>	ITS	100	OW983055.1/NR_182322.1
CF-164454	<i>Dactylonectria</i>	sp.	<i>Nectriaceae</i>	<i>Hypocreales</i>	<i>Sordariomyces</i>	ITS	100	JX231152.1/MN944923.1
CF-168993	<i>Fusarium</i>	<i>oxysporum</i>	<i>Nectriaceae</i>	<i>Hypocreales</i>	<i>Sordariomyces</i>	ITS	100	LT841208.1

CF-164444	<i>Fusarium</i>	sp.	Nectriaceae	Hypocreales	Sordariomycetes	ITS	100	MT453281.1
CF-164275	<i>Fusarium</i>	incarnatum-equiseti complex	Nectriaceae	Hypocreales	Sordariomycetes	ITS	100	MG274307.1
CF-164460	<i>Volutella</i>	sp.	Nectriaceae	Hypocreales	Sordariomycetes	ITS	99	OU989510.1
CF-164466	<i>Tolypocladium</i>	sp.	Ophiocordycipitaceae	Hypocreales	Sordariomycetes	ITS	97	NR_155019.1
CF-169007	<i>Sirastachys</i>	phaeospora	Stachybotryaceae	Hypocreales	Sordariomycetes	ITS	100	KU846667.1
CF-164453	<i>Acremonium</i>	antarcticum	Incertainae sedis	Hypocreales	Sordariomycetes	ITS	100	MG250387.1
CF-166074	<i>Sarocladium</i>	sp.	Incertainae sedis	Hypocreales	Sordariomycetes	ITS	100	MK579174.1/GU189520.1
CF-166160	<i>Myrmecridium</i>	sp.	Incertainae sedis	Myrmecridiales	Sordariomycetes	ITS	99	KX306762.1
CF-169032	<i>Phaeoacremonium</i>	africanum	Togniniaceae	Togniniales	Sordariomycetes	ITS	99	NR_135940.1
CF-166113	<i>Phaeoacremonium</i>	sp.	Togniniaceae	Togniniales	Sordariomycetes	ITS	96	EU552161.1
CF-166109	<i>Anthostomella</i>	sp.	Xylariaceae	Xylariales	Sordariomycetes	ITS	98	NR_153510.1
CF-164421	<i>Anthostomella</i>	sp.	Xylariaceae	Xylariales	Sordariomycetes	ITS	99	NR_175686.1
CF-166110	<i>Anthostomelloides</i>	sp.	Xylariaceae	Xylariales	Sordariomycetes	ITS	98	NR_153510.1
CF-164462	<i>Neoanthostomella</i>	viticola	Xylariaceae	Xylariales	Sordariomycetes	ITS	100	ON400757.1
CF-164440	<i>Neoanthostomella</i>	sp.	Xylariaceae	Xylariales	Sordariomycetes	ITS	99	ON400757.1
CF-164451	<i>Neoanthostomella</i>	sp.	Xylariaceae	Xylariales	Sordariomycetes	ITS	93	NR_174847.1
CF-166165	<i>Pleurophoma</i>	sp.	Incertainae sedis	Xylariales	Sordariomycetes	ITS	98	OQ410705.1
CF-166159	<i>Pleurophoma</i>	pleurospora	Incertainae sedis	Xylariales	Sordariomycetes	ITS	100	OQ410705.1
CF-166146	<i>Arthrimum</i>	sp.	Apiosporaceae	Incertainae sedis	Sordariomycetes	ITS	100	KF144883.1
CF-164427	<i>Arthrimum</i>	sp.	Apiosporaceae	Incertainae sedis	Sordariomycetes	ITS	98	NR_166043.1
CF-164418	<i>Arthrimum</i>	kogelbergense	Apiosporaceae	Incertainae sedis	Sordariomycetes	ITS	100	NR_120272
CF-164467	<i>Sordariomycetes</i>	sp.	Incertainae sedis	Incertainae sedis	Sordariomycetes	ITS	91	MT183990.1
CF-166101	<i>Ochroconis</i>	sp.	Incertainae sedis	Incertainae sedis	Incertainae sedis	ITS+28S	97	AB564619.1
CF-164346	<i>Polyscytalum</i>	vaccinii	Incertainae sedis	Incertainae sedis	Incertainae sedis	ITS	100	NR_175211.1
CF-166052	<i>Rhexodenticula</i>	sp.	Incertainae sedis	Incertainae sedis	Incertainae sedis	ITS	98	NR_154447.1
CF-164484	<i>Scolecobasidium</i>	sp.	Incertainae sedis	Incertainae sedis	Incertainae sedis	ITS	88	OQ917081.1
CF-164413	<i>Pseudosigmoidea</i>	sp.	Incertainae sedis	Incertainae sedis	Incertainae sedis	ITS	96	NR_185383
CF-164400	<i>Dendrosporium</i>	sp.	Incertainae sedis	Incertainae sedis	Incertainae sedis	ITS+28S	93	MH855767.1
CF-164475	<i>Gyrophthrix</i>	sp.	Incertainae sedis	Incertainae sedis	Incertainae sedis	ITS	99	ON400759.1
CF-164406	unidentified	fungus	Incertainae sedis	Incertainae sedis	Incertainae sedis	-	-	-
CF-164396	unidentified	fungus	Incertainae sedis	Incertainae sedis	Incertainae sedis	-	-	-
CF-166114	unidentified	fungus	Incertainae sedis	Incertainae sedis	Incertainae sedis	-	-	-
CF-166103	unidentified	fungus	Incertainae sedis	Incertainae sedis	Incertainae sedis	-	-	-
CF-168963	unidentified	fungus	Incertainae sedis	Incertainae sedis	Incertainae sedis	-	-	-
CF-166098	<i>Cryptomarasmius</i>	sp.	Physalacriaceae	Agaricales	Agaricomycetes	ITS	94	OQ725929.1
CF-164455	<i>Coprinellus</i>	micaceus	Psathyrellaceae	Agaricales	Agaricomycetes	ITS	100	MK656239.1
CF-164301	<i>Serpula</i>	himantioidea	Serpulaceae	Boletales	Agaricomycetes	ITS	99	GU187545.1

Annexes

CF-164389	<i>Clavulina</i>	sp.	<i>Hydnaceae</i>	<i>Cantharellales</i>	<i>Agaricomycetes</i>	ITS	92	HQ022108.1
CF-164252	<i>Sistotrema</i>	sp.	<i>Hydnaceae</i>	<i>Cantharellales</i>	<i>Agaricomycetes</i>	ITS	93	KF218968.1
CF-164409	<i>Sistotrema</i>	sp.	<i>Hydnaceae</i>	<i>Cantharellales</i>	<i>Agaricomycetes</i>	ITS	99	KC965692.1
CF-164268	<i>Tulasnella</i>	sp.	<i>Tulasnellaceae</i>	<i>Cantharellales</i>	<i>Agaricomycetes</i>	ITS	99	AB369940.1
CF-166036	<i>Corticium</i>	sp.	<i>Corticaceae</i>	<i>Corticiales</i>	<i>Agaricomycetes</i>	ITS	92	MH520061.1
CF-164227	<i>Corticium</i>	sp.	<i>Corticaceae</i>	<i>Corticiales</i>	<i>Agaricomycetes</i>	ITS	92	MW805881.1
CF-164430	<i>Marchandiomyces</i>	sp.	<i>Corticaceae</i>	<i>Corticiales</i>	<i>Agaricomycetes</i>	28S	97	AY583332.1
CF-169012	<i>Phanerochaete</i>	sp.	<i>Phanerochaetaceae</i>	<i>Polyporales</i>	<i>Agaricomycetes</i>	ITS	99	NR_175173.1
CF-164344	<i>Trametes</i>	<i>versicolor</i>	<i>Polyporaceae</i>	<i>Polyporales</i>	<i>Agaricomycetes</i>	ITS	100	NR_154494.1
CF-166155	<i>Cystobasidium</i>	<i>slooffiae</i>	<i>Cystobasidiaceae</i>	<i>Cystobasidiales</i>	<i>Cystobasidiomycetes</i>	28S	99	AB025994.2
CF-166083	<i>Sporobolomyces</i>	<i>roseus</i>	<i>Sporidiobolaceae</i>	<i>Sporidiobolales</i>	<i>Microbotryomycetes</i>	ITS	100	KY611834.1
CF-166129	<i>Wallemia</i>	<i>mellicola</i>	<i>Wallemiaceae</i>	<i>Wallemiales</i>	<i>Wallemiomycetes</i>	ITS	100	OP596062.1
CF-164405	<i>Umbelopsis</i>	sp.	<i>Umbelopsidaceae</i>	<i>Umbelopsidales</i>	<i>Incertae sedis</i>	28S	99	MF417090.1

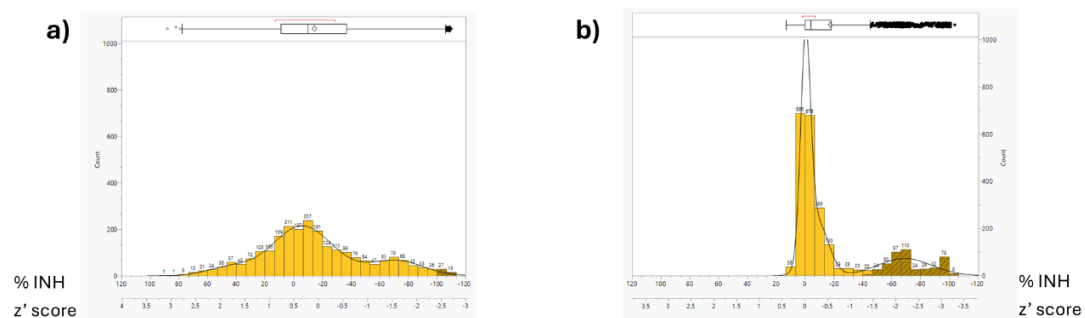


Figure S1. Distribution of antifungal activity based on (a) absorbance and (b) fluorescence data against *Magnaporthe grisea* CF-105765, including extracts from BRFT medium. The x-axis shows the range of percentage of inhibition and the corresponding z' score values, while the y-axis shows the frequency of occurrences.

Table S2. Categorization of the active strains according to their activity profiles obtained from conditions without SAHA (**n**), induced by SAHA (**S**) or common to both fermentation conditions with and without SAHA (**c**), against the four fungal phytopathogens **BC** (*Botrytis cinerea*), **CA** (*Colletotrichum acutatum*), **FP** (*Fusarium proliferatum*) and **MG** (*Magnaporthe grisea*), and the HepG2 cell line.

Strain	Taxonomy	BC			CA			FP			MG			HepG2			LC-MS Dereplication
		n	c	S	n	c	S	n	c	S	n	c	S	n	c	S	
CF-164279	<i>Phomatodes nebulosa</i>	0	1	0	0	1	0	0	1	0	0	1	0	0	1	0	palmarumycins B1, B9, C12, C13, C15 & C16, preussomerins B & L, stemphytoxin I
CF-164387	<i>Phomatodes nebulosa</i>	0	1	0	0	1	0	0	1	0	0	1	0	0	1	0	palmarumycins C15 & C16, preussomerin B, stemphytoxin I
CF-164398	<i>Arachnopeziza</i> sp.	0	1	0	0	1	0	0	1	0	0	1	0	0	1	0	myriocin
CF-168994	<i>Tremateia</i> sp.	0	1	0	0	1	0	0	1	0	0	1	0	0	0	0	lecanorin, hyalodendrin
CF-168996	<i>Phoma</i> sp.	0	1	0	0	1	0	0	1	0	0	1	0	0	0	0	lecanorin, hyalodendrin
CF-164385	<i>Nodulosphaeria cirsi</i>	0	1	0	0	0	1	0	1	0	0	1	0	0	1	0	integrastatins A & B, radicicol, heptelidic acid, massarilactone H
CF-168984	<i>Alföldia</i> sp.	0	1	0	1	0	0	1	0	0	0	1	0	1	0	0	hyalodendrin, gliovictin
CF-164467	<i>Sordariomycetes</i> sp.	1	0	0	1	0	0	0	0	0	0	1	0	1	0	0	leucinostatin A/U, B & K, pyrenocine G
CF-166102	<i>Phomatodes nebulosa</i>	0	0	0	1	0	0	1	0	0	0	1	0	0	1	0	palmarumycins C15 & C16, preussomerin B, stemphytoxin I, zearalenone
CF-164236	<i>Flammeascooma</i> sp.	0	0	1	0	0	0	1	0	0	0	1	0	0	1	0	6-(1-Hydroxyethyl)-5-hydroxy-2,7-dimethoxy-1,4-naphthoquinone, mycophenolic acid, rubellin A
CF-164341	<i>Cryptocoryneum</i> sp.	0	0	1	0	0	0	0	1	0	0	1	0	0	1	0	palmarumycins B9, C15 & C16, preussomerins B & L, stemphytoxin I
CF-164386	<i>Phomatodes nebulosa</i>	0	0	1	0	0	0	0	1	0	0	1	0	0	1	0	palmarumycins C16 & C15, preussomerin B, stemphytoxin I, zearalenone
CF-164451	<i>Neoanthostomella</i> sp.	0	0	0	0	0	0	0	0	1	0	1	0	0	1	0	antibiotic TMC 264, cinatrin C1/C2/C3, rhizopicin A
CF-164254	<i>Alternaria</i> sp.	0	0	0	0	0	0	0	0	1	0	0	0	1	0	0	7-O-ethylfulvic acid, 3-hydroxy-5,7-dimethoxy-2-(2-oxopropyl)naphthalene-1,4-dione, altenuene
CF-164344	<i>Trametes versicolor</i>	1	0	0	0	0	0	0	0	0	1	0	0	1	0	0	
CF-169007	<i>Sirastachys phaeospora</i>	1	0	0	0	0	0	0	0	0	0	1	0	0	0	0	mellein
CF-164345	<i>Cylindrium</i> sp.	1	0	0	0	0	0	0	0	0	0	0	1	0	0	0	mellein and 4/3-hydroxymellein
CF-164389	<i>Clavulina</i> sp.	1	0	0	0	0	0	0	0	0	0	0	0	0	1	0	
CF-166074	<i>Sarocladium</i> sp.	1	0	0	0	0	0	0	0	0	0	0	0	0	0	0	
CF-164227	<i>Corticium</i> sp.	0	1	0	0	0	0	0	0	0	0	1	0	0	1	0	connatusin B
CF-166114	unidentified fungus	0	1	0	0	0	0	0	0	0	0	1	0	0	1	0	chaetoglobosin N & K
CF-166164	<i>Neostagonospora</i> sp.	0	1	0	0	0	0	0	0	0	0	1	0	0	0	0	2-(3,4-epoxy-5-heptenyl)-5-methylpyrrole, mellein
CF-164425	<i>Microsphaeropsis arundinis</i>	0	1	0	0	0	0	0	0	0	0	0	0	0	0	0	deoxydihydrofusicin, LL-D-253g, resorcylic acid
CF-164396	unidentified fungus	0	1	0	0	0	0	0	0	0	0	0	0	0	0	0	
CF-164382	<i>Dothidea eucalypti</i>	0	0	1	0	0	0	0	0	0	0	0	1	0	0	1	
CF-164331	<i>Chalara</i> sp.	0	0	1	0	0	0	0	0	0	0	0	1	0	1	0	emestrin
CF-164488	<i>Dothiora coronillae</i>	0	0	1	0	0	0	0	0	0	0	0	1	1	0	0	monocerin
CF-166187	<i>Oidiodendron</i> sp.	0	0	1	0	0	0	0	0	0	0	1	0	0	1	0	asteric acid, bisdechlorodihydrogeodin
CF-164416	<i>Pleosporales</i> sp.	0	0	1	0	0	0	0	0	0	0	1	0	1	0	0	radicidin
CF-166098	<i>Cryptomarasmius</i> sp.	0	0	1	0	0	0	0	0	0	0	1	0	0	1	0	diocinol
CF-164483	<i>Equiseticola</i> sp.	0	0	1	0	0	0	0	0	0	0	1	0	0	1	0	aspothalasins, infectopyrone
CF-164261	<i>Mollisia novobrunsvicensis</i>	0	0	1	0	0	0	0	0	0	0	1	0	0	0	0	cerebroside B
CF-166041	<i>Pyrenochaeta pinicola</i>	0	0	1	0	0	0	0	0	0	0	1	0	0	0	0	9-chloro-10-hydroxy-8-methoxycarbonyl-4-methylene-2,5-dioxabicyclodec-7-en-3-one, radicidin
CF-164378	<i>Sclerostagonospora</i> sp.	0	0	1	0	0	0	0	0	0	0	1	0	0	0	0	11,12-hydroxyeudesm-4-en-o-one, dihydroilludinal M
CF-164440	<i>Neoanthostomella</i> sp.	0	0	1	0	0	0	0	0	0	0	1	0	0	0	0	cinatrin B, connatusin B, illudinal M
CF-164281	<i>Neoonothium</i> sp.	0	0	1	0	0	0	0	0	0	1	0	0	0	0	0	antibiotic L 783277, cochliomycin D/E/F
CF-166036	<i>Corticium</i> sp.	0	0	1	0	0	0	0	0	0	0	0	0	0	1	0	leucinostatin K
CF-166144	<i>Juncaceicola</i> sp.	0	0	1	0	0	0	0	0	0	0	0	0	0	1	0	6-(1-hydroxyethyl)-5-hydroxy-2,7-dimethoxy-1,4-naphthoquinone, radicicol
CF-164233	<i>Neocrinula lambertiae</i>	0	0	1	0	0	0	0	0	0	0	0	0	0	1	0	leucinostatin A/U & B
CF-166157	<i>Ascochyta</i> sp.	0	0	1	0	0	0	0	0	0	0	0	0	0	1	0	brefeldin A, ovalacin
CF-166110	<i>Anthostomelloides</i> sp.	0	0	1	0	0	0	0	0	0	0	0	0	0	1	0	anhydrosepedonin, cytochalasins H & E, heptelidic acid, ternatin
CF-166109	<i>Anthostomella</i> sp.	0	0	1	0	0	0	0	0	0	0	0	0	0	1	0	anhydrosepedonin, cytochalasins, heptelidic acid, ternatin
CF-166063	<i>Penicillium</i> sp.	0	0	1	0	0	0	0	0	0	0	0	0	0	0	1	antibiotic NG 011

Annexes

CF-164445	<i>Wojnowiciella dactylidis</i>	0	0	1	0	0	0	0	0	0	0	0	0	0	0	0	0	0	1	11-desacetoxywortmannin, asteric acid, bisdechlorodihydrogeodin, epolone A, methylidihydromitorubin, nomofungin, pycnidione
CF-164478	<i>Thyridaria macrostomoides</i>	0	0	1	0	0	0	0	0	0	0	0	0	0	0	0	0	0	Oxasetin	
CF-166058	<i>Scleroconidioma sphagnicola</i>	0	0	1	0	0	0	0	0	0	0	0	0	0	0	0	0	0	0	antibiotic AS 2077715
CF-164234	<i>Neofusicoccum protearum</i>	0	0	1	0	0	0	0	0	0	0	0	0	0	0	0	0	0	0	mellein
CF-166091	<i>Sarcostroma</i> sp.	0	0	1	0	0	0	0	0	0	0	0	0	0	0	0	0	0	0	diorcinol, hyalodendrin, nemanolone A
CF-164337	<i>Magnibotryascoma mali</i>	0	0	1	0	0	0	0	0	0	0	0	0	0	0	0	0	0	0	connatusin B, deoxydihydrofusicin, diocinol F
CF-164439	<i>Didymosphaeria variabile</i>	0	0	1	0	0	0	0	0	0	0	0	0	0	0	0	0	0	0	
CF-164283	<i>Pyrenochaeta</i> sp.	0	0	1	0	0	0	0	0	0	0	0	0	0	0	0	0	0	0	ascomycone A, mellein
CF-164290	<i>Fortiomyces</i> sp.	0	0	1	0	0	0	0	0	0	0	0	0	0	0	0	0	0	0	
CF-164357	<i>Microsphaeropsis arundinis</i>	0	0	1	0	0	0	0	0	0	0	0	0	0	0	0	0	0	0	
CF-164362	<i>Dothiora maculans</i>	0	0	1	0	0	0	0	0	0	0	0	0	0	0	0	0	0	0	stemphol
CF-164383	<i>Pseudocamarosporium brabeji</i>	0	0	1	0	0	0	0	0	0	0	0	0	0	0	0	0	0	0	
CF-164466	<i>Tolypocladium</i> sp.	0	0	1	0	0	0	0	0	0	0	0	0	0	0	0	0	0	0	sch-217048, sch-218157, sch-378161, pleosporin A
CF-164471	<i>Coniothyrium</i> sp.	0	0	1	0	0	0	0	0	0	0	0	0	0	0	0	0	0	0	
CF-166027	<i>Cyphellophora</i> sp.	0	0	1	0	0	0	0	0	0	0	0	0	0	0	0	0	0	0	cordycerebroside A/B
CF-166040	<i>Nagrajchalara</i> sp.	0	0	1	0	0	0	0	0	0	0	0	0	0	0	0	0	0	0	
CF-166066	<i>Anungitea grevilleae</i>	0	0	1	0	0	0	0	0	0	0	0	0	0	0	0	0	0	0	
CF-166089	<i>Coleophoma</i> sp.	0	0	1	0	0	0	0	0	0	0	0	0	0	0	0	0	0	0	
CF-166103	unidentified fungus	0	0	1	0	0	0	0	0	0	0	0	0	0	0	0	0	0	0	
CF-168990	<i>Libertasomyces aloeticus</i>	0	0	1	0	0	0	0	0	0	0	0	0	0	0	0	0	0	0	libertamide
CF-164275	<i>Fusarium incarnatum-equiseti</i> complex	0	0	0	1	0	0	0	0	0	0	1	0	0	0	1	0			equisetin
CF-164329	<i>Tricladium attenuatum</i>	0	0	0	0	1	0	0	0	0	0	0	0	0	0	1	0			virgineone
CF-166146	<i>Arthrinium</i> sp.	0	0	0	0	1	0	0	0	0	0	0	0	0	0	0	0	0	0	
CF-166120	<i>Neodidymelliopsis</i> sp.	0	0	0	0	0	0	0	0	0	0	1	0	0	0	0	0	0	0	
CF-166181	<i>Keissleriella</i> sp.	0	0	0	0	0	0	0	0	0	0	0	1	0	0	0	0	0	0	
CF-166129	<i>Wallemia mellicola</i>	0	0	0	0	0	0	0	0	0	0	0	1	0	0	0	0	0	0	
CF-164257	<i>Acrostalagmus luteoalbus</i>	0	0	0	0	0	0	0	0	0	0	0	1	0	0	0	0	0	0	exophilic acid
CF-169011	<i>Phaeosphaeriaceae</i> sp.	0	0	0	0	0	0	0	0	0	0	0	1	0	0	0	0	0	0	coleophomone A/B
CF-164402	<i>Dothiora oleae</i>	0	0	0	0	0	0	0	0	0	0	0	1	0	0	0	0	0	0	
CF-164274	<i>Paraphaeosphaeria verruculosa</i>	0	0	0	0	0	0	0	0	0	0	0	1	0	0	0	0	0	0	secalonic acid C, violaceol I/II
CF-164414	<i>Immersidiscosia eucalypti</i>	0	0	0	0	0	0	0	0	0	0	0	1	0	0	0	0	0	0	
CF-164450	<i>Pleomonodictys</i> sp.	0	0	0	0	0	0	0	0	0	0	0	1	0	0	0	0	0	0	
CF-164479	<i>Pyrenochaetopsis leptospora</i>	0	0	0	0	0	0	0	0	0	0	0	1	0	0	0	0	0	0	
CF-166025	<i>Ramusculicola</i> sp.	0	0	0	0	0	0	0	0	0	0	0	1	0	0	0	0	0	0	
CF-166042	<i>Paracamarosporium leucadendri</i>	0	0	0	0	0	0	0	0	0	0	0	1	0	0	0	0	0	0	
CF-166119	<i>Plectania</i> sp.	0	0	0	0	0	0	0	0	0	0	0	1	0	0	0	0	0	0	
CF-166138	<i>Proliferodiscus</i> sp.	0	0	0	0	0	0	0	0	0	0	0	1	0	0	0	0	0	0	
CF-166147	<i>Didymella pinodella</i>	0	0	0	0	0	0	0	0	0	0	0	1	0	0	0	0	0	0	
CF-166142	<i>Paraconiothyrium brasiliense</i>	0	0	0	0	0	0	0	0	0	0	0	1	0	0	0	0	0	0	
CF-168971	<i>Phaeosphaeria</i> sp.	0	0	0	0	0	0	0	0	0	0	0	1	0	0	0	0	0	0	
CF-169016	<i>Pyrenochaeta nobilis</i>	0	0	0	0	0	0	0	0	0	0	0	1	0	0	0	0	0	0	
CF-169031	<i>Phaeosphaeria podocarpi</i>	0	0	0	0	0	0	0	0	0	0	0	1	0	0	0	0	0	0	
CF-169052	<i>Vaginatishpora fuckelii</i>	0	0	0	0	0	0	0	0	0	0	0	1	0	0	0	0	0	0	
CF-164301	<i>Serpula himantoides</i>	0	0	0	0	0	0	0	0	0	0	0	1	0	1	0	0	0	0	
CF-164438	<i>Forliomyces</i> sp.	0	0	0	0	0	0	0	0	0	0	0	1	0	1	0	0	0	0	
CF-164476	<i>Desertiserpentica</i> sp.	0	0	0	0	0	0	0	0	0	0	0	1	0	1	0	0	0	0	illudin M, MDN-0101, N-deoxykanthomycin
CF-164273	<i>Cryptocoryneum</i> sp.	0	0	0	0	0	0	0	0	0	0	0	1	0	0	1	0			palmarumycins B1, C15, preussomerin B
CF-164284	<i>Pyrenochaetopsis leptospora</i>	0	0	0	0	0	0	0	0	0	0	0	1	0	0	1	0			
CF-164330	<i>Angustimassarina</i> sp.	0	0	0	0	0	0	0	0	0	0	0	1	0	0	1	0			

CF-166111	<i>Acrospermum</i> sp.	0	0	0	0	0	0	0	0	1	0	0	0	1	questionomycin A
CF-168961	<i>Neosetophoma</i> sp.	0	0	0	0	0	0	0	0	1	0	0	0	1	6-(1-hydroxyethyl)-5-hydroxy-2,7-dimethoxy-1,4-naphthoquinone, methyl dihydromitorubin
CF-164269	<i>Pyrenochaetopsis leptospora</i>	0	0	0	0	0	0	0	0	1	0	0	0	1	preussomerin L, stemphytoxin III
CF-164238	<i>Austroafricana parva</i>	0	0	0	0	0	0	0	0	1	0	1	0	0	
CF-164444	<i>Fusarium</i> sp.	0	0	0	0	0	0	0	0	0	1	0	1	0	13a-hydroxylucilactaene, lucilactaene
CF-166183	<i>Curvularia protuberata</i>	0	0	0	0	0	0	0	0	1	0	1	0	0	11-Hydroxycurvularin, curvularin, resorcytide
CF-164333	<i>Oidiodendron tenuissimum</i>	0	0	0	0	0	0	0	0	1	0	1	0	0	deoxydihydrofusicin, infectopyrone
CF-164448	<i>Pseudocoleophoma</i> sp.	0	0	0	0	0	0	0	0	1	0	1	0	0	7-chloro-6-methoxymellein, dihydrohynophilitin, diorcinol F, preussin G
CF-164449	<i>Verrucocladosporium carpobroti</i>	0	0	0	0	0	0	0	0	0	1	1	0	0	
CF-164321	<i>Pleosporales</i> sp.	0	0	0	0	0	0	0	0	1	0	0	0	0	
CF-164376	<i>Xenopolyscytalum pinea</i>	0	0	0	0	0	0	0	0	1	0	0	0	0	
CF-166178	<i>Pseudoascochyta</i> sp.	0	0	0	0	0	0	0	0	1	0	0	0	0	
CF-164426	<i>Stagonospora</i> sp.	0	0	0	0	0	0	0	0	0	1	0	0	0	11,12-hydroxyeudesm-4-en-3-one, dihydrohynophilitin, fiscalins A & C
CF-164455	<i>Coprinellus micaceus</i>	0	0	0	0	0	0	0	0	1	0	0	0	0	
CF-166096	<i>Phaeomoniella</i> sp.	0	0	0	0	0	0	0	0	1	0	0	0	0	quinolactacin A2
CF-166132	<i>Cladophialophora</i> sp.	0	0	0	0	0	0	0	0	1	0	0	0	0	radicidin
CF-166148	<i>Didymella pinodella</i>	0	0	0	0	0	0	0	0	0	1	0	0	0	
CF-166185	<i>Botryobambusa</i> sp.	0	0	0	0	0	0	0	0	1	0	0	0	0	
CF-169051	<i>Chromolaenicola</i> sp.	0	0	0	0	0	0	0	0	1	0	0	0	0	funicone
CF-164349	<i>Anteaglonium</i> sp.	0	0	0	0	0	0	0	0	1	0	0	0	0	ascochitin, diorcinol F
CF-164411	<i>Dothiora oleae</i>	0	0	0	0	0	0	0	0	0	1	0	0	0	
CF-166060	<i>Cladophialophora</i> sp.	0	0	0	0	0	0	0	0	1	0	0	0	0	radicicol
CF-168985	<i>Banksiophoma</i> sp.	0	0	0	0	0	0	0	0	1	0	0	0	0	
CF-169002	<i>Neophaeomoniella zymoides</i>	0	0	0	0	0	0	0	0	1	0	0	0	0	
CF-169033	<i>Alfoldia</i> sp.	0	0	0	0	0	0	0	0	1	0	0	0	0	

No. of extracts	<i>B. cinerea</i>				<i>C. acutatum</i>				<i>F. proliferatum</i>				<i>M. grisea</i>			
Medium	none	common	SAHA	total	none	common	SAHA	total	none	common	SAHA	total	none	common	SAHA	total
BRFT	4	10	25	39	4	10	0	14	2	6	1	9	2	28	4	34
LSFM	2	8	10	20	2	4	0	6	4	8	0	12	6	26	16	48
MCKX	1	0	14	15	1	2	0	3	3	0	2	5	11	22	21	54
SMK-II	4	6	12	22	0	2	0	2	0	4	0	4	14	32	18	64
YES	0	2	15	17	0	2	2	4	1	4	1	6	8	28	18	54
total	11	26	76	113	7	20	2	29	10	22	4	36	41	136	77	254
hit-rate (%)	0.47	1.10	3.22	2362	0.30	0.85	0.08	2362	0.42	0.93	0.17	2362	1.74	5.76	3.26	2362
stains				60				12				13				83

Figure S2. Distribution of the hit population for each phytopathogen in the different fermentation media and in presence or absence of SAHA.

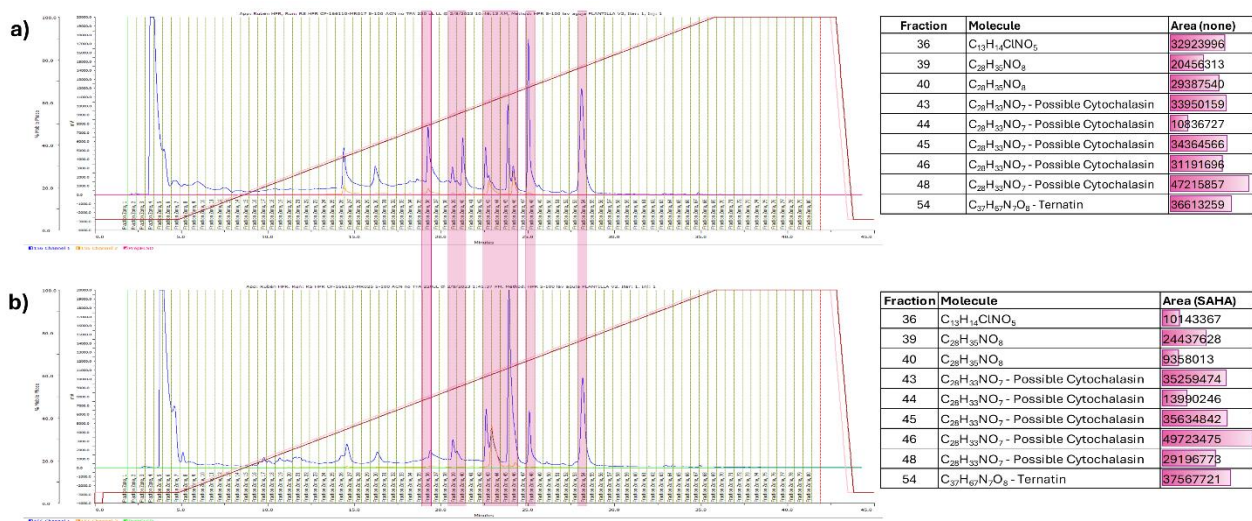


Figure S3. Comparative analysis of HPLC profiles of *Anthostomelloides leucospermi* CF-166110 grown in SMK-II in **(a)** absence and **(b)** presence of SAHA. HPLC/UV at 210 nm profiles in blue, 280 nm in orange and B gradient (5-100% ACN/H₂O) in red.

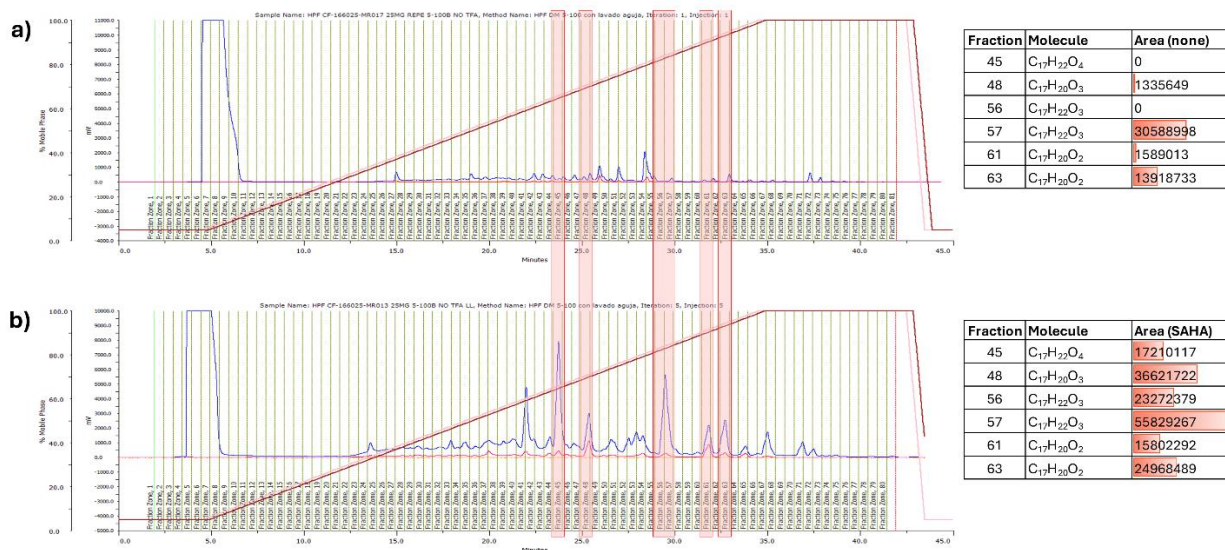


Figure S4. Comparative analysis of HPLC profiles of *Ramusculicola* sp. CF-166025 grown in SMK-II in **(a)** absence and **(b)** presence of SAHA. HPLC/UV at 210 nm profiles in blue, 280 nm in orange and B gradient (5-100% ACN/H₂O) in red.

Structural elucidation of the new compound *libertamide*

After LC-DAD-HRMS analysis, the target compound could not be dereplicated against our in-house library (Pérez-Victoria et al., 2016) and the molecular formula $C_{16}H_{27}NO_2$ was assigned based on the observed ion $[M+H]^+$ at m/z 266.2119 (calcd. for $C_{16}H_{28}NO_2 + = 266.2115$, $Dm = 1.7$ ppm). Attempts to dereplicate the compound based on its molecular formula and the fungal nature of the producer strain did not retrieve any candidate when querying the Dictionary of Natural Products or the Natural Products Atlas (Pérez-Victoria, 2024; van Santen et al., 2022), suggesting the putative novelty of the target compound. Structure elucidation was then pursued by NMR spectroscopy. A set of 1D (1H and ^{13}C) and 2D (COSY, TOCSY, NOESY, HSQC and HMBC) NMR spectra were recorded for the structural determination. Interpretation of the 1H , ^{13}C , HSQC and HMBC spectra revealed the presence of 2 quaternary carbons (corresponding to ketone and amide carbonyls at δ_C 209.2 and δ_C 165.2 respectively), 4 methines (including two olefinic carbons at δ_C 111.2 and δ_C 128.9, and two aliphatic methines at δ_C 43.1 and δ_C 52.7), 7 aliphatic methylenes in the range δ_C 23-46 and finally 3 methyls (one as a triplet corresponding to an aliphatic chain end and two as doublets). Detailed analysis of the COSY and TOCSY correlations identified different spin systems which could be connected using the key long-range correlations observed in the HMBC spectrum rendering the final connectivity of the compound (Figure S4). The key NOEs observed between the olefinic proton H-1' and both H-2 and H-11 (Figure S4) determined the stereochemistry of the tertiary amide bond, placing olefinic C-1' in a *cis* display with respect to C-2. Interestingly, EXSY-type cross peaks due to chemical exchange are likewise clearly observed in the NOESY spectrum involving the protons at the five-membered heterocycle, indicating an equilibrium with the minor *trans* isomer along the amide bond (Figure S5). Such *cis/trans* amide bond equilibrium (at a ratio ca. 70:30 according to signal integration in the 1H NMR spectrum) resembles that frequently found for proline residues in peptides. Additionally, the NMR spectra likewise showed minor signals of closely related species which must correspond to diastereomers with different relative stereochemistry at the two chiral centers C-2 and C-4. The relative stereochemistry for the main diastereomer of the *cis* isomer could not be determined though. Epimerization at C-2, surrounded by two carbonyl groups, must proceed easily in solution, explaining the presence of diastereomers as it has been reported for the structurally related *scalusamides* A–C (Tsuda et al., 2005).

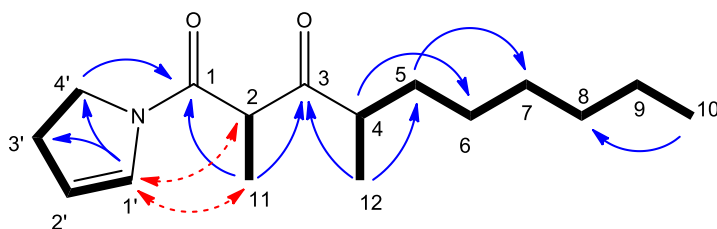


Figure S5. Key COSY and TOCSY correlations (bold bonds) determined the different spin systems of *libertamide*. Key HMBC correlations (H to C, blue arrows) connect the different spin systems and render the connectivity of the compound. Key NOEs (dashed red arrows) were observed for the main *cis* isomer along the tertiary amide bond of the compound.

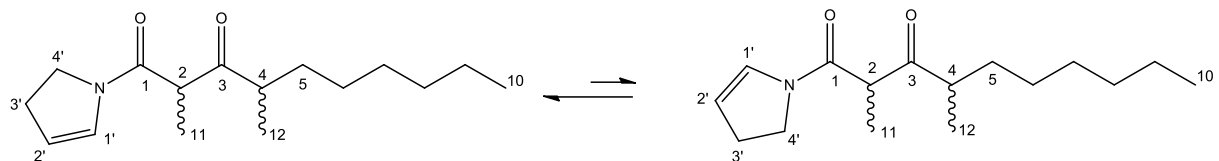


Figure S6. Amide bond cis/trans equilibrium in the new compound *libertamide*.

Table S3. NMR data for *libertamide* (main *cis* isomer) (500 MHz, CD₃OD 24 °C)

Position	δ_C , type	δ_H , mult. (<i>J</i> in Hz)
1	165.2, C	
2	52.7, CH	3.35, m
3	209.2, C	
4	43.1, CH	2.72, dq (13.4, 6.4)
5	33.6, CH ₂	1.21, m
		1.77, m
6	27.7, CH ₂	1.18, m
7	29.9, CH ₂	1.18, m
8	32.2, CH ₂	1.19, m
9	23.1, CH ₂	1.24, m
10	14.31, CH ₃	0.88, t (6.9)
11	13.0, CH ₃	1.29, d (6.9)
12	18.0, CH ₃	0.92, d (6.9)
1'	128.9, CH	6.23, ddd (7.0, 2.5, 2.5)
2'	111.2, CH ₃	4.71, dd (7.0, 2.5)
3'	28.0, CH ₂	2.03, m
		2.00, m
4'	45.6, CH ₂	3.62, m
		3.59, m

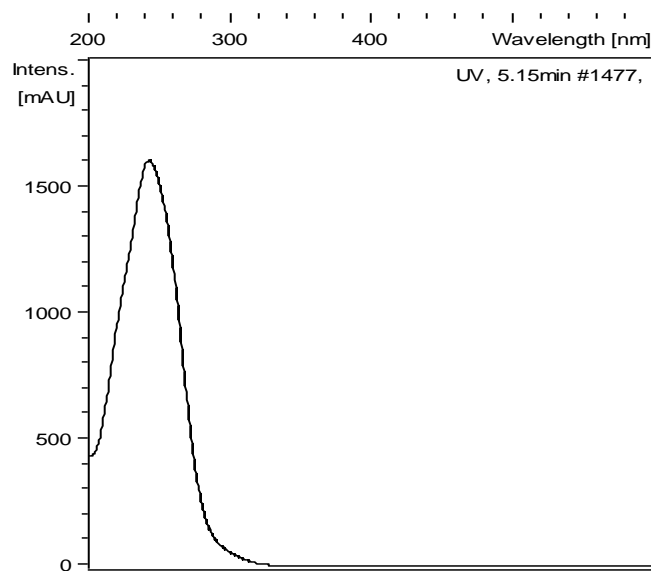


Figure S7. UV (DAD) spectrum of *libertamide*.

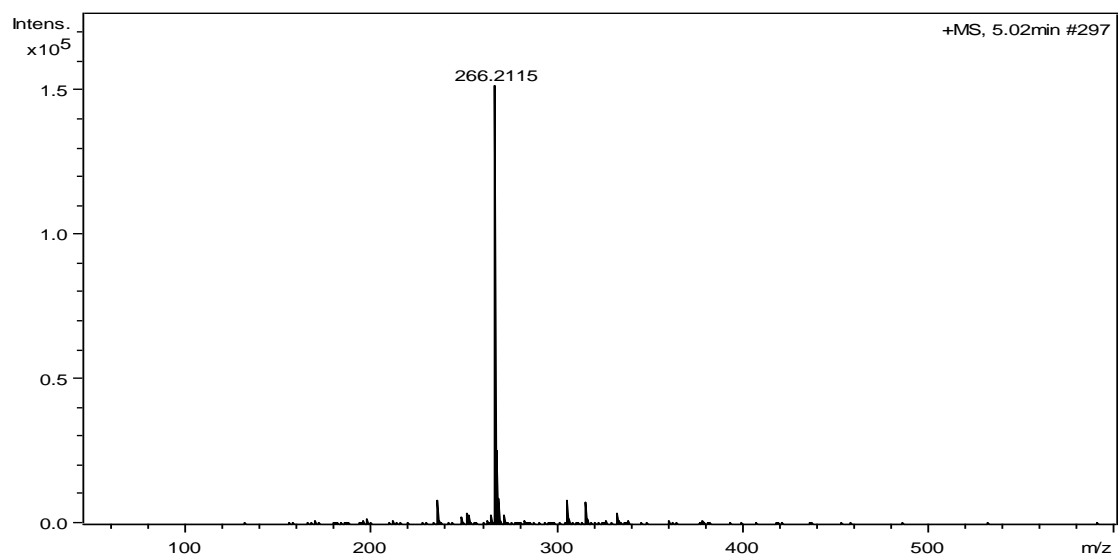


Figure S8. ESITOF HRMS spectrum of *libertamide*.

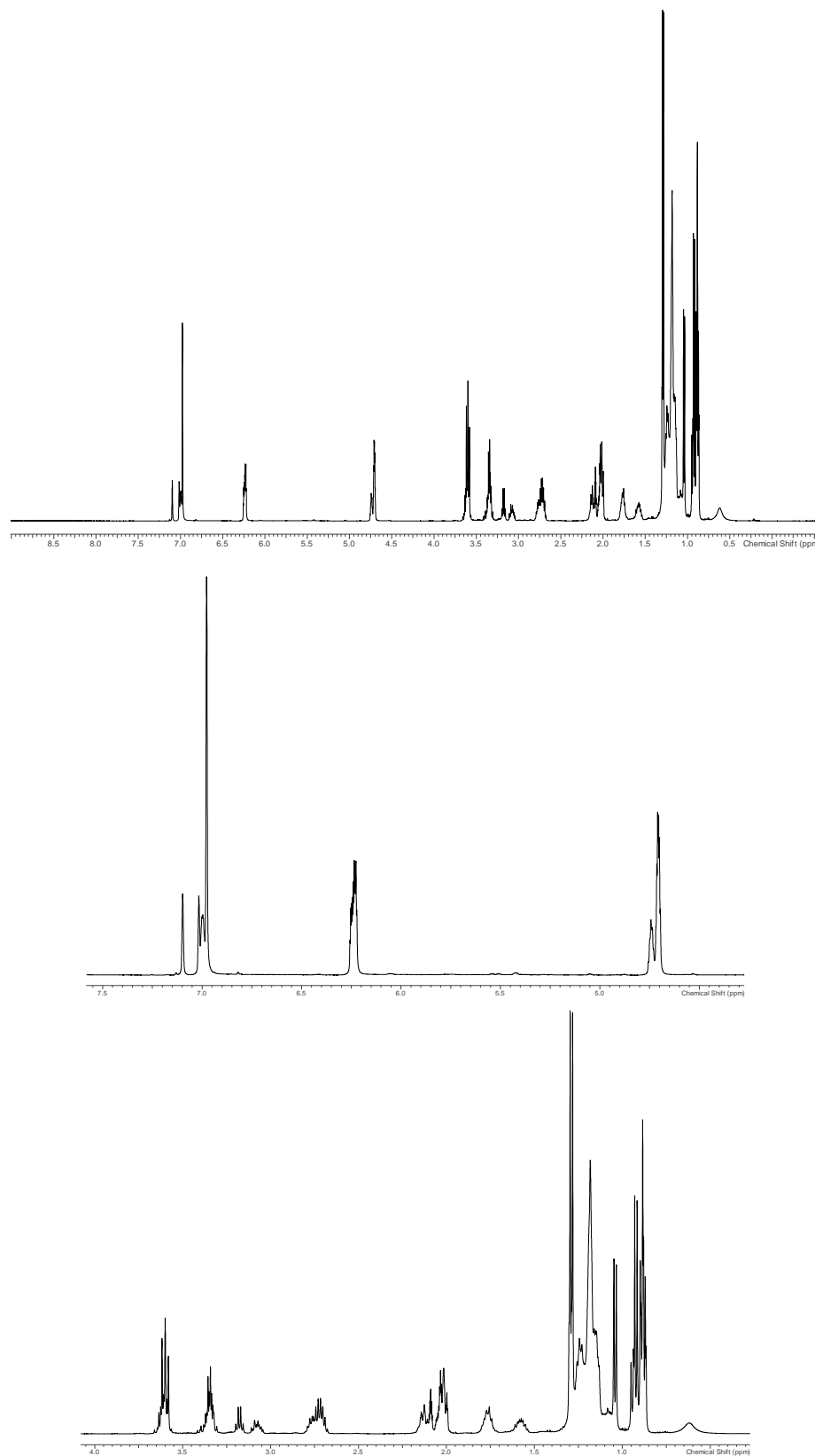


Figure S9. ^1H NMR spectrum of *libertamide*, showing expanded regions (500 MHz, CD_3OD 24 °C).

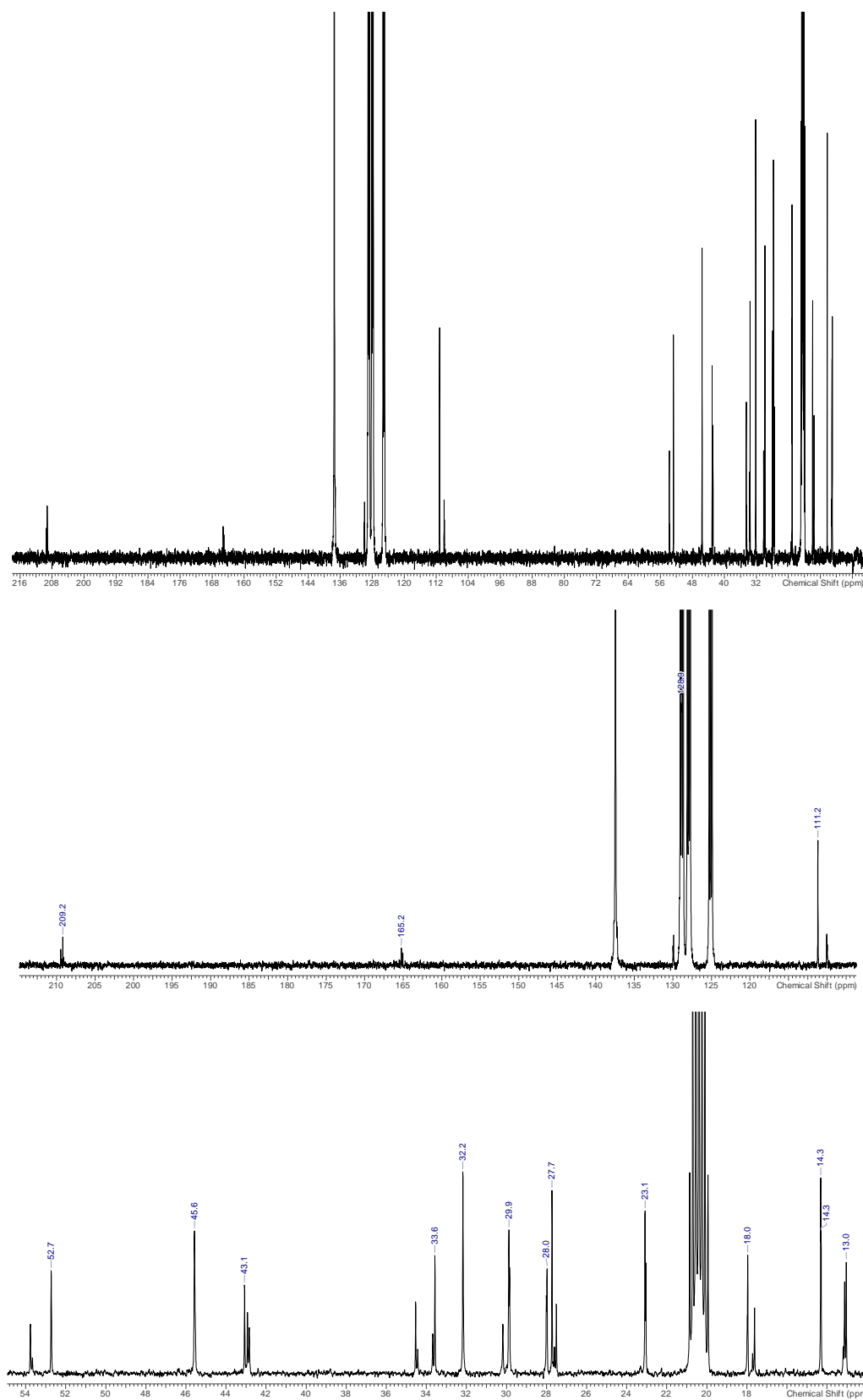


Figure S10. ^{13}C NMR spectrum of *libertamide*, showing expanded regions (125 MHz, CD_3OD 24 °C).

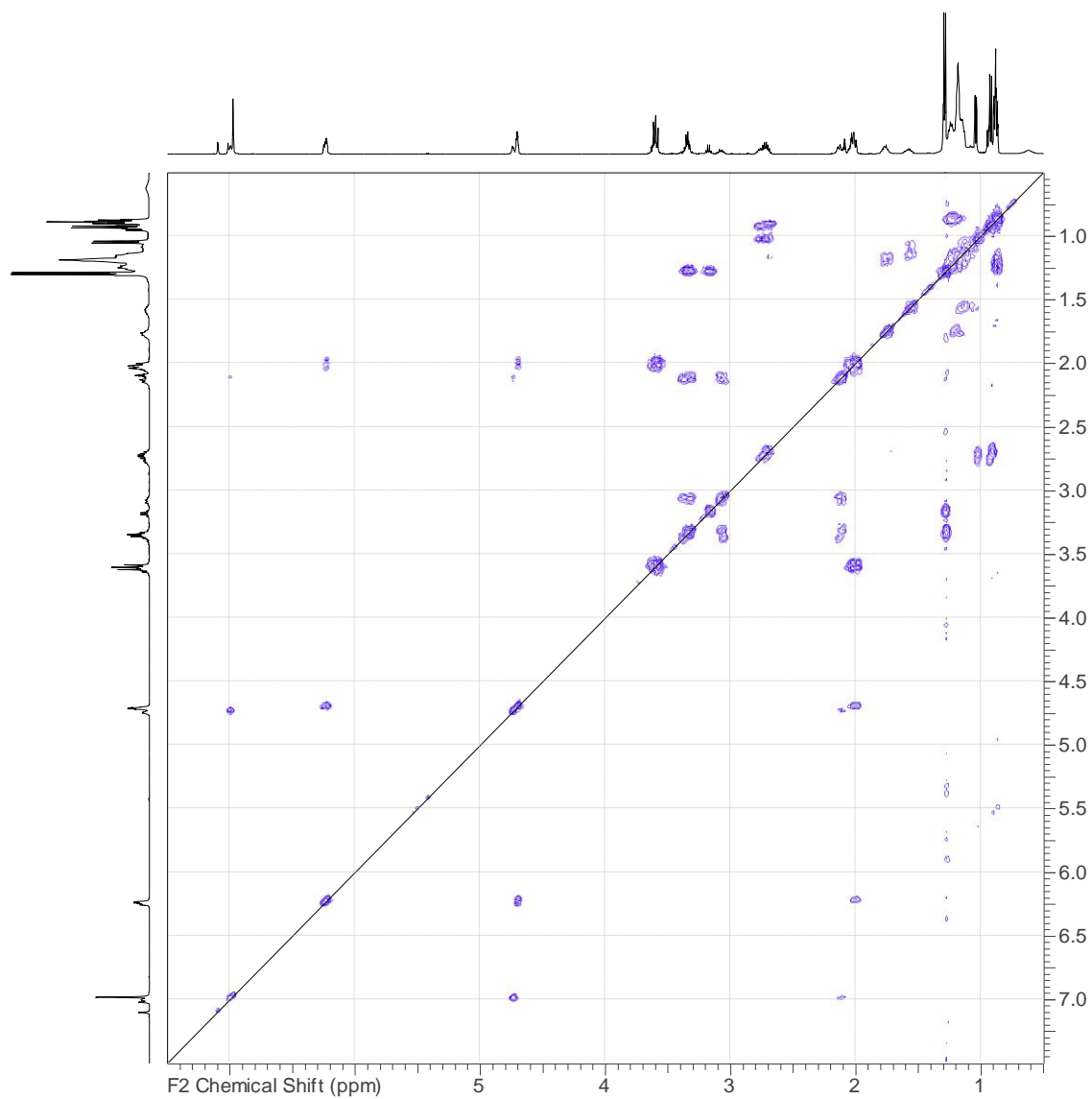


Figure S11. COSY spectrum of *libertamide*.

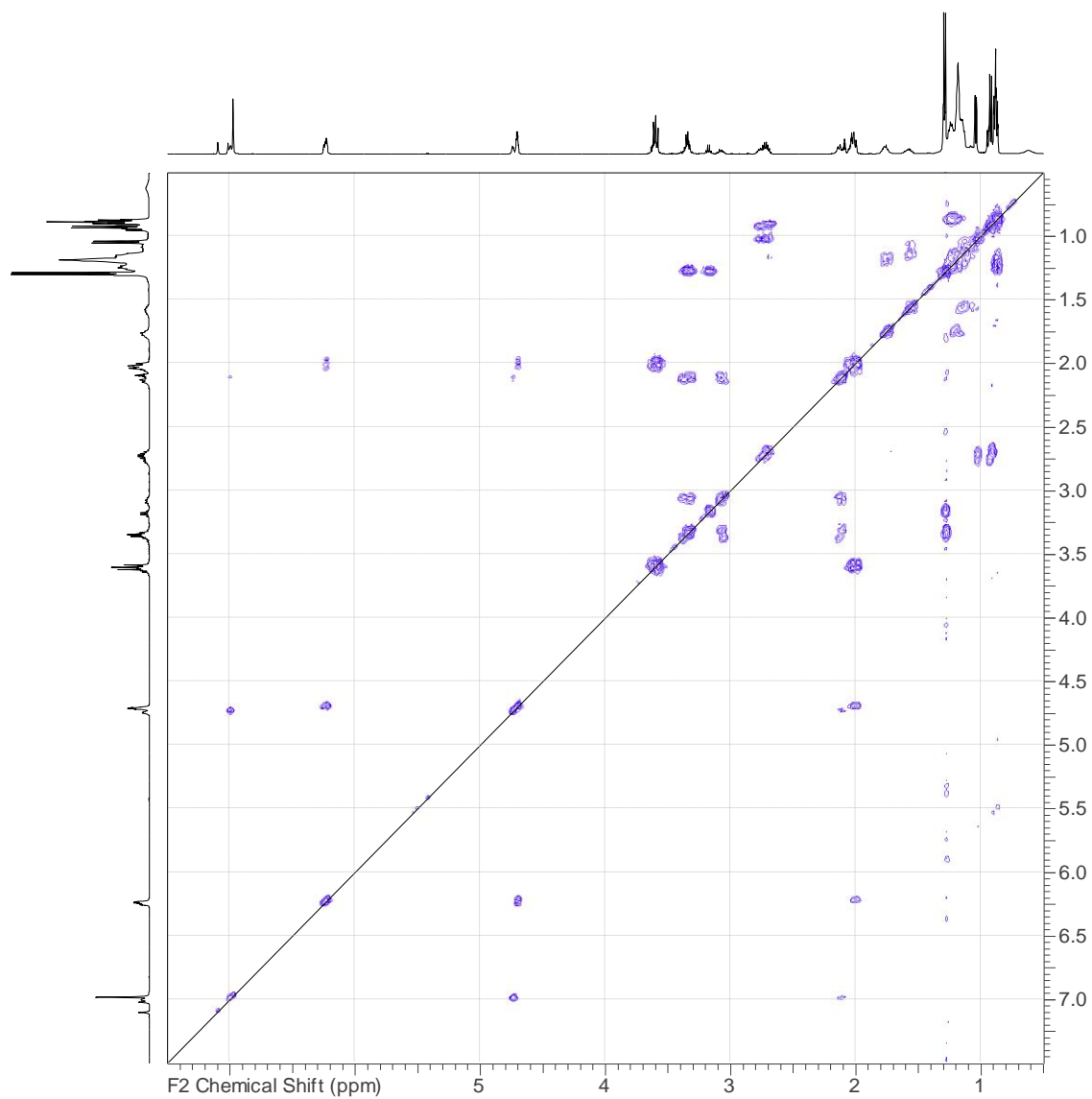


Figure S12. TOCSY spectrum of *libertamide*.

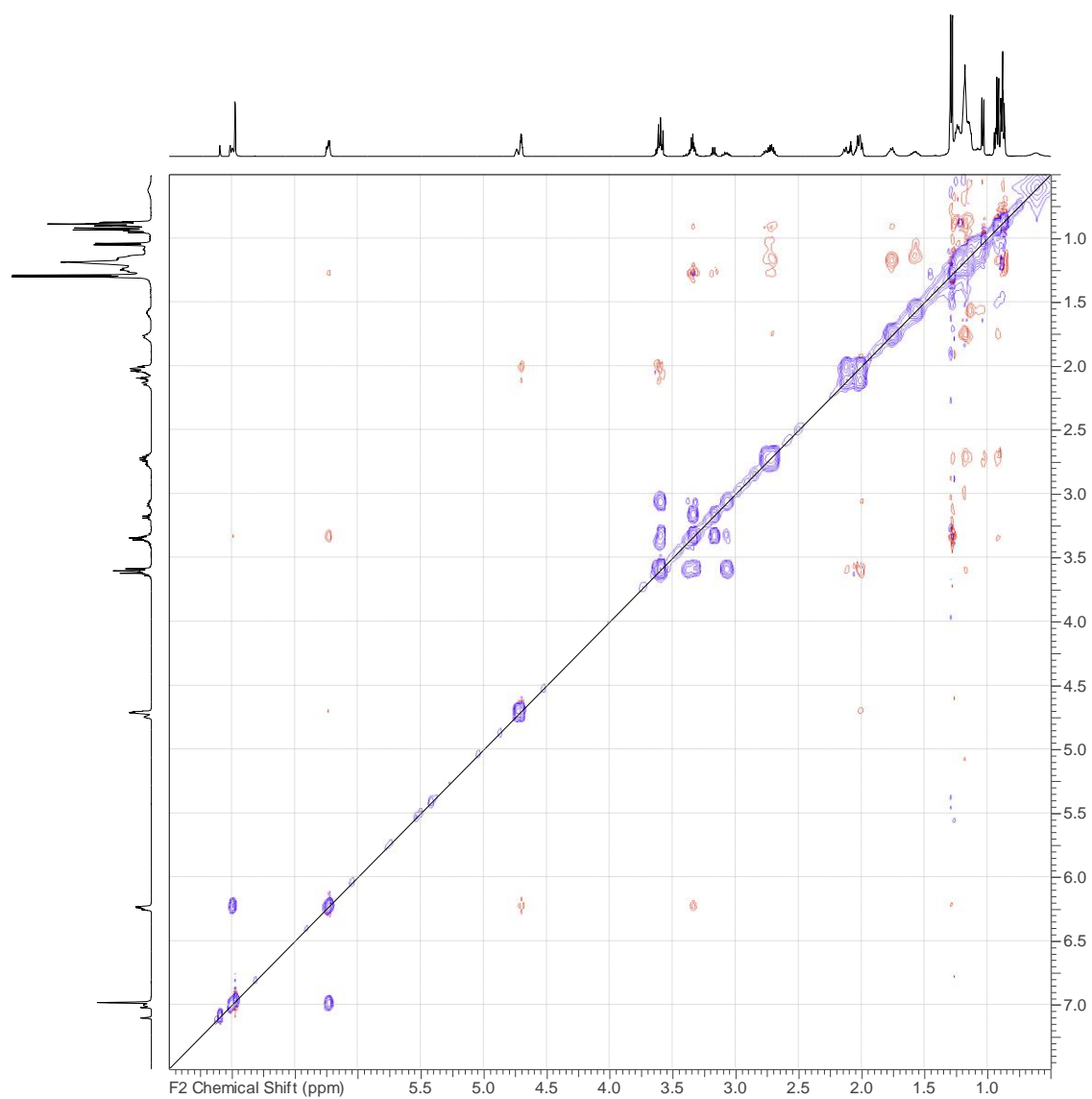


Figure S13. NOESY spectrum of *libertamide*.

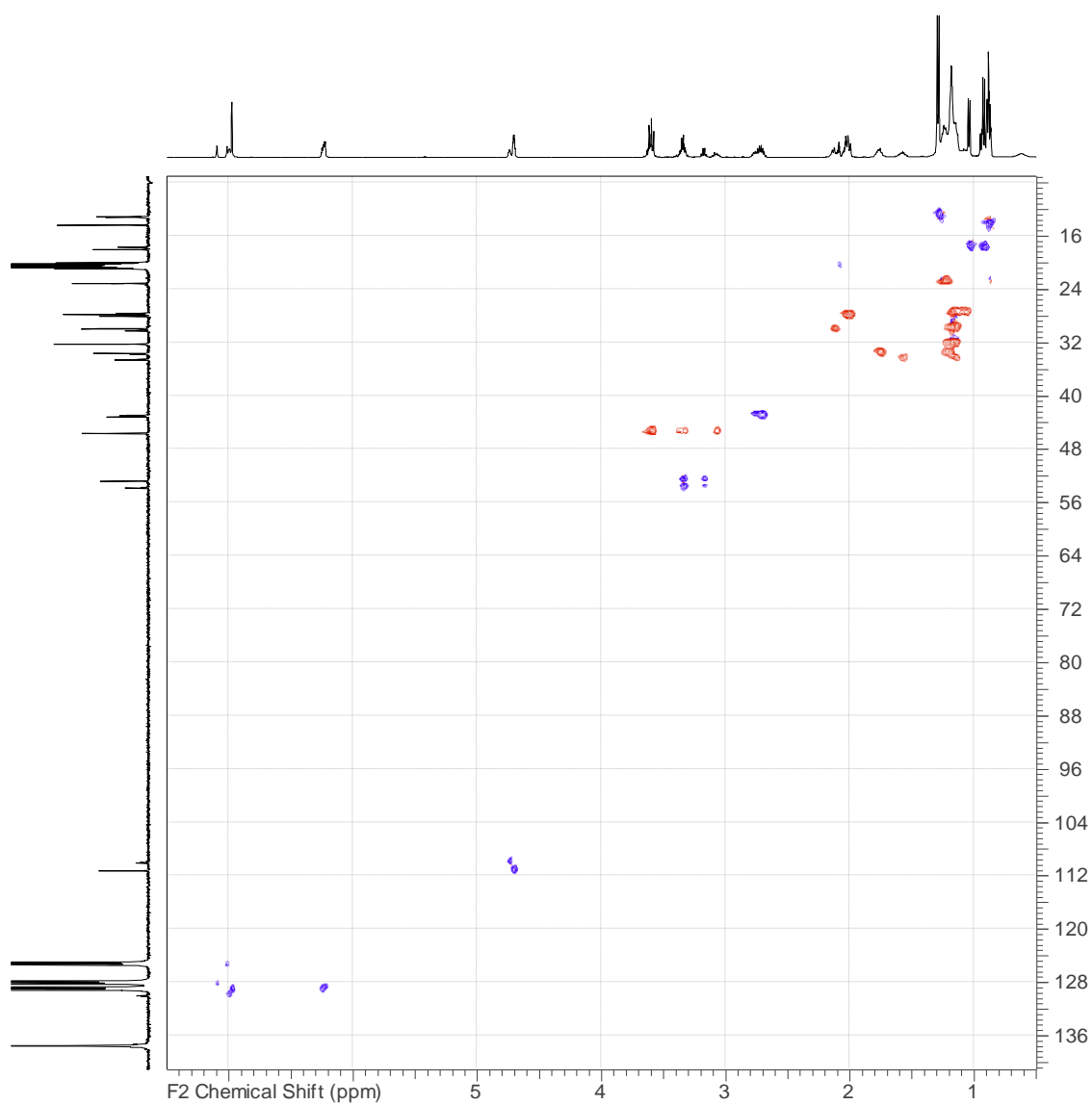


Figure S14. Multiplicity edited HSQC spectrum of *libertamide*.

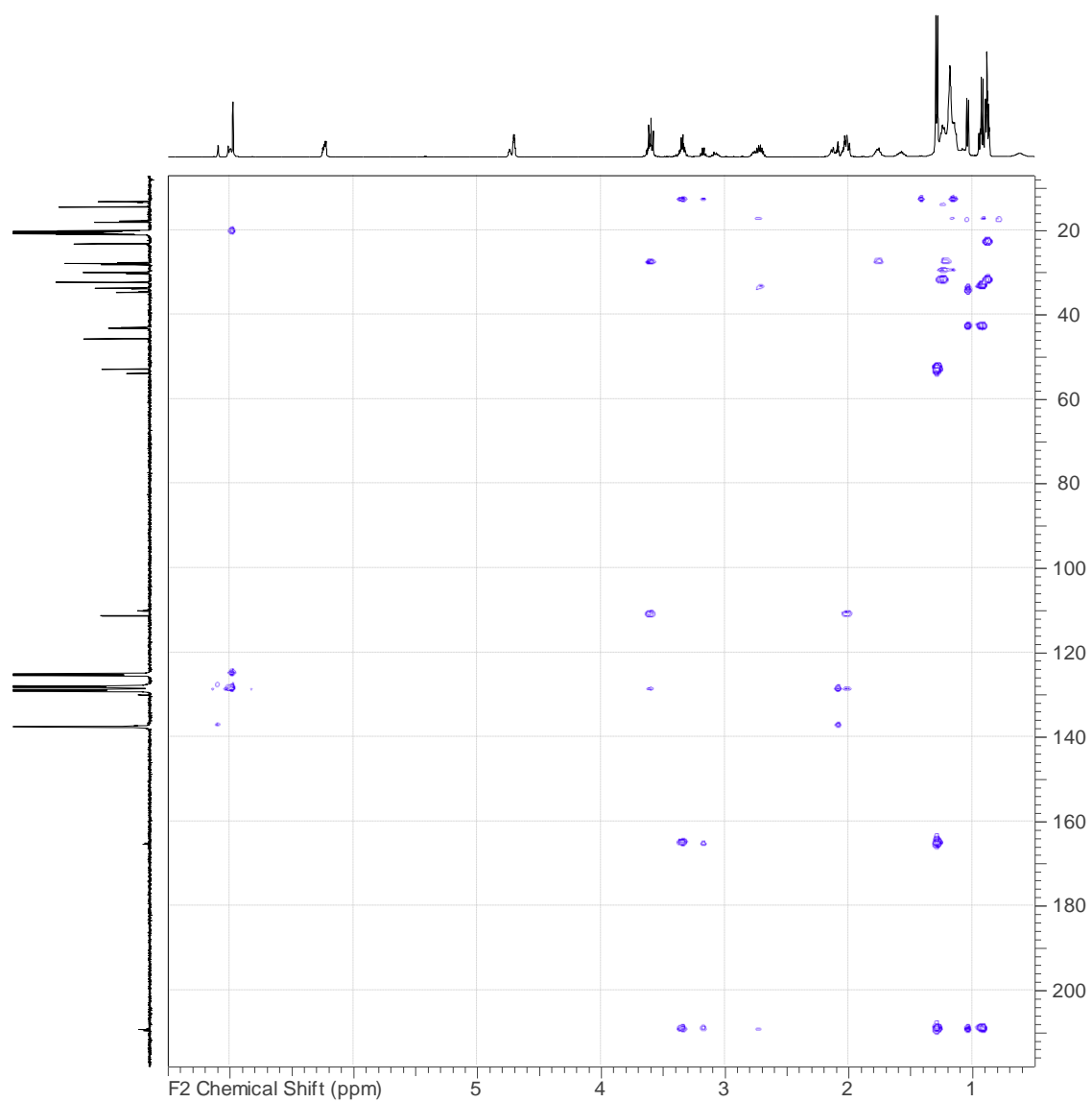


Figure S15. HMBC spectrum of *libertamide*.

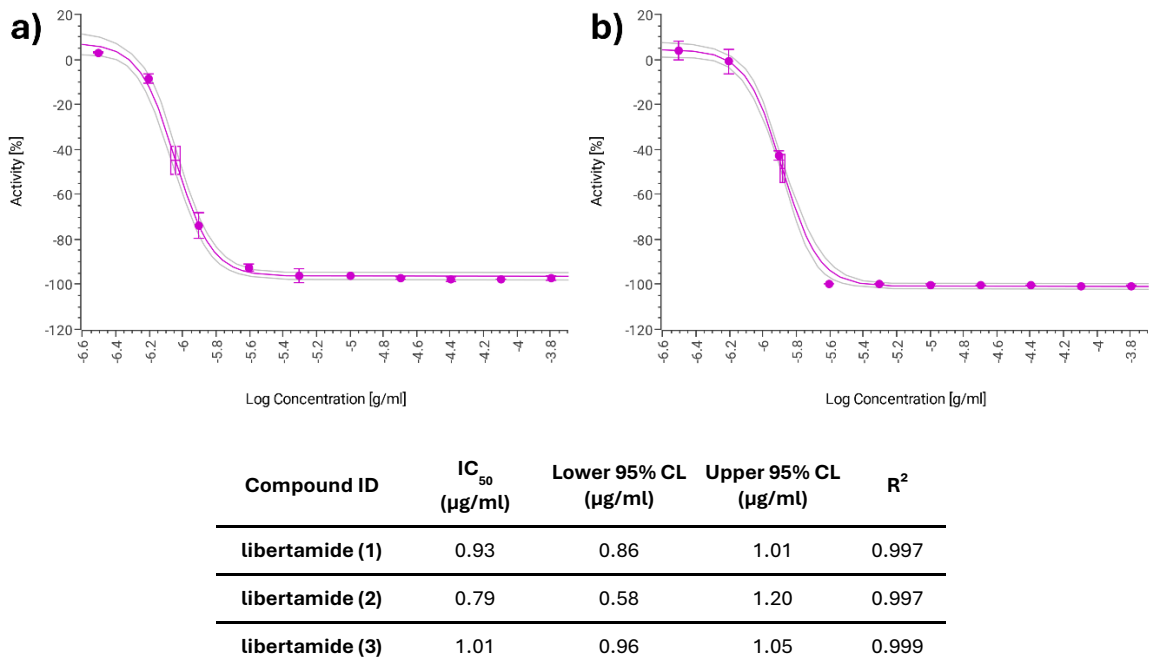


Figure S16. Dose-response curves of *libertamide* C₁₆H₂₇NO₂ and IC₅₀ (μg/mL) with their corresponding 95% confidence intervals against *Zymoseptoria tritici* CBS 115943 per triplicate, based on (a) absorbance and (b) fluorescence data.

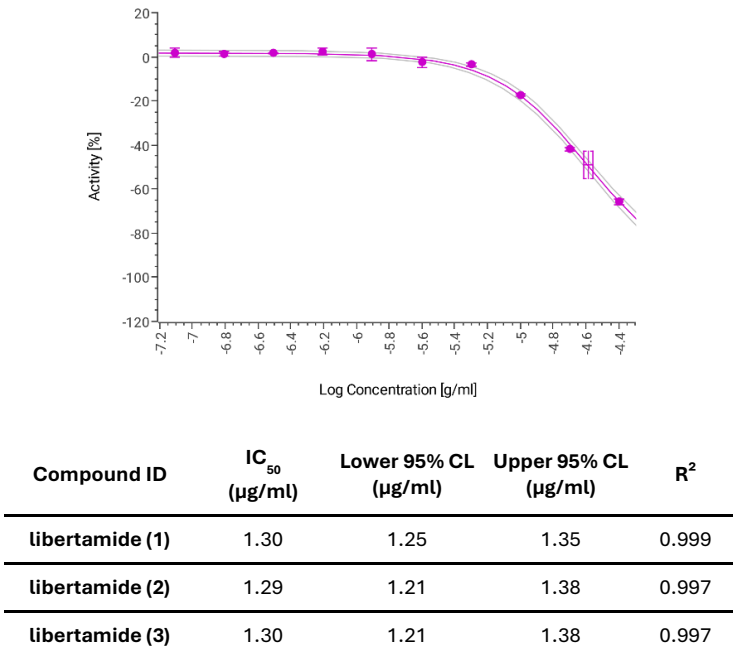


Figure S17. Dose-response curves of *libertamide* C₁₆H₂₇NO₂ and ED₅₀ (μg/mL) with their corresponding 95% confidence intervals for cytotoxicity evaluation in HepG2 cell line per triplicate.

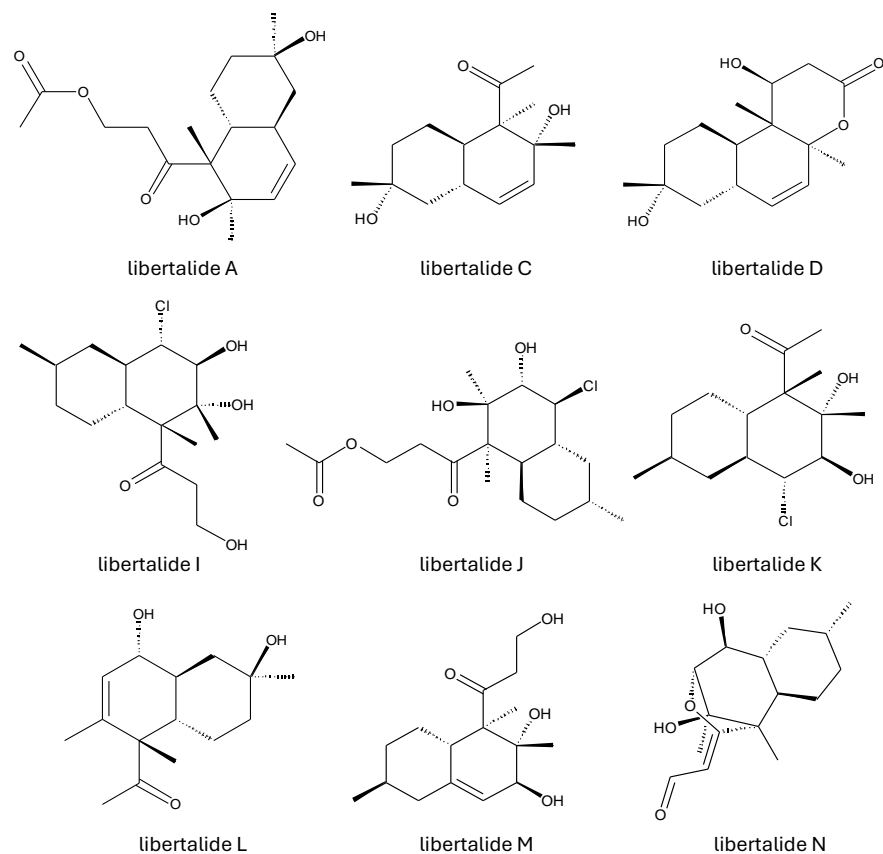


Figure S18. Examples of structural chemical diversity within the family of *libertalides*.

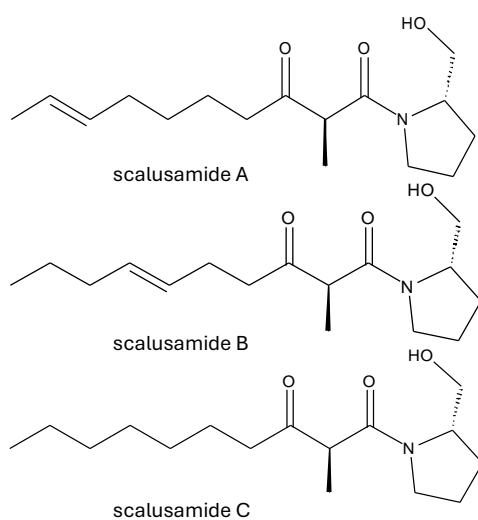


Figure S19. Chemical structure of *scalusamide A-C*.